

ALLOSTERIC MODULATION OF THE MU OPIOID RECEPTOR

by

Kathryn Elsa Livingston

A dissertation submitted in partial fulfillment
of the requirements for the degree of
Doctor of Philosophy
(Pharmacology)
in The University of Michigan
2016

Doctoral Committee:

Professor John R. Traynor, Chair
Professor Margaret E. Gnegy
Associate Professor Georgios Skiniotis
Professor John J. G. Tesmer

© Kathryn Elsa Livingston

2016

Acknowledgements

First, I would like to thank Dr. John Traynor. He has been an immensely supportive mentor who has always taken an interest in my development as a scientist and student. I am grateful for his patience, wisdom, and trust. Secondly, I wish to thank the additional members of my thesis committee: Drs. Margaret Gnegy, Georgios Skiniotis, and John Tesmer who have provided valuable comments and insight into my project.

Nest, I would like to thank all of the members of the Traynor laboratory, both past and present, including Aaron Chadderdon, Chao Gao, Abigail Fenton, Nicholas Griggs, James Hallahan, Dr. Todd Hillhouse, Dr. Jennifer Lamberts, Claire Meurice, Dr. Lauren Purington, Evan Schramm, Nicolas Senese, Alex Stanczyk, Omayra Vargas-Morales, Dr. Qin Wang, and Wyatt Wells. They have all made the lab a wonderful, vibrant environment.

I would also like to thank the various colleagues and collaborators for their contributions to this thesis. From the University of Michigan, I would like to thank Dr. Emily Jutkiewicz and her laboratory for helpful discussions and suggestions, Drs. Yoichi Osawa and Jorge Iñiguez-Lluhi for use of laboratory equipment, the Center for Chemical Genomics and the staff for help using the OctetRed[®], and Jacob Mahoney for purification of proteins and help in establishing the interferometry technique in the rHDL system for use in Chapter 5.

I would like express gratitude to Drs. Andrew Alt and Neil Burford from Bristol-Myers Squibb for their long-term collaborative input which made this project possible. I would also like to acknowledge additional collaborators that have been helpful in moving this project forward: Drs. Arthur Christopoulos and Meritxell Canals from University of Monash, Drs. Brian Kobilka and Aashish Manglik from Stanford University, and Dr. Roger Sunahara from University of California-San Diego.

I am also grateful for the sources of funding that have supported my graduate studies and thesis work including the Program in Biomedical Sciences (University of Michigan), the Endowment for the Basic Sciences (University of Michigan), the NIDA Neuroscience Training Program (NIH T32 DA7281-17), the Substance Abuse Interdisciplinary Training Grant (NIH T32 DA007267), and the Department of Pharmacology (University of Michigan) as well as the administration who helped arrange these fellowships and other details outside of the science including: Josh Daniels, Eileen Ferguson, Denise Gakle, Lisa Garber, Nancy Katon, Dar-Weia Liao, Dennis Ondreyka, and Ingrid Shriner-Ward.

Table of Contents

Acknowledgements	ii
List of Figures	v
List of Tables	viii
List of Appendices	ix
List of Abbreviations	x
Abstract	xii
CHAPTER 1: General Introduction	1
OPIOID RECEPTORS	1
RECEPTOR THEORY	4
CELLULAR CONSEQUENCES OF MU OPIOID RECEPTOR ACTIVATION	6
BIASED AGONISM AND IMPLICATIONS FOR NOVEL OPIOID THERAPEUTICS	8
ALLOSTERY AT OPIOID RECEPTORS	9
HYPOTHESIS AND AIMS	11
CHAPTER 2: Disruption of Na⁺-Ion Binding Site as a Mechanism of Positive Allosteric Modulation of the Mu Opioid Receptor	14
SUMMARY	14
INTRODUCTION	15
RESULTS	16
DISCUSSION.....	30
MATERIALS AND METHODS	36
CHAPTER 3: Two Chemically Distinct Allosteric Modulators Bind to a Conserved Site on Mu and Delta Opioid Receptors	38
SUMMARY	38
INTRODUCTION	39
RESULTS	41
DISCUSSION.....	49
MATERIALS AND METHODS	54
CHAPTER 4: Stabilization of Active-State Mu Opioid Receptor by Orthosteric and Allosteric Ligands: Implications for Agonist Efficacy	58
SUMMARY	58
INTRODUCTION	58
RESULTS	61
DISCUSSION.....	71

MATERIALS AND METHODS	75
CHAPTER 5: A Biased Mu-Opioid Receptor Positive Allosteric Modulator that Does Not Alter Morphine-Mediated Desensitization	78
SUMMARY	78
INTRODUCTION	79
RESULTS	81
DISCUSSION.....	86
MATERIALS AND METHODS	92
CHAPTER 6: Discussion and Future Directions.....	96
FUTURE DIRECTIONS	97
OVERALL CONCLUSIONS	103
APPENDICES.....	104
BIBLIOGRAPHY	157

List of Figures

CHAPTER 1

- Figure 1.1: Structures of various opioid ligands and crystal structures of inactive and active MOPr 3
- Figure 1.2: Sodium binding site collapses in active state of A_{2A}AR 7

CHAPTER 2

- Figure 2.1: Structure of BMS-986122 15
- Figure 2.2: Structure of opioid ligands..... 18
- Figure 2.3: Comparison of the effect of BMS-986122 on Met-Enk and morphine .. 19
- Figure 2.4: Affinity of morphine to bind MOPr is unaltered, even in the presence of 30 μ M BMS-986122..... 22
- Figure 2.5: Buprenorphine stimulation of G protein is concentration-dependently increased by BMS-986122..... 24
- Figure 2.6: BMS-986122 enhances the affinity and potency of (RS)-methadone 25
- Figure 2.7: Competition binding of orthosteric ligands in the absence or presence of 100 mM NaCl and 10 μ M GTP γ S 27
- Figure 2.8: Relationship between BMS-986122 and Na⁺ ions 28
- Figure 2.9: Correlation between the degrees of shift in affinity caused by the addition of BMS-986122 and the shift in potency at activating G protein 29
- Figure 2.10: BMS-986122 fails to stimulate GTP γ ³⁵S binding over basal levels, even with decreased (10 mM) NaCl..... 31

CHAPTER 3

- Figure 3.1: The chemical structures of BMS-986122 and BMS-986187 40
- Figure 3.2: BMS-986187 is an allosteric ligand and can enhance the affinity, potency, and maximal stimulation of several opioid ligands at MOPr 42
- Figure 3.3: BMS-986187 has a concentration-dependent effect on the potency of methadone to activate G protein 43
- Figure 3.4: Effects of BMS-986187 on adenylate cyclase inhibition and arrestin recruitment 45
- Figure 3.5: Negative cooperativity between NaCl and BMS-986187 at DOPr 47
- Figure 3.6: The mu-SAM BMS-986123 blocks the action of BMS-986187 at MOPr..... 48
- Figure 3.7: mu-SAM reverses activity of BMS-987187 at DOPr, implying a conserved opioid allosteric binding site..... 50

Figure 3.8: mu-PAM BMS-986182 is weak PAM at DOPr capable of reversing BMS-986187 activity	51
--	----

CHAPTER 4

Figure 4.1: Orthosteric ligand-mediated Nb39 association and dissociation in MOPr-rHDL	62
Figure 4.2: Correlation of association times of Nb39 with various measures of agonist efficacy	64
Figure 4.3: Allosteric modulation of MOPr rHDL by small molecule PAMs	67
Figure 4.4: Binding kinetics of Nb39 driven by allosteric ligands	70
Figure 4.5: Effects of mu-PAMs on morphine-mediated association and dissociation of Nb39 from MOPr-rHDL.....	72

CHAPTER 5

Figure 5.1: Desensitization of MOPr by various ligands in C6MOPr cell membranes as determined by loss of GTP γ ³⁵ S binding	82
Figure 5.2: BMS-986122 does not enhance agonist-mediated phosphorylation of S375 of MOPr	85
Figure 5.3: Internalization of MOPr is not enhanced by BMS-986122	87
Figure 5.4: BMS-986122 mediated ERK1/2 activation in C6MOPr cells.....	88

CHAPTER 6

Figure 6.1: BMS-986122 antinociception mediated through MOPr.....	102
---	-----

APPENDIX A

Figure A.1: Prototypic results from Mahan-Motulsky experiments	106
Figure A.2: Structures of BU97008, PPOM, BU9609, and BU72.....	109
Figure A.3: Mahan-Motulsky experiments of BU72 in the presence or absence of Nb39.....	111
Figure A.4: Enhancement in affinity of BU72 to bind MOPr rHDL in the presence of Nb39.....	112
Figure A.5: Time course of BU72 mediated ERK1/2 activation	113
Figure A.6: BU72 internalizes MOPr to the same extent as the endogenous ligand Leu-Enk.....	114

APPENDIX B

Figure B.1: β -Arrestin recruitment response to 2 in agonist mode and in PAM mode in PathHunter cells expressing δ receptors and μ receptors.....	124
Figure B.2: Effect of 2 on ³ H-diprenorphine binding and the effect of 10 μ M 2 on leu-enkephalin, SNC80, and TAN67 competition binding curves in CHO-hDOPr membranes	127
Figure B.3: Effect of increasing concentrations of 2 on leu-enkephalin concentration–response curves in β -arrestin recruitment and in inhibition of forskolin-stimulated cAMP accumulation in CHO-OPRD1 cells.	129

Figure B.4: Effect of increasing concentrations of 2 on leu-enkephalin concentration–response curves in GTP ³⁵ γS binding in CHO-hDOPr membranes and in pERK in CHO-hDOPr cells	123
--	-----

APPENDIX C

Figure C.1: Clustering results of the 1336 analogs of BMS-986121 and BMS-986122 extracted from eMolecules.....	146
Figure C.2: Allosteric EC ₅₀ shifts of endomorphin-1-stimulated β-arrestin recruitment in CHO-μ PathHunter cells in the presence of increasing concentrations of PAM.....	149
Figure C.3: Effects of MS1 on the binding of various orthosteric μ-opioid receptor agonists	151
Figure C.4: Effects of MS1 on the potency of various orthosteric μ-opioid receptor agonists to activate G-protein	152
Figure C.5: Ligand-based 3D pharmacophore model built from μ-PAMs	154

List of Tables

Table 2.1: Binding affinity of MOPr ligands in the presence or absence of BMS-86122.....	20
Table 2.2: Stimulation of GTP γ ³⁵ S binding by MOPr ligands in the absence or presence of BMS-986122	21
Table 2.3: Efficacy of MOPr agonists	33
Table 4.1: Association and dissociation kinetics of Nb39 to MOPr rHDL in the presence of various agonists	65
Table 4.2: Alteration in Nb39 kinetics in the presence of MOPr PAMs	69
Table 5.1: Saturation binding with ³ H-DPN reveals no change in Bmax or Kd following morphine treatment	83
Table B.1: Structure–Activity Relationship of the δ -PAM Chemotype in PathHunter CHO-OPRD1 and CHO-OPRM1 Cells in a β -Arrestin Recruitment Assay	125
Table B.2: Effect of 2 (10 μ M) on Orthosteric Agonist Competition Binding Ki Values in CHO-hDOPr Cell Membranes.....	128
Table B.3: Allosteric Parameters for 2 at the δ Receptor	131
Table C.1: Structure Activity Relationship of a New μ -PAM/SAM Chemotype in a PathHunter β -Arrestin Recruitment Assay	148

List of Appendices

Appendix A: Identification of slowly dissociating mu opioid receptor agonists for use in X-ray crystallography	104
Appendix B: .Discovery and characterization of positive allosteric modulators of the delta opioid receptors.....	119
Appendix C: Discovery of novel scaffold of positive allosteric modulations for mu opioid receptor using virtual docking	143

List of Abbreviations

5-HT1A	serotonin 1A receptor
6 x His	hexa histadine tag
Å	angstrom
aa	amino acid
α 2AR	alpha2-adrenergic receptor
AC	adenylate cyclase
ago-PAM	positive allosteric modulator with agonist properties
Apo-A1	apolipoprotein-A1
β 1AR	beta1-adrenergic receptor
β 2AR	beta2-adrenergic receptor
β -FNA	beta-funaltrexamine
CaMKII	Ca ²⁺ /calmodulin-dependent protein kinase II
cAMP	cyclic adenosine monophosphate
CB1	cannabinoid receptor type 1
CBD	cannabidiol
CHO	Chinese hamster ovary cells
CI	confidence interval
D2R	dopamine receptor D2
DAMGO	[D-Ala ² ,N-Me-Phe ⁴ ,Gly-ol ⁵]-enkephalin
DMEM	Dulbecco's Modified Eagle Medium
DMSO	dimethyl sulfoxide
DOPr	delta opioid receptor
DPN	diprenorphine
EC ₂₀	20% effective concentration
EC ₅₀	50% effective concentration
ERK	extracellular regulated kinase
FBS	fetal bovine serum
FLAG epitope	DYKDDDDK
G protein	guanine nucleotide binding protein
GDP	guanosine diphosphate
GIRK	G protein-coupled inwardly rectifying potassium channel
GPCR	G protein-coupled receptor
GRK	G protein-coupled receptor kinase
GTP	guanosine-5'-triphosphate

GTP γ S	guanosine-5'-O-(3-thio)triphosphate
GTP γ ³⁵ S	guanosine-5'-O-(3-[³⁵ S]thio)triphosphate
HEK293	human embryonic kidney 293 cells
IBMX	3-isobutyl-1-methylxanthine
ICV	intracerebroventricularly
K _d	dissociation constant
Leu-Enk	leucine-enkephalin
M2R	muscarinic acetylcholine receptor M2
MAPK	mitogen-activated protein kinase
MD	molecular dynamics
Mg/kg	milligram/kilogram
Met-Enk	methionine-enkephalin
MOPr	mu opioid receptor
mu-PAM	positive allosteric modulator of the mu opioid receptor
mu-SAM	silent allosteric modulator of the mu opioid receptor
MWC	Monod-Wyman-Changeux
Na ⁺	sodium ion
NAM	negative allosteric modulator
NLX	naloxone
NTI	naltrindole
Nb	nanobody
NOPr	nociceptin/orphanin FQ peptide receptor
PAM	positive allosteric modulator
PDB	protein data bank
PKC	protein kinase C
PLC	phospholipase C
PTX	pertussis toxin
RGS	regulators of G protein signaling
SAM	silent allosteric modulator
SDS-PAGE	sodium dodecyl sulfate-polyacrylamide gel electrophoresis
SEM	standard error of the mean
SNC80	4-[(R)-[(2 <i>S</i> ,5 <i>R</i>)-4-allyl-2,5-dimethylpiperazin-1-yl](3-methoxyphenyl)methyl]- <i>N,N</i> -diethylbenzamide
TEV	tobacco etch virus
THC	(-)- Δ 9-tetrahydrocannabinol
TM	transmembrane

Abstract

The mu opioid receptor (MOPr), a G protein-coupled receptor (GPCR), is the pharmacological site of action of morphine and related opioid narcotic agonists that bind to the orthosteric site on MOPr, evolutionarily developed to accommodate the endogenous opioid peptides. MOPr activation results in analgesia but also causes a number of unwanted effects including constipation, respiratory depression, tolerance, and euphoria leading to a high addictive liability. In contrast, small molecule positive allosteric modulators of MOPr (MOPr-PAMs) bind to alternative sites on the protein to modulate receptor function. MOPr PAMs represent a potential avenue for pain relief with a better therapeutic profile.

Studies described in this thesis seek to understand the mechanism of action of MOPr PAMs. The results show that MOPr-PAMs promote an active state of MOPr by disruption of the Na⁺ binding site on the receptor, a mechanism that may be applicable to other GPCRs. Furthermore, this active state can be captured and measured by the camelid antibody Nb39 providing a novel method for quantifying orthosteric and allosteric agonist efficacy. The work also demonstrates that the allosteric site on MOPr can accommodate structurally diverse ligands, and is somewhat conserved on the related delta opioid receptor. Lastly, this thesis explores the effects of chronic allosteric enhancement of MOPr signaling on the downstream processes of receptor desensitization and cellular tolerance *in vitro*.

CHAPTER 1

General Introduction

Opium, the dried latex obtained from the *papaver somniferum* plant, has been used by humans for spiritual and medical uses for thousands of years (Brownstein, 1993) and contains dozens of active alkaloids, including codeine, thebaine, and morphine (Kalant, 1997). Morphine, the primary molecule responsible for opium's actions, makes up at least 10% of opium by weight and the first reported extraction of morphine occurred in the early 1800's by Friedrich Sertürner.(Sertürner,1805; Frick *et al.*, 2005). Presently, medical use of opioid ligands exceeds 250 million prescriptions per year in the United States (Paulozzi *et al.*, 2014). The most commonly prescribed opioids include morphine and its semisynthetic analogues oxycodone and hydrocodone (IMS 2011). Though these drugs are effective at causing analgesia, they have a number of unwanted side effects including respiratory depression, suppression of gastric motility, and nausea (Kromer, 1988; Dhawan *et al.*, 1996; Yaksh TL *et al.*, 2011). In addition, long-term administrations of opioids results in tolerance and dependence, with drug cessation causing a withdrawal syndrome. Appreciation for the pharmacological effects of morphine led to in depth research about how and where morphine acts. Over 150 years after the isolation of morphine, the endogenous opioids and their receptors were discovered, opening the door for further structure-activity-relationship (SAR) studies of opioid ligands (Hughes *et al.*, 1975; Mains *et al.*, 1977; Goldstein *et al.*, 1979; Chavkin and Goldstein, 1981).

Opioid receptors

Clinically used opioids exert their analgesic and side effects by activating the mu opioid receptor (MOPr), a class A G protein-coupled receptor (GPCR) (Matthes *et al.*, 1996). There are three other members of the opioid receptor family: delta (DOPr), kappa (KOPr) and the nociceptin receptor (NOPr), each with unique expression patterns and physiological roles (for

review see (Waldhoer *et al.*, 2004)). In particular, MOPr is expressed throughout the central nervous system with enrichment in the periaqueductal gray region, nucleus accumbens, cerebral cortex, amygdala, and the nucleus of the solitary tract and is also highly expressed in the gastrointestinal tract. All clinically used opioids bind to the site where the endogenous opioid peptides bind, known as the orthosteric site (Fig 1.1). In addition to small morphine-like molecules from opium and their derivatives, MOPr binds endogenous peptide ligands that range from 5 amino acids (aa) (leucine-enkephalin and methionine-enkephalin) to the 31-aa peptide β -endorphin (Fig 1.1).

MOPr Structure

The orthosteric site of MOPr has been well-characterized by X-ray crystallography, mutagenesis, and a rich structure-activity relationship library. The MOPr has been crystallized in both an inactive state in complex with the irreversible antagonist β -funaltrexamine (β -FNA) as well as in an active form in complex with the high efficacy agonist BU72 and the G protein mimetic Nb39 ((Manglik *et al.*, 2012; Huang *et al.*, 2015); Appendix A).

To accommodate such a wide range of structurally dissimilar ligands, the binding pocket for MOPr is large in contrast to aminergic receptors like β 2- adrenergic (β 2AR) and muscarinic receptors (Rasmussen, DeVree, *et al.*, 2011; Kruse *et al.*, 2013). The binding of opioids involves a phenolic hydroxyl group that engages in a water-mediated interaction with H297^{6.52} (superscript indicates Ballesteros-Weinstein nomenclature (Ballesteros and Weinstein, 1995)) and the interaction of the morphinan tertiary amine with D147^{3.32} (Fig 1.1). The importance of this phenolic hydroxyl has been established by SAR. While no crystal structure of a peptide-bound MOPr has been determined, mutagenesis studies probing the binding of the synthetic peptide full MOPr agonist DAMGO ([D-Ala²,N-Me-Phe⁴,Gly-ol⁵]-enkephalin) show that there are extensive interactions between DAMGO and residues spanning the pocket (K303^{6.58}, W318^{7.35} and H319^{7.36}) as well as residues in extracellular loop 3 (Seki *et al.*, 1998).

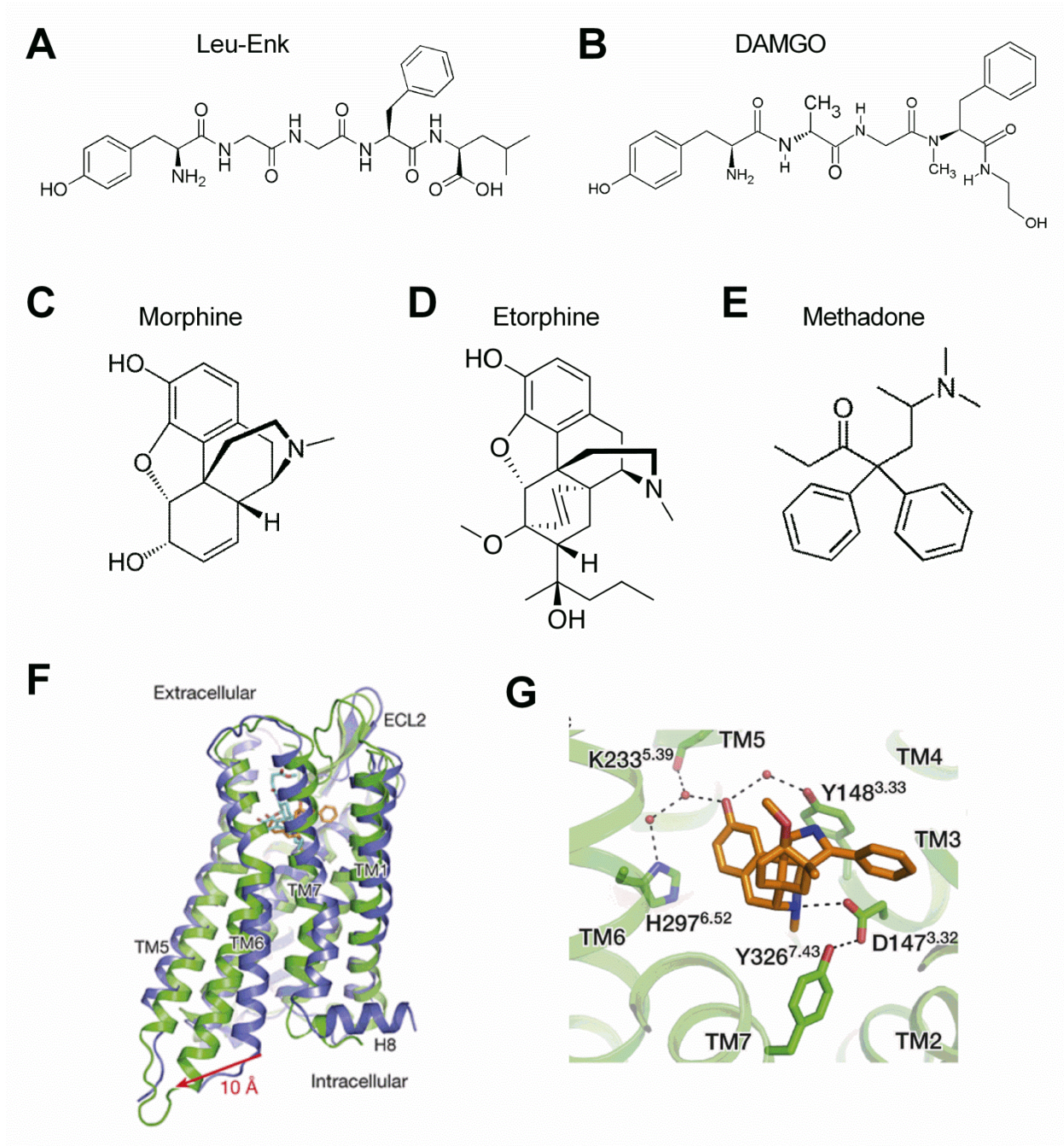


Figure 1.1: Structures of various opioid ligands and crystal structures of inactive and active MOPr. Structures of A) Leu-Enk, B) DAMGO, C) morphine, D) etorphine, and E) methadone. F) Overlay of the inactive (PDB 4DKL; purple) and the active (PDB 5C1M; green) crystal structure of MOPr. G) The orthosteric binding pocket of active MOPr with the agonist BU72 shown in orange. [Figures F and G taken from (Huang *et al.*, 2015)].

Receptor theory

GPCRs are allosteric machines that convey information from the extracellular side of a cell to the intracellular side. This propagation of signal occurs through conformational changes initiated by ligand binding that promotes G protein binding and nucleotide exchange. Receptor equilibrium can be simply thought of in terms of R (inactive) and R* (active receptor capable of signal transduction) populations. Although this model was originally proposed for ion channels that are either open or closed, it can also be generally applied to GPCRs (Del Castillo and Katz, 1957). Ligand-free receptors sample conformational space, with ligand-free sampling of R* being reflective of constitutive, or basal, receptor activity. By definition, agonists stabilize R* with the proportion of R* reflective of their intrinsic efficacy, neutral antagonists bind the receptor but do not perturb this equilibrium, and inverse agonists stabilize R, decreasing basal activity (Kofuku *et al.*, 2012).

Pharmacological characterization of novel ligands involves determining both their affinity and efficacy. These parameters can be considered largely independent and one does not predict the other. The affinity, or the strength of interaction between two molecules, is based upon the changes in free energy that occur following interaction (i.e. ligand and receptor) compared to the free energy of the entities in isolation and is often determined through the use of radiolabeled ligands. Affinity between a receptor and a ligand can change based upon the buffers and specifics of an assay, but is considered independent of tissue type and receptor expression. Efficacy, on the other hand, has been an ever evolving concept that can be measured and thought of in a multitude of ways.

History of pharmacological efficacy

The earliest ideas of efficacy derived from initial observations that some ligands caused a response in a tissue while others did not, and could only block the activity of another ligand. This was first described by Ariens and de Groot with the concept of “intrinsic activity” of a ligand (Ariens and De Groot, 1954). The word “efficacy” was first defined by Stephenson in 1956 by the following: “Different drugs may have varying capacities to initiate a response and consequently occupy different proportions of the receptors when producing equal response. This property will be referred to as the efficacy of the drug.” In the same paper, Stephenson defined partial agonists as “compounds with such a low efficacy that they possess properties intermediate

between agonists and antagonists (Stephenson, 1956).” Later, a method to analyze the relative ability of agonists to produce a response based on a given receptor occupancy was described by Furchgott (intrinsic efficacy; (Furchgott, 1967).

Stephenson’s definition allows for characterization of ligands on the basis of activity, but it was soon appreciated that the maximal response of a ligand depends greatly on the signaling output analyzed, degree of signal amplification, cell-type, and receptor expression level, in addition to many other factors. Partial agonists can display full agonist activity if signaling outputs far from the receptor, including physiological effects, are analyzed. This makes translation from *in vitro* to *in vivo* efficacy hard to predict. Due to this, many sought to determine a value for an “intrinsic efficacy,” or value reflective of the interaction of the specific ligand with a receptor that was less prone to differing between systems, much like affinity. Currently, the most well-accepted method for calculating the intrinsic efficacy of a ligand is the Black-Leff operational model (Black and Leff, 1983). This model was built to analyze an agonist-concentration response curve that obeyed the Law of Mass Action. In it, a ‘transducer function,’ tau (τ), is proposed that ‘transduces’ an agonist-occupied receptor into a pharmacological effect and defines the operational efficacy of a ligand. This model explicitly links receptor occupancy with functional response and for agonists, a τ value and K_A (agonist-receptor dissociation constant) can be calculated (Black and Leff, 1983) and be used to compare agonists and to calculate agonist bias (Kenakin *et al.*, 2012).

Role of sodium in receptor equilibrium and agonist activity

While receptor equilibrium between active and inactive states is readily perturbed by agonists in proportion to their efficacy, other factors can alter this equilibrium. In particular, Na^+ ions have been shown to alter the equilibrium between R and R* for many GPCRs, including MOPr (Pert *et al.*, 1973; Pert and Snyder, 1974; Motulsky and Insel, 1983; Carroll *et al.*, 1988; Emmerson *et al.*, 2004; Selent *et al.*, 2010; Liu *et al.*, 2012). Sodium ions bind in the central portion of the heptahelical bundle forming important water-mediated coordinations with residues in transmembrane 3 (TM3), TM7, and TM2 among others as seen in the four crystal structures of GPCRs so far obtained with Na^+ visible (A_{2A} adenosine receptor, β_1 adrenergic receptor, DOPr, and protease-activated receptor 1) ((Liu *et al.*, 2012; Zhang *et al.*, 2012; Fenalti *et al.*, 2014;

Miller-Gallacher *et al.*, 2014). In particular, a highly conserved aspartate residue (D2.50) in TM2 is shown to be required for Na⁺ to regulate receptor function.

Sodium regulates receptor function by stabilization of the inactive-state of the receptor. Na⁺ binding shifts receptor equilibrium to R and thereby causes a decrease in the basal activity of the receptor and a decrease in the affinity of agonists to bind. Inverse agonists are compounds that decrease basal binding and therefore show an increase in the affinity in the presence of Na⁺ ion (Appelmans *et al.*, 1986). Molecular dynamics simulations suggest that activation of the receptor causes conformational changes that restrict accessibility and space for the water, therefore driving it out of the Na⁺ ion binding pocket. Analyses performed by the Stevens group (Katritch *et al.*, 2014) have shown that the Na⁺/water pocket collapses in size from ~200 Å³ to 70 Å³ due to activation-related movement of the TM helices as seen in crystal structures (Fig 1.2). It is theorized that Na⁺ is then driven through the receptor and exits out the intracellular face, down its concentration gradient (Katritch *et al.*, 2014), although the fate of Na⁺ following receptor activation is not completely understood. The incompatibility of Na⁺ and active-states of GPCRs has been confirmed by the lack of Na⁺ found in GPCR structures, including the crystal structure of MOPr which shows occlusion of the sodium-binding site. These data, and others, support the hypothesis that sodium stabilizes R and that removal of Na⁺ either drives R* or destabilizes the receptor, much like an agonist, allowing for transition to R*. In support of this, sodium ions enhance the thermal stability of the A_{2A} adenosine receptor (Liu *et al.*, 2012) as well as the β1 adrenergic receptor (Miller-Gallacher *et al.*, 2014).

Cellular consequences of MOPr activation

Agonist occupation of MOPr leads to activation of heterotrimeric G proteins of the G_{α_{i/o}} class including G_{α_{i1}}, G_{α_{i2}}, G_{α_{i3}}, G_{α_o}, and G_{α_z}. Nucleotide exchange on the alpha subunit leads to an active GTP-bound G_α and an activated G_{βγ} that interact with effector enzymes and second messengers including: adenylate cyclase (AC), G protein-coupled inwardly rectifying potassium channel (GIRK), mitogen-activated protein kinase (MAPK), N-type calcium channels, and phospholipase C (PLC). Termination of G protein signaling occurs when GTP is hydrolyzed by the intrinsic GTPase activity of the G_α subunit, which can be accelerated by regulators of G protein signaling (RGS) proteins in some cases (for review see (Hollinger and Hepler, 2002)).

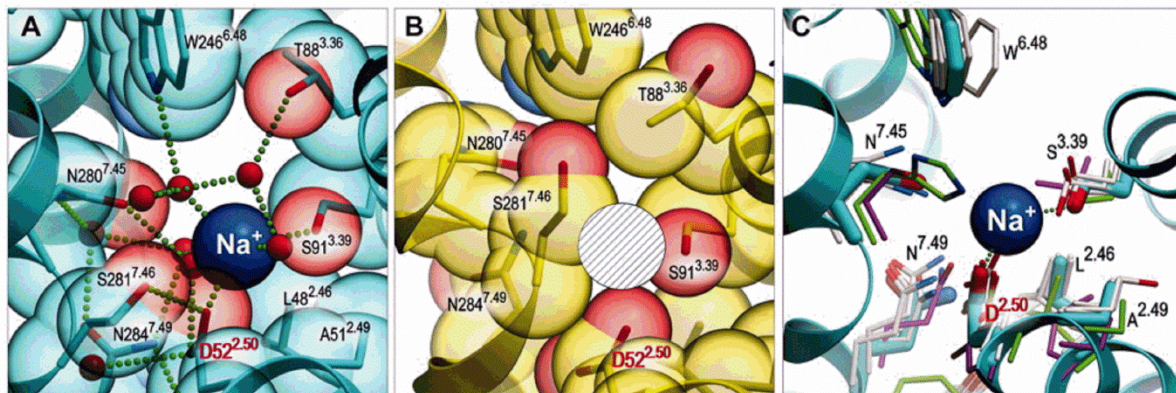


Figure 1.2: Sodium binding site collapses in active state of $A_{2A}AR$. A) Na^+ (blue sphere) in the middle of the transmembrane bundle of the $A_{2A}AR$ receptor structure with water molecules as red spheres. B) The sodium-pocket collapses in the active-like state of $A_{2A}AR$ which disables sodium from binding. C) The conservation of the sodium-binding site in a number of Class A GPCRs ($A_{2A}AR$ - cyan, chemokine receptor type 4- green, rhodopsin- magenta, and all other ($\beta 2AR$, histamine 1 receptor, dopamine D3 receptor, kappa opioid receptor, sphingosine-1 phosphate receptor) in gray). [Figure from (Liu *et al.*, 2012). Reprinted with permission from AAAS]

Signal transduction from the receptor terminates through various forms of homologous or heterologous desensitization. Homologous desensitization occurs when kinases recruited by activated G proteins, namely G protein-coupled receptor kinase 2 and 3 (GRK2/3), recognize and bind to agonist-bound receptor to phosphorylate residues on the intracellular loops and C-terminal tail of MOPr. Heterologous desensitization occurs when kinases, including protein kinase C (PKC) and Ca²⁺/calmodulin-dependent protein kinase II (CaMKII) phosphorylate intracellular residues of MOPr, independent of agonist occupancy. Phosphorylation enhances the binding of arrestin-2 and arrestin-3 to MOPr (Zhang *et al.*, 1998; McPherson *et al.*, 2010). Arrestin-binding leads to clathrin-mediated endocytosis of MOPr which results in the majority of MOPr being degraded, with a small percentage being returned to the plasma membrane once phosphatases remove and resensitize the receptor. Desensitization and downregulation occurs through prolonged administration of opioid ligands (Williams *et al.*, 2001, 2013).

Biased agonism and implications for novel opioid therapeutics

The concept of intrinsic efficacy became more complicated when inconsistencies arose as newer methods of measuring signal outputs were developed. Studies moved from measuring physiological responses in animal tissues (i.e. contraction) to detection of second messenger production in immortalized cell lines expressing high levels of receptors. Many levels of the signal transduction pathway may now be measured and quantified. In addition to the G protein mediated pathways, both the G α and G $\beta\gamma$ arms, G protein-independent signaling pathways have also been elucidated. The activation of these latter pathways, mainly mediated by arrestin, can now also be quantified. It has been shown for many GPCRs that a ligand may not signal through each arm (G protein or arrestin) to the same extent and as such may exhibit varying intrinsic efficacies depending upon the pathway. For example, binding of parathyroid hormone (PTH1-34) results in full activation of both Gs and Gq/11 at the parathyroid 1 (PTH1) receptor. In contrast, a synthetic derivative PTH-barr is an inverse agonist of G protein signaling at this receptor but induces arrestin-dependent ERK activation (Gesty-Palmer *et al.*, 2006). Indeed, signaling by this ligand is abrogated in arrestin-3 knockout mice (Gesty-Palmer *et al.*, 2009). Another example is the activation of GPR109A by niacin, also known as vitamin B3. Niacin administration has the clinical benefit of increasing high-density lipoproteins and reducing triglycerides through activation of Gi/o proteins through this receptor. In contrast, activation of

arrestin-2 and subsequent binding to activated cytosolic phospholipase A2 (cPLA2) generates arachidonate, resulting in the uncomfortable flushing associated with niacin administration (Walters *et al.*, 2009). As such, the GPR109A agonist MK-0354 has been developed that has a G protein bias and shows therapeutic benefits without the flushing (Semple *et al.*, 2008).

At MOPr, it has been proposed that G protein-privileged ligands would be the most clinically beneficial with decreased tolerance and respiratory depression, but robust analgesia. This hypothesis is supported by experiments conducted with arrestin-3 knockout mice (Bohn *et al.*, 1999, 2002; Raehal *et al.*, 2005). These mice are resistant to both acute tolerance following one administration of a high dose of the opioid agonist morphine (100 mg/kg) and also show a lack of tolerance formation following 9 days of morphine administration (10 mg/kg once a day) or after morphine-pellet implantations which slowly release morphine continuously over the course of 3 days (Bohn *et al.*, 2000).

Based on data like these, there has been an effort to develop MOPr agonists that are G protein-biased. One of the first such ligands was herkinorin, a derivative of the kappa opioid receptor agonist salvinorin A, which was shown to activate G protein mediated ERK1/2 phosphorylation. But, herkinorin administration failed to cause robust phosphorylation of MOPr, arrestin recruitment, and arrestin-mediated internalization of MOPr in cultured HEK293 cells stably expressing MOPr (Groer *et al.*, 2007). Another ligand, TRV130, has also been purported to be a G protein-biased ligand capable of potent antinociception with reduced gastrointestinal and respiratory depression as compared to the traditional ligand morphine (Dewire *et al.*, 2013). The degree of this ligand's bias has been questioned, though. It may be that TRV130 is not biased, but is actually a balanced, but low efficacy partial agonist when the Black-Leff operational model is applied to analysis of TRV130 signaling (Thompson *et al.*, 2015). Nonetheless, TRV130 has recently moved into Phase 3 clinical trials for the treatment of moderate to severe pain, with a focus on acute postoperative pain (www.trevenainc.com).

Allostery at opioid receptors

A recent avenue of research in the pharmacology of GPCRs is the study of allosteric ligands (Conn *et al.*, 2009; Wootten *et al.*, 2013). Allosteric ligands bind to regions on GPCRs spatially distinct from the orthosteric site and can alter affinity, potency, and efficacy of a ligand binding at the orthosteric site. Classically, positive allosteric modulators (PAMs) enhance

agonist binding and activity while negative allosteric modulators (NAMs) decrease such features. Muscarinic receptors have the most well studied allosteric ligands. A crystal structure of the human M2 muscarinic acetylcholine receptor (M2R) in complex with an agonist and a positive allosteric modulator was recently reported (Kruse *et al.*, 2013). The structure reveals that the allosteric site of the M2 receptor lies directly above the orthosteric site. When an agonist binds, a ‘shelf’ is created by the rotation of residues over the orthosteric site. This ‘shelf’ provides a pocket for allosteric ligands to bind and has direct consequences on the association and dissociation kinetics of orthosteric ligand binding. In addition, the structure provided a molecular basis for the cooperativity seen between allosteric and orthosteric ligands. The binding site for the allosteric ligand was only present when the receptor was occupied by an agonist and in an active-like state.

Allosteric ligands offer many advantages over orthosteric ligands including preservation of spatial/temporal regulation and specificity. First, due to their mechanism of action, these ligands often have no activity in the absence of an orthosteric ligand. This means that activity is dependent upon endogenous ligands being synthesized and released, allowing for signal timing and distribution to more closely mimic the body’s natural timing and endogenous ligand release. Secondly, it is often difficult to create a selective drug that targets one receptor subtype of a family (muscarinic for example) due to the endogenous orthosteric ligand(s) they share. In contrast, in the absence of an endogenous allosteric ligand there is no evolutionary pressure to conserve other potential pockets on the receptor. Consequently, selective M1 and M4 allosteric ligands have been discovered and represent novel ways to treat certain diseases such as schizophrenia (Felder *et al.*, 2000; Seager *et al.*, 2009; Farrell and Roth, 2010).

Allostery at opioid receptors remains a relatively unexplored avenue of research. Cannabidiol (CBD) and the closely related cannabidiol receptor 1 agonist (CB1) (-)- Δ^9 -tetrahydrocannabinol (THC) have been postulated to be negative allosteric modulations (NAMs) at both MOPr and DOPr (Kathmann *et al.*, 2006). In rat brain homogenates, the dissociation of the MOPr selective agonist ^3H -DAMGO was shown to be 12-fold faster in the presence of 100 μM CBD and 2-fold faster in the presence of 100 μM THC. In addition, they were both shown to accelerate the dissociation of the DOPr selective antagonist naltrindole (NTI). But, allosteric modulation by THC and CBD was not confirmed to be mediated by direct binding to MOPr. The preparation used (rat brain homogenate) contains CB1 receptors as well as many of the putative

targets of CBD including CB1, GPR55, the serotonin 1A (5-HT_{1A}) receptor, and peroxisome proliferator-activated receptor (PPAR)-gamma receptors (Russo *et al.*, 2005; Campos *et al.*, 2012; Hegde *et al.*, 2015; Walsh *et al.*, 2015). As such, the effects of CBD and THC may not be through a direct allosteric interaction at MOPr, but instead indirectly through the interactions of another receptor with MOPr. There are reports of heterodimer formation between MOPr with both CB1 and 5-HT_{1A} receptors and it is also possible that CBD has allosteric effects across this heteromeric interface as has been seen with the dopamine receptor allosteric ligand SB269652 that acts as a NAM of dopamine D2 receptor (D₂R) dimers (Kathmann *et al.*, 2006; Hojo *et al.*, 2008; Cussac *et al.*, 2012; Lane *et al.*, 2014). The description of CBD and THC as NAMs at MOPr is also in contrast to the numerous studies showing synergism between cannabinoids and opioids in causing antinociception and analgesia in rodents and humans, respectively (for review see (Cichewicz, 2004)).

In collaboration with Bristol-Myers Squibb, our lab discovered several small molecule PAMs of MOPr (Burford *et al.*, 2013) from a 1.2 million compound library using a DiscoverX® high-throughput screen to measure agonist-mediated arrestin recruitment. Specifically, compounds were screened alone and in the presence of an EC₂₀ concentration of the MOPr agonist endomorphin-1. Those compounds that selectively enhanced agonist-response while having no response alone were evaluated further. This screen yielded several PAMs as well as several ‘silent’ (neutral) allosteric molecules (SAMs) that show no activity but instead bind competitively to displace the PAMs. The lead compound, BMS-986122, was then shown to enhance the affinity and potency of several opioids agonists to bind MOPr and cause G protein activation as measured by GTPγ³⁵S binding (Burford *et al.*, 2013).

Hypothesis and Aims

The overall goal of the work described in this thesis is to further explore allosteric modulation of MOPr. Specifically, the goals are to determine the mechanism of allosteric modulation of this receptor, to probe the interaction between allosteric modulator and MOPr, and to understand the acute and chronic effects of allosteric modulation at the cellular level. Given that allosteric modulators of GPCRs are a possible drug avenue; this work will provide the *in vitro* data required for proof of principle that this may be a beneficial strategy to target MOPr.

Chapter 2: Investigate the probe dependence and mechanism of action of BMS-986122.

Chapter 2 investigates the probe dependence of the MOPr PAM BMS-986122. Probe dependence, or the variance of allosteric action based on the orthosteric ‘probe’ used, is a well-known phenomenon for allosteric modulators (Valant *et al.*, 2012). Though it is known that BMS-986122 enhances the affinity of MOPr agonists DAMGO and endomorphin-1, it is unknown if BMS-986122 can enhance the binding and activity of endogenous peptides or commonly used opioid drugs, such as morphine and methadone. The studies in this chapter utilize radioligand binding assays and functional assays using GTP γ ³⁵S in cultured cells expressing rat MOPr to understand which orthosteric ligands are cooperative with BMS-986122. In analyzing the probe dependence of BMS-986122, an understanding of the mechanism of action of this mu-PAM, namely an allosteric interaction with the Na⁺ binding site was uncovered and will be explored.

Chapter 3: Investigate the action of BMS-98618 and the possibility of a conserved opioid binding site across MOPr and DOPr.

Chapter 3 focuses on the recently discovered DOPr PAM, BMS-986187. Although discovered as a high affinity and high efficacy DOPr PAM, BMS-986187 was found to have allosteric activity at MOPr. In this chapter, we investigated if BMS-986187 has the same mechanism of action as BMS-986122 at both MOPr and DOPr. Furthermore, we tested if BMS-986122 and BMS-986187 bind at the same site on MOPr or if they target different allosteric sites on the receptor.

Chapter 4: Investigate the ability of orthosteric and allosteric ligands to stabilize active-state MOPr

Chapter 4 investigates the minimal functional unit required to observe allosteric modulation of MOPr. All previous characterization of MOPr PAMs was performed in cell membranes and it is as of yet unknown if BMS-986122 or BMS-986187 bind directly to the receptor. In this chapter, purified MOPr reconstituted into high-density lipoproteins (MOPr-rHDL) and radioligand binding as well as interferometry was used to monitor ligand binding as well as the binding of the small camelid antibody, nanobody 39 (Nb39), which serves as an

active-state biosensor of MOPr. These tools were used to further probe the mechanism of MOPr-PAM activity and to create a novel assay for measuring both allosteric and orthosteric efficacy.

Chapter 5: Investigate the consequences of long-term exposure to BMS-986122 on cellular tolerance and desensitization.

The final data chapter focuses on the consequences of allosteric modulation on processes of cellular tolerance and desensitization which have direct relevance to the potential clinical benefit of these compounds. Using cultured cell lines expressing MOPr, the loss in signal transduction following chronic agonist exposure was measured in the absence or presence of BMS-986122 with the hypothesis that the MOPr PAM should enhance these processes. Furthermore, the ability of BMS-986122 to enhance MOPr phosphorylation and internalization was also measured. Lastly, these studies explored if BMS-986122 showed a bias in the signaling outputs that it potentiated.

The appendices contain studies related to the investigation of slowly dissociating ligands of MOPr for use in crystallography (Appendix A), the discovery of allosteric modulators of the delta opioid receptor (Appendix B), and the use of molecular dynamics simulations to find novel PAMs of MOPr (Appendix C).

CHAPTER 2

Disruption of the Na⁺-Ion Binding Site as a Mechanism for Positive Allosteric Modulation of the Mu-Opioid Receptor¹

Summary

Positive allosteric modulation of the mu opioid receptor (MOPr), the site of action of all clinically used opioids, represents a novel approach for the management of pain. We recently reported on positive allosteric modulators of MOPr (mu-PAMs), a class A G-protein coupled receptor (GPCR). This study was designed to examine the mechanism of allosteric modulation by comparing the degree to which opioid ligand structure governs modulation. To do this we examined the interaction of the mu-PAM, BMS-986122, with a chemically diverse range of MOPr orthosteric ligands. Generally, for full agonists BMS-986122 enhanced the binding affinity and potency to activate G protein with no alteration in the maximal effect. In contrast, lower efficacy agonists including morphine were insensitive to alterations in binding affinity and showed little to no change in potency to stimulate G protein. Instead, there was an increase in maximal G protein stimulation. Antagonists were unresponsive to the modulatory effects of BMS-986122. Sodium is a known endogenous allosteric modulator of MOPr and alters orthosteric agonist affinity and efficacy. The sensitivity of an orthosteric ligand to BMS-986122 was strongly correlated with its sensitivity to NaCl. In addition, BMS-986122 decreased the ability of NaCl to modulate agonist binding in an allosteric fashion. Overall, BMS-986122 displayed marked probe dependence that was based upon the efficacy of the orthosteric ligand and can be explained using the Monod-Wyman-Changeux two-state model of allosteric modulation. Furthermore, disruption of the Na⁺ ion binding site may represent a common mechanism for allosteric modulation of class A GPCRs.

¹This research was published in the Proceedings of the National Academy of Sciences. Livingston KE, Traynor JR. Disruption of the Na⁺ ion binding site as a mechanism of positive allosteric modulation of the mu-opioid receptor. *Proc Natl Acad Sci USA*. 2014 Dec 23;111 (51):18369-74. © National Academy of Sciences.

Introduction

The mu opioid receptor (MOPr) is the site of action of all clinically used opioid drugs. MOPr is a class A G protein-coupled receptor (GPCR) that couples to heterotrimeric Gi/o proteins. Clinically used opioid agonists bind to the orthosteric site on MOPr and though they are efficacious at causing pain relief, have a number of unwanted side effects resulting from direct MOPr activation. We have recently discovered and presented a preliminary characterization of positive allosteric modulators of MOPr (mu-PAMs) and are currently pursuing the idea that mu-PAMs could be a viable way to manage pain (Burford *et al.*, 2013; N Burford *et al.*, 2015). In particular, the ligand BMS-986122 (Fig 2.1) represents the most active mu-PAM currently identified. It was discovered in a high-throughput screen for its ability to enhance the recruitment of β -arrestin to MOPr by the agonist endomorphin-1. Though having little agonist activity on its own, this modulator has the ability to enhance the affinity, potency, and/or maximal response of MOPr agonists. In the same systems, BMS-986122 has no activity when the delta opioid receptor (DOPr) is expressed, indicating the importance of MOPr for BMS-986122 activity.

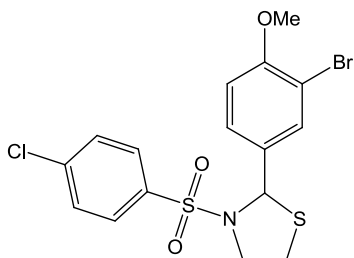


Figure 2.1 Structure of BMS-986122 (2-(3-Bromo-4-methoxyphenyl)-3-[(4-chlorophenyl) sulfonyl]-thiazolidine)

The study of allosteric modulation of GPCRs has recently gained momentum (Luttrell and Kenakin, 2011) and represents a novel avenue for drug development (Wootten *et al.*, 2013; Nickols *et al.*, 2014). Allosteric modulators have been discovered for several GPCRs including the muscarinic, cannabinoid, and metabotropic glutamate receptors (O'Brien *et al.*, 2004; Price *et al.*, 2005; May, Avlani, *et al.*, 2007) with a growing body of *in vitro* and *in vivo* literature describing allostery at GPCRs (Seager *et al.*, 2009; Kruse *et al.*, 2013; Byun *et al.*, 2014). In contrast, apart from our initial description of mu-PAMs, very little is known about allostery at MOPr.

Allosteric modulators exhibit probe dependence, meaning they show disparate effects depending on the agonist bound to the orthosteric site (Keov *et al.*, 2011). A striking example of this is LY2033298, a PAM of the muscarinic acetylcholine receptors M2 and M4. LY2033298 increases the affinity of the agonist oxotremorine, while having no effect on the binding of the agonists pilocarpine and McN-A-343 (Valant *et al.*, 2012). Currently, it is not known if all opioid agonists are equally sensitive to the PAM effect of BMS-986122, nor the mechanism underlying the allosteric modulation. Our initial characterization showed that BMS-986122 causes a shift in the potency of the agonist DAMGO ([D-Ala², N-MePhe⁴, Gly-ol]-enkephalin), but increases the maximal stimulation of G protein by morphine (Burford *et al.*, 2013). Opioid ligands are extremely diverse, ranging from the 31-amino acid endogenous peptide β -endorphin to small alkaloids like morphine. Therefore, this study sought to answer two questions: a) does BMS-986122 show probe dependence for the orthosteric ligand? and b) if probe dependence is seen, what is the mechanistic basis for this?

To address these questions we examined the effect of BMS-986122 on the MOPr properties of a wide range of opioid ligands from endogenous peptides to small molecules (Fig. 2.2). The results reveal that the PAM effects of BMS-986122 are dependent on the efficacy of the orthosteric ligand and not on the structure per se. We find a strong correlation between the positive action of BMS-986122 and the negative action of Na⁺ ions to inhibit agonist binding. Moreover, we also show that BMS-986122 allosterically inhibits the ability of Na⁺ ions to reduce agonist binding. The PAM effect of BMS-986122 can consequently be explained by an inhibition of the ability of Na⁺ ions to stabilize the inactive state of the receptor, thereby allowing the receptor to shift to an active conformation. Thus, the mechanism of positive allosteric modulation can be simply explained by the two-state Monod-Wyman-Changeux model of allosterism (Monod *et al.*, 1965).

Results:

We first investigated the effects of a maximally effective concentration (10 μ M; (Burford *et al.*, 2013)) of BMS-986122 on the MOPr activity of a range of endogenous opioid peptides (Fig. 2.2). Using cell membrane homogenates prepared from C6 glioma cells stably expressing MOPr (C6MOPr, (Clark *et al.*, 2003)), we performed radioligand competition binding assays using ³H-diprenorphine (DPN, an opioid antagonist) in the presence of GTP γ S and NaCl to

generate an inactive receptor state known to predominate in native membranes (Carroll *et al.*, 1988; Lee *et al.*, 1999). As shown in Fig. 2.3A and Table 2.1, BMS-986122 caused an approximate six-fold enhancement in the affinity of both methionine-enkephalin (Met-Enk) and leucine-enkephalin (Leu-Enk). A similar increase in affinity was seen for the smaller putative endogenous peptide endomorphin-1 (Zadina *et al.*, 1997). In addition to enhancing its affinity to bind MOPr, BMS-986122 caused a leftward shift in the concentration-response for Met-Enk to activate G protein, with no alteration in the maximal response (E_{max}), as measured by $GTP\gamma^{35}S$ binding in membrane homogenates (Fig. 2.3C, Table 2.2); an effect also seen with Leu-Enk and endomorphin-1 (Table 2.2). The endogenous opioid β -endorphin, a much larger 31-amino acid peptide, was also modulated by BMS-986122 with leftward shifts in both the affinity (fourfold; Table 2.1) and potency (six-fold; Table 2.2) to activate G protein.

Because we had previously seen that BMS-986122 increased the maximal G protein activation by morphine (Burford *et al.*, 2013), we determined the modulation of opioid affinity, potency, and maximal agonist effect of this small molecule MOPr agonist. There was no shift in the affinity of morphine to bind MOPr in the presence of BMS-986122 (Fig 2.3B and Table 2.1). Even at 30 μ M BMS-986122, a concentration approaching the limits of solubility, there was still no enhancement of morphine affinity (Fig 2.4; K_i (veh) = 163 ± 18 nM, K_i (BMS-986122; 30 μ M) = 250 ± 110 nM)). In contrast to this lack of effect on affinity, BMS-986122 did alter the ability of morphine to activate G protein. There was a small 2.9-fold decrease in the potency (EC_{50}), but the most striking effect was a significant increase in the degree of maximal activation. In the presence of BMS-986122, morphine was able to activate G protein to nearly the same extent as the full agonist DAMGO (Fig. 2.3D and Table 2.2). Moreover, the rate at which DAMGO activated G protein was unchanged in the presence of 10 μ M BMS-986122 whereas the rate of morphine-activated G protein was enhanced (Fig. 2.3E).

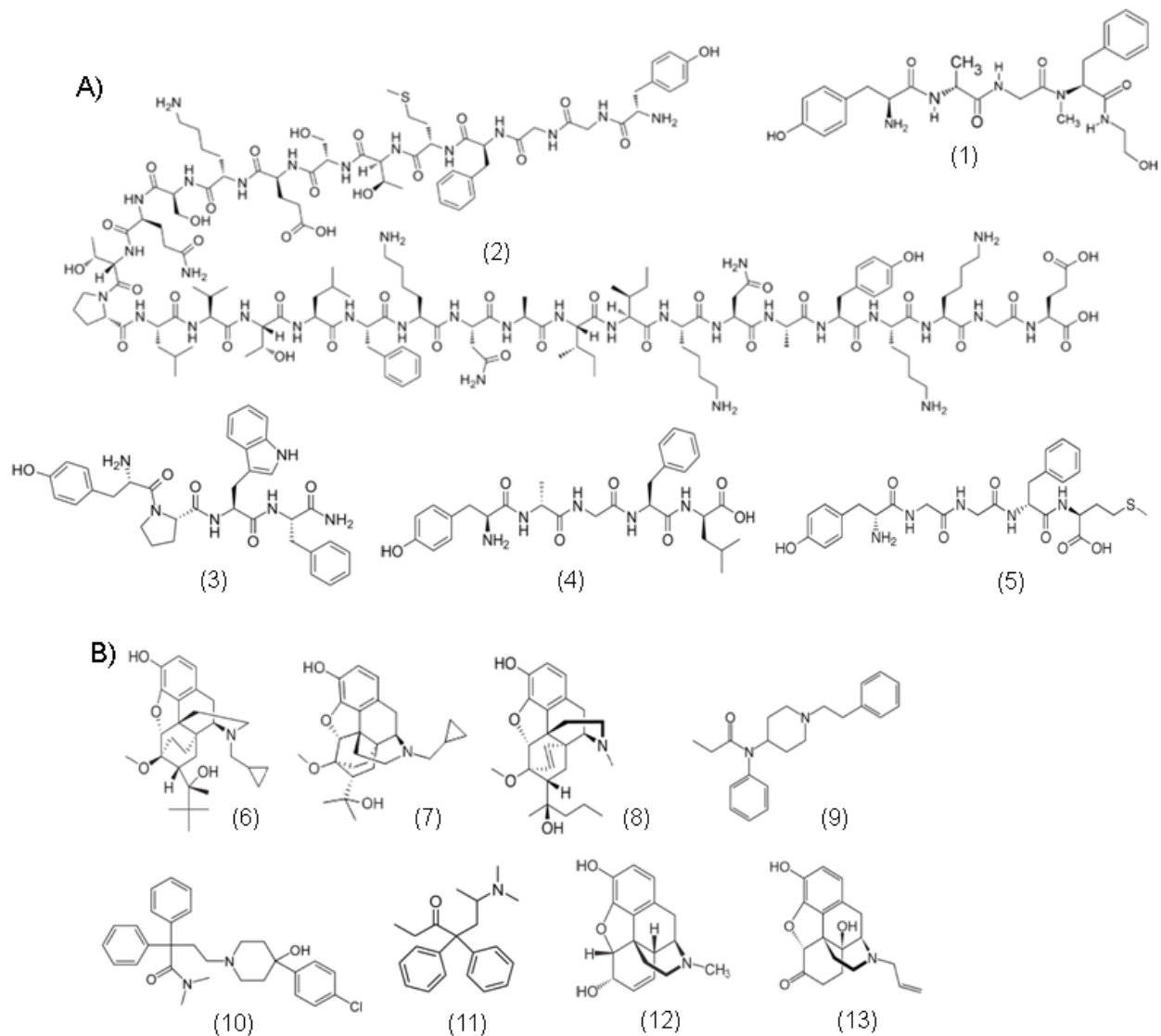


Figure 2.2: Structures of opioid ligands

A) Peptides: (1) DAMGO, (2) β -endorphin, (3) endomorphin-1, (4) leucine-enkephalin, (5) methionine-enkephalin.

B) Small molecules: (6) buprenorphine, (7) diprenorphine, (8) etorphine, (9) fentanyl, (10) loperamide, (11) methadone, (12) morphine, (13) naloxone

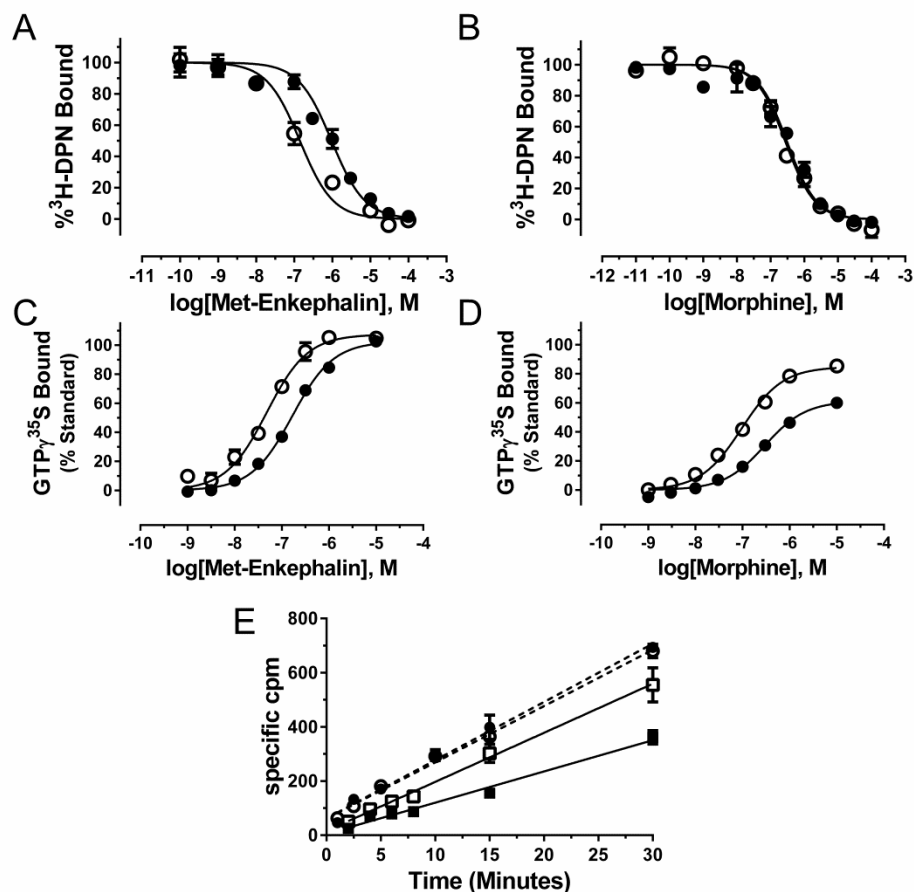


Figure 2.3: Comparison of the effect of BMS-986122 on Met-Enk and morphine. $^3\text{H-DPN}$ binding to MOPr was determined in membranes from C6MOPr cells in the presence of increasing concentrations of Met-Enk (A) or morphine (C) in the presence of vehicle (\bullet) or $10 \mu\text{M}$ BMS-986122 (\circ). The ability of increasing concentrations of Met-Enk (B) or morphine (D) to elicit $\text{GTP}\gamma^{35}\text{S}$ binding in C6MOPr cell membranes was measured in the absence (\bullet) or presence (\circ) of $10 \mu\text{M}$ BMS-986122 as described in the methods. Data are presented as % stimulation of a maximal concentration ($10 \mu\text{M}$) of the full agonist standard DAMGO. E) Rate of G protein activation by DAMGO (dotted line, circles) or morphine (solid line, squares) was measured in the presence of vehicle (closed symbols) or $10 \mu\text{M}$ BMS-986122 (open symbols). The rate of DAMGO-stimulated $\text{GTP}\gamma^{35}\text{S}$ was unchanged (vehicle: 21.5 ± 1.0 cpm/min; BMS-986122: 20.8 ± 0.7 cpm/min), while the rate of morphine-stimulated $\text{GTP}\gamma^{35}\text{S}$ was enhanced from 11.5 ± 0.7 cpm/min (vehicle) to 18.1 ± 0.5 cpm/min in the presence of BMS-986122. All plotted points are means \pm SEM of 3-5 independent experiments, each in duplicate.

Table 2.1: Binding affinity of MOPr ligands in the presence or absence of BMS-86122

Ligand	Ki (Vehicle, nM)	Ki (BMS-986122, nM)	Ki (Veh)/Ki (BMS)
Peptides			
β-Endorphin	194 ± 13	47 ± 8 ***	4.1
Endomorphin 1	104 ± 32	17 ± 8 *	6.1
Leu-Enk	664 ± 67	100 ± 15**	6.6
Met-Enk	423 ± 133	63 ± 16 *	6.7
Small molecules			
Buprenorphine	0.5 ± 0.1	0.4 ± 0.2	1.3
Etorphine	2.4 ± 0.3	1.5 ± 0.8	1.6
Fentanyl	222 ± 34	89 ± 25*	2.5
Loperamide	215 ± 54	14 ± 2 *	15.4
(RS)-Methadone	1076 ± 85	100 ± 4 ***	10.7
(R)-Methadone	382 ± 10	36 ± 10 ***	10.6
(S)-Methadone	6358 ± 2065	896 ± 35*	7.1
Morphine	163 ± 18	143 ± 42	1.1
Naloxone	2.5 ± 0.7	3.4 ± 1.0	0.7

Affinity (Ki values) were determined by competitive displacement of ³H-DPN binding from C6MOPr cell membranes in a buffer containing 10 μM GTPγS and 100 mM NaCl as described in the methods, in the absence or presence of 10 μM BMS-986122. * p < 0.05, ** p < 0.01, *** p < 0.001 compared to control (vehicle) data by Student's t test. Data shown are means ± SEM of 3-5 independent experiments each in duplicate.

Table 2.2: Stimulation of GTP γ ³⁵S binding by MOPr ligands in the absence or presence of BMS-986122

Ligand	Vehicle		BMS-986122 (10 μ M)		$\frac{EC_{50}(\text{veh})}{EC_{50}(\text{BMS})}$
	EC50 (nM)	Max (%) ^a	EC50 (nM)	Max (%) ^a	
Peptides					
β -endorphin	167 \pm 21	90 \pm 6	28 \pm 5 **	88 \pm 6	6.0
DAMGO	104 \pm 39	100	19 \pm 7	100	5.5
Leu-Enk	116 \pm 21	106 \pm 4	27 \pm 9 **	98 \pm 6	4.3
Met-Enk	169 \pm 16	103 \pm 2	49 \pm 7 **	107 \pm 1	3.5
Endomorphin 1	70 \pm 4	94 \pm 8	21 \pm 3 *	93 \pm 5	3.3
Small molecules					
Buprenorphine	0.5 \pm 0.2	21 \pm 3	0.5 \pm 0.2	52 \pm 1 ***	1.0
Etorphine	0.28 \pm 0.04	99 \pm 2	0.17 \pm 0.05	102 \pm 5	1.6
Fentanyl	459 \pm 173	61 \pm 3	156 \pm 24	85 \pm 1***	2.9
Loperamide	37 \pm 1	86 \pm 2	3.9 \pm 0.6***	91 \pm 1	9.5
(RS)-Methadone	542 \pm 149	85 \pm 1	47 \pm 6*	85 \pm 3	11.5
(R)-Methadone	273 \pm 12	95 \pm 4	31 \pm 0.6 ***	87 \pm 3	8.8
(S)-Methadone	7737 \pm 854	70 \pm 4	1275 \pm 216**	85 \pm 3*	6.1
Morphine	292 \pm 59	61 \pm 2	100 \pm 11 *	85 \pm 1***	2.9
Naloxone		dns		dns	

The GTP γ ³⁵S assay was performed as described in the methods. ^aMaximal values relative to the stimulation observed with 10 μ M DAMGO. * p < 0.05, ** p < 0.01, *** p < 0.001 compared to control (vehicle) data by Student's t test. Data shown are means \pm SEM of 3-5 independent experiments each in duplicate.

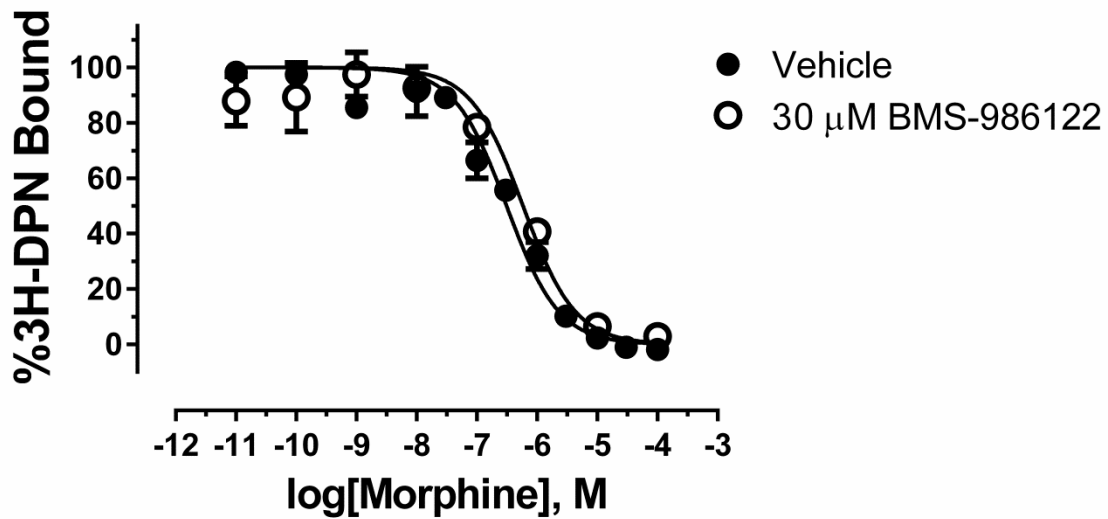


Figure 2.4: Affinity of morphine to bind MOPr is unaltered, even in the presence of 30 μ M BMS-986122. Competition binding was performed in the absence (\bullet), or presence (\circ) of 30 μ M BMS-986122. Data shown are means \pm SEM of 3 independent experiments each in duplicate.

We hypothesized that the disparate effects on orthosteric ligand binding seen with BMS-986122 might be explained by the structure of the ligand: peptides *versus* small molecules. All of the endogenous ligands tested are large, flexible peptides while morphine is a small, rigid molecule. To address this possibility, we measured the effect of BMS-986122 on additional small molecule MOPr agonists that are structurally distinct from morphine, namely buprenorphine, fentanyl, methadone, and loperamide as well as the antagonist naloxone (Tables 2.1 and 2.2, Fig 2.2B). Buprenorphine behaved like morphine, showing no increase in binding affinity for MOPr or potency in the GTP γ ³⁵S assay, but a marked concentration-dependent enhancement in maximal effect (Fig 2.5). With fentanyl, there was a small (2.5-fold) increase in its affinity for MOPr, together with a 2.9-fold shift in potency and an increase in the maximal level of ligand-stimulated GTP γ ³⁵S binding. Conversely, for the small molecule (RS)-methadone, there was a 10.9-fold shift in the MOPr binding affinity (Fig. 2.6A; Table 2.1) and a large (11.5) fold shift in the potency of (RS)-methadone to activate G protein, with no increase in the maximal effect (Fig. 2.6B; Table 2.2). Hill slopes of binding and GTP γ ³⁵S assays for all compounds were not significantly different from 1.0. We further characterized the effect of BMS-986122 on (RS)-methadone-mediated G protein activation by performing a series of concentration-response curves in the presence of increasing levels of BMS-986122 (Fig. 2.6C). Analyses of these curves using the allosteric ternary complex model afforded an alpha (α) value for functional cooperativity between (RS)-methadone and BMS-986122 of 18.4 and an affinity (K_B) of 1.7 μ M. This contrasts with our previously published cooperativity value of 8 for the interaction between endomorphin-1 and BMS-986122 recruitment of β -arrestin (Burford *et al.*, 2013). For loperamide, there was a similar 15-fold shift in affinity and a 9.5-fold shift in the potency (Tables 2.1 and 2.2).

The above experiments used racemic methadone. The (R)-isomer has a higher affinity for MOPr and a higher analgesic potency than the (S)-isomer (Scott *et al.*, 1948; Kristensen *et al.*, 1995). We therefore examined if the differential binding of the isomers to the MOPr affected the response to BMS-986122. The affinities of the individual isomers for MOPr as well as the racemate were all enhanced in the presence of BMS-986122 (Table 2.1). In the GTP γ ³⁵S assay for (R)-methadone, there was an 8.8-fold shift in potency in the presence of BMS-986122, with no change in maximal G protein stimulation. In contrast (S)-methadone, which is a partial agonist, responded to the presence of BMS-986122 with a 6-fold shift in potency as well as an

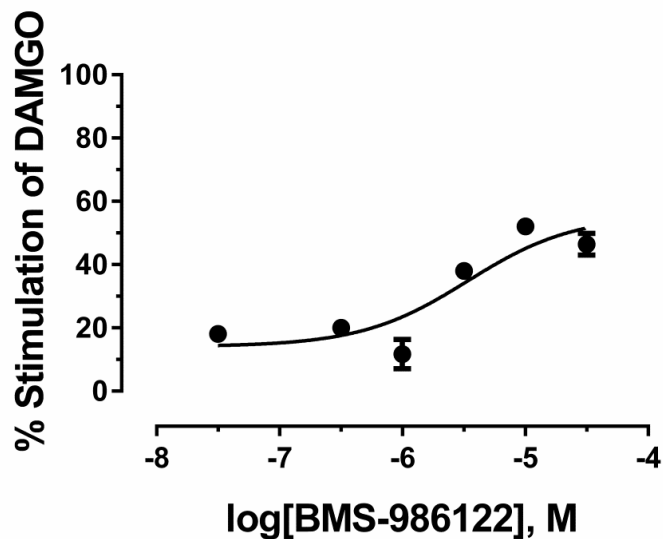


Figure 2.5: Buprenorphine stimulation of G protein is concentration-dependently increased by BMS-986122. GTP γ ³⁵S binding experiments were performed in C6MOPr cell membranes using 10 μ M buprenorphine in the presence of increasing concentrations of BMS-986122. Data are normalized to stimulation occurring from 10 μ M DAMGO. Data shown are means \pm SEM of 2 independent experiments each in duplicate.

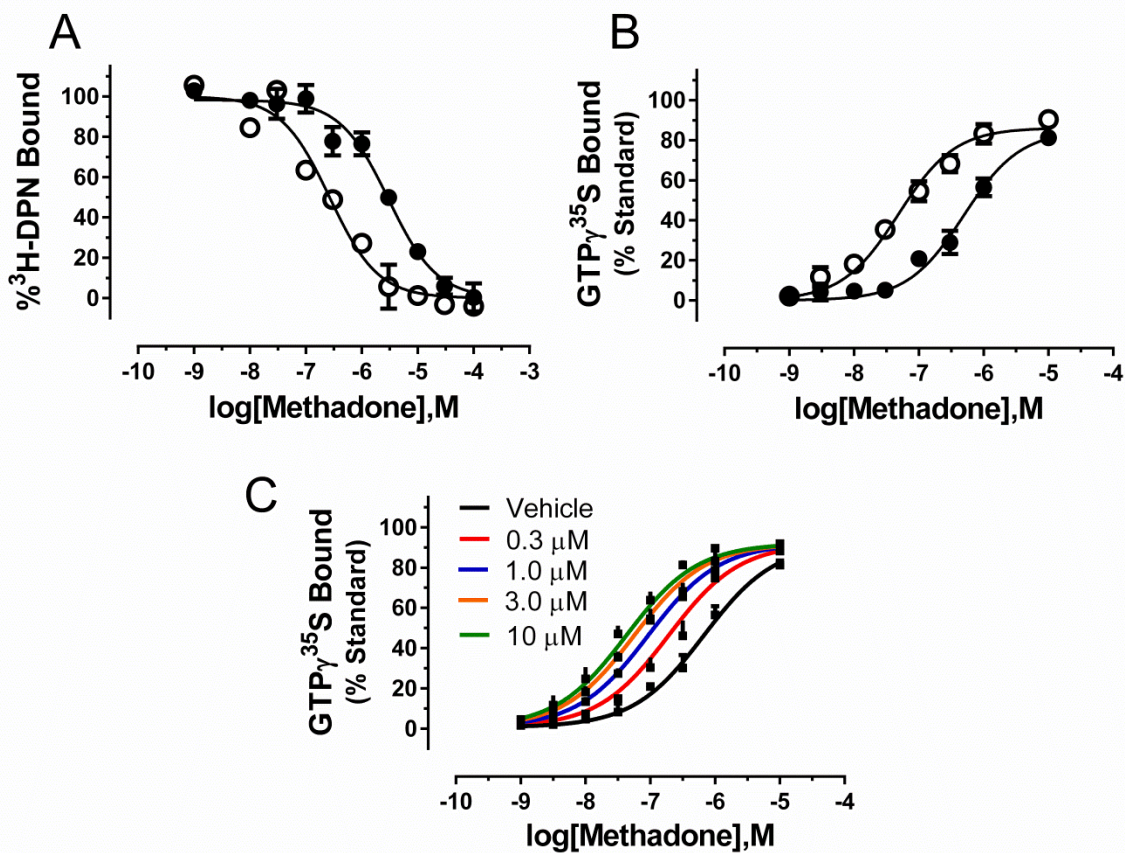


Figure 2.6: BMS-986122 enhances the affinity and potency of (RS)-methadone. A) Displacement of $^3\text{H-DPN}$ in C6MOPr membranes was measured in the presence of increasing concentrations of (RS)-methadone in the presence of vehicle (●) or 10 μM BMS-986122 (○). B) The ability of increasing concentrations of (RS)-methadone to elicit $\text{GTP}\gamma^{35}\text{S}$ binding in C6MOPr cell membranes was measured in the absence (●) or presence (○) of 10 μM BMS-986122. Experiments were performed as described in Fig 1. C) Stimulation of $\text{GTP}\gamma^{35}\text{S}$ binding by (RS)-methadone was performed in the presence of increasing concentrations (0.3-10 μM) of BMS-986122. Data were analyzed using the allosteric ternary complex model as described in the methods. Data shown are means \pm SEM of 3 independent experiments each in duplicate.

enhancement of the maximal stimulation. There was no effect of BMS-986122 on the affinity of the antagonist naloxone for MOPr (Table 2.1), nor did BMS-986122 impart any agonist activity to naloxone (Table 2.2).

The above findings suggest that it is the degree of agonist efficacy of the orthosteric ligands rather than their chemical structure that governs the response to BMS-986122 and so the observed probe dependence. Sodium ions are known to reduce the affinity of agonists to bind to GPCRs, including the MOPr (Pert *et al.*, 1973; Simon and Groth, 1975; Selley *et al.*, 2000), by stabilizing an inactive state of the receptor (Gutiérrez-de-Terán *et al.*, 2013; Fenalti *et al.*, 2014; Katritch *et al.*, 2014). Agonists vary in their response to Na⁺ ions such that sensitivity to Na⁺ ions generally correlates with the degree of intrinsic activity, with a continuum from antagonists that are insensitive to Na⁺ ions to full agonists that are the most sensitive. Since this matches the responsiveness to BMS-986122, we hypothesized that there would be a correlation between the sensitivity of a ligand to the mu-PAM and the sensitivity of a ligand to the presence of Na⁺ ions. Competition binding curves for orthosteric ligands were performed in Tris buffer in the absence or presence of NaCl/GTP γ S to calculate the ratio of binding affinity (as pKi values) to active and inactive states of MOPr. Under both conditions competition binding curves with Hill slopes not significantly different from one were obtained for all compounds (Fig 2.7). pKi values under the two conditions were then compared to the shift in affinity (Fig 2.8A) or potency (Fig 2.8B) of the orthosteric ligand caused by 10 μ M of BMS-986122. We observed a strong correlation between an orthosteric ligand's loss of binding affinity in the presence of Na⁺/GTP γ S and its increased affinity or potency in the presence of BMS-986122. As expected, there was a relationship between the shift in potency and affinity of orthosteric ligands caused by BMS-986122 (Fig 2.9).

To analyze whether Na⁺ ions and BMS-986122 were antagonistic, we investigated the ability of BMS-986122 to inhibit the effect of Na⁺ ions on agonist binding. As expected NaCl showed a concentration-dependent inhibition of DAMGO binding, determined as the inhibition of an EC₆₀ concentration of DAMGO (10 nM) to displace ³H-DPN (0.2 nM) (Fig. 2.8C). This gave an inhibitory concentration 50 (IC₅₀) value for NaCl of 6 \pm 1 mM. Addition of BMS-986122 resulted in a concentration-dependent rightward shift of the IC₅₀ of NaCl to 16 \pm 2 mM in the presence of 3 μ M BMS-986122 and 36 \pm 8 mM in the presence of 10 μ M BMS-986122.

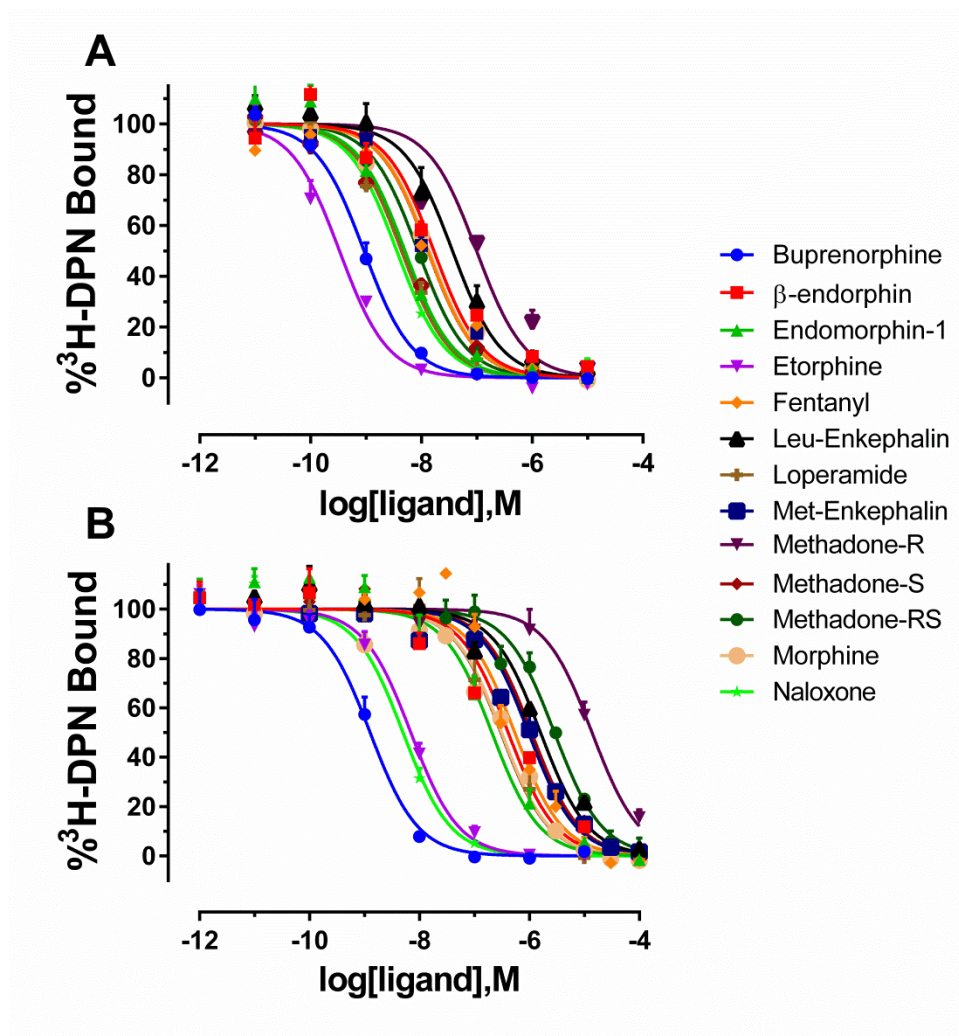


Figure 2.7: Competition binding of orthosteric ligands in the absence (A) or presence (B) of 100 mM NaCl and 10 μ M GTP γ S. Competition binding was performed using a variety of orthosteric ligands in C6MOPr cell membrane preparations. Nonlinear regression analysis fit all curves to one-site. Data shown are means \pm SEM of 3 independent experiments each in duplicate.

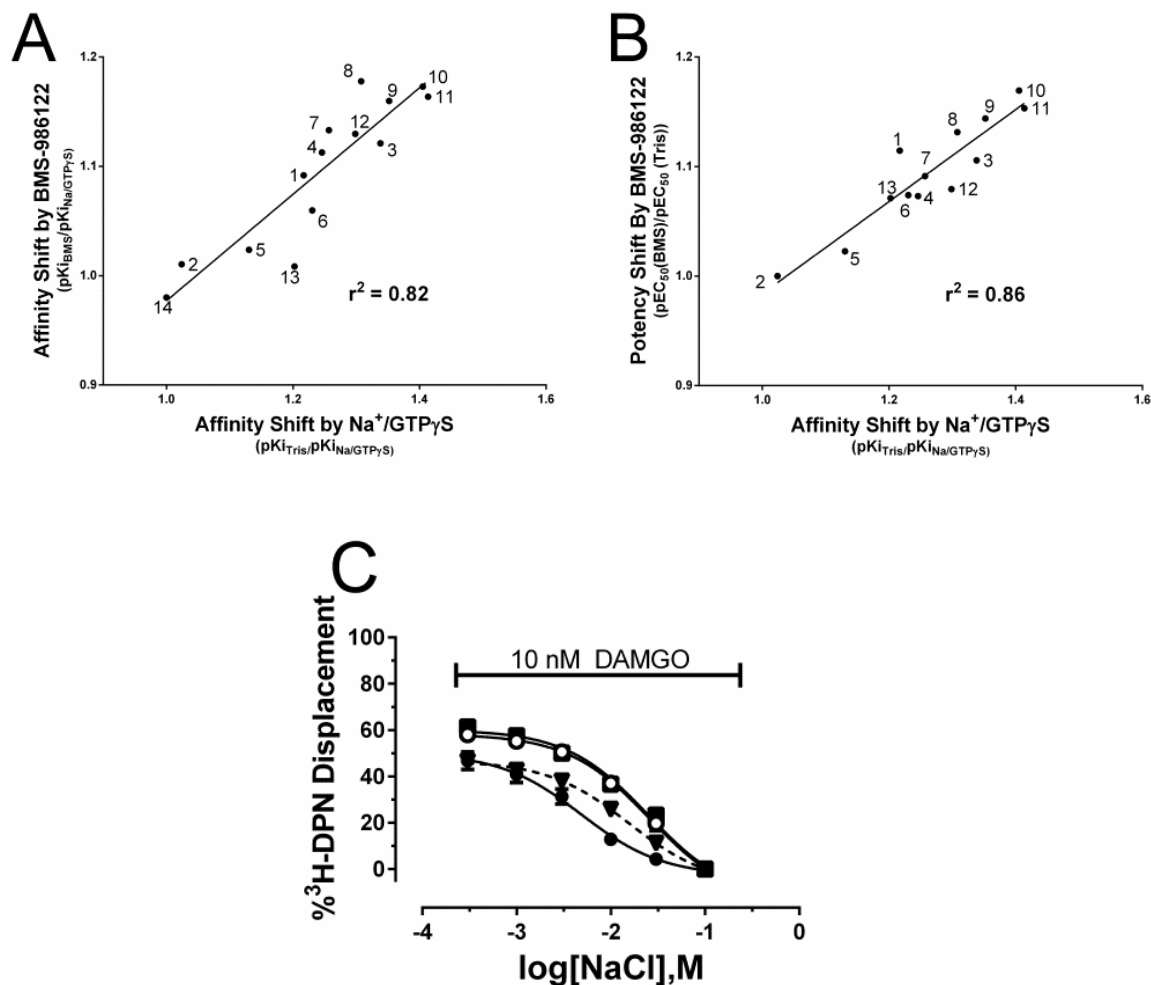


Figure 2.8: Relationship between BMS-986122 and Na⁺ ions. A) pKi values were obtained for each ligand in the presence and absence of 100 mM NaCl and 10 μM GTPγS with or without 10 μM BMS-986122. The ratio of the calculated pKi values is plotted. B) pEC₅₀ values were obtained for each ligand in the absence or presence of 10 μM BMS-986122. The ratio of these values is plotted compared to the ratio of pKi values with and without BMS-986122 obtained from A. C) Using C6MOPr membranes, DAMGO (10 nM) was incubated with 0.2 nM ³H-DPN and increasing concentrations of NaCl with 10 μM GTPγS in the presence of vehicle (●), 3 μM BMS-986122 (triangles with dashed line), 10 μM BMS-986122 (○), or 30 μM BMS-986122 (■). Data shown are means ± SEM of 3-10 independent experiments each in duplicate. (Legend for A/B: 1.β-endorphin 2.Buprenorphine 3.DAMGO 4.Endomorphin1 5.Etorphine 6.Fentanyl 7.Leu-enk 8.Loperamide 9.Methadone-R 10.Methadone-RS 11.Methadone-S 12.Met-enk 13.Morphine 14.Naloxone)

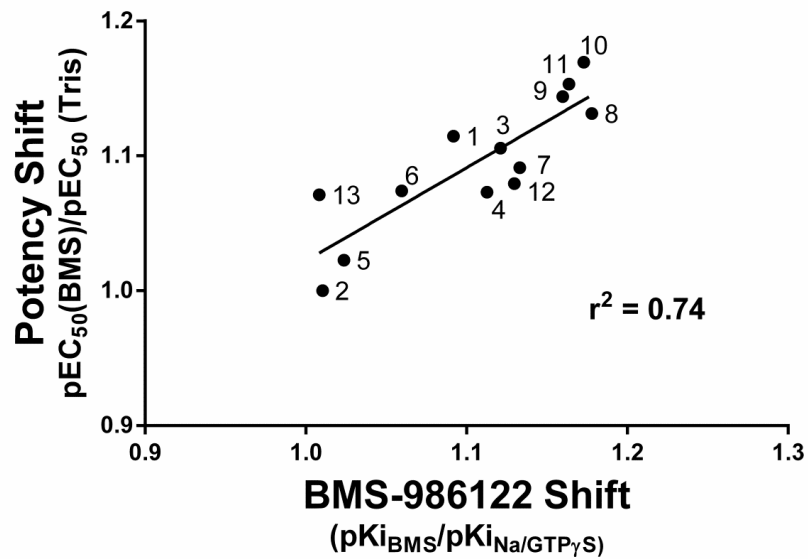


Figure 2.9: Correlation between the degree of shift in affinity caused by the addition of BMS-986122 and the shift in potency at activating G protein. pKi values were obtained for various orthosteric ligand in the absence or presence of 10 μ M BMS-986122. The ratio of these pKi is plotted against the ratio of pEC₅₀ values obtained for the orthosteric ligands in the absence or presence of 10 μ M BMS-986122.

This effect was saturable as the curve failed to shift any further right in the presence of 30 μ M BMS-986122 (Fig 2.8C).

Finally, to confirm a role for Na^+ ions we examined the ability of BMS-986122 to alter etorphine binding and activity. Etorphine (Fig. 2.10) is a potent full agonist at MOPr, but is relatively insensitive to Na^+/GTP ($K_i = 0.18 \pm 0.03$ nM in Tris and $K_i = 2.4 \pm 0.3$ nM with $\text{Na}^+/\text{GTP}\gamma\text{S}$) (see also (Lee *et al.*, 1999)) compared to other full agonists. We therefore hypothesized that etorphine would be less sensitive to BMS-986122. Indeed, BMS-986122 caused no shift in the affinity of etorphine (Table 2.1). In $\text{GTP}\gamma^{35}\text{S}$ binding assays, there was also no significant shift in potency and no alteration in the level of maximal stimulation (Table 2.2).

Discussion

In this study we show that the mu-PAM BMS-986122 exhibits marked probe dependence across a variety of structurally diverse agonists acting at the orthosteric site on MOPr. The sensitivity of orthosteric ligands to BMS-986122 correlated with the ratio of agonist affinities for active and inactive states of the receptor defined by the absence or presence of Na^+ ions and guanine nucleotide and was consistent with the hypothesis that probe dependence of BMS-986122 is defined by the efficacy of the orthosteric agonist. The effects of BMS-986122 are in line with the Monod-Wyman-Changeux two-state model of allosterism (Monod *et al.*, 1965; Canals *et al.*, 2012) involving a single active state, bound to G protein, and single inactive receptor state, uncoupled from G-protein and stabilized by Na^+ ions. BMS-986122 favors the active state, opposes the action of Na^+ ions, and therefore positively modulates the properties of the orthosteric agonist.

Though the degree of effect varied, BMS-986122 enhanced the affinity and potency of all endogenous opioid peptides tested and none showed any enhancement of maximal G protein activation. We initially hypothesized that the 31-amino acid β -endorphin may be a bitopic ligand, capable of binding to both the orthosteric site as well as the allosteric site (for review see (Lane *et al.*, 2013)). Thus, we predicted that β -endorphin would compete with BMS-986122 as well as with ^3H -DPN for binding to MOPr. However, BMS-986122 affected β -endorphin in a manner similar to other endogenous ligands, suggesting that it is not bitopic, at least for the allosteric site occupied by BMS-986122.

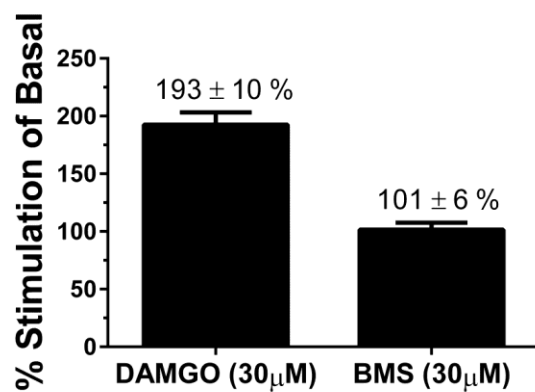


Figure 2.10: BMS-986122 fails to stimulate $\text{GTP}\gamma^{35}\text{S}$ binding over basal levels, even with decreased (10 mM) NaCl. $\text{GTP}\gamma^{35}\text{S}$ binding was performed with 30 μM concentrations of DAMGO or BMS-986122. While DAMGO stimulated $\text{GTP}\gamma^{35}\text{S}$ over basal, BMS-9896122 failed to show any detectable stimulation. Data shown are means \pm SEM of 3 independent experiments each in quadruplicate.

In contrast to the peptides, there were differences seen with small molecule MOPr agonists, indicating orthosteric probe dependence. Morphine, buprenorphine, and fentanyl showed an increase in maximal ability to stimulate $\text{GTP}\gamma^{35}\text{S}$ binding with little or no change in potency or affinity in the presence of BMS-986122. Opioid peptides have a message and address sequence (Chavkin and Goldstein, 1981; Schwyzer *et al.*, 1981) and occupy more of the MOPr binding pocket than smaller organic molecules (Manglik *et al.*, 2012) which could explain their different sensitivities to BMS-986122. However, our findings are not simply a matter of chemical structural differences in terms of peptide *versus* small molecules since (R)-methadone and loperamide were sensitive to BMS-986122 in the same ways as the endogenous peptides. Indeed, the allosteric action of BMS-986122 on these compounds was much greater than for the peptides.

Morphine, as well as fentanyl, buprenorphine, and (S)-methadone have reduced efficacy as compared to the endogenous peptides and (R)-methadone or loperamide. We have previously reported that binding of the opioid antagonist DPN was unaffected by BMS-986122 (Burford *et al.*, 2013) and have now demonstrated a lack of modulation of the opioid antagonist naloxone. Thus, a rational explanation for our findings is that the observed probe selectivity is dependent on agonist efficacy. Table 2.3 lists the intrinsic efficacy of the opioid compounds examined, determined by the method of Ehlert (Ehlert, 1985) using values for agonist affinity determined in the presence or absence of NaCl/ $\text{GTP}\gamma\text{S}$ and agonist potency in the $\text{GTP}\gamma^{35}\text{S}$ assay. The compounds with efficacy greater than or equal to β -endorphin (namely etorphine, Leu-Enk, loperamide, Met-Enk, (RS) - and (R)-methadone, endomorphin 1), all behaved similarly in their response to BMS-986122 with an increase in potency and ligand affinity, but no change in maximal response. In contrast, the lower efficacy agonists showed an increase in maximal effect with minimal alteration in potency or affinity, resulting in an increase in intrinsic efficacy (Table 2.3). With morphine we also demonstrated an increase in the rate of G protein activation, a property associated with ligand efficacy (Alt *et al.*, 2001). Finally (S)-methadone, that has an efficacy value between that of morphine and DAMGO, showed a shift in potency and an increase in maximal effect.

In a simple two-state model of GPCR activation, receptors are hypothesized to exist in conformational states that differ dramatically in their affinity for orthosteric agonists. Agonists

Table 2.3: Efficacy of MOPr agonists^a

<u>Ligand</u>	Efficacy^a	
	<u>Vehicle</u>	<u>BMS-986122</u>
Etorphine	4.7	5.0
Leu-Enk	3.6	2.3
Loperamide	2.9	2.1
DAMGO	2.1	2.0
Met-Enk	1.8	1.2
(RS)-Methadone	1.3	1.3
Endomorphin 1	1.2	0.8
(R)-Methadone	1.1	0.9
β-endorphin	1.0	1.2
(S)-Methadone	0.6	0.7
Fentanyl	0.5	0.7
Morphine	0.5	1.0
Buprenorphine	0.2	0.5
Naloxone	0	0

Ligands are listed in order of decreasing efficacy (vehicle). ^aEfficacy values were calculated from the ligand affinity and GTPγ³⁵S data in Tables 2.1 and 2.2 according to the method of Ehlert (Ehlert, 1985) as described in the methods.

have higher affinity for the active, G-protein bound state and preferentially stabilize this conformation, thus propelling agonist-induced activation of G protein and downstream cellular responses (Chung *et al.*, 2011; Kenakin, 2013). The inactive receptor state has lower affinity for orthosteric agonists and is stabilized in the presence of Na⁺ ions as well as guanine nucleotides that drive uncoupling of receptor and G-protein. The differential affinity of orthosteric agonists employed in this study for inactive and active MOPr states varied, but showed a strong correlation with their relative sensitivity to BMS-986122 and with their potency to stimulate GTP γ ³⁵S binding. Thus, BMS-986122 appears to shift the equilibrium towards the active receptor state thereby modulating the activity of the orthosteric agonists differentially, depending on their efficacy, an action that is opposite to the effects of Na⁺ ions (Selley *et al.*, 2000). The action of BMS-986122 on maximal response of the lower efficacy agonists is also in line with a two-state model of GPCR function. Utilizing the idea that efficacy is based upon an agonist's ability to shift the equilibrium of receptors towards an active state we would expect BMS-986122, by stabilizing an active receptor state, to enhance the efficacy of partial agonists. The appropriateness of the two-state model of allosterism to explain the probe dependence of BMS-986122 at MOPr mirrors the action of the M₁ muscarinic acetylcholine receptor modulator BQCA (benzylquinone carboxylic acid), which enhances the potency of orthosteric ligands or their maximal response depending on the efficacy requirements of the signaling assay (Canals *et al.*, 2012).

If a two-state model does explain the action of BMS-986122 then we should expect to see agonist activity of the modulator even in the absence of orthosteric agonist (Canals *et al.*, 2012). BMS-986122 alone fails to activate G protein to a detectable level as measured by the GTP γ ³⁵S assay, even with a lowered Na⁺ concentration to increase apparent efficacy (Fig 2.10;(Szekeres and Traynor, 1997)). Downstream of G proteins, MOPr orthosteric agonists inhibit adenylate cyclase (AC), a response that is more sensitive to lower efficacy compounds, due to increased amplification (Clark *et al.*, 2008). At high concentrations, BMS-986122 does inhibit AC (Burford *et al.*, 2013), thus confirming the appropriateness of the two-state model. In addition, we would predict BMS-986122 to have activity at even more amplified downstream signaling pathways (Canals *et al.*, 2012; Chapter 5).

An apparent anomaly to the hypothesis that probe dependence is based on orthosteric ligand efficacy and can be explained by a two-state model is that etorphine shows no cooperativity with BMS-986122, and is relatively insensitive to Na⁺ ions, yet this compound is a highly efficacious MOPr agonist (Table 2.3). Biophysical studies with the β 2-adrenergic receptor have shown that agonists destabilize the receptor, but the receptor exists in a variety of conformationally heterogeneous states that are not fully stabilized unless G protein is bound (Nygaard *et al.*, 2013). Thus, it is feasible that etorphine promotes a state that has very high affinity for G protein, but enriches this population to a lesser extent than other agonists.

Further support for the two-state model comes from the relationship between BMS-986122 and Na⁺ ions. High resolution X-ray structures of several class A GPCRs (Gutiérrez-de-Terán *et al.*, 2013), including the DOPr (Fenalti *et al.*, 2014), have identified the Na⁺ site as a Na⁺-H₂O cluster in a cavity in the middle of the 7-transmembrane (TM) helices. This cavity in the DOPr is formed by side chains of 16 residues distributed across TM domains 2, 3, 6 and 7 and is fully conserved in the MOPr (Fenalti *et al.*, 2014). Comparison of inactive and active GPCR structures and molecular dynamics simulations performed with the adenosine A2A receptor show that agonist binding causes molecular rearrangements that are not compatible with concurrent Na⁺ binding (Gutiérrez-de-Terán *et al.*, 2013). In particular, the addition of agonist dramatically reduces the size of the binding pocket for the Na⁺-H₂O cluster. BMS-986122 decreased the potency of Na⁺ ions to inhibit binding of the agonist DAMGO and there was a strong correlation between the opposite effects of the BMS-986122 and Na⁺/GTP on opioid ligands. Thus, the binding of both BMS-986122 and Na⁺ to MOPr is incompatible. We conclude that BMS-986122 favors the active receptor conformation with disruption of the Na⁺-H₂O cluster binding pocket and this explains its PAM activity. The interaction between Na⁺ and BMS-986122 could be through direct competition, for example as with the diuretic amiloride (Gao and Ijzerman, 2000), or indirectly through an allosteric interaction. However, the evidence favors an allosteric mechanism for several reasons. Firstly, BMS-986122 does cause a small increase in agonist affinity in the absence of Na⁺ ions (Burford *et al.*, 2013) suggesting it can stabilize an active receptor conformation. Secondly the same degree of shift in the inhibitory effect of NaCl on DAMGO binding is seen with both 10 μ M and 30 μ M BMS-986122, suggesting saturation is reached as expected for allosterism, rather than the surmountable parallel shifts expected if the antagonism were competitive (Arunlakshana and Schild, 1959). Thirdly, the Na⁺-H₂O cluster

binding pocket is conserved between MOPr and DOPr (Fenalti *et al.*, 2014) and indeed across all Class A GPCRs (Katritch *et al.*, 2014), yet the PAM activity of BMS-986122 is selective for MOPr over DOPr (Burford *et al.*, 2013). Current work is in progress to identify the allosteric site on MOPr.

In conclusion, this study further confirms the use of the Monod-Wyman-Changeux two-state model of allostery as the simplest mechanism to explain PAM activity at GPCRs (Canals *et al.*, 2012). Furthermore, the results directly relate the action of a small molecule PAM to interfere with Na⁺ binding at a GPCR. Disruption of the Na⁺ binding pocket during receptor activation may be a general mechanism for allosteric modulation across many class A GPCRs that have a conserved Na⁺-H₂O cluster binding pocket (Chapter 3). For example, the CB1 receptor PAM ORG27569 and the M₁ receptor PAM BQCA both enhance the high affinity state of their respective receptors (Ahn *et al.*, 2012; Canals *et al.*, 2012). This may, however, not be true for all agonists, in particular, those whose affinity is less sensitive to Na⁺ ions such as etorphine, or receptors such as the β₁ adrenergic receptor where Na⁺ does not appear to be involved in the transition from inactive to active states (Miller-Gallacher *et al.*, 2014). Nonetheless interference with the stability of the Na⁺-H₂O binding pocket of GPCRs may be a generally applicable mechanism that provides a basis for the discovery of novel modulators and the identification of potential endogenous modulators (for review see (Christopoulos, 2014)).

Materials and Methods

Materials: [³H]Diprenorphine and [³⁵S]GTPγS were from PerkinElmer Life Sciences. Cell culture materials were from Invitrogen (Carlsbad, CA). BMS-986122 (2-(3-Bromo-4-methoxyphenyl)-3-[(4-chlorophenyl)sulfonyl]-thiazolidine) was a gift from Bristol-Myers Squibb (Wallingford, CT). Morphine sulfate, leucine-enkephalin, methionine-enkephalin, β-endorphin, DAMGO, nalbuphine, and endomorphin-1 were from Sigma-Aldrich. All other chemicals, unless otherwise specified, were purchased from Sigma. All other opioids were from the Opioid Basic Research Center at the University of Michigan.

Cell lines and membrane preparation: Generation of C6 rat glioma cells heterologously expressing only the mu-opioid receptor (C6MOPr; B_{max} = 2.1 pmol/mg protein) and membrane preparation was as previously described (Emmerson *et al.*, 1996).

³H-DPN assays: Assays were performed using C6MOPr membranes by the method as described (Clark *et al.*, 2003). Competitive displacement of 0.2 nM ³H-DPN was measured using increasing concentrations of orthosteric ligand in the presence of vehicle (1% DMSO) or BMS-986122 at the indicated concentration.

GTP γ ³⁵S assays: Assays were performed using C6MOPr membranes as described (Clark *et al.*, 2003). Orthosteric and allosteric ligands were included where appropriate. For the rate experiments (Fig. 2.3E) maximal (10 μ M) concentrations of DAMGO or morphine were preincubated in the above buffer with C6MOPr membranes and vehicle or 10 μ M BMS-986122. After 1 h, 0.1 nM GTP γ ³⁵S was added and aliquots of the reaction were analyzed at various time points.

Data analysis: Data were analyzed using GraphPad Prism version 6 (GraphPad, San Diego, CA, USA). K_i values and EC₅₀ values were determined using nonlinear regression. The method of Ehlert (Ehlert, 1985) was used to calculate agonist efficacy based in the ability to stimulate GTP γ ³⁵S according to the equation: efficacy = 0.5 x (E_{max,A} / E_{max}) x (1 + K_i/EC₅₀), where E_{max,A} is the maximum stimulation by agonist A, E_{max} is the maximum stimulation by DAMGO, K_i is the affinity of agonist A, and EC₅₀ is the potency of agonist A. Hill slopes for all the binding and functional data were not significantly different from one (Fig 2.7), allowing use of the Ehlert equation. Functional cooperativity (α) between BMS-986122 and methadone, that describes the degree of change in ligand affinity between two separate but linked site both bound with appropriate ligand, and the affinity (K_B) value for BMS-986122 were obtained using an allosteric ternary complex model (Christopoulos and Kenakin, 2002) in GraphPad Prism, Version 6, from non-linear curve fitting of the series of parallel curves in Fig. 2.6C.

CHAPTER 3

Two Chemically Distinct Allosteric Modulators Bind to a Conserved Site on Mu and Delta Opioid Receptors

Summary

The mu and delta opioid receptors (MOPr and DOPr, respectively) are G protein-coupled receptors (GPCRs) that display a high degree of homology and share many endogenous peptide ligands. Even so, the recently described positive allosteric modulator (PAM) of MOPr (BMS-986122) is inactive at DOPr while the structurally unrelated delta-PAM, BMS-986187, exhibits PAM activity at both receptors, though shows a 100-fold higher potency at DOPr. Allosteric binding sites are generally not conserved due to a lack of evolutionary pressure and consequently, there may be more than one allosteric binding site on any given GPCR. Here we test the hypothesis that chemically distinct allosteric ligands, BMS-986122 and BMS-986187, bind to different allosteric sites on MOPr and may therefore possess different mechanisms of action. We compared the activity of BMS-986122 and BMS-986187 as PAMs at MOPr and DOPr expressed in C6 glioma and CHO cells. The results confirm the BMS-986187 is a highly efficacious, but low affinity, mu-PAM. Moreover, we demonstrate that the PAM activity of BMS-986187 at both MOPr and DOPr is due to disruption of the Na⁺ binding site, thus driving an active receptor state, in the same way as BMS-986122. Finally, a silent allosteric modulator (SAM) of MOPr blocks the action of BMS-986187 at both MOPr and DOPr and BMS-986122 acts as a SAM at DOPr, indicating that they may actually bind at the same site. Overall, the results are consistent with a hypothesis that there is a single allosteric binding site on MOPr that is able to accommodate a number of chemotypes and shows some degree of conservation with an allosteric site on DOPr.

Introduction

The mu opioid receptor (MOPr) represents the main pharmacological target of current pain-relieving agents including morphine and oxycodone. Such opioid drugs compete with the endogenous opioid peptides for binding and activation of MOPr and are therefore termed ‘orthosteric’ ligands. However, in addition to pain relief, orthosteric agonist activation of MOPr has unwanted effects including nausea, constipation, tolerance, and addiction, thus making separation of beneficial and unwanted effects very difficult. One approach that could result in analgesics with better therapeutic profiles is to target allosteric sites on MOPr with positive allosteric modulators (PAMs) (Burford *et al.*, 2015). Ideally, these ligands would have no activity alone and would instead serve to enhance signaling of endogenous opioid peptides, thereby preserving the spatial and temporal aspects of endogenous signaling. To help test this hypothesis, allosteric modulators of MOPr have been discovered and characterized (Burford *et al.*, 2013; Livingston and Traynor, 2014; Chapter 2). These ligands, as exemplified by BMS-986122, bind allosterically to MOPr and enhance the affinity, potency, and/or efficacy of various orthosteric ligands in an agonist-dependent manner, described as probe dependence.

Allosteric modulation of G protein-coupled receptors (GPCRs) has the potential for additional clinical benefits. The characteristic of probe dependence, which is the phenomenon in which an allosteric ligand will have distinct cooperativity with different orthosteric ligands, or probes, could be very beneficial in the clinical setting. For instance, a PAM displaying selective cooperativity with certain orthosteric ligands (e.g. endogenous peptides) over abused ligands (e.g. heroin) would help avoid overdoses and minimize abuse potential. Furthermore, the allosteric ligand-bound receptor can be thought of as an entirely new receptor with different sensitivities to activation and different patterns of second-messenger engagement. This gives the possibility of inducing biased signaling by initiating pathway-specific signal transduction. For MOPr, the ideal PAM would enhance analgesia without enhancing constipation, respiratory depression, or abuse liability (Raehal *et al.*, 2011). Lastly, there is the possibility of enhanced GPCR selectivity. In theory, allosteric sites on proteins face less evolutionary pressure to be conserved and therefore even closely related receptors can have different allosteric binding pockets (For review see Conn *et al.*, 2009). This has been demonstrated with the development of allosteric modulators selective for different muscarinic receptor subtypes (For review see Lindsley CW *et al.*, 2016).

At the opioid receptors, BMS-986122 is selective for MOPr and has no detectable activity at the closely related delta opioid receptor (DOPr; (Burford *et al.*, 2013)) which shares over 64% identity and also shares endogenous ligands (Chen *et al.*, 1993). But, this notion of allosteric specificity is not absolute. The muscarinic receptor (mAChR) allosteric modulator C₇/3-phth acts at all subtypes of mAChRs, although it has the highest affinity for the M₂ mAChR (Christopoulos *et al.*, 1999). SCH-202676 is a sulfhydryl reactive compound that acts as an ‘allosteric’ modulator of a variety of GPCRs, including MOPr and DOPr (Fawzi *et al.*, 2001; Gao *et al.*, 2004; Lewandowicz *et al.*, 2006). Finally, the recently discovered DOPr PAM, BMS-986187, has 100-fold binding selectivity for DOPr over MOPr, but initial studies suggested it retains efficacious mu-PAM activity (Appendix B; (Burford *et al.*, 2015)). In previous work we have demonstrated the mechanism of BMS-986122 action at MOPr is to allosterically disrupt the binding of Na⁺ ions (Chapter 2). Na⁺ ions modulate the activity of many class A GPCRs, including the opioid receptors (For review see Katritch *et al.*, 2014). The Na⁺ ion binds at a well-described site within the 7-transmembrane bundle and helps to stabilize the receptor in an inactive state with reduced affinity for agonists (Pert *et al.*, 1973; Pert and Snyder, 1974; Liu *et al.*, 2012). We hypothesized in Chapter 2 that allosteric disruption of Na⁺ binding may be a common mechanism for PAMs of class A GPCRs.

BMS-986187 is structurally different from the mu-PAM BMS-986122 (Fig 3.1). Here we confirm that BMS-986187 has PAM activity at MOPr and test our hypothesis of a general mechanism of action of allosteric modulation of GPCRs by studying whether the binding of BMS-986187 and Na⁺ ions are mutually incompatible at DOPr. Moreover, we assess whether the allosteric action of BMS-986187 at MOPr exhibits the same sodium-ion dependent mechanism. Finally, because BMS-986122 and BMS-986187 are structurally different we assess, if the binding sites for the two drugs at the MOPr and DOPr are conserved.

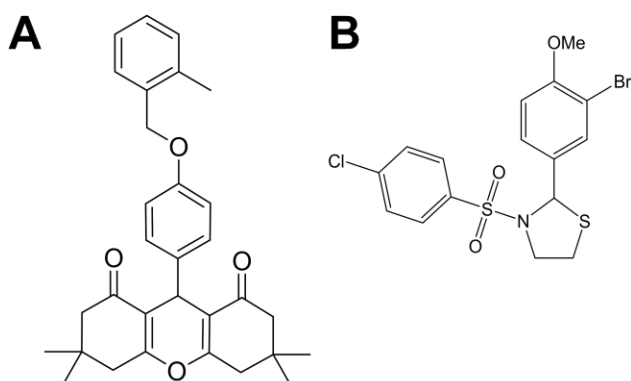


Figure 3.1: Structure of BMS-986187 (A) and BMS-986122 (B)

Results

Mu-PAM activity of the delta-PAM, BMS-986187

BMS-986187 shows 100-fold binding selectivity for DOPr as compared to MOPr, but, initial data suggest that BMS-986187 is an efficacious, but low affinity, PAM at MOPr (Appendix A; (Burford *et al.*, 2015)). To further examine PAM activity of BMS-986187 at MOPr, we studied the allosteric effect of BMS-986187 using cell membrane preparations from C6 rat glioma cells stably expressing rat MOPr (C6MOPr). We verified that BMS-986187 does not compete with the antagonist ³H-diprenorphine (DPN, Fig 3.2A) for the orthosteric site on MOPr. However, BMS-986187 was able to increase the affinity (K_i) of agonists for MOPr as measured by competition binding consistent with a positive allosteric ligand. Thus, in the presence of 10 μM BMS-986187 the affinity of the prototypic MOPr agonist DAMGO was enhanced 10-fold from 730 ± 40 nM to 70 ± 20 nM, while the affinity of methadone was increased 26-fold from 620 ± 100 nM to 25 ± 2 nM. In contrast, the affinity of morphine, a partial agonist, was enhanced to a much lesser extent from 230 ± 14 nM to 72 ± 9 nM (Fig 3.2).

BMS-986187 is an ago-PAM at DOPr, meaning that it can activate certain downstream signaling pathways in the absence of orthosteric agonist (Burford *et al.*, 2015) in addition to allosterically enhancing agonist affinity. In contrast, at MOPr, BMS-986187 alone (up to 30 μM; the solubility limit) was unable to significantly activate G protein as measured by GTPγ³⁵S binding (Fig 3.2B) in C6MOPr membranes. Though not an ago-PAM at MOPr, at a concentration of 1 μM BMS-986187 enhanced the potency of the full agonist DAMGO ([D-Ala², N-MePhe⁴, Gly-ol]-enkephalin) 5-fold (130 ± 23 nM to 20 ± 6 nM), methadone, by 6-fold (200 ± 33 nM to 30 ± 15 nM), and morphine by 3-fold (120 ± 9 nM to 40 ± 12 nM). There was also an increase in the maximal effect of morphine, from 70 ± 1 % to 90 ± 2 % of the DAMGO response (Fig 3.2). Performing GTPγ³⁵S binding of methadone in the presence of increasing concentrations of BMS-986187 allowed for the generation of a series of concentration-response curves that, when analyzed using the allosteric ternary complex model, resulted in an alpha value of cooperativity between methadone and BMS-986187 of 28.8. The K_B, or affinity of BMS-986187 for the unoccupied MOPr, was determined to be 2.2 μM (Fig 3.3). Thus overall, BMS-986187 acts as a PAM at MOPr with probe-dependent effects that are

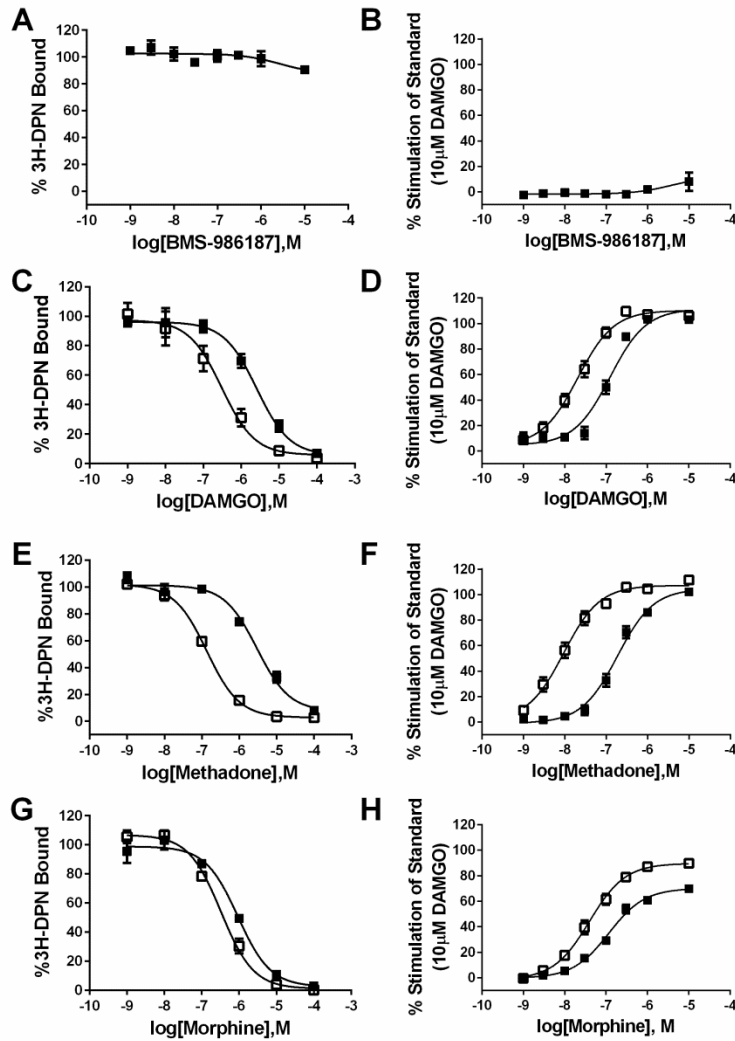


Figure 3.2: BMS-986187 is an allosteric ligand and can enhance the affinity, potency, and maximal stimulation of several opioid ligands at MOPr. A) The ability of BMS-986122 alone (A) or orthosteric ligands (DAMGO (C), methadone (E), and morphine (G)) in the absence (■) or presence (□) or 10 μ M BMS-986122 to displace 3 H-DPN binding in C6MOPr cell membranes was measured. Concentrations response curves of BMS-986122 alone (B) or the orthosteric ligands DAMGO (D), methadone (F), and morphine (H) in the absence (■) or presence (□) or 1 μ M BMS-986122 were performed to measure stimulation of $GTP\gamma^{35}S$ binding. The stimulation at 10 μ M BMS-986187 alone was not significant. Data are presented as % stimulation of a maximal concentration (10 μ M) of the full agonist standard DAMGO. Nonlinear regression analysis fit all curves to one-site. Data shown are means \pm SEM of 3-4 independent experiments each performed in duplicate.

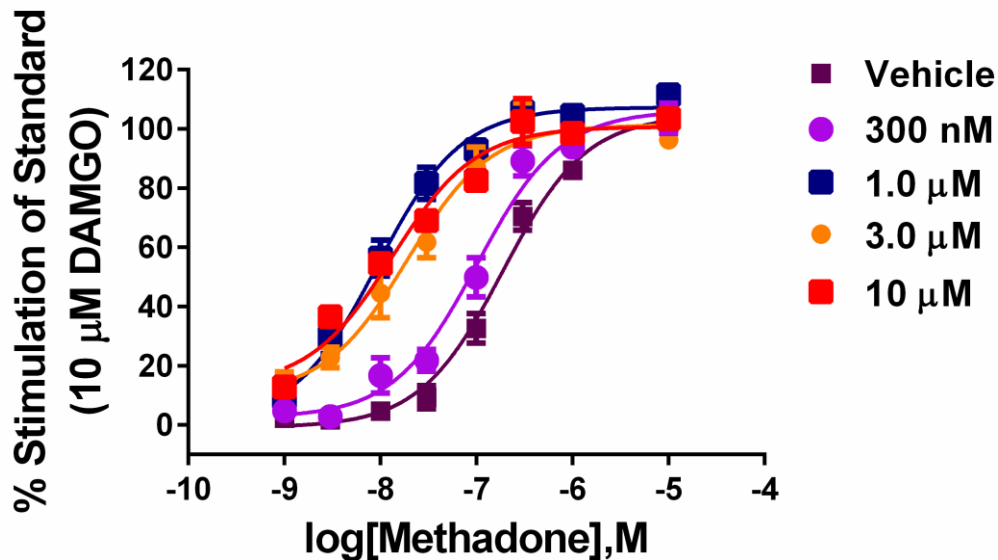


Figure 3.3: BMS-986187 has a concentration-dependent effect on the potency of methadone to activate G protein. Stimulation of $GTP\gamma^{35}S$ binding in C6MOPr cell membranes by methadone was performed in the presence of increasing concentrations (0.3-10 μ M) of BMS-986187. Data were analyzed using the allosteric ternary complex model as described in the methods. Data shown are means \pm SEM of 3 independent experiments each in duplicate.

qualitatively the same as that seen with BMS-986122 at MOPr. The determined affinity of BMS-986187 was similar to that of BMS-986122 ($K_B = 1.7 \mu\text{M}$, Chapter 2) but BMS-986187 showed a higher cooperativity with methadone compared to BMS-986122 which has an alpha value of 18.4 (Chapter 2).

BMS-986187 has agonist effects at MOPr in the absence of orthosteric agonist

Although at MOPr, BMS-986187 was unable to increase $\text{GTP}\gamma^{35}\text{S}$ binding in the absence of orthosteric agonist it is possible that BMS-986187 may display agonist activity at a more amplified downstream pathway. We investigated the ability of BMS-986187 to inhibit adenylate cyclase using CHO cells expressing human MOPr. In these cells, BMS-986187 alone inhibited forskolin-stimulated cAMP accumulation to almost the extent seen with DAMGO giving an EC_{50} value of 380 nM (Fig 3.4A), thus acting as an “ago-PAM” (Schwartz and Holst, 2007). BMS-986187 also enhanced the inhibitory effect of DAMGO in the cAMP accumulation assay by a maximum of 10-fold (from 66 pM with vehicle to 7 pM) (Fig 3.4B). If BMS-986187 shows any signaling bias this would not be evident by measuring G protein signaling so we also determined if BMS-986187 alone could produce arrestin-3 recruitment. For these studies we employed CHO PathHunter cells expressing enzyme-acceptor tagged arrestin-3 and PK-tagged human MOPr from DiscoverX to investigate arrestin-3 recruitment. BMS-986187 alone failed to recruit arrestin-3 up to the highest concentration (30 μM) tested (Fig 3.4C). In contrast, DAMGO was an efficient agonist in this assay with an EC_{50} of 170 nM. BMS-986187 enhanced the potency of DAMGO in a concentration-dependent manner to 3 nM, representing a 58-fold shift (Fig 3.4D).

BMS-986187 acts to disrupt Na^+ binding at both MOPr and DOPr

We have previously proposed that the original MOPr PAM, BMS-986122, acts to allosterically disrupt the Na^+ ion binding site on MOPr. Na^+ ion binding contributes to stabilization of an inactive state of the receptor and disruption of this leads to an increased level of active-state MOPr with cooperativity with agonist binding and activity. We therefore tested if BMS-986187 has the same mechanism of action at DOPr. We performed a Schild analysis of the ability of NaCl to inhibit basal $\text{GTP}\gamma^{35}\text{S}$ binding in membranes prepared from CHO cells expressing human DOPr in the presence of increasing BMS-986187 concentrations. These cells

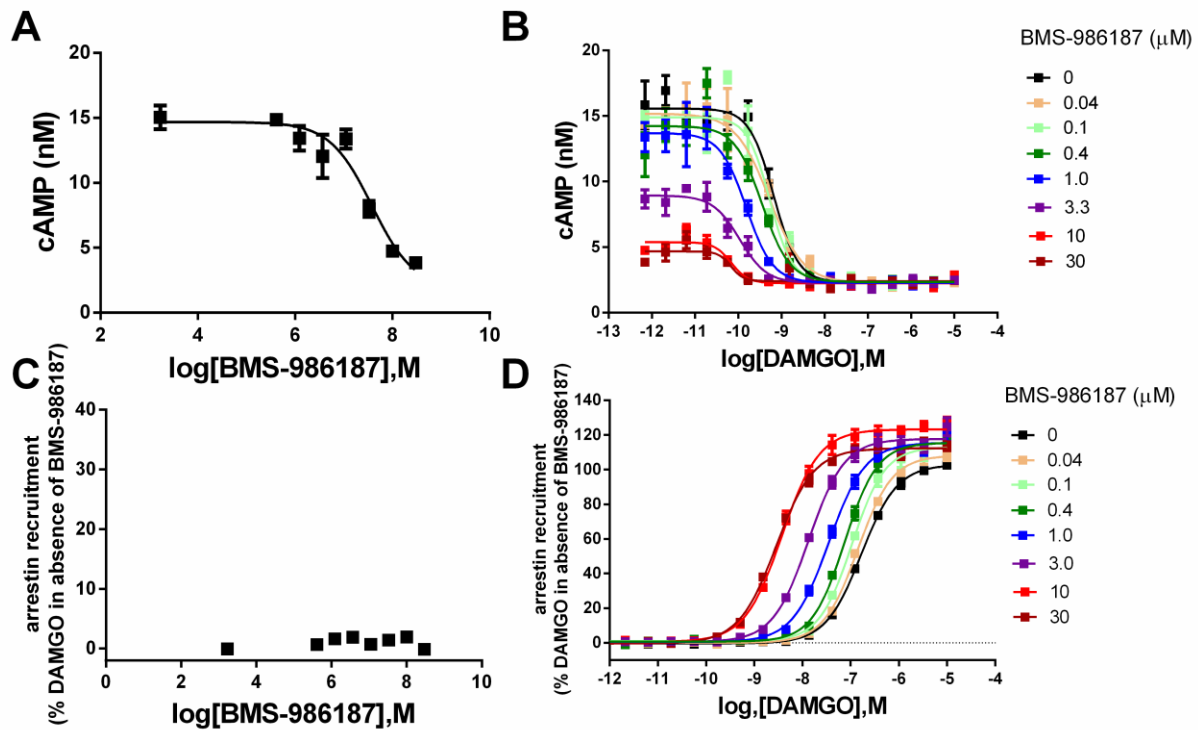


Figure 3.4: Effects of BMS-986187 on adenylate cyclase inhibition (AC) and arrestin recruitment. Using CHO-MOPr cells, the ability of BMS-986187 alone to inhibit AC was measured (A). Concentration-response curves of the full MOPr agonist DAMGO were performed in the presence of vehicle (black) or in the presence of increasing concentrations of BMS-986187 (B). Using CHO cells, the ability of BMS-986187 to cause arrestin recruitment alone was measured (C). In addition, concentration-response curves of DAMGO were performed in the presence of vehicle (black) or of increasing concentrations of BMS-986187. (D) These data were fit using the allosteric ternary complex model as described in the methods. All data were analyzed GraphPad Prism and data shown are means \pm SEM of 3 independent experiments done in quadruplicate.

were used instead of C6DOPr cells because we have previously shown that BMS-986187 has greater agonist activity in the CHO line. In contrast to parallel rightward shifts with the addition of increasing BMS-986187, which is indicative of competitive antagonism, we observed rightward shifts that saturated, revealing a negative allosteric interaction between Na⁺ ions and BMS-986187. Analysis of this set of curves using the allosteric ternary complex model resulted in a K_B of BMS-986122 for the Na⁺ ion-free receptor of 110 nM [95% CI 48 nM to 230 nM] and an alpha value of cooperativity of 0.16, indicative of negative cooperativity (Fig 3.5).

Furthermore, we investigated if BMS-986187 would also inhibit the effects of Na⁺ ions at MOPr. Using C6MOPr membranes, we found that BMS-986187 reduced the potency of NaCl to inhibit the binding of leucine-enkephalin (Leu-Enk) at MOPr. The potency of NaCl was decreased 4-fold in the presence of BMS-986187, suggesting the mechanism of allosteric disruption of Na⁺ binding is not unique to molecules structurally related to BMS-986122 and is also not unique for MOPr.

BMS-986122 and BMS-986187 bind to the same site on MOPr and DOPr

BMS-986122 and BMS-986187 have the same probe dependence and mechanism of action at MOPr. To determine if they bind at the same site on MOPr we used the mu-silent allosteric modulator (mu-SAM) BMS-986123. BMS-986123 has been previously shown to displace BMS-986122 from MOPr while having no effects alone (Burford *et al.*, 2013). We therefore tested if BMS-986123 could also displace BMS-986187 at MOPr. BMS-986187 at 10 μM produced a 5-fold increase in the EC₅₀ of DAMGO to stimulate GTPγ³⁵S binding in C6MOPr cell membranes. The addition of increasing amounts of the mu-SAM concentration-dependently decreased the EC₅₀ of DAMGO such that the positive allosteric effects of BMS-986187 were no longer observed (Fig 3.6). We used DAMGO for this experiment because although previously designated as a mu-SAM BMS-986123 showed a low degree of positive allosteric cooperativity with methadone, increasing methadone's affinity for MOPr by 3-fold (from 620 ± 100 nM with vehicle to 200 ± 20 nM with 10 μM BMS-986123; *data not shown*), indicating that it is not truly silent.

We then sought to determine if BMS-986123 was also a SAM at DOPr. GTPγ³⁵S binding assays were performed using membranes prepared from C6 cells expressing rat DOPr (C6DOPr)

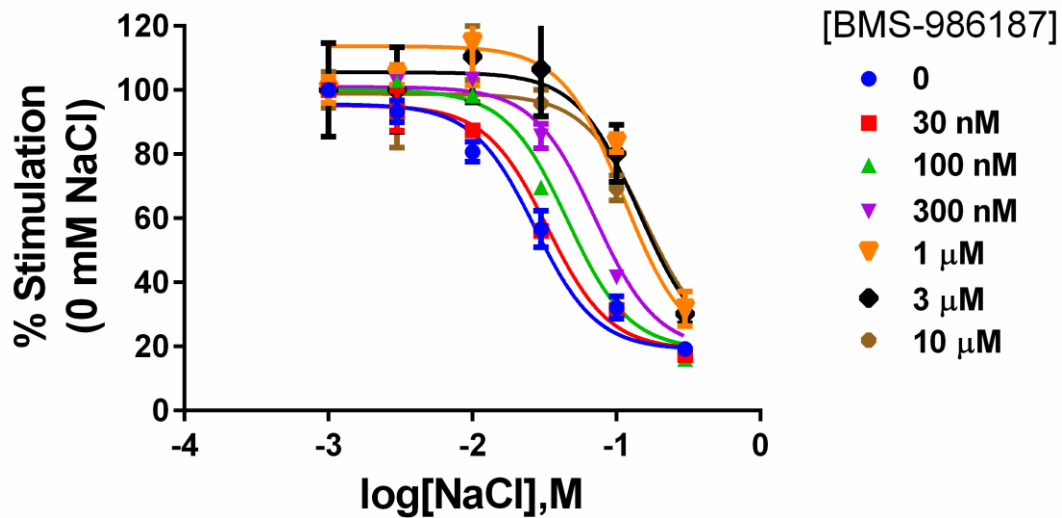


Figure 3.5 Negative cooperativity between NaCl and BMS-986187 at DOPr. The ability of increasing concentrations of NaCl to decrease basal $\text{GTP}\gamma^{35}\text{S}$ binding the presence of increasing concentrations of BMS-986187 was measured using CHO cells expressing human DOPr. Data were fitted using an allosteric ternary complex model and the K_B of BMS-986187 to the sodium-free receptor to be 110 nM [95% CI 48 nM to 130 nM]. The $\log(\alpha)$ value of cooperativity between sodium and BMS-986187 is -0.79 [95% CI -0.93 to -0.64]. Data shown are mean \pm SEM from 2 experiments performed in duplicate.

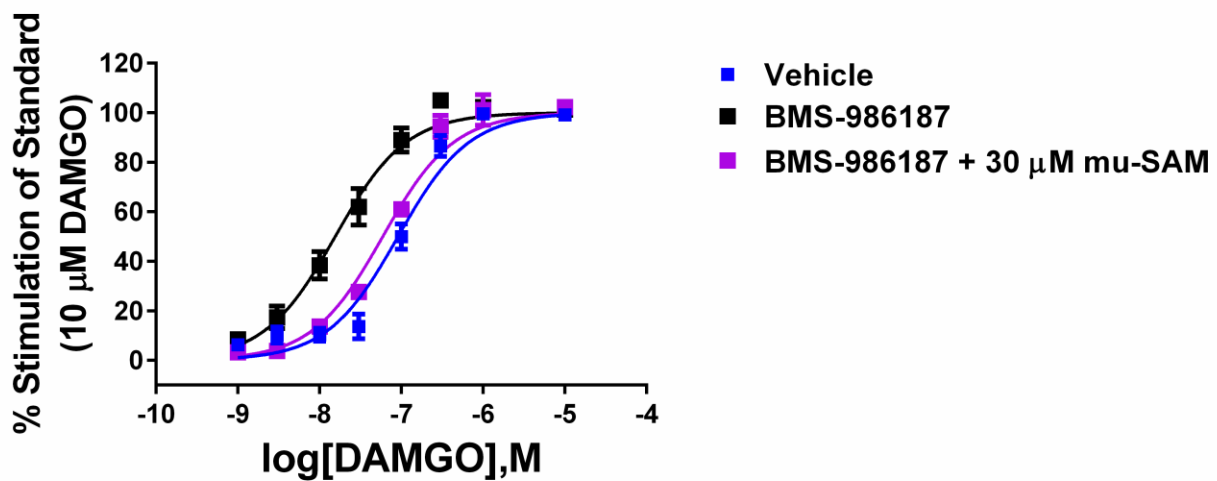


Fig 3.6: The mu-SAM BMS-986123 blocks the action of BMS-986187 at MOPr. Using C6MOPr cell membranes, the ability of 10 μM BMS-986187 to enhance the potency of DAMGO-mediated $GTP\gamma^{35}S$ stimulation was measured in the presence or absence of 30 μM of the mu-SAM BMS-986123. An intermediate concentration of 10 μM mu-SAM was also tested but left out for graph clarity. Data shown are mean \pm SEM from 3 experiments done in duplicate.

with the orthosteric ligand Leu-Enk. BMS-986187 (300 nM) displayed no agonism alone but enhanced the potency of Leu-Enk to stimulate $\text{GTP}\gamma^{35}\text{S}$ by 4-fold. This effect was absent in the presence of BMS-986123 (Fig 3.7).

Finally, since BMS-986123 blocks the action of BMS-986122 at MOPr and BMS-986187 at DOPr, we predicted that BMS-986122 would be a SAM at DOPr. To test this, we measured the ability of Leu-Enk to stimulate $\text{GTP}\gamma^{35}\text{S}$ in C6DOPr cell membranes. This gave an EC_{50} for Leu-Enk of 650 nM. The presence of BMS-986187 (300 nM) shifted the dose response 5-fold leftward to 120 nM and the addition of 30 μM BMS-986122 shifted the EC_{50} back to 250 nM. (Fig 3.8)

Discussion

Here, we confirmed that BMS-986187, initially described as a delta-PAM, is also a highly efficacious PAM for MOPr and likely has the same mechanism of action, allosteric disruption of the Na^+ binding site, at both MOPr and DOPr as the previously described, yet structurally distinct, BMS-986122. Finally, we show that the known mu-SAM (BMS-986123) acts to reverse the activity of BMS-986187 at both MOPr and DOPr. Together, our data are consistent with an allosteric binding site on both MOPr and DOPr that is conserved enough to recognize the same ligands and sufficiently promiscuous to recognize structurally diverse compounds.

At DOPr, BMS-986187 is an ago-PAM ligand capable of both allosteric activity and direct agonist activity as measured by G protein activation, AC inhibition, and ERK activation (Appendix A; (Burford *et al.*, 2015)), even though it does not bind to the orthosteric site. In contrast, the agonist activity of BMS-986187 at MOPr cannot be observed at the G protein level but can be seen as amplified AC inhibition, consistent with a low efficacy (Traynor and Nahorski, 1995). In addition, DOPr is known to have a higher constitutive activity compared to MOPr (Polastron *et al.*, 1992; Neilan *et al.*, 1999) and so is less constrained in the inactive state. It therefore should be easier for a PAM to drive the receptor to an active state.

BMS-986187 has the ability to enhance the affinity of DAMGO to bind MOPr by 10-fold. We also tested if BMS-986187 was cooperative with methadone, which we had previously found to be the most sensitive orthosteric ligand to allosteric modulation by BMS-986122

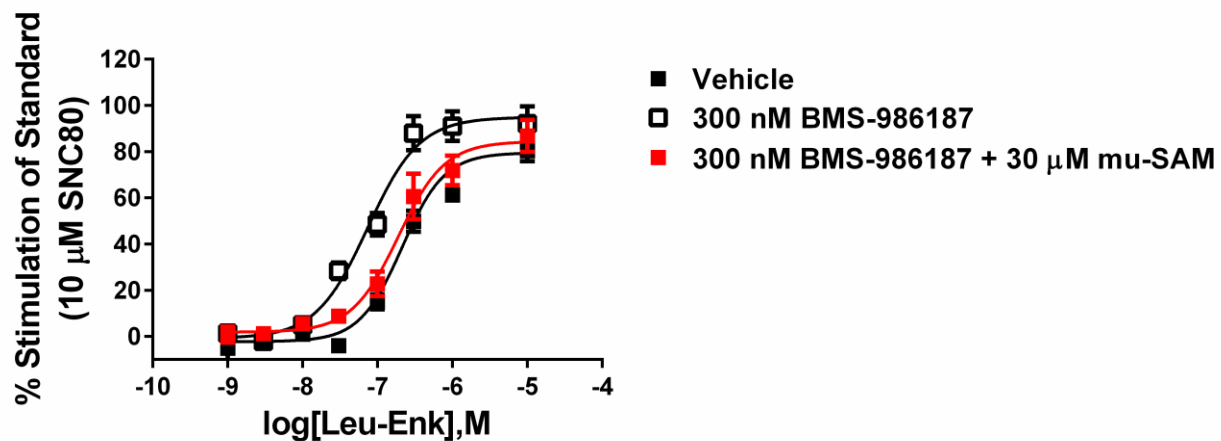


Figure 3.7: mu-SAM reverses activity of BMS-987187 at DOPr, implying a conserved opioid allosteric binding site. Using C6DOPr cell membranes, the ability of 300 nM BMS-986187 to enhance the potency of Leu-Enk-mediated $GTP\gamma^{35}S$ stimulation was measured in the presence or absence of 30 μM of the mu-SAM BMS-986123. Data shown are mean \pm SEM from three experiments in duplicate. Potency values were obtained from fitting the data by linear regression with Hill slopes of unity using GraphPad Prism 6.01.

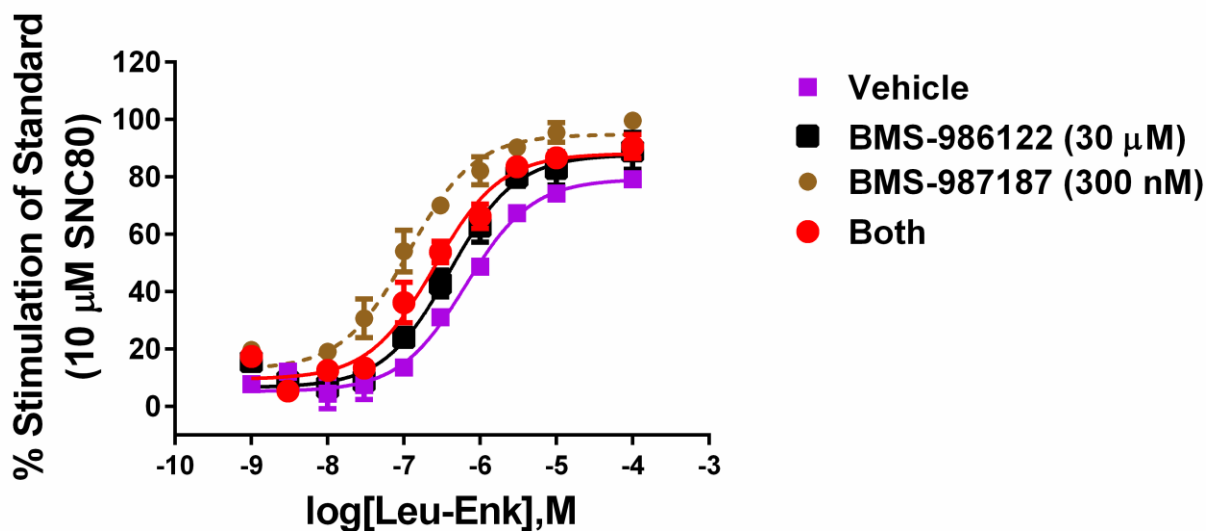


Figure 3.8: mu-PAM BMS-986182 is weak PAM at DOPr capable of reversing BMS-986187 activity. Using C6DOPr cell membranes, the ability of 300 nM BMS-986187 to enhance the potency of Leu-Enk-mediated $GTP\gamma^{35}S$ stimulation was measured in the presence or absence of 30 μM of the mu-PAM BMS-986122. Data shown are mean \pm SEM from three experiments in duplicate. Potency values were obtained from fitting the data by linear regression with Hill slopes of unity using GraphPad Prism 6.01.

Indeed, BMS-986187 caused a 28-fold shift in the affinity of methadone to bind MOPr. This means that for BMS-986187, BMS-986122, and the recently reported mu-PAM MS1 (Appendix B; (Bisignano *et al.*, 2015)), methadone is more sensitive to modulation relative to DAMGO. Methadone is also more sensitive to the inhibitory effects of Na⁺ (Chapter 2), suggesting increased sensitivity to both positive and negative modulators that is presumably driven by the way in which methadone binds to the orthosteric site of MOPr. Molecular dynamics simulations recently performed with methadone, Na⁺, and BMS-986122 at MOPr may also provide insight into this sensitivity (Bartuzi *et al.*, 2016). In this paper, the authors found several poses that methadone could adopt- one more reflective of a full agonist than the other and that the presence of BMS-986122 in the simulations shifted the methadone to preferring the full-agonist specific position.

BMS-986187 appears to display the same efficacy-based probe dependence as we reported with the mu-PAM BMS-986122 (Chapter 2). For full agonists such as DAMGO and methadone, BMS-986187 causes an enhancement in both the affinity to bind MOPr as well as the potency to activate G protein. For the partial agonist morphine, BMS-986187 causes a small shift in affinity but significantly increases the level of maximal activation. This efficacy-based probe dependence falls in line with the Monod-Wyman-Changeux theory of allostery (Monod *et al.*, 1965), and has also been reported with the M2 mAChR PAM benzyl quinolone carboxylic acid (Canals *et al.*, 2012) which demonstrates a probe selectivity reflective of a two-state model of GPCR signaling.

The K_B, or affinity of BMS-986187 for MOPr, was found to be 2.2 μM which is not different than the K_B of BMS-986122 for MOPr (1.7 μM; Chapter 2). The alpha value (α) of cooperativity between BMS-986187 and methadone was found to be 29; this is higher than the alpha value between BMS-986122 and methadone of 18 showing improved allosteric cooperativity of BMS-986187. Similarly, single concentrations of BMS-986187 showed larger shifts in the DAMGO affinity and potency to stimulate GTPγ³⁵S binding than BMS-986122 and whereas both BMS compounds caused an increase in the maximal response to morphine, BMS-986187 also afforded an increase in morphine potency. We are currently testing the hypothesis that these efficacy differences are due to variation in the ability of the two BMS compounds to stabilize active-state MOPr (Chapter 4).

Opioid receptor bias has been implicated in the selection of specific physiological effects resulting from MOPr activation. For instance, β -arrestin signaling is heavily implicated in the development of opioid tolerance (Bohn *et al.*, 2000, 2002; Raehal and Bohn, 2011). Consequently, we analyzed the ability of BMS-986187 to alter both G-protein signaling (through GTP γ ³⁵S binding and AC inhibition assays) as well as arrestin-3 recruitment. Using the prototypic MOPr agonist DAMGO, it was found that BMS-986187 was able to enhance the potency of DAMGO in all pathways tested. There was enhanced cooperativity seen in the arrestin recruitment assay but this difference may be due to differences in the assay kinetics, ceiling, and lack of amplification. There seems to be no obvious bias, though there could well be a probe dependence to any bias. For example endomorphin-2 was shown to be biased (Rivero *et al.*, 2012) and BMS compounds could potentially alter this bias. It was noted that BMS-986187 alone was unable to cause arrestin-3 recruitment. The arrestin assay relies on enzyme complementation with no amplification and is therefore a high efficacy requiring system which could account for the lack of BMS-986187 agonist activity in this assay. A more amplified arrestin-mediated pathway, like ERK, may be more sensitive (Chapter 5).

One of the proposed advantages of allosteric ligands is thought to lie in their selectivity as they target regions of proteins that faced little to no evolutionary pressure to remain conserved. However, both BMS-986187 and BMS-96122 bind to MOPr and both are antagonized by the mu-SAM BMS-986122. Indeed both the mu-SAM and BMS-986122 act as SAMs against the delta-PAM activity of BMS-986187. Although it is feasible that there could be negative allosteric interference between modulators, our data are consistent with a competitive interaction suggesting some form of a common site. Given the diversity in structure between BMS-986187 and BMS-986122 the specific amino-acid contacts are however, likely to be different. Based on two recent molecular dynamics studies, the proposed binding of BMS-986122 at MOPr and BMS-986187 at DOPr rely upon residues that are conserved. In particular both studies emphasize the importance of residues Asn2.63, Tyr2.64, Trp7.35, and His7.36, which are conserved across MOPr and DOPr (Bartuzi *et al.*, 2016; Shang *et al.*, 2016). MOPr and DOPr share a high degree of homology, especially in the transmembrane domains and the orthosteric ligand binding pockets (Fenalti *et al.*, 2014; Huang *et al.*, 2015), which has evolved to bind the same ligands, including β -endorphin and the enkephalins. Because our data suggest a common allosteric site, it is tempting to speculate there may be an endogenous allosteric

modulator that binds to MOPr and DOPr. There are very few examples reported thus far of endogenous allosteric modulators (for review see (van der Westhuizen *et al.*, 2015)) including dynorphin A, a putative allosteric modulator of M2 acetylcholine receptor (Hu and El-Fakahany, 1993), and glutathione, an allosteric ligand at the calcium sensing receptor (CaSR) (Wang *et al.*, 2006; Broadhead *et al.*, 2011).

In conclusion we have provided evidence that a common allosteric binding site exists on MOPr and DOPr, although this does not rule out the presence of other, as yet unidentified, allosteric sites on these receptors. Our support for a common allosteric site is based on several arguments. First, BMS-986187 and BMS-986122 are structurally very different yet both are effective PAMs for MOPr and the previously “selective” mu-PAM BMS-986122 is actually a SAM for DOPr. Secondly, the mechanism of allosterism of both BMS compounds at MOPr and DOPr involves disruption of the Na⁺ binding site thereby driving formation of active receptor conformations. Finally, data from molecular dynamics simulations suggests that involvement of similar residues in MOPr and DOPr. However, the difference in chemical structure between BMS-986122 and BMS-986187 suggests this site is capable of accommodating a wide range of structures.

Materials and Methods

Materials: [³H]Diprenorphine and [³⁵S]GTPγS were from PerkinElmer Life Sciences. All tissue culture medium, penicillin-streptomycin, geneticin (G148), trypsin, and fetal bovine serum were from Invitrogen (Carlsbad, CA). DAMGO, naloxone, and morphine sulfate were from Sigma-Aldrich. PathHunter detection reagents were from DiscoveRx (Freemont, CA). Lance-Ultra cAMP detection reagents were from PerkinElmer Life Sciences (Cambridge, MA). BMS-986122, BMS-986123, and BMS-986187 were gifts from Bristol Myers Squibb. Methadone was from the Opioid Basic Research Center at the University of Michigan. All other chemicals, unless otherwise specified, were purchased from Sigma (St. Louis, MO).

Cell Lines and Membrane Preparation: The generation and maintenance of C6 rat glioma cells stably transfected with rat mu opioid receptor (MOPr) or rat delta opioid receptor (DOPr) were performed as described (Clark *et al.*, 2008). FlpIn Chinese Hamster Ovary (CHO) expressing human DOPr were generated and maintained as described. Cell membranes were prepared for

binding assays as described (Burford *et al.*, 2015). Briefly, cells were grown to confluence and washed twice with 37 °C phosphate-buffered saline (pH 7.4). Cells were detached in harvesting buffer (20 mM HEPES, 150 mM NaCl, 0.68 mM EDTA, pH7.4) and pelleted by centrifugation at 200 x g for 3 min at room temperature. The pellet was resuspended in ice-cold 50mM Tris (pH 7.4) and homogenized using a Tissue Tearor (Dremel). This homogenate was centrifuged at 20000 x g at 4 °C for 20 min. The pellet was then resuspended, homogenized, and centrifuged once more. The final pellet was resuspended in 50 mM Tris (pH 7.4) using a glass dounce homogenizer and aliquots were flash frozen in liquid nitrogen. Aliquots were stored at -80 °C until use. Concentration was determined using BCA quantification method with bovine serum albumin as the standard.

CHO PathHunter cells expressing enzyme acceptor (EA)-tagged β -arrestin 2 and ProLink (PK)-tagged MOPr receptor (CHO-OPRM1) were from DiscoverRx (Freemont, CA). Cells were grown in F-12 media (Invitrogen 11765), containing Hyclone FBS 10%, Hygromycin 300 μ g/mL, Geneticin (G418) 800 μ g/mL and maintained at 37 °C in a humidified incubator containing 5% CO₂. These cells were used for β -arrestin recruitment assays and inhibition of forskolin-stimulated cAMP accumulation assays described below.

Radioligand Binding Assays: Ligand binding assays were performed using the cell membrane homogenates described above. Competition binding assays were performed as previously described (Livingston and Traynor, 2014). Briefly, displacement of ³H-diprenorphine (DPN; 0.2-0.3 nM) was incubated in assay buffer (50 mM Tris pH 7.4, 100 mM NaCl, 5 mM MgCl₂, 1 mM EDTA, 10 μ M GTP γ S) with 10 μ g membrane protein, orthosteric ligand, and allosteric ligand (or vehicle). Nonspecific binding as determined in the presence of 10 μ M naloxone. Assays were incubated for 75 minutes to reach equilibrium and then terminated and counted as described (Lamberts *et al.*, 2011).

GTP γ ³⁵S Assays: GTP γ ³⁵S binding experiments were performed as described (Livingston and Traynor, 2014) using cell membrane homogenates prepared as described above. Briefly, 10 μ g of membrane proteins were incubated for 1 h at 25°C in buffer [50 mM Tris pH 7.4, 100 mM NaCl, 5 mM MgCl₂, 1 mM EDTA] with 0.1 nM GTP γ ³⁵S (guanosine-5'-O(3-thio)triphosphate), 30 μ M GDP (guanosine 5'-diphosphate), orthosteric ligand, and allosteric ligand (or vehicle). An internal standard at 10 μ M (DAMGO [(D-Ala², N-MePhe⁴, Gly-ol]-enkephalin)) for MOPr,

SNC80 [(+)-4-[(αR)- α -((2*S*,5*R*)-4-Allyl-2,5-dimethyl-1-piperazinyl)-3-methoxybenzyl]-*N,N*-diethylbenzamide] for DOPr) was used to define maximal activation and water/vehicle defined basal binding. The assays were terminated and counted as described above.

PathHunter β -Arrestin Assay: Confluent flasks of CHO-OPRM1 cells were harvested with TrypLE Express, and resuspended in F-12 media supplemented with 10 % FBS and 25 mM HEPES, at a density of 6.67×10^5 cells /mL and plated (3 μ L / well) into white solid TC-treated 1536-well plates (Corning, NY). Plates were incubated overnight at 37 °C in a 5% CO₂ humidified incubator. The next day, increasing concentrations of BMS-986187 (40 nL of 100 x final concentration in 100% DMSO) were added to separate rows of the assay plates by acoustic dispense using an Echo-550 (Labcyte, Sunnyvale, CA) from Echo-qualified 1536-well source plates (Labcyte). Next, 1 μ L of increasing concentrations of DAMGO (4 x final concentration in assay buffer) were added to separate columns of the assay plates containing cells. Plates were covered with a lid and incubated at room temperature for 90 min. Incubations were terminated by the addition of 2 μ L PathHunter Reagent (DiscoverX). One hour later luminescence was detected using a Viewlux imaging plate reader (PerkinElmer).

Inhibition of Forskolin-Stimulated cAMP Accumulation Assays: CHO-OPRM1 cells were grown to confluence then harvested and resuspended at 10^6 cells / mL in assay buffer (HBSS + 25 mM HEPES, + 0.05% BSA). Increasing concentrations of BMS-986187 (30 nL of 100 x final concentration in 100% DMSO) were added to separate rows of 1536-well white solid NT plates by acoustic dispense using an Echo-550 (Labcyte, CA). Next, 1 μ L of increasing concentrations of DAMGO (at 3 x final concentration in assay buffer) were added to separate columns of the plates. Next, 1 μ L of cells (1000 cells / well) were added to all wells followed by 1 μ L of forskolin (3 x final concentration in assay buffer). Plates were lidded and incubated for 45 min at RT. Incubations were terminated by the addition of Lance-Ultra cAMP detection reagent (Perkin Elmer) (1.5 μ L of Eu-cryptate-labelled cAMP tracer in lysis buffer, followed by 1.5 μ L of U-light conjugated anti-cAMP antibody in lysis buffer). After a 1 h incubation at room temperature, time-resolved fluorescence (TRF) was detected on a Viewlux or Envision plate reader (PerkinElmer) with excitation at 337 nm and emission reads at 615 nm and 665 nm. The ratiometric data (665 nm read/615 nm read)*10,000 were then converted to cAMP (nM) based

on a standard curve for cAMP (replacing the cell addition step) run at the same time and under identical conditions to the assay.

Data Analysis: Data were analyzed using GraphPad Prism version 6 (GraphPad, San Diego, CA, USA). K_i values and EC_{50} values were determined using nonlinear regression. The method of Ehlert (Ehlert, 1985) was used to calculate agonist efficacy based in the ability to stimulate $GTP\gamma^{35}S$ according to the equation: $efficacy = 0.5 \times (E_{max,A} / E_{max}) \times (1 + K_i / EC_{50})$, where $E_{max,A}$ is the maximum stimulation by agonist A, E_{max} is the maximum stimulation by DAMGO, K_i is the affinity of agonist A, and EC_{50} is the potency of agonist A. Hill slopes for all the binding and functional data were not significantly different from one, allowing use of the Ehlert equation. Functional cooperativity (α) and the affinity (K_B) value for allosteric modulators were obtained using an allosteric ternary complex model (Christopoulos and Kenakin, 2002) in GraphPad Prism, Version 6, from non-linear curve fitting of the series of parallel curves.

CHAPTER 4

Stabilization of Active-State Mu Opioid Receptor by Orthosteric and Allosteric Ligands: Implications for Agonist Efficacy

Summary

The mu opioid receptor (MOPr) represents one of the most pharmacologically targeted G protein-coupled receptors (GPCRs). Activation by an orthosteric agonist such as morphine causes robust pain relief, but also results in unwanted effects including respiratory depression, constipation, and addiction. However, these actions have different agonist efficacy requirements. Consequently, an understanding of the factors governing efficacy and a quantitative way to measure efficacy is needed. Utilizing purified MOPr reconstituted into high density lipoprotein (rHDL) particles we studied binding of the MOPr state-sensitive sensor nanobody39 (Nb39) by interferometry to monitor abundance of the MOPr active state following agonist binding. Differences in orthosteric ligand efficacy were shown to correlate with different kinetics of Nb39 association and dissociation. In addition, we have recently described a series of positive allosteric modulators (PAMs), exemplified by BMS-986122 and BMS-986187, that enhance the affinity and/or efficacy of orthosteric MOPr ligands. BMS-986122 and BMS-986187 enhanced the on-rates of Nb39 in the absence of orthosteric ligand and they also showed cooperativity with agonist to promote Nb39 binding, but differences were seen in the allosteric efficacies. Finally, we show that allosteric cooperativity between agonist and BMS-986187 is the same in membrane systems containing G protein and in the MOPr rHDL system without G protein, suggesting that the allosteric modulators alone are able to stabilize of an active state of MOPr and induce of high-affinity agonist binding.

Introduction

Pain is an unavoidable condition for which millions of people worldwide seek medical treatment and intervention. The leading medications for moderate to severe pain are opioid

ligands such as morphine and oxycodone. These drugs bind and activate the mu opioid receptor (MOPr), a G protein-coupled receptor (GPCR), at its orthosteric site and compete with the endogenous opioid peptides. Though efficacious at causing pain relief, MOPr activation at the orthosteric site also results in constipation, respiratory depression, and euphoria which enhances the addictive liability of opioid agonists. We are currently pursuing the idea that allosteric modulation of MOPr could represent a better method of pain relief with the potential for an improved therapeutic profile. In contrast to traditional activation by orthosteric agonists, allosteric enhancement of the actions of endogenous opioid peptides would preserve the spatial and temporal regulation of opioid peptide release (Burford *et al.*, 2015). This may allow for analgesia while avoiding long-term adaptations that manifest as tolerance and dependence. In addition, allosteric ligands have been known to alter or promote the bias of orthosteric agonists (Leach *et al.*, 2007; Ahn *et al.*, 2012; Baillie *et al.*, 2013). Induction of a bias of MOPr signaling could potentially result in analgesia with reduced adverse effects. For example, G protein biased signaling has been suggested to promote analgesia while decreasing the potential for tolerance and dependence (Bohn *et al.*, 1999, 2000; Raehal *et al.*, 2011).

Positive allosteric modulators (PAMs) of MOPr, exemplified by BMS-986122 (Burford *et al.*, 2013), enhance the affinity and/or efficacy of orthosteric ligands for MOPr, but show a distinct dependence on which orthosteric ligand is used to probe the allosteric interaction ((Burford *et al.*, 2013; Livingston and Traynor, 2014); Chapter 2). We have shown that BMS-986122 allosterically disrupts the binding of the endogenous negative allosteric modulator Na⁺ and promotes formation of active state MOPr with the degree of agonist cooperativity dependent upon the intrinsic efficacy of the ligand ((Livingston and Traynor, 2014); Chapter 2). In order to fully validate the hypothesis that BMS-986122 promotes active-state MOPr, we sought to design and implement a method to investigate the formation and stabilization of active state MOPr in response to various orthosteric and allosteric ligands.

The side effects of opioid agonists result from on-target activation of MOPr (Matthes *et al.*, 1996), although it is known that the initiation of these physiological effects requires different degrees of efficacy. Evidence exists that the discriminative stimulus of opioid agonists varies depending on efficacy (Walker *et al.*, 2004), suggesting that opioid agonist efficacy is a determinant of abuse potential. Indeed, it has been shown that higher efficacy ligands carry more of an addictive liability as compared to lower efficacy opioid ligands (Center for Substance

Abuse Treatment, 2004). For example, the low efficacy ligands nalbuphine, (Nubain[®]), and buprenorphine (Buprenex[®]), both carry lower addictive liability, but exhibit robust pain relief in humans indicating that the efficacy requirements for euphoria and pain relief are different. Indeed, extremely high efficacy opioid agonists including etorphine, have shown limits in their clinical value due to propensity to cause severe respiratory depression in addition to analgesia (Blane *et al.*, 1967) and have a narrow therapeutic index. In order to be able to predict the ability of MOPr agonists to cause various physiological effects, an understanding of their intrinsic efficacy is required.

The majority of approaches to determine intrinsic efficacy rely upon cell-based systems and the measurement of signaling downstream of the receptor. Despite best efforts, the calculated intrinsic efficacy of ligands can vary based on the signaling output measured due to signal amplification, ligand bias, kinetics of the assay, and the species of the cell system used (Kenakin, 2002; Kenakin and Christopoulos, 2011; Luttrell and Kenakin, 2011; Herenbrink *et al.*, 2016). For example, using the same cellular background, the putatively biased ligand TRV130 initiates robust arrestin recruitment (74% of standard) downstream of mouse MOPr, less with human MOPr (14% of standard), and shows undetectable levels using rat MOPr (Dewire *et al.*, 2013). Complications such as these make correlations of physiological effects to values of efficacy and bias difficult to interpret. In this study we sought to establish a method to evaluate the intrinsic efficacy of opioid ligands utilizing a cell-free assay independent of signaling outputs and signal amplification. We then sought to utilize this method to further probe the mechanism by which small molecule PAMs alter the efficacy of ligands at MOPr.

The recent crystal structure of MOPr in complex with the highly efficacious agonist BU72 utilized nanobody 39 (Nb39), a camelid antibody, to stabilize active MOPr (Huang *et al.*, 2015). Nb39 enhances the affinity of agonists to bind MOPr and stabilizes conformational changes in MOPr associated with an active-like state, including an outward movement of transmembrane helix 6. Nanobodies are small, monomeric proteins that can be utilized as conformational biosensors. Nanobodies have recently been used as tools to monitor formation of active-state β 2 adrenergic receptors (β 2AR) in live cells (Irannejad *et al.*, 2013). Consequently, we sought to use Nb39 as a probe to detect active-state conformation of MOPr using a variety of orthosteric and allosteric ligands in a cell-free setting. We predicted that the intrinsic efficacy of an agonist will determine the extent and rate at which the agonists promote the binding of Nb39.

Results

Measure of orthosteric agonist efficacy using interferometry-based technique

Nb39 enhances the affinity of agonists such as BU72 to bind MOPr ((Huang *et al.*, 2015), Appendix A) by stabilizing active (R*) states of MOPr. Because agonists shift the equilibrium of receptor to R* in proportion to their efficacy to activate downstream signaling, we predicted that agonists should enhance the binding of Nb39 in an efficacy-dependent manner. To test this, we implemented an interferometry-based technique to study the association and dissociation kinetics of Nb39 binding to monomeric MOPr in reconstituted high-density lipoproteins (rHDL). Briefly, MOPr rHDL particles are immobilized on a probe which is dipped in buffers containing ligands and Nb39. As shown in Figure 4.1, there was no detectable binding of Nb39 to MOPr in the absence of ligand. This indicates there is no spontaneous formation of active MOPr even with Nb39 present. Indeed, published research indicate very low levels of constitutive activity of MOPr (Divin *et al.*, 2009; Connor and Traynor, 2010). In contrast, a wide range of agonists caused binding of Nb39, although to varying degrees (Table 4.1). In particular, the presence of a saturating concentration (30 μ M) of BU72 drives robust and rapid binding of Nb39 (Fig 4.1, Table 4.1). The high-efficacy peptide agonist DAMGO displayed a similar association rate, but drove less overall binding of Nb39. In contrast, the partial agonist morphine led to slower Nb39 association and less overall binding of Nb39 (Fig 4.1, Table 4.1). Neither of the orthosteric antagonists naloxone or diprenorphine promoted MOPr:Nb39 interaction (Table 4.1).

To determine if the association rates of Nb39 to agonist-bound receptor reflect the efficacy of the agonist, we compared Nb39 association with three methods of efficacy measurement. In particular we studied the i) maximal efficacy to stimulate G protein signaling (Strange, 2008), ii) intrinsic efficacy as defined by Ehlert's equation (Ehlert, 1985), and iii) reduction in agonist affinity in the presence of Na⁺ ions and GTP nucleotide (Lee *et al.*, 1999). These complimentary methods of efficacy determination generally agree with one another, but reflect different factors of efficacy, which will be discussed later.

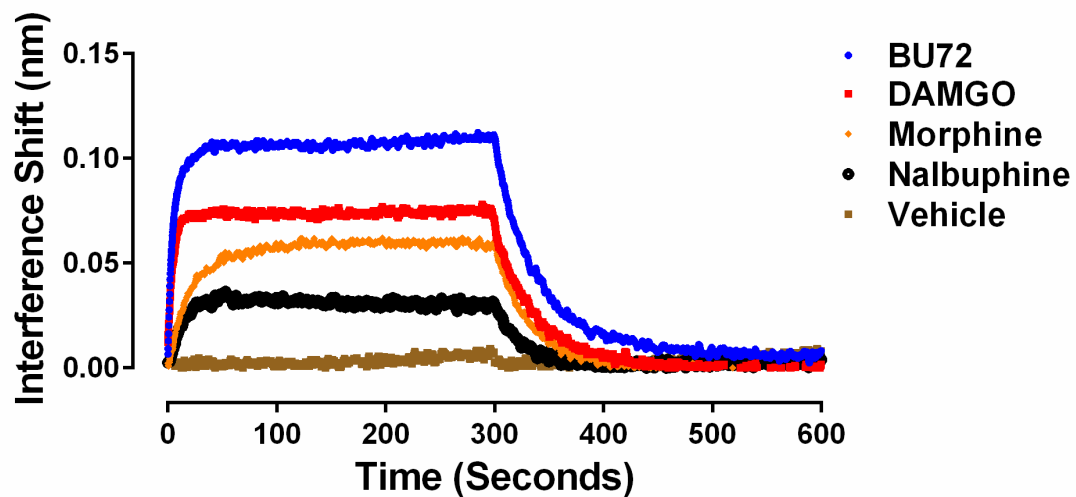


Figure 4.1: Orthosteric ligand-mediated Nb39 association and dissociation in MOPr-rHDL. As described in the methods, the association and dissociation of Nb39 (1 μM) was measured using OctetRed[®]. Shown is a representative experiment comparing four orthosteric agonists at 30 μM.

First, we compared the Nb39 association half-time ($t_{1/2}$) and the ability to stimulate G protein activation for each ligand. The $\text{GTP}\gamma^{35}\text{S}$ response elicited (taken from Chapter 2; (Livingston and Traynor, 2014)) by a saturating (10 μM) concentration of ligand correlated with the $t_{1/2}$ for Nb39 recruitment. ($r^2 = 0.75$, $p < 0.0001$ Fig 4.2A). Next, we correlated these association data with the intrinsic efficacy of the various orthosteric ligands. Intrinsic efficacy was calculated using the Ehlert equation ((Ehlert, 1985); see Methods) with potency and maximal response obtained from $\text{GTP}\gamma^{35}\text{S}$ binding assays and affinity values obtained using radioligand competition binding in the same buffer as the $\text{GTP}\gamma^{35}\text{S}$ assays. There was a statistically significant correlation. For instance, both etorphine and BU72 have equivalent Ehlert values (4.7) and both ligands show the same association rate for Nb39 ($t_{1/2} = 3.5$ sec for BU72, 3.9 sec for etorphine). The correlation was weaker than the comparison with the $\text{GTP}\gamma^{35}\text{S}$ maximum stimulation, but was still significant ($r^2 = 0.44$, $p = 0.02$ Fig 4.2B). For this analysis, we had to exclude nalbuphine as an EC_{50} value could not be determined due to its extremely low efficacy to activate G protein.

To avoid the use of a signaling measure, we used an additional readout of intrinsic efficacy, specifically the Na^+/GTP shift. It is known that addition of Na^+ and guanine nucleotide decreases the affinity of agonists to bind MOPr and that this effect is larger for higher efficacy ligands (Lee *et al.*, 1999). Using previously published data (Chapter 2), we plotted the shift in affinity of the orthosteric ligands by the addition of NaCl/GTP (100 mM and 10 μM respectively) versus the calculated $t_{1/2}$ of Nb39 association to ligand-bound MOPr. This correlation was significant (Fig 4.2C, $r^2 = 0.73$, $p = 0.002$). Of note, the ligands BU72 and etorphine were excluded from this analysis due to their paradoxical lack of Na^+/GTP shift (Chapter 2; Appendix A).

Our interferometry technique also allows for measurement of the dissociation of Nb39 from ligand-bound MOPr. In contrast to the association rates observed, the dissociation of Nb39 was fairly constant across the various ligands (Table 4.1). As an example, the Nb39 dissociation rate was the same from both morphine-bound MOPr ($0.033 \pm 0.001 \text{ min}^{-1}$) and BU72-bound MOPr ($0.031 \pm 0.001 \text{ min}^{-1}$), despite their markedly different efficacies. In contrast, L-methadone and loperamide were outliers and Nb39 dissociated more rapidly than with other

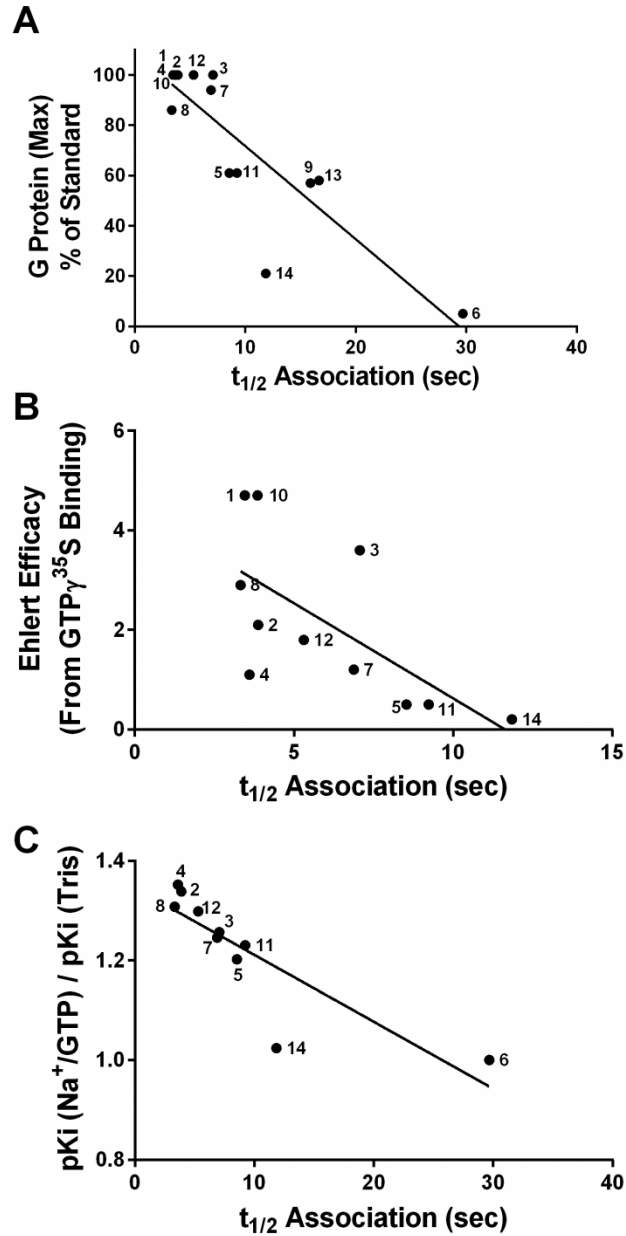


Figure 4.2: Correlation of association times of Nb39 with various measures of agonist efficacy. The $t_{1/2}$ of association of Nb39 in the presence of saturating agonist was measured and is plotted against A) maximal stimulation of $GTP\gamma^{35}S$ binding by agonist ($r^2 = 0.75$, $p < 0.0001$), B) the calculated Ehlert efficacy (Ehlert, 1985) values for each agonist to activate G protein ($r^2 = 0.44$, $p = 0.02$), and C) the shift in affinity of the agonist as measured by radioligand competition binding in the absence or presence of Na^+/GTP ($r^2 = 0.73$, $p = 0.002$). The ligands are: 1) BU72, 2) DAMGO, 3) Leu-Enk, 4) L-methadone, 5) Morphine, 6) Nalbuphine, 7) Endomorphin2, 8) Loperamide, 9) Oxycodone, 10) Etorphine 11) Fentanyl, 12) Met-Enk, 13) Hydrocodone, and 14) Buprenorphine

Table 4.1: Association and dissociation kinetics of Nb39 to MOPr rHDL in the presence of various agonists.

Ligand	$k_{obs} \pm SEM$ (min⁻¹)	$t_{1/2}$ Association (sec)	k_{off} (min⁻¹)	$t_{1/2}$ Dissociation (sec)
BU72	0.20 ± 0.01	3.5	0.031 ± 0.001	22
DAMGO	0.179 ± 0.008	3.9	0.030 ± 0.001	23
Leu-Enk	0.098 ± 0.02	7.1	0.031 ± 0.001	23
L-Methadone	0.19 ± 0.02	3.6	0.052 ± 0.003	13
Morphine	0.08 ± 0.01	8.5	0.033 ± 0.003	21
Nalbuphine	0.023 ± 0.008	30	0.036 ± 0.004	19
Endomorphin 2	0.101 ± 0.002	6.9	0.036 ± 0.002	19
Loperamide	0.208 ± 0.009	3.2	0.044 ± 0.003	16
Oxycodone	0.044 ± 0.001	16	0.028 ± 0.001	25
Etorphine	0.180 ± 0.007	3.9	0.026 ± 0.001	27
Fentanyl	0.075 ± 0.005	9.2	0.035 ± 0.002	20
Met-Enk	0.131 ± 0.004	5.3	0.027 ± 0.001	26
Hydrocodone	0.042 ± 0.004	17	0.029 ± 0.001	24
Buprenorphine	0.058 ± 0.009	12	0.025 ± 0.001	27
Naloxone	n/a	----	n/a	----
Diprenorphine	n/a	----	n/a	----
BMS-986122	0.012 ± 0.001	56	0.027 ± 0.003	25
BMS-986187	0.025 ± 0.006	28	0.037 ± 0.005	19

k_{obs} and k_{off} were fit for each independent experiment (3-10 individual experiments) and averaged. One-phase association and single-phase exponential decay models were used. Half-time values ($t_{1/2}$) numbers were calculated from the respective K values ($t_{1/2} = 0.693/k$).

ligands ($t_{1/2}$ of dissociation of 13 and 16 sec for L-methadone and loperamide, respectively; see Table 4.1). This difference can be interpreted as a distinct methadone-(or loperamide-) bound MOPr with decreased affinity for Nb39 as compared to other ligands.

Allosteric modulation of MOPr rHDL by small molecule PAMs and measurement of allosteric efficacy

Previously, we have shown that the MOPr PAM, BMS-986122, enhances agonist affinity and efficacy by stabilizing the active state of MOPr. To test this hypothesis using the interferometry method, we first wanted to validate that BMS-986122 had detectible allosteric activity in monomeric MOPr rHDL, as all previous work was done in cell membranes. The affinity of L-methadone was measured using competition binding with ^3H -diprenorphine in the presence or absence of 10 μM BMS-986122. The affinity of L-methadone was enhanced 3-fold in the presence of 10 μM BMS-986122 (Fig 4.3). This shift is much smaller than seen in membranes prepared from C6 rat glioma cells stably expressing MOPr (C6MOPr; Chapter 2; (Livingston and Traynor, 2014)). In order to determine if this diminished BMS-986122 activity in the MOPr rHDL system was a property of BMS-986122 or a property of purified MOPr, we investigated BMS-986187, another PAM that is structurally distinct from BMS-986122 (Fig 4.3). Though initially discovered as a PAM of the closely related delta opioid receptor (DOPr) we have shown it is a low affinity PAM of MOPr that binds at the same site on the receptor as BMS-986122 (Chapter 3; (Burford et al., 2015)). In contrast to BMS-986122, BMS-986187 enhanced the affinity of L-methadone to bind MOPr by over 10-fold in the rHDL system (Fig 4.3). By performing competition assays in the presence of increasing concentrations of BMS-986187, the allosteric ternary complex model was used to calculate an α value of cooperativity (58) and K_B (4.5 μM), representing the affinity of BMS-986187 for the unoccupied MOPr in rHDL, similar to that seen for MOPr in C6 membranes (Chapter 3). From this we determined the affinity of BMS-986187 for the methadone-bound MOPr in rHDL (K_B/α) to be 77 nM.

The discrepancy in BMS-986122 and BMS-986187 activity in MOPr rHDL was surprising as we have previously shown that both ligands have the same probe dependence, same mechanism of action, and bind at the same site on MOPr (Chapter 3). To verify that this probe

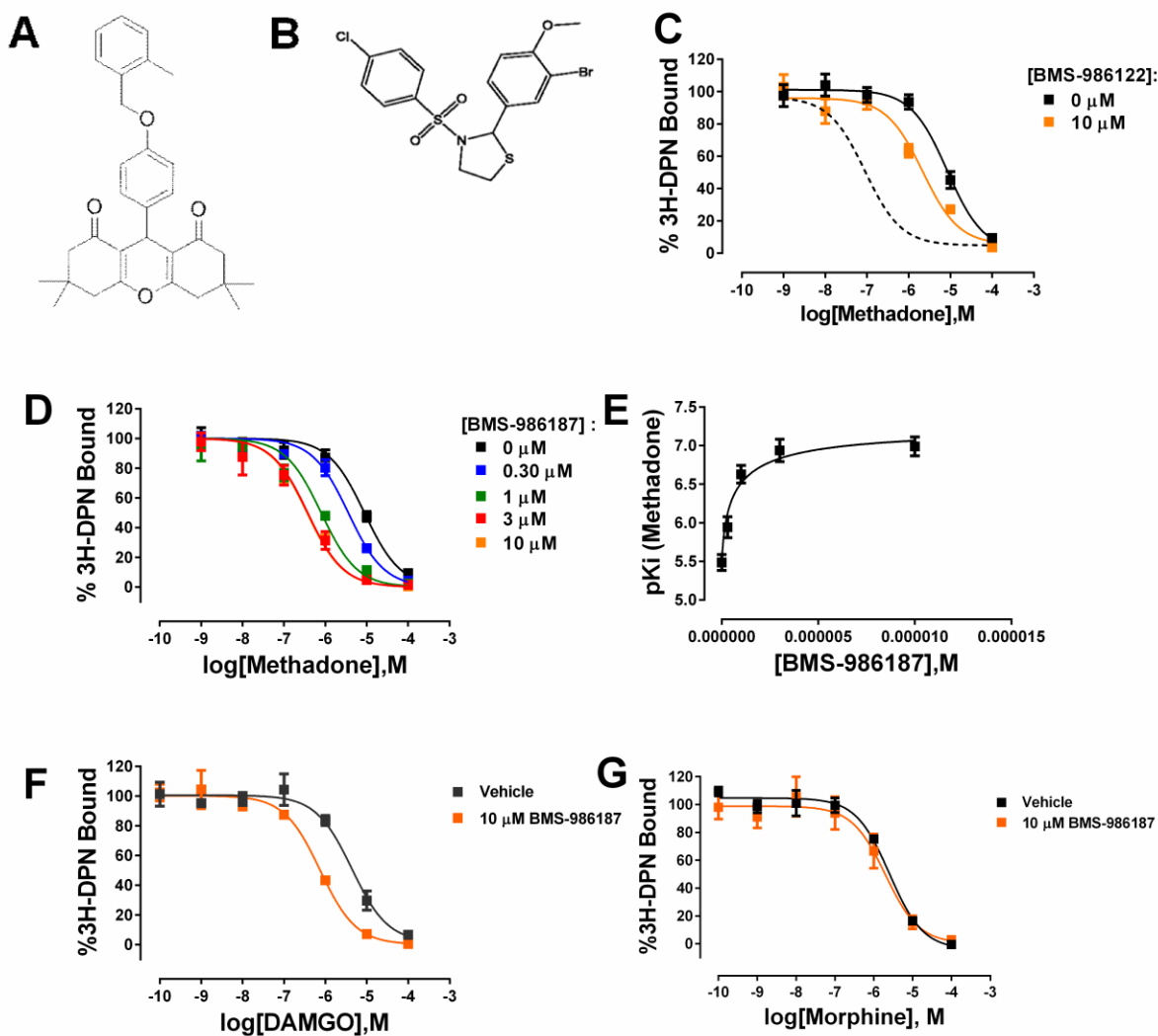


Figure 4.3: Allosteric modulation of MOPr rHDL by small molecule PAMs. Structures of BMS-986187 (A) and BMS-986122 (B). The ability of increasing concentrations of BMS-986122 (C) or BMS-986187 (D) to enhance the binding affinity of methadone was measured using displacement of ^3H -diprenorphine. The effect of BMS-986187 on methadone affinity is plotted in (E) and these data were analyzed using the allosteric ternary complex model to calculate K_B and alpha value of cooperativity. The ability of 10 μM BMS-986122 to enhance the affinity of DAMGO (F) or morphine (G) is also shown. All plotted points are means \pm SEM of 3-5 independent experiments, each in duplicate.

dependence of BMS-986187 we had previously seen (Chapter 3) was based upon direct ligand:receptor interaction and not due to the cellular membrane environment, we studied the ability of BMS-986187 to enhance affinity of three orthosteric ligands in rHDL-MOPr. The probe dependence was the same in the rHDL-MOPr system as in the C6MOPr membranes; BMS-986187 was able to enhance the affinity of DAMGO by six-fold ($\log K_i$ (veh) = -5.8 [95% C.I. -6.1 to -5.5] and $\log K_i$ (BMS-986187) = -6.6 [95% C.I. -6.7 to -6.4]) and methadone, but failed to alter that of morphine ($\log K_i$ (veh) = -6.2 [95% C.I. -6.4 to -6.0 and $\log K_i$ (BMS-986187) = -6.3 [95% C.I. -6.7 to -5.9]) (Fig 4.3). Furthermore, this probe dependence matches that seen for BMS-986122 and can be most simply explained by a two-state model of GPCR function ((Monod *et al.*, 1965; Livingston and Traynor, 2014), Chapter 2) in which BMS-986187 drives R*.

We hypothesized that both PAMs stabilize active-states of MOPr but that BMS-986187 has a higher allosteric efficacy compared to BMS-986122 as seen by the enhanced cooperativity with L-methadone in the MOPr rHDL. Therefore we hypothesized that both ligands alone would result in the binding of Nb39 but BMS-986187 would do so to a greater extent and at a more rapid rate. We found that both allosteric ligands were able to cause Nb39 binding but that it was quite slow (Fig 4.4, Table 4.1) compared to orthosteric agonists. In addition, the k_{off} of Nb39 from the BMS-986122-bound or BMS-986187-bound MOPr showed the same kinetics as the orthosteric agonists. This suggests that the active state stabilized by these PAMs is similar to those stabilized by traditional orthosteric agonists.

In addition to stabilizing active-state alone, we were interested to investigate the effect of the allosteric ligands on the ability of orthosteric agonists to promote Nb39 binding. Since both allosteric ligands have the ability to increase the efficacy of various orthosteric ligands in cell-based signaling assays, we hypothesized that this increase in efficacy would manifest as an increase in the observed on rate of Nb39 and that BMS-986187 would have a larger effect on Nb39 association than BMS-986122. Shown in Fig 4.5 is the ability of the two MOPr PAMs to enhance morphine-driven recruitment of Nb39. As predicted, both allosteric ligands enhanced the rate of Nb39 association and also enhanced maximal Nb39 binding. We did the same experiments with the orthosteric ligands L-methadone and DAMGO. Both PAMs enhanced the rate of DAMGO-driven Nb39 binding (Table 4.2) and slowed the dissociation of Nb39 from

Table 4.2: Alteration in Nb39 kinetics in the presence of MOPr PAMs

Morphine (1 μM Nb39)				
	k_{obs} (min^{-1})	$t_{1/2}$ Assoc (sec)	k_{off} (min^{-1})	$t_{1/2}$ diss (sec)
Vehicle	0.08 \pm 0.01	8.5	0.033 \pm 0.001	21
BMS-986122	0.11 \pm 0.001	6.4	0.032 \pm 0.0002	22
BMS-986187	0.13 \pm 0.01 ***	5.3	0.024 \pm 0.0004	29
L-Methadone (100 nM Nb39)				
	k_{obs} (min^{-1})	$t_{1/2}$ Assoc (sec)	k_{off} (min^{-1})	$t_{1/2}$ diss (sec)
Vehicle	0.087 \pm 0.009	8.0	0.050 \pm 0.004 §	14
BMS-986122	0.077 \pm 0.007	9.0	0.047 \pm 0.004 ++	15
BMS-986187	0.055 \pm 0.004 *	13	0.033 \pm 0.002 **	21
DAMGO (100 nM Nb39)				
	k_{obs} (min^{-1})	$t_{1/2}$ Assoc (sec)	k_{off} (min^{-1})	$t_{1/2}$ diss (sec)
Vehicle	0.051 \pm 0.003	14	0.035 \pm 0.003 ¥	20
BMS-986122	0.05 \pm 0.01	13	0.029 \pm 0.003	24
BMS-986187	0.050 \pm 0.004	14	0.022 \pm 0.001*	31

Two-way ANOVA with a Tukey post-hoc test was performed. * indicated statistically significance compared to vehicle condition for each orthosteric ligand. (* $p < 0.05$, ** $p < 0.01$, *** $p < 0.001$). ++ indicates $p < 0.01$ as compared to L-methadone/BMS-986187 combination. § indicates $p < 0.01$ as compared to morphine/vehicle combination. ¥ indicates $p < 0.01$ as compared to DAMGO/vehicle combination.

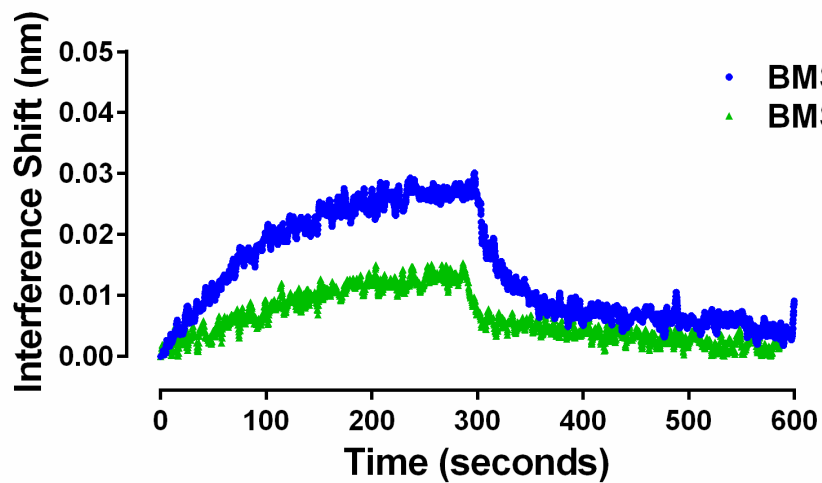


Figure 4.4: Binding kinetics of Nb39 driven by allosteric ligands. The association and dissociation of Nb39 (1 μM) was measured using OctetRed®. Shown is a representative experiment comparing two allosteric agonists 30 μM.

MOPr with BMS-986187 having a larger effect. Unexpectedly, the association of Nb39 to L-methadone bound MOPr was actually *slowed* in the presence of either BMS-986122 or BMS-986187. Additionally, the dissociation of L-methadone is unchanged by BMS-986122 but is slowed significantly by BMS-986187 (Table 4.2)

Discussion

We have described a novel method for examining the efficacy of both orthosteric and allosteric ligands of a prototypic class A GPCR, MOPr, which relies upon the ability of Nb39 to recognize the active state of the receptor. The ability of a ligand to stabilize active states (R*) of a GPCR is the first requirement in displaying physiological agonist effects. For MOPr, activation results in a variety of effects depending on the efficacy and bias of the ligand as well as the location of the receptor. Understanding the actions of ligands at this first step is crucial in predicting their activity downstream and *in vivo*. The technique presented here is a way of quantitatively examining the efficacy of both orthosteric and allosteric ligands at MOPr and should readily be applied to other GPCRs. This technique is independent of signaling and does not depend upon calculations of efficacy derived in the operational model from Black and Leff (Black and Leff, 1983) or the method of Ehlert (Ehlert, 1985). Measurement of Nb39 binding has no amplification and is dependent upon only receptor:ligand interaction. This enables fine-tune detection of ligand differences that may be masked when measuring an amplified signaling output. Indeed, if we were to perform the same correlation analysis presented in Fig 4.2 with a more amplified output (adenylate cyclase), the correlation falls dramatically (*data not shown*).

As predicted based on data from previous studies with Nb39 and Nb80 (Rasmussen, Choi, *et al.*, 2011; Irannejad *et al.*, 2013; Huang *et al.*, 2015), the presence of an agonist resulted in robust Nb39 binding while the antagonists naloxone or diprenorphine failed to promote detectable Nb39 binding. Our findings show that the ability of an agonist to promote Nb39 binding is well-correlated with its ability to promote signal transduction through G protein as measured by GTP γ ³⁵S binding. In fact, this technique was more sensitive as some of the ligands were able to promote Nb39, but failed to show measurable G protein activity using the GTP γ ³⁵S binding assay, including the MOPr PAMs (Chapter 2, Chapter 3, (Livingston and Traynor, 2014)).

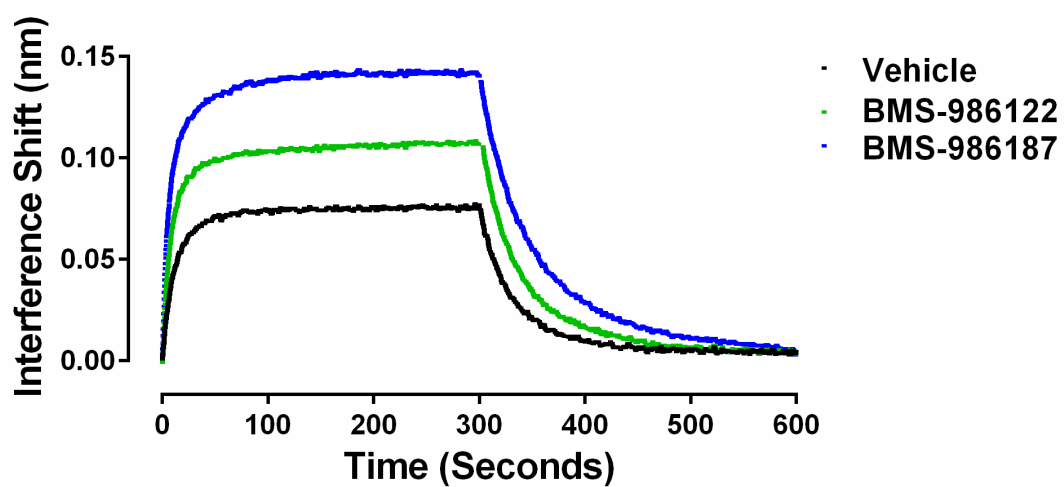


Figure 4.5: Effects of mu-PAMs on morphine-mediated association and dissociation of Nb39 from MOPr-rHDL. As described in the methods, the association and dissociation of Nb39 (1 μ M) was measured using OctetRed[®]. Shown is a representative experiment comparing the kinetics in the presence of morphine plus vehicle (black), BMS-986122 (green), or BMS-986187 (blue).

While theoretically measuring the same process (active-state promotion) the GTP $\gamma^{35}\text{S}$ assay can vary dramatically based upon nucleotide concentration, receptor:G protein ratios, MgCl_2 concentration, NaCl concentrations, time, and temperature (Traynor and Nahorski, 1995; Szekeres and Traynor, 1997; Remmers *et al.*, 2000; Heusler *et al.*, 2016). Indeed, it may be possible for there to be initiation of R*:G complexes that do not result in nucleotide exchange and GTP $\gamma^{35}\text{S}$ binding and therefore would not be detectable by this method. In contrast, Nb39 binding is not an enzymatic process like nucleotide exchange and instead represents a bimolecular binding event.

It is important to note that the range of active MOPr conformations recognized by Nb39 is, as of yet, unknown but it is known that Nb39 stabilizes an active state of MOPr displaying the prototypic outward movement of TM6 associated with active GPCRs. Also, the affinity of the agonist BU72 for Nb39-bound MOPr and Gi-bound MOPr is the same, suggesting the states of MOPr are similar (Huang *et al.*, 2015). The correlation experiments leave room for interpretation of the nature of states that Nb39 can bind. If Nb39 was an active state sensor capable of recognizing and binding *all* active-like conformations capable of initiating downstream signal transduction, there should theoretically be perfect correlations in Fig 4.2. As evidenced, the correlation with Ehlert efficacy values shows this is not the case. Though a well-accepted method for determining intrinsic efficacy, Ehlert's measure still relies upon data collected from a signaling assay which means that if a ligand is biased the results may differ depending on which signaling output is chosen. The Ehlert equation relies upon an EC_{50} , affinity value, and an E_{max} that is relative to a chosen standard. The EC_{50} of an assay will be heavily reliant on the system: receptor reserve, time of incubation, and inherent system maximum and is therefore not an absolute number (Strange, 2008). It is possible that there are active states recognized by Nb39 that are not as efficient as others at activating G protein.

Data from the interferometry experiments correlated more strongly with the Na^+/GTP shift of orthosteric agonists. This is likely because affinity is ideally system-independent and so the Na^+/GTP shift appears to be more reflective of true intrinsic efficacy of a ligand with no dependence on selection and measurement of a signaling output. Of note, etorphine and BU72 are unique ligands in that they exhibit no Na^+/GTP shift despite their high efficacy. This high efficacy and induction of rapid Nb39 binding is not predicted by their lack of sensitivity to Na^+/GTP . It is possible that this relatively small shift in affinity is not an absolute lack of

sensitivity to Na⁺, but perhaps a decrease in the potency of sodium to alter etorphine's affinity compared to other agonists and that a higher concentration of Na⁺ could further shift the affinity of BU72 and etorphine. The lack of the ability of Na⁺/GTP to alter affinity is in agreement with the lack of allosteric effects of the PAMs on these ligands (Chapter 2), suggesting that their affinity may be too high to be altered by allosteric ligands/ions. It is also possible that etorphine and BU72 promote a distinct state of the receptor that is not negatively cooperative with sodium. Indeed, recent NMR work has suggested that BU72 is a superagonist capable of stabilizing MOPr in an active-state without G protein and etorphine may be similar (Sounier *et al.*, 2015).

Generally most orthosteric ligands examined, as well as the allosteric ligands, induced a conformation of MOPr that displayed the same dissociation rate of Nb39. There were two outliers though: L-methadone and loperamide. The dissociation rates of Nb39 from the methadone-bound and loperamide-bound MOPr were statistically much faster than with other agonists as well as the allosteric ligands. This difference could arise for various reasons. Presumably, dissociation of Nb39 is driven by the relaxation of the R* to inactive R conformation; this could indicate that the methadone-bound MOPr produces an active state with a shorter lifetime than other agonists, despite L-methadone being present in concentrations ten-fold greater than its affinity. In contrast, if we take the dissociation to be a product of the affinity of Nb39 for a methadone-bound receptor, this indicates that the methadone-bound receptor has decreased affinity for Nb39. The same can be said for loperamide, though to a lesser extent.

Although the dissociation of Nb39 from the methadone-occupied receptor was faster than the other ligands, it was still sensitive to the PAMs in the same way (Table 4.2) in that the dissociation was slowed by the PAMs. In contrast to the other orthosteric ligands tested however, BMS-986122 and BMS-986187 both *slowed* association of Nb39 in the presence of methadone, indicating a negative cooperativity. This is in sharp contrast to both of these PAMs increasing potency and affinity of L-methadone to bind and activate MOPr (Fig 4.3, (Livingston and Traynor, 2014), Chapter 2, Chapter 3), but fits with a decrease in the Ehlert efficacy of L-Methadone that was seen in the presence of BMS-986122 (Chapter 2). One plausible explanation is that Nb39 recognizes only a subset of all possible conformations that are capable of activating G protein such that the efficiency of MOPr to activate nucleotide exchange may not be reflected in differences in Nb39 binding. In addition, methadone is the most sensitive orthosteric ligand for allosteric modulation with three different chemicals scaffolds (BMS-986122, BMS-986187,

and MS1 (Appendix C; (Bisignano *et al.*, 2015)). It is suggestive that methadone engages with MOPr in distinct ways that can be seen both in Nb39 binding characteristics as well as in sensitivity to allosteric modulation.

The differences in the efficacy of BMS-986122 and BMS-986187 are intriguing. Both ligands exhibit the same probe dependence, same mechanism of action, and appear to bind at the same site. Both are capable of driving Nb39 binding alone, but BMS-986187 does so to a greater extent at a faster rate. In line with this enhanced allosteric efficacy, only BMS-986187 is capable of driving high-affinity agonist binding alone (Fig 4.3). In addition, the dissociation rate of Nb39 from allosteric ligand-bound receptors is the same as that of agonist-bound receptors suggesting that they are similar active states that recognize Nb39 in the same manner (Table 4.1). Indeed, this is an example of a G protein-independent high affinity state. It would be interesting to determine if a BMS-986187:Receptor:Agonist complex adopts the same conformation as a Receptor:Agonist:G protein complex. Crystallographic work is underway to determine the mode of BMS-986187 binding and to determine the structural features that govern allosteric modulation of MOPr.

In summary, these data show a novel method for the quantitative evaluation of efficacy of both orthosteric and allosteric ligands using purified MOPr in rHDL particles and demonstrate that allosteric modulators of MOPr that work by displacement of Na⁺ ions are capable of forming active state receptor and of driving G protein-independent high affinity agonist binding. This technique is more sensitive than traditional measures of efficacy and is not reliant upon signal amplification. In the future, the methodology could also be applied to other GPCRs and other interacting proteins, such as arrestin, in order to determine a ligands' bias at the purely receptor level, independent of second messengers and cell type.

Materials and Methods

Purification of MOPr: Full length *Mus musculus* MOPr bearing an amino-terminal Flag epitope tag and a carboxy-terminal 6xHis tag was expressed in Sf9 insect cells using the BestBac baculovirus system (Expression Systems). A tobacco etch virus (TEV) protease recognition sequence was inserted after residue 51 and a rhinovirus 3C protease recognition sequence was inserted before residue 359 for cleavage during purification. Insect cells were infected with

baculovirus encoding MOPr 48–60h at 27 °C. Receptor was solubilized and purified in a final buffer comprised of 25 mM HEPES pH 7.4, 100 mM NaCl, 0.01% MNG (Anatrace), and 0.001% cholesterol hemisuccinate (CHS), as previously described (Manglik *et al.*, 2012).

Purification of Nb39: Nb39 was purified as described (Huang *et al.*, 2015). Briefly, Nb39 bearing a carboxy-terminal His tag were expressed in the periplasm of Escherichia coli strain WK6 grown in Terrific Broth medium containing 0.1% glucose, 2 mM MgCl₂, and 50 mg/ml ampicillin and induced with 0.5 mM isopropyl-b-D-thiogalactoside (IPTG). Cells were harvested after overnight growth at 25 °C and incubated in a buffer containing 200 mM Tris, pH 8.0, 0.5 mM EDTA, 500 mM sucrose and 0.5 mg/ml lysozyme for 1 h at 25 °C. Bacteria were osmotically lysed by rapid dilution in water. The periplasmic fraction was isolated by centrifugation of cell debris, and was supplemented with NaCl (150 mM final) and imidazole (25 mM final). Nb39 was isolated from the periplasmic fraction by nickel affinity chromatography, and subsequently purified by size-exclusion chromatography in a buffer comprised of 25 mM HEPES pH7.5 and 100 mM NaCl. Peak fractions were pooled and concentrated to approximately 5mM.

Apolipoprotein purification and biotinylation: Apolipoprotein-AI (Apo-AI) was purified as described previously (Whorton *et al.*, 2007). Apo-AI was biotinylated using NHS-PEG4-biotin (Pierce Biotechnology) at a 1:1 molar ratio. Following a 30-min biotinylation reaction at room temperature, the sample was dialyzed to remove free biotin.

MOPr rHDL Reconstitution: Purified MOPr was reconstituted into high-density lipoprotein (HDL) particles comprised of the lipids POPC and POPG (Avanti Polar Lipids) in a 3:2 molar ratio as previously described (Whorton *et al.*, 2007). For OctetRed® experiments, rHDL particles containing receptor were isolated from empty rHDL by FLAG affinity chromatography and elution fractions positive for ³H-diprenorphine binding were pooled.

Nb39 Kinetic Assays: Nb39 binding to MOPr in the presence or orthosteric and/or allosteric ligands was measured using the OctetRED biolayer interferometry system (Pall Forte Bio). In this assay, biotinylated apolipoprotein-containing rHDL-MOPr sample is immobilized on a streptavidin-coated fiber optic probe that is incubated into buffers containing ligands in the presence or absence of Nb39. Dissociation of bound-Nb39 is initiated by placing the probe in

buffer containing ligands but no Nb39. Specifically, biosensors (Pall Forte 'Bio) were loaded with biotinylated MOPr-rHDL particles for 15 min at room temperature and the biosensors were transferred to the OctetRED instrument. Sensors were placed into assay buffer (20 mM HEPES, pH 7.7, 100 mM NaCl, 1 mM EDTA, 0.05% (w/v) BSA) with vehicle or various orthosteric/allosteric ligands for 10 min to reach equilibrium. To measure Nb39 association, the probe was transferred to assay buffer with Nb39 (at indicated concentrations) for 5min, followed by a 10 min dissociation step in assay buffer (preliminary studies showed that dissociation of Nb39 was quite rapid). All ligands (orthosteric and allosteric), once introduced to the probe remained in each subsequent buffer during association and dissociation. All experiments were carried out at 25 °C with the assay plate shaking at 2,000 r.p.m. Nonspecific binding was measured using a vehicle control with no ligands and this was subtracted to account for baseline drift. Raw data were processed to remove baseline using Octet Data Analysis 7.0 software (Pall Forte Bio) and exported to GraphPad Prism 6.0 for curve fitting. Association and dissociation curves were fit using a single-phase exponential association or decay curves, respectively.

Radioligand binding assays: For competition binding experiments in MOPr- rHDL, a mixture of MOPr-rHDL and ³H-diprenorphine (³H-DPN) was incubated with varying concentrations of agonist in a binding buffer comprised of 25 mM HEPES pH 7.4, 100 mM NaCl, and 0.1% BSA in the presence or absence of 3 μM Nb39. For assays performed using cell membranes, conditions listed were kept the same except for exclusion of BSA and inclusion of 10μg protein per well. Binding reactions were incubated for 2 h at 25 °C. Free radioligand was separated from bound radioligand by rapid filtration onto a Whatman GF/C filter pretreated with 0.1% polyethylenimine using a 24-well harvester (Brandel). Nonspecific binding was measured in the presence of 10μM naloxone, an opioid antagonist. Radioligand activity was measured by liquid scintillation counting using a Wallac 1450 MicroBeta counter (Perkin Elmer). Competition binding data were fit to a one-site model using GraphPad Prism 6.0.

CHAPTER 5

A Biased Mu-Opioid Receptor Positive Allosteric Modulator that Does Not Alter Morphine-Mediated Desensitization

Summary

Currently used opioid analgesics, in particular morphine, compete with endogenous opioid peptides by binding to the orthosteric site of the mu opioid receptor (MOPr), a G protein coupled receptor (GPCR). Activation of MOPr causes analgesia but also results in respiratory depression, sedation, constipation, and euphoria leading to a high addictive liability. Furthermore, long-term treatment with opioids leads to tolerance, or the requirement for larger doses to maintain adequate pain relief. Our lab is pursuing the idea that positive allosteric modulators (PAMs) of MOPr may represent a way to treat pain with a better therapeutic profile. Such compounds, including BMS-986122, enhance the affinity, potency, and/or efficacy of orthosteric opioid ligands, including morphine, to bind MOPr and activate G protein. Here, we sought to determine if the enhancement in the efficacy of morphine to activate G protein signaling by BMS-986122 also results in enhanced desensitization and tolerance. The results demonstrate that BMS-986122 alone did not cause any long-term adaptations in MOPr signaling and also fails to enhance morphine-induced desensitization as measured by receptor downregulation, receptor phosphorylation, and loss of receptor mediated signaling following long-term agonist exposure. Furthermore, we show that BMS-986122 initiates activation of extracellular signal-regulated kinase 1/2 in a pertussis-toxin insensitive manner supporting a G protein independent mechanism and demonstrates that BMS-986122 is a biased “ago-PAM.” Development of biased allosteric ligands at GPCRs represents a novel avenue for analgesic drug development and future work will determine the physiological consequences for this biased MOPr PAM in rodent models of pain.

Introduction

Pain is one of the leading causes of doctor visitations and is responsible for an estimated \$600 billion per year in health costs and loss in work productivity in the United States (Debono *et al.*, 2013). Currently used opioids, including the gold standard morphine, cause analgesia by activation of the mu opioid receptor (MOPr), a G protein-coupled receptor (GPCR). Though MOPr agonists are effective at managing moderate to severe pain, they cause undesirable on-target effects including respiratory depression, constipation, dependence, and also have an addiction liability. Most prescription opioids, including buprenorphine, oxycodone, and morphine, are partial agonists that bind to the orthosteric site on MOPr, or the site where the endogenous opioid peptides bind.

The use of opioid drugs for the management of chronic pain is problematic as long term administration produces tolerance with dose escalation being required to maintain adequate pain relief. Tolerance does not develop to all MOPr effects at equivalent rates (Jaffe, 1985; Roerig *et al.*, 1987; Buntin-Mushock *et al.*, 2005), leading to severe and dose-limiting constipation. Morphine, in particular, is known to cause robust tolerance in animal models as well as in humans (Huidobro *et al.*, 1976; de Leon-Casasola *et al.*, 1993; Buntin-Mushock *et al.*, 2005) though it remains one of the most commonly used opioid agonists. Physiological tolerance initiates at the level of the receptor. Generally, exposure to MOPr agonists results in phosphorylation of the intracellular loops and C-terminal tail of the MOPr that enhances arrestin-2/3 binding. Arrestin-binding blocks subsequent G protein activation resulting in receptor desensitization and also initiates internalization of the receptor which can then be recycled or degraded. Indeed, chronic stimulation of MOPr, both *in vitro* and *in vivo*, leads to downregulation of MOPr (Stafford *et al.*, 2001; Yoburn *et al.*, 2003). In contrast to its robust physiological tolerance and desensitization, morphine generally does not induce robust internalization and phosphorylation of MOPr, but can do so in certain tissues or with particular alterations in cellular environment (Whistler and von Zastrow, 1998; Whistler *et al.*, 1999; Rodríguez-Muñoz *et al.*, 2007). For instance, if GRK2 is overexpressed, the ability of morphine to internalize is increased (Zhang *et al.*, 1998). However, the effect of increased receptor internalization on physiological tolerance remains controversial.

We are currently pursuing the idea that positive allosteric modulation of MOPr may represent a strategy for pain management with fewer side effects, including lower tolerance

development. Positive allosteric modulators (PAMs) bind to sites distinct from the orthosteric site, or the site where endogenous ligands and clinical opioids bind, and enhance the binding and activity of orthosteric ligands. A MOPr PAM could be given alone to cause pain relief by enhancement of endogenous opioid peptide activity, preserving spatial and kinetic peptide regulation, or be given in combination with a traditional opioid ligand, enhancing its activity while enabling a lower dose to be used (Burford *et al.*, 2015).

Another benefit of allosteric modulation of GPCR activity is the potential for the induction of signaling bias, or the preferential activation of one pathway (e.g. G protein-mediated) over other pathways (e.g. arrestin-mediated). Allosteric ligands acting at other GPCRs have been shown to induce bias of orthosteric ligands *in vitro*, including ORG27569 at the cannabinoid CB1 receptor and PDC113.824 at the prostaglandin F2alpha (PGF2 α) receptor (Goupil *et al.*, 2010; Ahn *et al.*, 2012; Baillie *et al.*, 2013). Accumulating literature suggests that many of the detrimental effects of opioid agonists result from arrestin mediated signaling, including MOPr internalization. For example, arrestin-3 knockout mice display increased morphine-induced analgesia, decreased respiratory depression, and decreased constipation following acute morphine administration and also show decreases in tolerance development following chronic exposure to morphine (Bohn *et al.*, 1999, 2000, 2002; Raehal *et al.*, 2005). Therefore a MOPr PAM that enhances G protein signaling at the expense of arrestin-mediated signaling of traditional opioids would enhance the clinical value of opioid drugs.

The first MOPr PAM discovered, BMS-986122 (Burford *et al.*, 2013), increases the affinity of full agonists like the endogenous enkephalins and β -endorphin to bind MOPr and the potency of these full agonists to activate G_{i/o} protein as measured by GTP γ ³⁵S binding (Chapter 2; Livingston and Traynor, 2014). In addition, the PAM enhances the efficacy of partial agonists such as morphine (Chapter 2, Chapter 4). Agonist efficacy is correlated with ability to cause phosphorylation and desensitization of MOPr (McPherson *et al.*, 2010), therefore we hypothesized that BMS-986122 should enhance these events. To address this, we studied the effects of BMS-986122 on the action of morphine in cellular models of desensitization (Elliott *et al.*, 1997). Results indicate that BMS-986122 does not enhance morphine-induced cellular desensitization or downregulation of MOPr despite enhancing the efficacy of morphine. Moreover during these studies we also found that BMS-986122 is biased and can activate extracellular signal-regulated kinase 1/2 (ERK1/2) through a G protein-independent manner.

Results

To assess the ability of BMS-986122 to cause MOPr desensitization alone, membranes prepared from C6 glioma cells stably expressing rat MOPr (C6MOPr) were treated overnight with vehicle or 10 μ M BMS-986122. The ability of MOPr to signal to G protein in a concentration-dependent manner when occupied by morphine was then assessed using GTP γ ³⁵S binding. The potency and maximal activity of morphine was unaltered by overnight pretreatment with BMS-986122 (Fig 5.1A).

Next, as BMS-986122 has been shown to increase the efficacy of morphine as determined by the method of Ehlert (Ehlert, 1985; Chapter 2), we investigated if this also would result in an enhancement in desensitization. As a comparison, we studied the effect of BMS-986122 on the desensitization of a ligand whose efficacy was not altered by BMS-986122, namely the full-agonist peptide [D-Ala²,N-Me-Phe⁴,Gly-ol⁵]-enkephalin (DAMGO). C6MOPr cells were pretreated overnight (18 h) with 10 μ M DAMGO in the presence or absence of 10 μ M BMS-986122. The membranes were challenged with DAMGO across several concentrations using a GTP γ ³⁵S binding assay. Results show that, as expected, pretreatment with DAMGO did cause a reduction in the ability of the challenge DAMGO to elicit G protein activation, indicative of desensitization. But, the presence of BMS-986122 did not enhance this desensitization (Fig 5.1B). As DAMGO is a high efficacy ligand that may cause maximal desensitization, we needed to verify that an effect of BMS-986122 was not being masked so we also challenged these membranes with morphine, a lower efficacy partial agonist with a smaller receptor reserve. Results using a morphine challenge were the same: pretreatment of C6MOPr cells with DAMGO caused a reduction in the ability of morphine to signal but that this was not enhanced by co-treatment with BMS-986122 (Fig 5.1C). Similarly, BMS-986122 did not enhance desensitization mediated by the partial agonist morphine (10 μ M) (Fig 5.1D).

We then examined whether BMS-986122 could ‘rescue’ MOPr coupling to G proteins, following desensitization with morphine, predicting that the PAM should enhance the activity of the remaining non-desensitized receptors or be capable of enhancing signal transduction through a desensitized receptor. Cells treated overnight with morphine were challenged with a range of

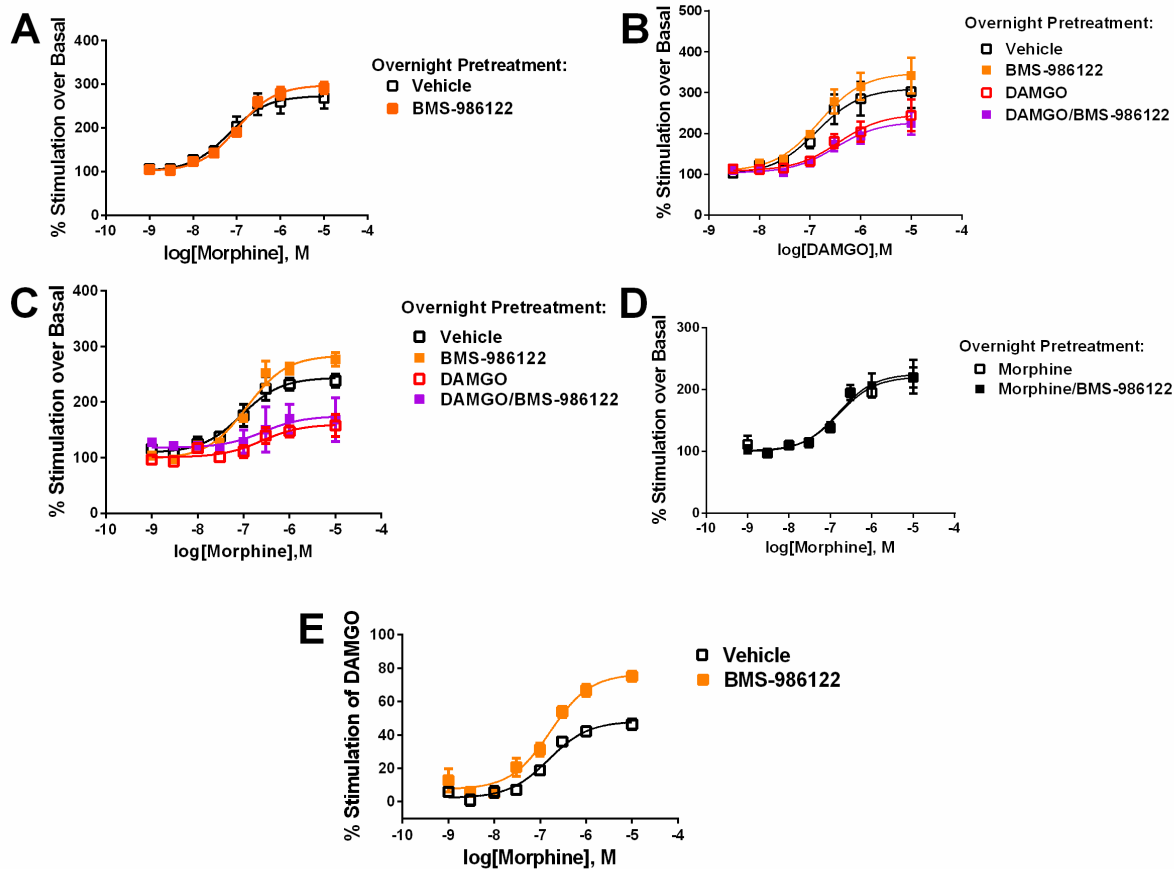


Figure 5.1: Desensitization of MOPr by various ligands in C6MOPr cell membranes as determined by loss of $GTP\gamma^{35}S$ binding. A) C6MOPr cells were treated with vehicle or 10 μ M BMS-986122 for 18 h. The ability of morphine to initiate $GTP\gamma^{35}S$ binding was measured in both membranes. B) C6MOPr cells were treated overnight (18 h) with vehicle, BMS-986122 (10 μ M), DAMGO (10 μ M), or DAMGO and BMS-986122 (both 10 μ M). Membranes prepared from each condition were challenged with increasing concentrations of DAMGO or morphine (C) for the ability to stimulate $GTP\gamma^{35}S$ binding. D) C6MOPr cells were pretreated with morphine (10 μ M) with or without BMS-986122 (10 μ M) for 18 h and then challenged with varying concentrations of morphine. E) Membranes were pretreated with morphine (10 μ M) for 18 h and then a morphine concentration-response $GTP\gamma^{35}S$ assay was performed in the presence of vehicle or BMS-986122 (10 μ M). All data shown are means \pm SEM of 2-4 individual experiments in duplicate. Data are expressed as percent over basal $GTP\gamma^{35}S$ binding calculated by binding in the absence of any ligand or expressed as percent of a 10 μ M DAMGO standard.

Table 5.1: Saturation binding with ³H-DPN reveals no change in Bmax or Kd following morphine treatment.

	<u>K_d</u>	<u>pmol/mg</u>
Vehicle	0.25 ± 0.05	4.6 ± 0.7
BMS-986122	0.21 ± 0.05	5.9 ± 0.7
Morphine	0.21 ± 0.06	4.3 ± 0.6
Morphine + BMS-986122	0.39 ± 0.10	4.2 ± 0.5

All ligands are at 10 μM. K_d and Bmax were calculated by performed saturation binding in membranes prepared from C6MOPr cells treated 18 h with the indicated vehicles/ligands. Nonspecific binding in the presence of saturating (10 μM) naloxone was subtracted before fitting curves using GraphPad Prism. Data shown were calculated from 3 separate saturation binding experiments in duplicate from three separate pretreatment/membrane preparations as described in the methods.

morphine concentrations in the presence of vehicle or 10 μ M BMS-986122. Overnight treatment with morphine cause a significant reduction in morphine-mediated GTP γ ³⁵S binding and this was reversed back to control conditions in the presence of BMS-986122 (Fig 5.1E).

In addition to diminished functional responses, chronic exposure to MOPr agonists has been shown to cause downregulation of the receptor (Stafford *et al.*, 2001; Patel *et al.*, 2002) both *in vitro* and *in vivo*, and the degree of downregulation of positively correlated with ligand efficacy (Chakrabarti *et al.*, 1997; Yoburn *et al.*, 2003, 2004). However, in the C6MOPr cells saturation binding using the non-selective opioid antagonist ³H-diprenorphine revealed no differences in K_d or Bmax after overnight treatment with BMS-986122, morphine, or the combination of both (Table 5.1).

The diminished functional response after morphine or DAMGO exposure could be a result of several processes including MOPr phosphorylation, arrestin binding and internalization. Using an antibody specific for MOPr phosphorylated at serine-375 (S375), a site known to be targeted by GPCR receptor kinase 2/3 (GRK2/3) as well as GRK5 (Doll *et al.*, 2011; Just *et al.*, 2013; Allouche *et al.*, 2014), we evaluated the ability of BMS-986122 to afford phosphorylation of this site and/or or to increase the ability of morphine to induce MOPr phosphorylation. C6MOPr cells were exposed to BMS-986122 (10 μ M) for 10 min (peak time for agonists as determined by time course; *data not shown*) and analyzed using SDS-PAGE followed by Western blot to probe for phosphorylated S375. As shown in Fig 5.2, basal levels of phosphorylated S375-MOPr are very low, as reported (Just *et al.*, 2013). BMS-986122 exposure failed to result in significant phosphorylation of this residue, while the positive control DAMGO (10 μ M) resulted in robust phosphorylation of this site. The partial agonist morphine (10 μ M) resulted in no phosphorylation of S375, as has been previously reported (McPherson *et al.*, 2010) and BMS-986122 was unable to enhance phosphorylation induced by morphine (Fig 5.2).

To quantify the internalization of MOPr by BMS-986122, HEK293T cells were transiently transfected with MOPr that has a FLAG epitope on the extracellular N-terminus of the receptor. Following ligand treatment at 37°C, cells were fixed and cell surface receptors were quantified using an alkaline phosphatase-conjugated anti-FLAG antibody. As shown in Fig 5.3, BMS-986122 (10 μ M) alone did not cause a significant decrease in cell surface receptors, but the positive control DAMGO (10 μ M) caused robust internalization. Morphine (10 μ M) exposure

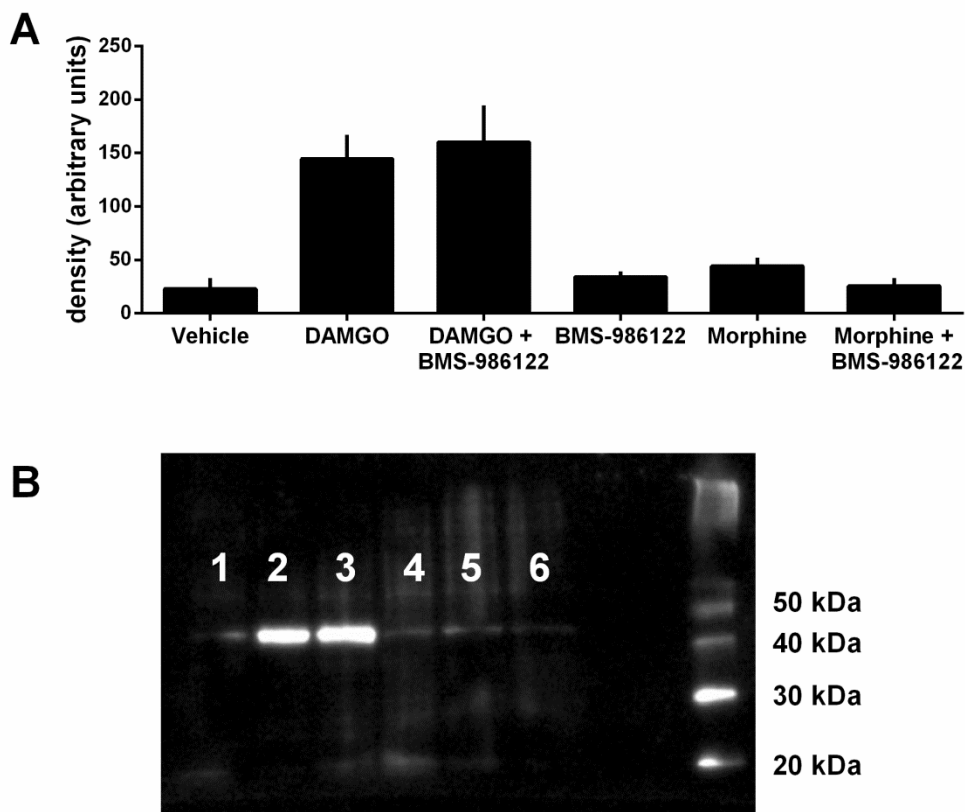


Figure 5.2: BMS-986122 does not enhance agonist-mediated phosphorylation of S375 of MOPr. C6MOPr were treated with 10 μ M ligands (or vehicle) for ten mins and then examined using SDS-PAGE followed by western blot against phosphorylated S375 of MOPr. Shown is the mean \pm SEM quantification of 3 separate experiments (A) and a representative image (B) with lanes as follows 1) vehicle, 2) DAMGO, 3) DAMGO + BMS-986122, 4) BMS-986122, 5) Morphine, and 6) Morphine + BMS-986122

resulted in less internalization than DAMGO as was expected but this was unaltered in the presence of 10 μ M BMS-986122.

It has been previously shown that BMS-986122 does not recruit arrestin-3 alone using the DiscoverX PathHunter[®] assay (Burford *et al.*, 2013), but does enhance the ability of orthosteric ligands to recruit arrestins. As BMS-986122 was unable to alter cellular desensitization and internalization which are events largely regulated by arrestins, we wanted to confirm that BMS-986122 did not engage arrestin-mediated signaling. We investigated the ability of BMS-986122 to activate extracellular regulated kinase 1/2 (ERK1/2), which can be mediated by both arrestin and G protein pathways. In C6MOPR cells, BMS-986122 (10 μ M) alone activated ERK1/2 with a peak time occurring at 30 min (Fig 5.4). Using this peak time, we then performed a concentration response of BMS-986122 that give an EC₅₀ of approximately 100 nM. Pretreatment of the cells with pertussis toxin (PTX; 100 ng/mL) for 18 h did not alter ability of BMS-986122 to activate ERK1/2, suggesting this pathway was not G protein mediated. Importantly, BMS-986122 did not stimulate ERK1/2 phosphorylation in the parental C6 glioma cell line which expresses no MOPr, indicating the effect was receptor-mediated (*data not shown*).

Discussion

Here we report that BMS-986122, despite enhancing the efficacy of morphine to activate G protein, does not enhance morphine's ability to cause MOPr desensitization, downregulation, phosphorylation MOPr at S375, or MOPr internalization. Furthermore, we show that BMS-986122 can rescue agonist-mediated signaling in membranes expressing MOPr that have been functionally desensitized by prolonged agonist treatment. Finally, we find that BMS-986122 is capable of activating MOPr in the absence of orthosteric ligand in a way that leads to G protein-independent activation of ERK1/2 indicating that BMS-986122 is a signaling biased "ago-PAM".

As we have previously shown, BMS-986122 can drive active-MOPr by allosterically disrupting Na⁺ binding (Chapter 2; (Livingston and Traynor, 2014)) thereby forming a state of MOPr that is captured and stabilized by the active-state sensor nanobody 39 (Chapter 4). However, the lack of G protein activation (Burford *et al.*, 2013) and slow rates of nanobody 39

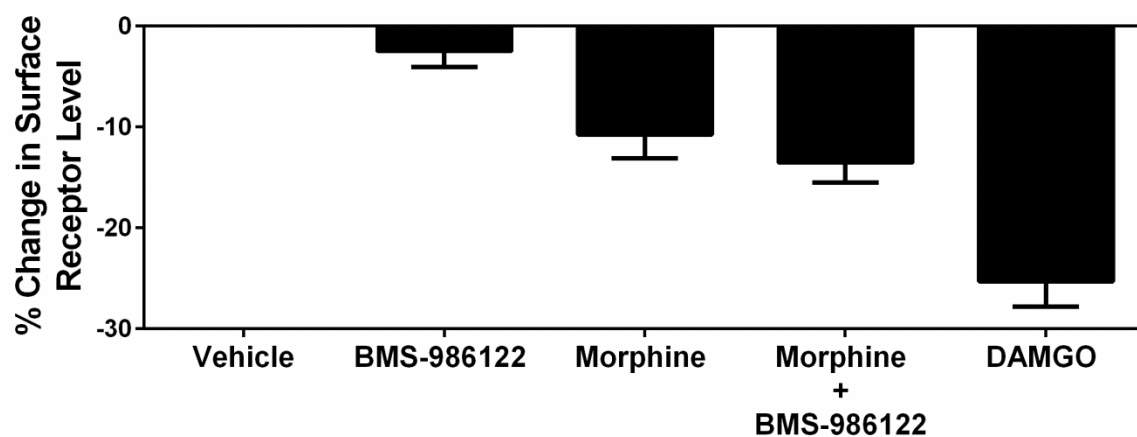


Figure 5.3: Internalization of MOPr by various ligands. As described in the methods, the ability of various ligands (all at 10 μ M) to cause internalization of MOPr following 10 min of treatment was measured in HEK293T cells transiently transfected with FLAG-tagged MOPr. Data are presented as percent change from vehicle condition and data shown are means of 3-4 experiments performed in triplicate.

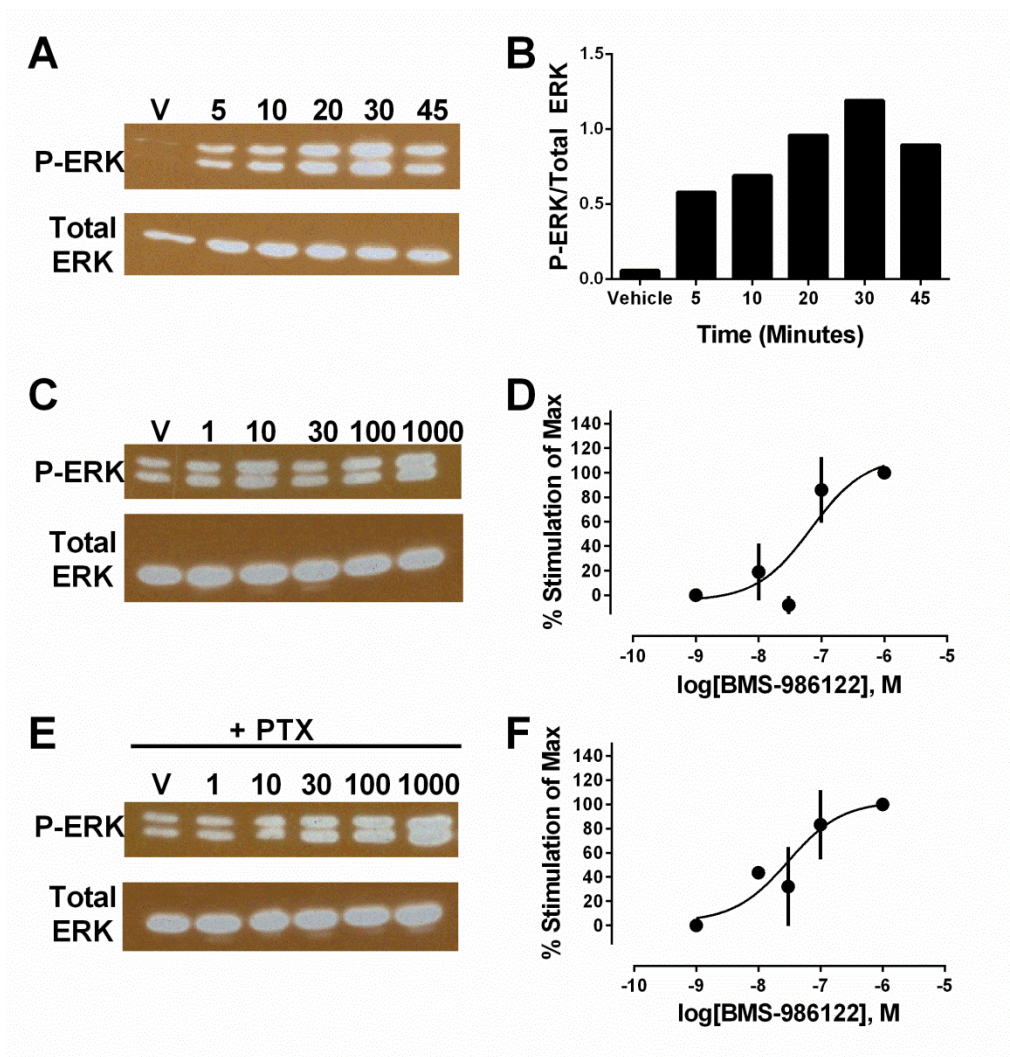


Figure 5.4: BMS-986122 mediated ERK1/2 activation in C6MOPr cells. Shown are representative western blot images of the time course (A), dose response at 30 min (A) and dose response at 30 min following 18 h pretreatment with PTX (100 ng/mL). The numbers above A are minutes and C/E represents concentrations of BMS-986122 in nM. B, D, and E show the average quantification of 1-3 experiments for each point. Data from D and F were fitted using linear regression to calculate pEC_{50} values of Vehicle: -7.22 ± 0.35 and PTX: -7.53 ± 0.66 which are not statistically different ($p=0.67$).

association (Chapter 4) driven by BMS-986122 suggest that its efficacy or ability to stabilize active-state MOPr is low. As such, the lack of functional desensitization and MOPr internalization by BMS-986122 alone (Fig 5.1) is explained as these outputs are correlated with ligand efficacy. But, this active-state formation is responsible for the ability of BMS-986122 to enhance the efficacy of morphine which is exemplified by the ability of BMS-986122 to rescue the desensitized response. This is likely due to enhancement in the functionality of the non-desensitized receptors and an apparent enhancement in receptor reserve.

Given the ability of BMS-986122 to enhance the efficacy of morphine to initiate G protein signaling, it is surprising that we do not see enhancement of morphine-mediated phosphorylation of S375 as this site is phosphorylated by G protein-recruited kinases, specifically GRK2/3. It is true the BMS-986122 could drive phosphorylation of other residues on MOPr, including sites in the ³⁷⁰TREHPSTANT³⁷⁹ and ³⁵⁴TSST³⁵⁷ sequences. But, S375 is the initiating residue phosphorylated and is a necessary prerequisite for phosphorylation of other sites (e.g. S363, T376, and T379) (Just *et al.*, 2013). In addition, morphine has been shown to only cause phosphorylation of S375 and only in certain cell types (Doll *et al.*, 2011). It may be that BMS-986122 changes the phosphorylation ‘bar-code’ of morphine (Lau *et al.*, 2011; Nobles *et al.*, 2011), but the lack of enhancement of the initiating residue (S375) suggests this will not be the case. In addition, S375 has been shown to be the residue that enhances the affinity of arrestin to bind MOPr (El Kouhen *et al.*, 2001).

The lack of BMS-986122 mediated phosphorylation of S375 on its own fits with previous studies that showed no recruitment of arrestin-3 by BMS-986122 alone using the DiscoverX PathHunter assay (Burford *et al.*, 2013). This also explains why BMS-986122 alone did not cause internalization of MOPr alone (Fig 5.3). Importantly, the DiscoverX assay only measured arrestin-3 recruitment and the ability of BMS-986122 to promote arrestin-2 recruitment is unknown. BMS-986122 has been shown to enhance endomorphin-1 mediated recruitment of arrestin-3 (Burford *et al.*, 2013), suggesting that BMS-986122 can enhance arrestin recruitment for some ligands. It is important to note though, that the PathHunter assay measures enzyme complementation resulting from proximity of arrestin with MOPr and the functional consequence of this arrestin-receptor interaction that BMS-986122 enhanced is not known. Not all receptor:arrestin interactions result in receptor internalization (For review see (Shenoy and Lefkowitz, 2011)). It would be interesting to determine if BMS-986122 enhances endomorphin-1

internalization as the arrestin data would suggest and conversely if BMS-986122 enhances morphine mediated arrestin-3 recruitment, which we would predict it does not as it does not enhance morphine driven internalization of MOPr.

The physiological consequence of the enhancement in efficacy of morphine to active G protein but lack of enhancement in morphine-mediated MOPr internalization by BMS-986122 is unknown. Though this is seen as a lack of enhanced functional desensitization in C6MOPr cells (Fig 5.1), the effects on more chronic tolerance and dependence *in vivo* can only be speculated. According to studies performed using arrestin-3 knockout mice, lack of arrestin-3 resulted in morphine-mediated analgesia with less tolerance development as compared to wildtype controls (Bohn *et al.*, 1999; Raehal and Bohn, 2011) which suggests that BMS-986122 coadministration with morphine should enhance analgesia without enhancing tolerance. It is important to note that the arrestin-3 knockout animals would show decreased MOPr internalization but also decreased arrestin-mediated signaling. As BMS-986122 has no effect on internalization but does appear to signal through arrestin (*see below*), this complicates the prediction. On the other hand, the RAVE (relative activity versus endocytosis) theory proposed by Whistler and colleagues states that arrestin-mediated internalization is actually *beneficial* in avoiding tolerance as it enables recycled, resensitized receptors to return to the surface (Finn and Whistler, 2001; Martini and Whistler, 2007). In this theory, agonists that do not cause robust internalization cause more tolerance due to the accumulation of desensitized, non-functional receptors at the cell surface. According to this theory, the lack of enhancement of morphine-mediated MOPr internalization with the accompanied enhancement in the efficacy of morphine could actually *enhance* tolerance development.

The ability of BMS-986122 to activate ERK1/2 while failing to inhibit adenylate cyclase (AC; up to 30 μ M in the C6MOPr cells; *data not shown*) is indicative of a bias because opioid agonists, including DAMGO, are more potent at inhibition of AC as compared to ERK1/2 activation (Clark *et al.*, 2003) in these cells. The mechanism of ERK1/2 activation by BMS-986122 is independent of G α i/o proteins as shown by the insensitivity of the response to PTX pretreatment (Fig 5.4). While there is evidence of MOPr coupling to the PTX-insensitive G α z subunit (Tso and Wong, 2000; Sánchez-Blázquez *et al.*, 2001), C6 glioma cells have been shown to not express this subtype (Charpentier *et al.*, 1993). This suggests an arrestin-mediated activation of ERK1/2. The slow time to peak (30 min) also matches literature data for arrestin-

mediated ERK1/2 activation compared to faster (5-10 min) G protein mediated ERK1/2 activation for MOPr (Clark *et al.*, 2003). Furthermore, the lack of arrestin-3 recruitment as measured by the PathHunter assay (Burford *et al.*, 2013) suggests it is not arrestin-3 mediated. This leaves arrestin-2, which has been shown to be less involved in regulating agonist-mediated internalization of MOPr. Therefore, we propose that BMS-986122 promotes ERK1/2 activation selectively by arrestin-2, and does not engage arrestin-3 which is why internalization of MOPr is not enhanced (*see Chapter 6 for further discussion*). A remaining question is the cellular fate of this activated ERK1/2 as it has been reported the arrestin-activated ERK1/2 is translocated to the nucleus and is responsible for alteration in gene transcription (Zheng *et al.*, 2008). Indeed, if this ERK1/2 does translocate to the nucleus, then knowing the transcriptional targets would enable prediction of the long term consequences of BMS-986122 administration.

Activation of ERK1/2 by BMS-986122 occurs at much lower concentrations than the published affinity for BMS-986122 for MOPr (2 μ M; (Burford *et al.*, 2013)) would predict. The reported K_B was found utilizing both whole-cell and membrane based assay in various cell types, including the same C6MOPr cells, so this does not account for the difference. The discrepancy is indicative of a high level of efficacy for BMS-986122 to activating this pathway. It is unknown if this high efficacy of BMS-986122 to activate ERK1/2 is specific to BMS-986122 or is a more common feature of positive allosteric modulation of MOPr or even other opioid receptors. Indeed, the recently discovered PAM of the delta opioid receptor (DOPr), BMS-986187, is also able to activate ERK1/2 alone as well as activate G protein, inhibit AC, and trigger recruitment of β -arrestin ((Burford *et al.*, 2015); Appendix B), and the cannabinoid CB1 receptor PAM, ORG27569, can activate ERK1/2 through a G protein-independent mechanism (Ahn *et al.*, 2012).

Overall this study has investigated the effects of chronic PAM activity at MOPr and the consequences of enhancement of the efficacy of the gold standard opioid, morphine. It has been found that while BMS-986122 can enhance acute G protein signaling, it does not enhance cellular desensitization, or MOPr phosphorylation and internalization or downregulation. On the other hand BMS-986122 does enhance agonist-mediated signaling in membranes that express desensitized MOPrs suggesting that a PAM may be beneficial for patients already tolerant to opioid medications. Finally, we have shown that BMS-986122 is actually a biased “ago-PAM” and can activate ERK1/2 through a G protein independent pathway. Future work will focus on

understanding the mechanism and consequences of BMS-986122-mediated ERK phosphorylation.

Materials and Methods

Materials: [³H]diprenorphine and [³⁵S]GTPγS (guanosine-5'-(3-thio)triphosphate) were purchased from PerkinElmer. Guanosine diphosphate (GDP), *p*-nitrophenyl phosphate (pNPP), and M2 mouse anti-FLAG antibody conjugated to alkaline phosphatase were from Sigma-Aldrich (St Louis, MO, USA). PTX was from List Biological Laboratories Inc. (Campbell, CA, USA). All tissue culture supplies, including Lipofectamine 2000, were from Invitrogen (Carlsbad, CA, USA) unless otherwise stated.

Cell line and transfection: C6 glioma cells were stably transfected with rat MOPr as described previously. Cells were grown in DMEM containing 10% fetal bovine serum, 1% pen/strep, and 100 μg/mL geneticin (G148) in a 37 °C incubator containing 5% CO₂. HEK293T cells (from AATC) were grown in DMEM supplemented with 10% FBS and 1% pen-strep. (Pen/strep was removed 24 h prior to transient transfection). For transient transfection, cDNA (FLAG-MOPr) in complex with Lipofectamine 2000 reagent in minimal media was added to cells in log phase of growth. Cells were used 48 hours following transfection.

Membrane Preparation: Confluent C6MOPr cells were rinsed with phosphate buffered saline and then detached using harvesting buffer (20 mM HEPES pH 7.4, 0.68 mM EDTA, and 150 mM NaCl). Cells were pelleted following centrifugation at 300g for 3 min at room temperature. Supernatant was discarded and pellet was resuspended in ice-cold 50mM Tris buffer, pH 7.4. Pellet was homogenized using a Tissue Tearor (company) and then centrifuged at 20000g for 20 min at 4 °C. The supernatant was discarded and the pellet as resuspended, homogenized, and centrifuged once more. The final pellet was homogenized in 50 mM Tris, pH 7.4 using a glass dounce homogenizer and aliquots were flash frozen and stored at -80 °C until use in assays. Concentration of protein was determined using a BCA protein assay with bovine serum albumin as the standard.

³H-DPN Saturation Binding Assay: C6- MOPr cell membranes (5 μg/well) were incubated for 90 minutes at room temperature with shaking. Membranes were diluted in 50 mM Tris pH7.4

with various concentrations of ^3H -DPN (0.02-4.0 nM). Nonspecific binding was measured in the presence of saturating naloxone (10 μM).

GTP γ ^{35}S Binding Assays: C6MOPr cell membranes (10 μg /well; prepared as described above) were incubated while shaking for 60 min at 25 $^\circ\text{C}$ in assay buffer (50 mM Tris pH 7.4, 1 mM EDTA, 5 mM MgCl_2 , 100 mM NaCl) containing 30 μM GDP, 0.1 nM $\text{GTP}\gamma^{35}\text{S}$, orthosteric ligand and allosteric ligand (or vehicle). Basal binding was measured in the absence of orthosteric ligand and maximal binding was determined using 10 μM of the full agonist internal standard DAMGO. The reaction was terminated using rapid filtration onto glass GF/C fiber filters (Whatman) and rinsed 6-8 times using 1 mL of cold wash buffer (50 mM Tris pH 7.4, 5 mM MgCl_2 , 100 mM NaCl). The filters were dried and radioactivity was measured using liquid scintillation counting with EcoLume liquid scintillation cocktail (MP Biomedicals) in a Wallac 1450 MicroBeta counter.

P-ERK Assays: C6MOPr cells were plated in 24-well plates the day before the assay to reach 80-90% confluency on the day of the assay and treated with vehicle or pertussis toxin (PTX; 100 ng/mL). The medium was replaced with serum-free DMEM two hours prior to addition of vehicle or BMS-986122 at the indicated concentration. The assay was stopped by aspirating the medium and rinsing the cells twice with ice-cold phosphate buffered saline. Lysates were collected with radioimmuno-precipitation assay buffer [50 mM Tris, pH 7.4, 150 mM NaCl, 1% Triton X-100, 1% sodium deoxycholic acid, 0.1% SDS] plus protease inhibitor, 2mM EDTA, 100 μM NaF, and 10 μM sodium orthovanadate. Lysates were sonicated for 30 seconds and centrifuged at 10000 x g at 4 $^\circ\text{C}$ for 10 min. Supernatant was taken and diluted into SDS sample buffer (62.5 mM Tris-HCl, pH 6.8, 2% SDS, 10% glycerol, 0.0008% bromophenol blue) and beta-mercaptoethanol. Samples were loaded on 12% polyacrilamide gel and subjected to SDS-PAGE followed by transfer to PVDF nitrocellulose membranes for Western blotting. The blot was probed with a 1:2000 dilution of anti-phospho-p44/42 MAPK (ERK1/2) antibody and visualized using horseradish peroxidase (HRP) -conjugated anti-mouse IgG. To ensure equal loading, membranes were stripped and total ERK levels were assessed using 1:1000 dilution of anti-p42/44 MAPK (ERK1/2) antibody.

Phosphorylation of MOPr S375 Assays: C6 MOPr cells were split into 6-well plates to reach 90% confluency for the day of the assay. Briefly, ligand/vehicles were added to the media to reach the indicated concentrations. Media was aspirated at the indicated time and cells were quickly rinsed with ice-cold phosphate buffered saline. Lysates were collected with radioimmuno-precipitation assay buffer [50 mM Tris, pH 7.4, 150 mM NaCl, 1% Triton X-100, 1% sodium deoxycholic acid, 0.1% sodium dodecyl sulfate (SDS)] plus protease inhibitor, 2 mM EDTA, 100 μ M NaF, and 10 μ M sodium orthovanadate. Lysates were sonicated for 30 seconds and centrifuged at 10000 x g at 4 °C for 10 min. The resulting pellet was resuspended in SDS sample buffer and loaded onto a 10% polyacrylamide gel and subjected to SDS-PAGE followed by transfer to PVDF nitrocellulose membranes for Western blotting. The blot was incubated overnight at 4 °C with a 1:1000 dilution of the anti phosphor- S375 MOPr antibody and visualized using HRP conjugated secondary antibody.

Internalization Assays: HEK293T cells were grown to 80% confluency prior to transient transfection with FLAG tagged MOPr. 24 h following transfection, cells were seeded (0.75×10^6 cells per well) onto poly-d-lysine coated 24-well plates. 24 h following splitting, the cells were treated with drug (or vehicle) in the presence of allosteric ligand (or vehicle) for 10 min at 37C in DMEM. At the end of the incubation period, the cells were fixed with 3.7% formaldehyde in Tris-buffered saline [(TBS), 25 mM Tris-HCl, pH 7.4, 2.7 mM KCl, 140 mM NaCl] for 5 min at 4 °C. The cells were washed three times with TBS, blocked with 1% non-fat dry milk made up in TBS for 1 h at room temperature and washed two times with TBS and incubated with monoclonal anti-FLAG M2 alkaline phosphatase antibody for 1 h at 23 °C. Cells were washed five times and incubated with *p*-nitrophenyl phosphate for 30 min at 23 °C. 0.2 mL aliquots were added to 0.05 mL 3 N NaOH in a 96-well plate. Absorbance at 405 nm was measured using a VERSAmax tunable microplate reader (Molecular Devices, Sunnyvale, CA, USA). The percentage of receptors internalized was calculated using the following equation: $[1 - (\text{Drug O.D.} - \text{Background O.D.}) / (\text{Control O.D.} - \text{Background O.D.})] \times 100$, where O.D. is optical density. Background was defined as the absorbance of untransfected HEK293 cells and control as absorbance from untreated FLAG MOPr expressing cells.

Data analysis: Concentration-effect curves from GTP γ ³⁵S binding assays and ERK1/2 activation Western blots were fit to sigmoidal concentration-effect curves using GraphPad Prism 6.01 to

determine EC_{50} values and maximal effects. Saturation binding data were fit to a one-site hyperbolic function after nonspecific binding was subtracted. K_d and B_{max} values were obtained using GraphPad Prism 6.01. Data presented are means and SEM from at least 3 independent experiments unless otherwise noted.

CHAPTER 6

Discussion and Future Directions

Summary and significance

Studies described in this thesis investigated allosteric modulation of the mu opioid receptor (MOPr) in the context of receptor:ligand interactions and cellular signaling, both acutely and chronically. The positive allosteric modulators (PAMs) discussed in this thesis, particularly BMS-986122, represent the first molecules unequivocally shown to be PAMs at MOPr.

I have shown that BMS-986122 functions at the MOPr by allosterically disrupting the binding of Na⁺ ion, an endogenous negative allosteric modulator of MOPr, and that the actions of BMS-986122 are probe dependent, that is they are contingent on the ligand occupying the orthosteric binding site. Moreover this probe dependence is based on the efficacy of the orthosteric agonist. I have also demonstrated that this mechanism of allosteric activity is not unique to MOPr or to BMS-986122, and have described the non-selective positive allosteric ligand BMS-986187 as a PAM of both the delta opioid receptor (DOPr) and MOPr with the same mechanism of action at both. This work also indicates that MOPr and DOPr may share a common allosteric binding site capable of recognizing structurally diverse ligands. Next, I developed and implemented a biophysical technique to quantify intrinsic efficacy of both allosteric and orthosteric ligands of the MOPr in a cell-free manner and used it to verify our hypothesis that MOPr PAMs stabilize active state conformations of MOPr. Finally, I have explored the effects of chronic MOPr PAM activity in cellular models of desensitization and tolerance, finding that BMS-986122 selectively enhances signaling through G protein over enhancement of receptor desensitization.

This work provides proof of principle of a novel way to target MOPr, one of the most pharmacologically important G protein-coupled receptors (GPCRs). Such an approach could lead to major changes in the management of pain, as a MOPr PAM could be capable of pain relief through the enhancement of endogenous opioid peptide activity which would preserve their

spatial and temporal regulation. In addition, the mechanism of allostery I have proposed is likely to be important for other class A GPCRs that bind to and are regulated by Na⁺ ions. Indeed, I have already shown this to be the case for an additional GPCR, DOPr (Chapter 3). Furthermore, the novel assay I present in Chapter 4 for the determination of intrinsic efficacy of orthosteric and allosteric ligands can readily be applied to other GPCRs as a way to measure efficacy of ligands in preclinical settings to better predict *in vivo* activity. This measurement of efficacy is cell-free and does not depend on signaling output. Finally, work in Chapter 5 suggests that allosteric ligands at MOPr have the potential for signaling bias and also the potential to enhance the desired effects (i.e. G protein activation), but not detrimental signaling (i.e. desensitization and tolerance) of clinically used opioids, such as morphine. This raises the possibility of creating an allosteric ligand that can enhance the pain-relieving effects of currently used opioids while not increasing tolerance, thereby enhancing their therapeutic potential.

Future directions

Though this body of work has answered many questions regarding the mechanisms and consequences of PAM activity at MOPr, it has also raised additional questions regarding allosteric modulation at MOPr and DOPr that should be a focus of future research. In the following sections, I will discuss these future directions and provide both my hypotheses and possible methods for addressing them.

Identification of MOPr-PAM binding site

One of the most pressing questions involves the binding site of BMS-986122 and the other allosteric ligands. From Chapter 4, we know that BMS-986122 and BMS-986187 bind directly to the receptor to modulate receptor function. They do not bind at a secondary protein or at the interface of the receptor with any other protein since they both show allosteric activity at purified MOPr reconstituted as monomers into high-density lipoproteins (rHDL). We can make some provisional inferences of the binding site of BMS-986122 based on published work of other GPCRs.

Several class A GPCR X-ray crystallographic structures in complex with an allosteric ligand have recently been solved. What stands out is that each allosteric ligand binds in a different location on the GPCR, highlighting the possibility that there are several allosteric sites

on any given GPCR. For instance, the free fatty acid receptor (FFAR1) structure in complex with the allosteric ligand TAK-875 shows the ligand binding via the lipid bilayer with extensive contacts in TM3, TM4, and extracellular loop 2 (ECL2) (Srivastava *et al.*, 2014). Whereas FFAR1 and opioid receptors share low sequence homology and there is no support for MOPr PAMs binding in a similar manner, it cannot be ruled out. Indeed, all of our MOPr PAMs are lipophilic with several halogen groups (Burford *et al.*, 2013; Bisignano *et al.*, 2015; NT Burford *et al.*, 2015) so they could potentially partition into the membrane bilayer. In addition, the C-C chemokine receptor type 5 (CCR5) in complex with the HIV drug maraviroc was recently solved (Tan *et al.*, 2013). While maraviroc is allosteric and does not compete with the endogenous chemokine, it was observed to bind to a site analogous to the orthosteric site of MOPr (Tan *et al.*, 2013). However, the allosteric site on MOPr is not the orthosteric site as my work shows that PAMs do not displace orthosteric ligands (Burford *et al.*, 2013; Livingston and Traynor, 2014; Bisignano *et al.*, 2015).

Presently, there is only one X-ray crystal structure of a Class A GPCR in complex with an allosteric ligand *and* an agonist: the M2 acetylcholine receptor in complex with the agonist iperoxo and the PAM LY2119620 (Kruse *et al.*, 2013). The binding site of LY2119620 may share some commonalities with the BMS-986122 binding site on MOPr. Indeed, recent molecular dynamics simulation studies performed with MOPr using BMS-986122 hypothesized that the MOPr PAM interacts with residues 6.58 and 7.35, analogous to those residues that LY2119620 interacts with in the M2R (Bartuzi *et al.*, 2016). In addition, another group performed simulations using BMS-986187 at DOPr and also found that residues 6.58 and 7.35 play a role in PAM binding (Shang *et al.*, 2016). From Chapter 3, I hypothesize that these allosteric sites on MOPr and DOPr are analogous. These data support that the binding site of the PAMs described in this thesis may be analogous to the binding site of LY2119620 on the M2R. Mutagenesis of residues 6.58 and 7.35 should be performed to determine the role of these residues in the activity of BMS-986122.

Currently, our lab is working with collaborators to obtain a crystal structure of MOPr in complex with a PAM. One of the problems is the poor solubility of the current modulators and the low affinity they have for agonist-free receptor (μM range; Chapter 2; Chapter 3). This means that the structure will likely need to be a co-crystal in the presence of both an agonist and Nb39 or G protein. In the presence of an agonist, the affinity of BMS-986187 improves to ~ 100

nM (Chapter 4) which is more amenable to crystallography. As such, we are concurrently working with medicinal chemists to develop novel MOPr PAMs with enhanced affinity and solubility more suited for both crystallography as well as *in vivo* work (discussed later). Also conceivable would be the crystallization of inactive MOPr with a SAM or NAM that would not depend on the presence of an agonist or G protein. Currently, the SAMs we have also have μ M affinity and there are no known NAMs of MOPr.

A more straightforward approach that could be done is to analyze the activity of BMS-986187 at various species of MOPr (human, rat, mouse, etc). As most species' opioid receptors bind opioid peptides (although some species have lost opioid peptide expression while retaining the receptors (Dores *et al.*, 2002)), divergence arises in areas of the proteins not involved in the binding of orthosteric ligands- namely allosteric sites (Dreborg *et al.*, 2008). This evolutionarily-driven mutagenesis could yield information regarding the BMS-986122 binding site and could be determined by calculating K_B at each of the receptor types.

Identification of potential endogenous opioid receptor PAM

Due to the ability of both MOPr and DOPr to bind the same allosteric ligands (Chapter 3), albeit with different affinities, I hypothesize that there is an allosteric site that is somewhat conserved between the two receptors. Phylogenetically, it is thought that MOPr and DOPr share a common ancestral GPCR and that they are more similar to one another compared to the other opioid receptors (Dreborg *et al.*, 2008). It is possible that the PAMs in this thesis, specifically BMS-986122 and BMS-986187, also bind to kappa opioid receptor (KOPr) and the nociceptin/orphanin FQ opioid receptor (NOPr). Preliminary work has failed to show PAM activity at either of these receptors (*data not shown*), but due to probe dependence, we may not have used the correct agonist. In addition, these PAMs may be silent allosteric ligands at KOPr and NOPr. However, due to a lack of PAMs at these receptors, it is currently impossible to test this theory. In the future, if PAMs for KOPr and NOPr are discovered, their reversal by BMS-986122 and BMS-986187 could be evaluated.

Due to this possible conservation between allosteric sites on MOPr and DOPr, it is tempting to speculate the existence of an endogenous allosteric modulator of MOPr and DOPr. Attempts to find a potential endogenous allosteric ligand could be made using metabolomics screens or screens of known endogenous molecules (such as the Screen-Well from Enzo® that

contains compounds with biological activity whose target proteins have not yet been identified). Screens could be performed looking for enhancement of signaling by the endogenous opioid peptides, with cooperativity being presumed but not certain. Another approach that would be independent of a chosen orthosteric ligand would be to look for displacement of a radiolabeled PAM, although to date we do not have compounds with sufficiently high affinity

Identification of signaling pathway for BMS-986122 mediated activation of MAPK

In Chapter 6, I found that BMS-986122 activates MAPK in a G protein independent manner and I hypothesize occurs through arrestin-2. From the initial discovery of BMS-986122, we know that BMS-986122 does not recruit arrestin-3 alone as measured using the DiscoverX® PathHunter assay (Burford *et al.*, 2013). But, because the G protein independent MAPK activation is slow to peak and sustained, it is presumably arrestin-mediated, leaving arrestin-2 as the subtype capable of generating this signal. Furthermore, recent studies I have performed using the AlphaScreen® system (Garbison *et al.*, 2015) have found that BMS-986122-activated MAPK is not cytosolic (*unpublished data*).

Downstream of MOPr, G protein activated MAPK stays in the cytosol while arrestin-activate MAPK translocates to the nucleus (Zheng *et al.*, 2008). Furthermore, ligands that can internalize MOPr robustly can recruit both arrestin-2 and arrestin-3, suggesting the arrestin-3 may play more of a role in trafficking of MOPr whereas arrestin-2 may be involved in other signaling, though this is speculative. From these data, I hypothesize that BMS-986122 fails to enhance internalization and receptor desensitization because it selectively engages arrestin-2 and activates MAPK. Mouse embryonic fibroblasts (MEFs) that lack arrestin-2, arrestin-3, or both arrestin-2/3 stably expressing MOPr can be employed to further probe the mechanism of BMS-986122-mediated MAPK activation.

Validation of MOPr-PAM activity in rodent models of antinociception

Potential therapeutic use of the allosteric modulators is predicated by their ability to enhance antinociception in rodent models of acute and chronic pain. But, this must be validated. BMS-986122 has recently been tested *in vivo* in our laboratory using rodent models of antinociception, particularly the hot plate assay that measures thermal latency (Woolfe and MacDonald, 1944; O'Callaghan and Holtzman, 1975). Due to the unknown pharmacokinetic

profile of BMS-986122 (and limited compound), BMS-986122 was administered intracerebroventricularly (i.c.v.) and it was found that it enhanced thermal latency on its own. Importantly, this enhancement was blocked by pretreatment of the animal with the opioid antagonist naloxone and or when using MOPr global knockout mice (Fig 6.1). As stated above, we are working with chemists to develop higher affinity compounds that could potentially cross the blood brain barrier for future studies.

In addition to acute antinociception, the ability of a MOPr PAM to treat pain chronically should be evaluated. As shown in Chapter 5, BMS-986122 did not cause desensitization and cellular tolerance on its own nor did it enhance the ability of agonists to cause these effects. This suggests that BMS-986122 should not cause tolerance *in vivo*, but the studies I performed were in cultured cells that lack neuronal connections and circuitry. While tolerance does begin at the level of the receptor, it is hypothesized that circuit-level adaptations also occur with the formation of tolerance and dependence in animals and humans (Williams *et al.*, 2001; Kosten and George, 2002).

Investigation of abuse potential of MOPr PAMs

Opioid agonists used in the clinic cause euphoria and therefore have an addictive liability. MOPr PAMs should be evaluated in rodent models of self-administration and conditioned place preference as well as antinociception. If BMS-986122 causes conditioned place preference or elicits self-administration alone in animal models, this is indicative of addictive liability (Cunningham *et al.*, 2006; O'Connor *et al.*, 2011). Ideally, a MOPr PAM would have enough allosteric efficacy and/or signaling bias to enhance enkephalin-mediated analgesia but not other effects, especially because the PAM maintains the temporal and spatial activity of the endogenous opioid peptides.

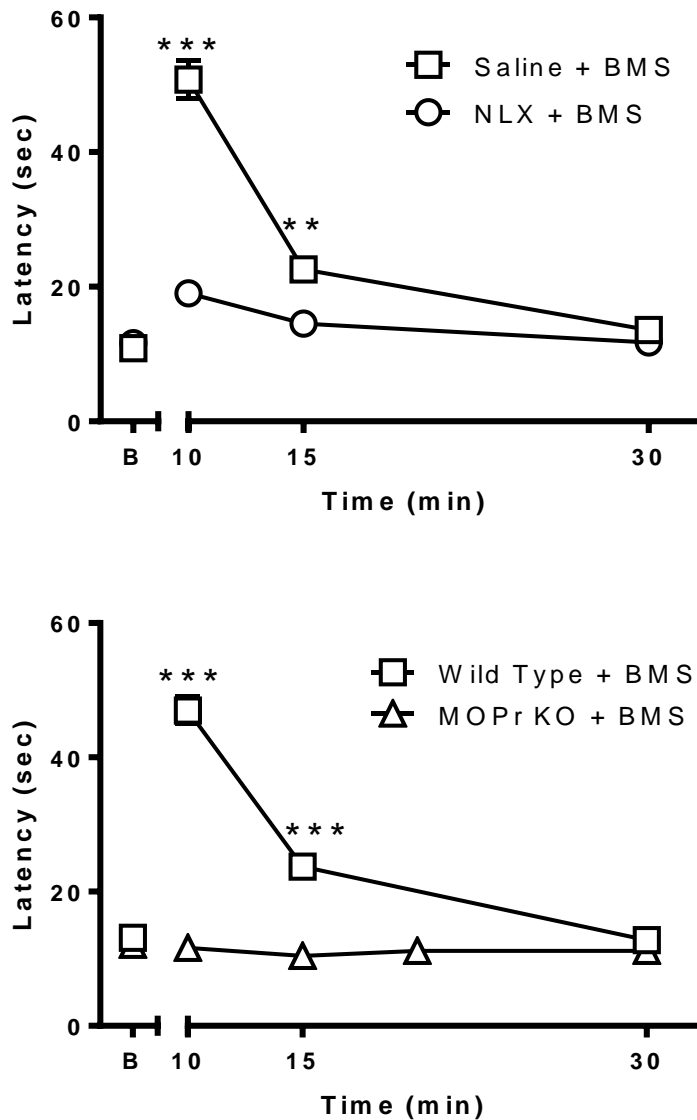


Figure 6.1: BMS-986122 antinociception mediated through MOPr. Pretreatment (30 min) with the nonselective opioid antagonist naloxone (1.0 mg/kg) blocked the antinociceptive effects of BMS-986122 (1.5 nmols) ($n = 6$ per group) (top figure). Antinociceptive effects of 1.5 nmols BMS-986122 are abolished in MOPr homozygous null (-/-) knockout mice ($n = 8$) (bottom figure). ** $P < 0.01$; *** $P < 0.001$ vs. vehicle control groups. NLX = naloxone; BMS = BMS-986122 [Experiments performed by Todd Hillhouse and James Hallahan].

Overall conclusions

As a whole, this body of works mechanistically describes the acute and chronic cellular and receptor-level consequences of PAM activity at the MOPr. It provides the basis for future preclinical studies to develop a novel method of pain management in humans and establishes a new method for assessing the efficacy of allosteric and orthosteric ligand for this receptor. MOPr PAMs can enhance the intrinsic efficacy of both endogenous opioid peptides as well as clinically used opioids while sparing the enhancement of tolerance and desensitization that result from chronic exposure. These ligands have great potential as novel therapeutics and future work will aim to push these ligands closer to clinical studies.

APPENDIX A

Identification of Slowly Dissociating Mu Opioid Receptor Agonists for Use in X-ray Crystallography²

Recent technological advances in biochemical methods have aided in solving x-ray structures of many different G protein-coupled receptors (GPCRs), proteins once thought too dynamic for such endeavors (for review see (Ghosh *et al.*, 2015)). Since the first structures of rhodopsin (Palczewski *et al.*, 2000) and the β 2-adrenergic receptor ((β_2AR) ;(Cherezov *et al.*, 2007)) in 2000 and 2007 respectively, over 125 structures of GPCRs in both inactive and active states have been solved. Mechanistic insights into the binding and activation of receptors by agonists have been examined for both the β 2AR and the M2 muscarinic acetylcholine receptor (M2R), with both inactive and active state crystal structures existing for both (Rasmussen, DeVree, *et al.*, 2011; Haga *et al.*, 2012; Kruse *et al.*, 2013).

In 2012, the crystal structure of the inactive mouse mu opioid receptor (MOPr) in complex with the irreversible morphinan antagonist β -funaltrexamine (β -FNA) was solved (Manglik *et al.*, 2012). With this structure came the confirmation of decades of structure-activity and mutagenesis work concerning the crucial residues involved in ligand recognition, including W318^{7,35}, a residue proposed to be involved with the ‘address’ portions of opioid ligands in the “message-address” hypothesis of opioid selectivity (Lipkowski *et al.*, 1986). While the inactive-state structure provides a lot of information, active-state structures give insights into determinants of agonist activity which would be beneficial for MOPr, one of the most pharmacologically targeted GPCRs in the world.

² Parts of this work were published in Nature. Huang W, Manglik A, Venkatakrisnan AJ, Laeremans T, Feinberg EN, Sanborn AL, Kato H, Livingston KE, Thorsen TS, Kling R, Granier S, Gmeiner P, Traynor JR, Weis WI, Steyaert J, Dror RO, Kobilka BK. “Structural Insights into μ -Opioid Receptor Activation.” *Nature*. 2015 Aug 20; 524: 315-321. © Nature Publish Group 2015.

One of the impediments in obtaining active-state structures of GPCRs is having an agonist capable of stabilizing an active-state receptor long enough to develop an active-state antigen *in vivo* following immunization and also to grow homogenous crystals (Steyaert and Kobilka, 2011). Ligands with fast kinetics of binding, particularly those with fast dissociation rates, are not well-suited due to the protein dynamics associated with binding and unbinding. In order to find a slowly dissociating ligand compatible with crystallography of active-state MOPr, we utilized the method of Motulsky-Mahan to measure the dissociation rates of various unlabelled opioid agonists (Motulsky and Mahan, 1984).

Briefly, for this method the association rate of a radiolabeled antagonist with known kinetics is measured in the presence of varying concentrations of cold ligand with two basic phenotypes resulting (Fig A.1). For competitive ligands with dissociation rates that are faster than the radiolabeled ligand, all curves will be exponential with a decrease in max as the concentration of cold ligand increases. In contrast, if the cold ligand dissociates slower than the labeled ligand, the association will be exponential at first (assuming the association rates of the labeled and unlabelled ligands are relatively equal) but soon diminish as receptor sites are occupied with the slowly dissociating cold ligand, creating an ‘overshoot.’ Mathematical models can be used which incorporate the known k_{on} , k_{off} , and concentration of radioligand as well as the concentration of cold ligand in order to calculate the k_{on} and k_{off} of the cold ligand. Validity of the assay was confirmed by calculating K_d values from the calculated rates and comparing them with known affinity values for the test ligands.

In order to choose ligands to screen, we focused on MOPr agonists that were high efficacy (at least 90% stimulation compared to the endogenous ligand standard), high affinity (K_i less than 1 nM), and molecules that were non-peptidic to minimize ligand flexibility. In addition, several clinical compounds known to be slowly dissociating, namely methadone and buprenorphine, were also tested (Kosterlitz *et al.*, 1975; Virk *et al.*, 2009).

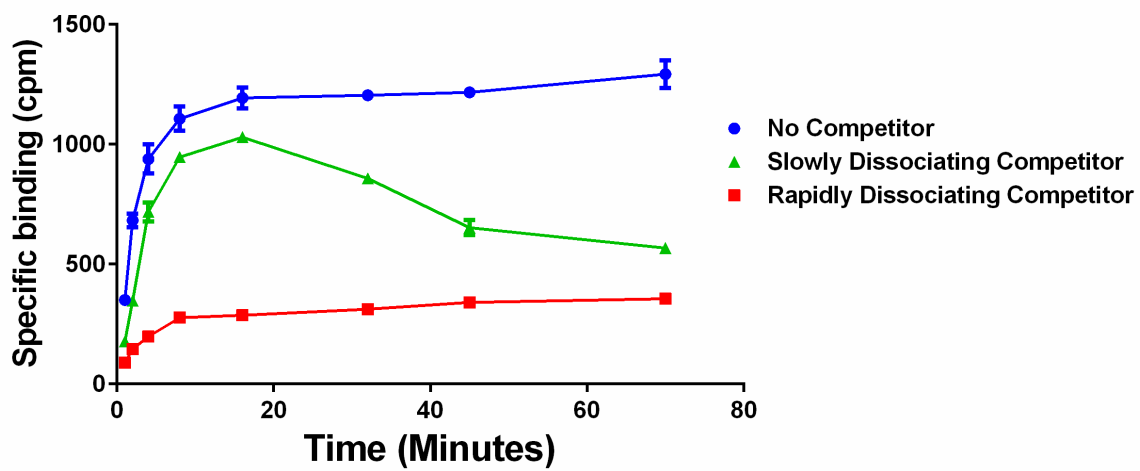


Figure A.1: Prototypic results from Mahan-Motulsky. The association of a radiolabelled antagonist over time is shown in blue. The association is altered in the presence of either a slowly dissociating competition (green) or a rapidly dissociating competitor (red).

The β 2AR-Gas structure was solved in complex with the highly efficacious, high affinity agonist BI-167107 which had a dissociation half-time ($t_{1/2}$) of over 30 hours (Rasmussen, DeVree, *et al.*, 2011). While this was the goal for MOPr, such a slowly dissociating ligand was not found. After screening over a dozen ligands, the slowest ligands were: BU97008, 14-phenylpropoxymetopon (PPOM;(Schutz *et al.*, 2003)), BU9609, and BU72 (Fig A.2) with $t_{1/2}$ dissociation times of approximately 231, 122, 100, and 70 min respectively. In addition, all four ligands were full agonists at activation of GTP γ ³⁵S binding in C6MOPr cell membranes with affinity of less than 0.5 nM (*data not shown*).

Of these four ligands, only one succeeded in producing crystals that diffracted: BU72. BU72 is a buprenorphine analog with subnanomolar affinity and agonist activity at MOPr, delta opioid receptor, and kappa opioid receptor (Neilan *et al.*, 2004; Divin *et al.*, 2008). It is a potent analgesic in rodents, but has a very narrow therapeutic index with high levels of respiratory depression, limiting its utility as a drug. In contrast to our general hypothesis, BU72 was not the slowest dissociating ligand tested, emphasizing that other characteristics of the ligand are important for successful crystal formation and diffraction (Hassell *et al.*, 2006).

All of the ligands were initially screened used cell membranes prepared from C6 cells stably expressing rat MOPr. Once the crystals were shown to diffract and the structure was in the process of being resolved, the kinetics of BU72 at the purified MOPr construct used for crystallography were examined. Purified MOPr was reconstituted into high-density lipoproteins (MOPr-rHDL) and, using the Motulsky-Mahan method, the $t_{1/2}$ of dissociation of BU72 from MOPr-rHDL was found to be 43 min (Fig A.3). For the crystal structure, the receptor was stabilized in the active state using camelid antibody nanobody 39 (Nb39). To understand the influence of Nb39 on BU72 affinity and binding kinetics, competition binding of BU72 for 3H-diprenorphine (³H-DPN) was performed in the MOPr-HDL system with and without Nb39. As expected, Nb39 (3 μ M) increased the affinity of BU72 by 10-fold from 0.8 nM (95% CI: 0.4 - 1.6 nM) to 0.09 nM (95% CI: 0.06 - 0.13 nM) (Fig A.4). (This concentration of Nb39 was chosen because at higher concentrations, Nb39 inhibited ³H-DPN binding. *Data not shown*). In addition, the effect of Nb39 on the dissociation kinetics of BU72 was tested. The Motulsky-Mahan method was performed and the $t_{1/2}$ of dissociation of BU72 was 140 minutes in the presence of 3 μ M Nb39 (Fig A.3).

Another facet of BU72 binding that is unique is its sensitivity to Na⁺. Opioid agonist binding is highly dependent on the concentration of Na⁺ present (Pert and Snyder, 1976; Selley *et al.*, 2000). In addition, this sensitivity to Na⁺ is correlated with the efficacy of the ligand with higher efficacy ligands showing greater shifts in the affinity by the addition of sodium. Using Ehlert's equation, the intrinsic efficacy of BU72 is 4.7 which is the same as etorphine (Chapter 2; (Livingston and Traynor, 2014)). In contrast to this high efficacy, the shift in affinity of BU72 by the addition of Na⁺/GTP is quite small (six-fold) from 0.38 ± 0.04 nM (in 100 mM NaCl/ 10 μ M GTP) to 0.06 ± 0.02 nM (in Tris pH 7.4) as found doing competition binding in C6MOPr cells. As we have previously shown the sodium-insensitive ligand etorphine to also be insensitive to allosteric modulation by BMS-986122 (Chapter 2), we investigated if the affinity of BU72 would be enhanced by BMS-986122. The data matched etorphine in that BU72 was also insensitive to enhancement in affinity by BMS-986122 ($K_i = 0.39 \pm 0.02$ nM with 10 μ M BMS-986122).

In addition to understanding the binding kinetics of BU72 and its cooperativity with Nb39, we investigated the potential to BU72 to be a biased ligand. In order to validate this, the ability of BU72 to activate ERK1/2 in C6MOPr cells was determined by using SDS-PAGE followed by western analysis. BU72 (10 nM; $\sim 10 \times K_d$) exposure caused robust ERK1/2 activation that peaked at 5 min. Overnight pretreatment of the C6MOPr cells with PTX (100 ng/mL) blocked the early phase of ERK1/2 activation, indicating that the majority of ERK1/2 activation was caused by G proteins (Fig A.4). To validate that BU72 was also not overtly biased towards G protein, we assessed the ability of it to cause MOPr internalization. Utilizing an ELISA based internalization method, the ability of BU72 to cause MOPr internalization was compared to an endogenous ligand that is known to be unbiased, leucine-enkephalin (Leu-Enk) (McPherson *et al.*, 2010). BU72 caused the same degree of internalization as Leu-Enk, indicating no overt bias (Fig A.5).

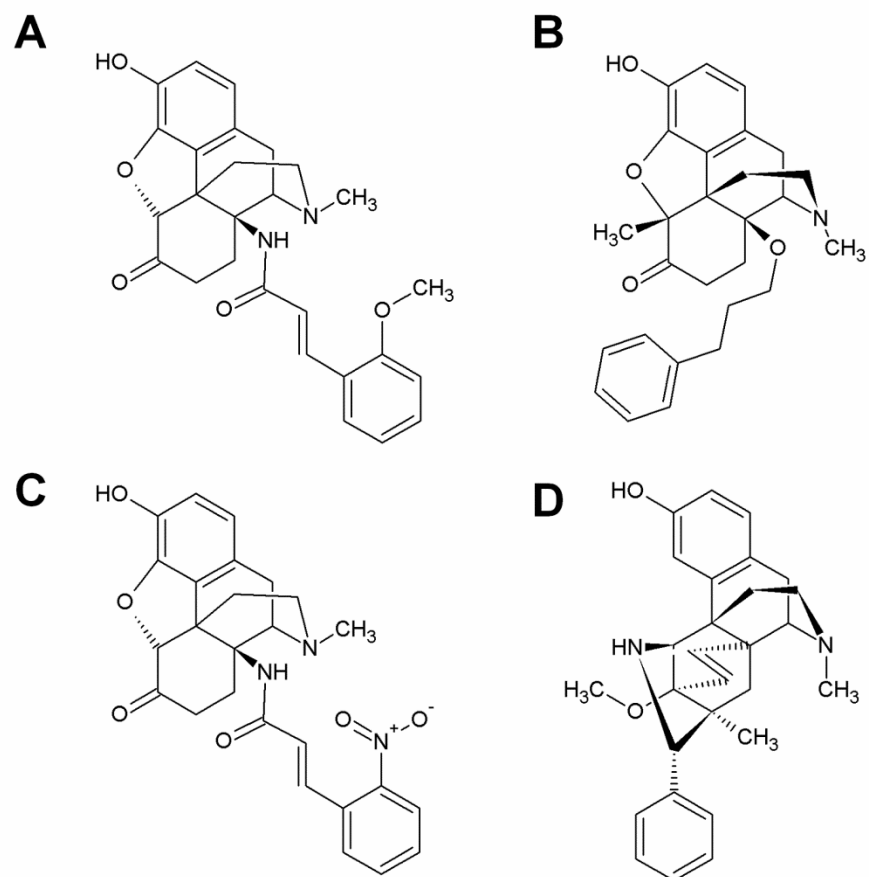


Figure A.2: Structures of BU97008 (A), PPOM (B), BU9609 (C), and BU72 (D).

Upon final refinement and solving of the crystal structure of active MOPr in complex with Nb39 and BU72, the relatively fast dissociation of BU72 compared to BI-167107 could be explained (Huang *et al.*, 2015). The binding pocket of MOPr, even in an active state, is more open than compared to the β 2AR and the M2R (Rasmussen, DeVree, *et al.*, 2011; Kruse *et al.*, 2013). This orthosteric site, which must be large enough to accommodate the binding of the endogenous β -endorphin (31 amino acids), remains open even in the active state which supports the generally fast association and dissociation of even the highest affinity opioid agonists. In addition, subsequent NMR studies on BU72 association with MOPr revealed BU72 to be a “superagonist” that was able to stabilize active-state MOPr better than traditional full agonists like DAMGO (Sounier *et al.*, 2015), indicating that this ligand may have unique properties that engender its ability to stabilize the MOPr-Nb39 crystal complex as compared to the other slower dissociating agonists BU9609 and PPOM. Overall, this study established the use of the Motulsky-Mahan method in a purified MOP-rHDL system to find tools to aid in the crystallography of an active-state GPCR.

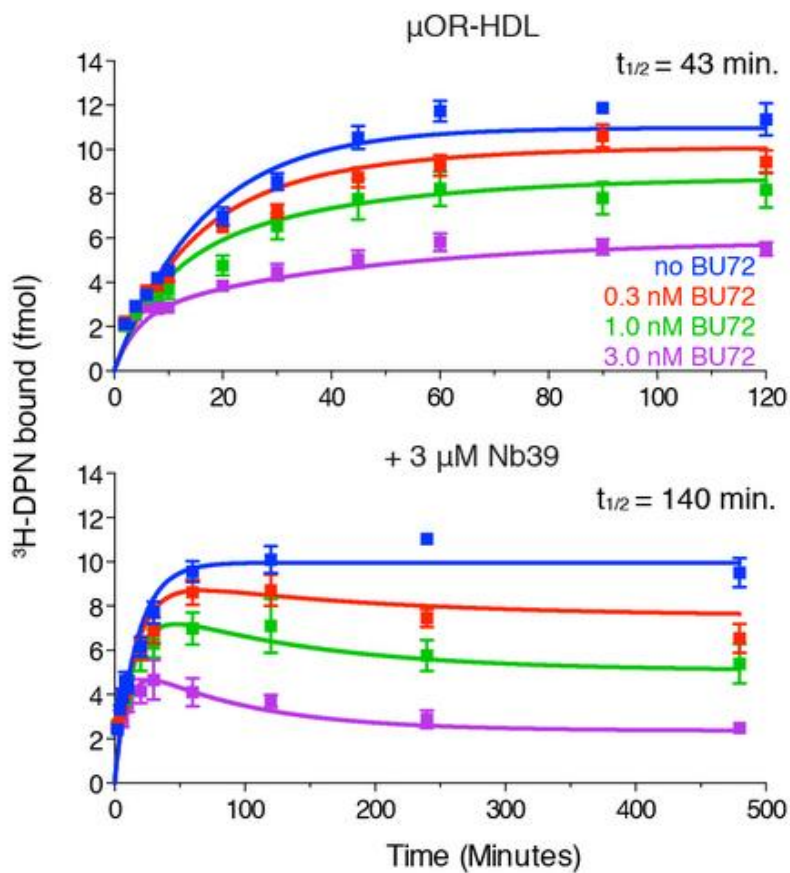


Figure A.3: Motulsky-Mahan experiments of BU72 in the absence or presence of Nb39. The dissociation half-life ($t_{1/2}$) of BU72 was determined by measuring the association rate of the antagonist ³H-DPN in the presence of the indicated concentrations of BU72. The dissociation $t_{1/2}$ of BU72 is 43 min (top) and increases to 140 min in presence of Nb39 (bottom) (Figure from (Huang *et al.*, 2015)).

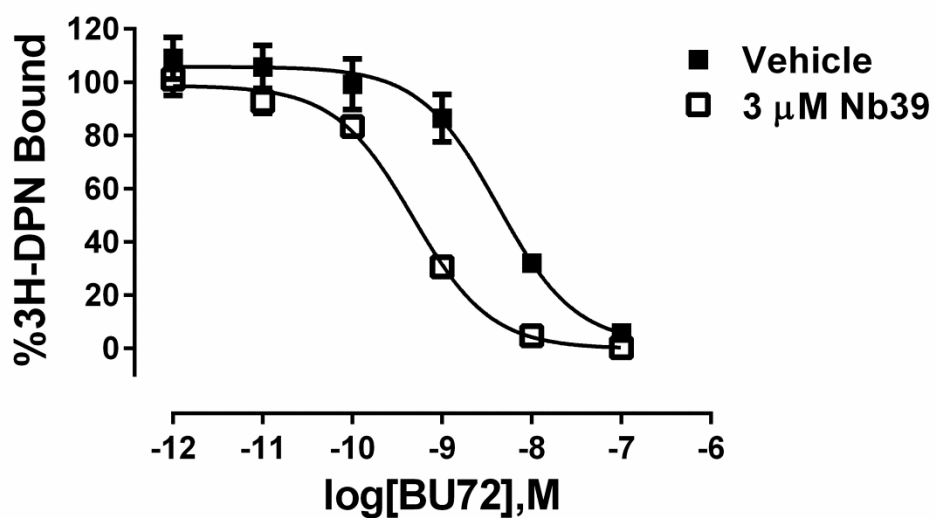


Figure A.4: Enhancement in affinity of BU72 to bind MOPr rHDL in the presence of Nb39. The ability of BU72 to displacement ³H-DPN in MOPr rHDL was measured in the absence or presence of 3 μM Nb39. Data shown are means ± SEM of 3 independent experiments each in duplicate. Data were fit using nonlinear regression to a one-site curve using GraphPad Prism 6.02.

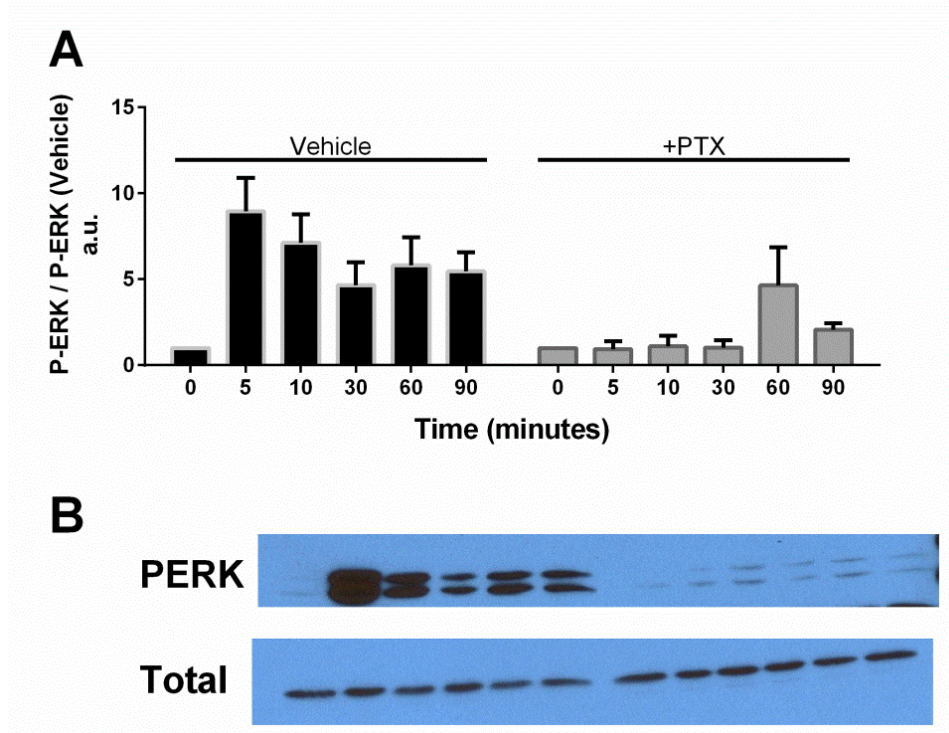


Figure A.5: Time course of BU72 mediated ERK1/2 activation. Time course of BU72 (10 nM) was performed in C6MOPr cells pretreated overnight with vehicle or PTX (100 ng/mL). Samples were analyzed using SDS-PAGE followed by western blot. A) Quantified data for 3 separate experiments. B) Representative image showing samples loaded in the same order as the bar graph in A.

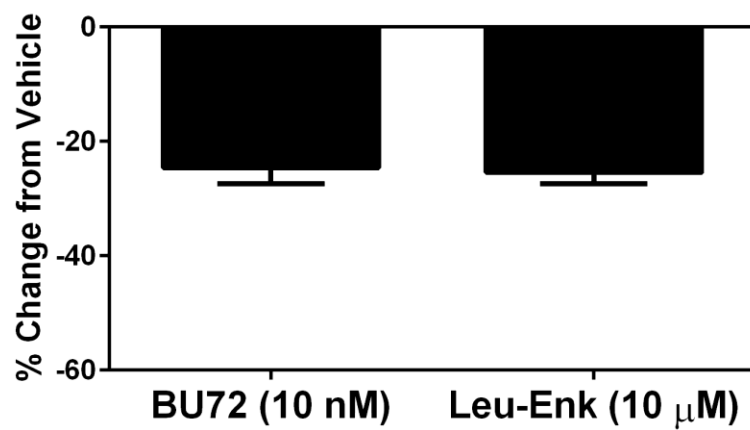


Figure A.6: BU72 internalizes MOPr to the same extent as the endogenous ligand Leu-Enk. HEK293T cells transiently expressing FLAG tagged MOPr were used to monitor the internalization caused by agonist exposure for 10 minutes. Data shown are mean and SEM from 3 independent experiments performed in quadruplicate.

Materials and Methods

Materials: [³H]diprenorphine and [³⁵S]GTPγS (guanosine-5'-(3-thio)triphosphate) were purchased from PerkinElmer. Guanosine diphosphate (GDP), *p*-nitrophenyl phosphate (pNPP), and M2 mouse anti-FLAG antibody conjugated to alkaline phosphatase were from Sigma-Aldrich (St Louis, MO, USA). PTX was from List Biological Laboratories Inc. (Campbell, CA, USA). All tissue culture supplies, including Lipofectamine 2000, were from Invitrogen (Carlsbad, CA, USA) unless otherwise stated.

Cell line and transfection: C6 glioma cells were stably transfected with rat MOPr as described previously. Cells were grown in DMEM containing 10% fetal bovine serum, 1% pen/strep, and 100 μg/mL geneticin (G148) in a 37 °C incubator containing 5% CO₂. HEK293T cells (from AATC) were grown in DMEM supplemented with 10% FBS and 1% pen-strep. (Pen/strep was removed 24 h prior to transient transfection). For transient transfection, cDNA (FLAG-MOPr) in complex with Lipofectamine 2000 reagent in minimal media was added to cells in log phase of growth. Cells were used 48 h following transfection.

Membrane Preparation: Confluent C6-MOPr cells were rinsed with phosphate buffered saline and then detached using harvesting buffer (20 mM HEPES pH 7.4, 0.68 mM EDTA, and 150 mM NaCl). Cells were pelleted following centrifugation at 300 g for 3 min at room temperature. Supernatant was discarded and pellet was resuspended in ice-cold 50 mM Tris buffer, pH 7.4. Pellet was homogenized using a Tissue Tearor (company) and then centrifuged at 20000 g for 20 min at 4 °C. The supernatant was discarded and the pellet as resuspended, homogenized, and centrifuged once more. The final pellet was homogenized in 50 mM Tris, pH 7.4 using a glass dounce homogenizer and aliquots were flash frozen and stored at -80 °C until use in assays. Concentration of protein was determined using a BCA protein assay with bovine serum albumin as the standard.

Reconstitution of MOPr: Purified MOPr was reconstituted into high-density lipoprotein (HDL) particles comprised of the lipids POPC and POPG (Avanti Polar Lipids) in a 3:2 molar ratio as previously described (Whorton *et al.*, 2007).

Radioligand binding assays: For competition binding experiments in MOPr- rHDL, a mixture of MOPr-rHDL and ³H-diprenorphine (³H-DPN) was incubated with varying concentrations of agonist in a binding buffer comprised of 25mM HEPES pH 7.4, 100mM NaCl, and 0.1% BSA in the presence or absence of 3 μM Nb39. For assays performed using cell membranes, conditions listed were kept the same except for exclusion of BSA and inclusion of 10μg protein per well. Binding reactions were incubated for 2 h at 25°C. Free radioligand was separated from bound radioligand by rapid filtration onto a Whatman GF/C filter pretreated with 0.1% polyethylenimine using a 24-well harvester (Brandel). Nonspecific binding was measured in the presence of 10μM naloxone, an opioid antagonist. Radioligand activity was measured by liquid scintillation counting using a Wallac 1450 MicroBeta counter (Perkin Elmer). Competition binding data were fit to a one-site model using GraphPad Prism 6.0.

Mahan Motulsky Assay: Dissociation studies for BU72 were performed using the method of Motulsky and Mahan (Motulsky and Mahan, 1984). ³H-DPN was diluted in an assay buffer comprised of 20 mM Tris, pH 7.4, 150 mM NaCl, and 0.05% BSA containing MOPr in HDL particles with either vehicle or different concentrations of BU72 alone or in the presence of Nb39. Binding reactions were incubated at 25 °C in the dark and nonspecific binding was determined in the presence of 10 μM naloxone. Aliquots of this binding reaction were removed at specified time points over the course of 2-8 h and filtered through Whatman GF/C filters with the aid of a Brandel harvester. As above, radioligand activity was measured by liquid scintillation counting. Dissociation rates for BU72 were determined by fitting data in the ‘kinetics of competitive binding’ program in GraphPad Prism 6.02. For K1 and K2, rates of 3H-DPN association and dissociation were determined through independent studies following the same method as above.

Purification of MOPr: Full length *Mus musculus* MOPr bearing an amino-terminal Flag epitope tag and a carboxy-terminal 6xHis tag was expressed in Sf9 insect cells using the BestBac baculovirus system (Expression Systems). A tobacco etch virus (TEV) protease recognition sequence was inserted after residue 51 and a rhinovirus 3C protease recognition sequence was inserted before residue 359 for cleavage during purification. Insect cells were infected with baculovirus encoding MOPr 48–60 h at 27 °C. Receptor was solubilized and purified in a final

buffer comprised of 25 mM HEPES pH 7.4, 100 mM NaCl, 0.01% MNG (Anatrace), and 0.001% cholesterol hemisuccinate (CHS), as previously described (Manglik *et al.*, 2012).

Purification of Nb39: Nb39 was purified as described (Huang *et al.*, 2015). Briefly, Nb39 bearing a carboxy-terminal His tag were expressed in the periplasm of Escherichia coli strain WK6 grown in Terrific Broth medium containing 0.1% glucose, 2 mM MgCl₂, and 50 mg/ml ampicillin and induced with 0.5 mM isopropyl-b-D-thiogalactoside (IPTG). Cells were harvested after overnight growth at 25 °C and incubated in a buffer containing 200 mM Tris pH 8.0, 0.5 mM EDTA, 500 mM sucrose and 0.5 mg/ml lysozyme for 1 h at 25 °C. Bacteria were osmotically lysed by rapid dilution in water. The periplasmic fraction was isolated by centrifugation of cell debris, and was supplemented with NaCl (150 mM final) and imidazole (25 mM final). Nb39 was isolated from the periplasmic fraction by nickel affinity chromatography, and subsequently purified by size-exclusion chromatography in a buffer comprised of 25 mM HEPES pH7.5 and 100 mM NaCl. Peak fractions were pooled and concentrated to approximately 5mM.

Apolipoprotein purification and biotinylation: Apolipoprotein-AI (Apo-AI) was purified as described previously (Whorton *et al.*, 2007). Apo-AI was biotinylated using NHS-PEG4-biotin (Pierce Biotechnology) at a 1:1 molar ratio. Following a 30-min biotinylation reaction at room temperature, the sample was dialysed to remove free biotin.

P-ERK Assays: C6MOPr cells were plated in 24-well plates the day before the assay to reach 80-90% confluency on the day of the assay and treated with vehicle or pertussis toxin (PTX; 100ng/mL). The medium was replaced with serum-free DMEM two hours prior to addition of vehicle or BMS-986122 at the indicated concentration. The assay was stopped by aspirating the medium and rinsing the cells twice with ice-cold phosphate buffered saline. Lysates were collected with radioimmuno-precipitation assay buffer [50 mM Tris, pH 7.4, 150 mM NaCl, 1% Triton X-100, 1% sodium deoxycholic acid, 0.1% SDS] plus protease inhibitor, 2mM EDTA, 100 μM NaF, and 10 μM sodium orthovanadate. Lysates were sonicated for 30 seconds and centrifuged at 10000 x g at 4 °C for 10 min. Supernatant was taken and diluted into SDS sample buffer (62.5 mM Tris-HCl, pH 6.8, 2% SDS, 10% glycerol, 0.0008% bromophenol blue) and beta-mercaptoethanol. Samples were loaded on 12% polyacrylamide gel and subjected to SDS-PAGE followed by transfer to PVDF nitrocellulose membranes for Western blotting. The blot

was propped with a 1:2000 dilution of anti-phospho-p44/42 MAPK (ERK1/2) antibody and visualized using horseradish peroxidase (HRP) -conjugated anti-mouse IgG. To ensure equal loading, membranes were stripped and total ERK levels were assessed using 1:1000 dilution of anti-p42/44 MAPK (ERK1/2) antibody.

Internalization Assays: HEK293T cells were grown to 80% confluency prior to transient transfection with FLAG tagged MOPr. 24 hours following transfection, cells were seeded (0.75×10^6 cells per well) onto poly-d-lysine coated 24-well plates. 24 h following splitting, the cells were treated with drug (or vehicle) in the presence of allosteric ligand (or vehicle) for 10 minutes at 37C in DMEM. At the end of the incubation period, the cells were fixed with 3.7% formaldehyde in Tris-buffered saline [(TBS), 25 mM Tris-HCl, pH 7.4, 2.7 mM KCl, 140 mM NaCl] for 5 min at 4 °C. The cells were washed three times with TBS, blocked with 1% non-fat dry milk made up in TBS for 1 h at room temperature and washed two times with TBS and incubated with monoclonal anti-FLAG M2 alkaline phosphatase antibody for 1 h at 23°C. Cells were washed five times and incubated with *p*-nitrophenyl phosphate for 30 min at 23°C. 0.2 mL aliquots were added to 0.05 mL 3 N NaOH in a 96-well plate. Absorbance at 405 nm was measured using a VERSAmax tunable microplate reader (Molecular Devices, Sunnyvale, CA, USA). The percentage of receptors internalized was calculated using the following equation: $[1 - (\text{Drug O.D.} - \text{Background O.D.}) / (\text{Control O.D.} - \text{Background O.D.})] \times 100$, where O.D. is optical density. Background was defined as the absorbance of untransfected HEK293 cells and control as absorbance from untreated FLAG mu-opioid receptor expressing cells.

APPENDIX B

Discovery, Synthesis, and Molecular Pharmacology of Selective Positive Allosteric Modulators of the δ -Opioid Receptor³

Summary

Allosteric modulators of G protein-coupled receptors (GPCRs) have a number of potential advantages compared to agonists or antagonists that bind to the orthosteric site of the receptor. These include the potential for receptor selectivity, maintenance of the temporal and spatial fidelity of signaling *in vivo*, the ceiling effect of the allosteric cooperativity which may prevent overdose issues, and engendering bias by differentially modulating distinct signaling pathways. Here we describe the discovery, synthesis, and molecular pharmacology of δ -opioid receptor-selective positive allosteric modulators (δ PAMs). These δ PAMs increase the affinity and/or efficacy of the orthosteric agonists leu-enkephalin, SNC80 and TAN67, as measured by receptor binding, G protein activation, β -arrestin recruitment, adenylyl cyclase inhibition, and extracellular signal-regulated kinases (ERK) activation. As such, these compounds are useful pharmacological tools to probe the molecular pharmacology of the δ receptor and to explore the therapeutic potential of δ PAMs in diseases such as chronic pain and depression.

Introduction

The δ -opioid receptor is a seven transmembrane domain (7TMD) receptor that belongs to the class A family of G protein-coupled receptors (GPCRs). Agonists of the δ receptor have been shown to be antinociceptive especially in chronic pain models (Gavériaux-Ruff and Kieffer, 2011) and to have potential as antidepressant agents (Lutz and Kieffer, 2013). The possible dual

³ This research was originally published in the Journal for Medicinal Chemistry. Burford NT, Livingston KE, Canals M, Ryan M, Budenholzer L, Han Y, Banks M, Zhang L, Filizola M, Bassoni D, Wehrman T, Christopoulos A, Traynor J, Gerritz S, Alt A. "Discovery, Synthesis and Pharmacological Characterization of Selective Positive Allosteric Modulators of the δ -Opioid Receptor." *J Med Chem*. 2015 May 28;58(10):4220-9.
© 2015 American Chemical Society.

effects of δ receptor agonists to alleviate chronic pain and mitigate emotional disorders provide a particularly attractive therapeutic strategy because of the high level of comorbidity between chronic pain and depression. However, agonists acting directly at the δ receptor can show proconvulsant effects in animal models, including non-human primates. Indeed, it has been proposed that these seizurogenic properties of δ receptor agonists may be responsible for their antidepressant-like activity analogous to electroconvulsive therapy (Broom *et al.*, 2002). On the other hand, slowing the rate of administration of the δ receptor agonist SNC80 reduces seizurogenic activity but has no effect on anti-depressant-like effects (Jutkiewicz *et al.*, 2005). Also, some δ receptor agonists (e.g., ADL5859) show no seizures in rat or mouse models (Le Bourdonnec *et al.*, 2008). These and other findings suggest that the convulsive properties of δ receptor agonists can be separated from their antidepressant-like effects (Jutkiewicz *et al.*, 2006; Chu Sin Chung and Kieffer, 2013; Chu Sin Chung *et al.*, 2015).

Allosteric modulators for GPCRs bind to a site on the receptor that is topographically distinct from the site that binds the orthosteric (or endogenous) agonist. Positive allosteric modulators (PAMs) increase the affinity and/or efficacy of bound orthosteric agonist ligands. The operational model of allosterism allows the quantification of allosteric effects, and as such, it can estimate the binding affinity of the allosteric ligand to the free receptor (pK_B), the allosteric cooperativity factor ($\alpha\beta$), as well as any intrinsic agonist efficacy (τ_B) of the allosteric ligand. PAMs that have little or no intrinsic efficacy (τ_B) but modulate the orthosteric agonist response have a number of advantages over orthosteric ligands (Christopoulos and Kenakin, 2002; May, Leach, *et al.*, 2007; N Burford *et al.*, 2015). In particular, these PAMs can theoretically maintain the temporal and spatial fidelity of endogenous receptor activation *in vivo*. The allosteric modulator binds to the target receptor but remains effectively silent until the endogenous orthosteric agonist is presented to the receptor. Therefore, PAMs can amplify the effect of endogenous signaling molecules without disrupting normal physiological regulation of receptor activation and might therefore be expected to exhibit superior efficacy and side effect profiles compared to traditional orthosteric agonists. Studies with δ receptor selective ligands, or utilizing a genetic deletion of the δ receptor (Gavériaux-Ruff and Kieffer, 2011), suggest that native opioid peptide signaling at the δ receptor mediates an increase in pain threshold in models of chronic pain and modulates mood states in rodent models (Pradhan *et al.*, 2011). Therefore, positive allosteric modulation of the δ receptor should enhance responses to the endogenous

agonist peptides and thereby be therapeutically efficacious. In addition, the finite nature of the agonist potency shift (defined by the allosteric cooperativity factor), which saturates when the allosteric site is fully occupied, may increase the safety margin between therapeutic effect and possible side effects associated with overactivation of the target receptor. Finally, and pertinent to the δ -receptor system which is known to exhibit ligand-biased signaling (Pradhan *et al.*, 2012), PAMs can modulate the signaling bias of receptor activation toward desired pathways or engender bias from previously unbiased ligands (Leach *et al.*, 2010; Kenakin and Christopoulos, 2012). Thus, δ PAMs may provide a greater therapeutic window between pain relieving and antidepressant-like effects and proconvulsive activity, compared with traditional δ receptor orthosteric agonists.

In this study we report the synthesis and structure–activity relationships (SAR) of the first described δ PAMs. One of the most potent compounds identified, 3,3,6,6-tetramethyl-9-(4-((2-methylbenzyl)oxy)phenyl)-3,4,5,6,7,9-hexahydro-1*H*-xanthene-1,8(2*H*)-dione (**2**, BMS-986187), was further characterized in radioligand binding assays and using a range of cellular functional assays. **2** was shown to positively modulate orthosteric agonist binding affinity and functional potency at the δ receptor and enhance the efficacy of the partial agonist TAN67.

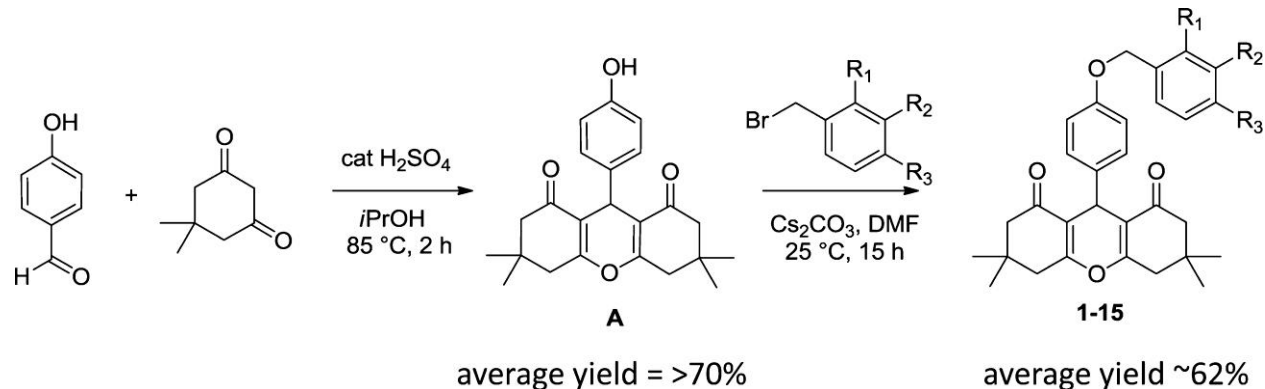
Results

Discovery and Structure–Activity Relationship (SAR) of δ Receptor PAMs

The δ PAM chemotype was identified from a high throughput screen (HTS) using a β -arrestin recruitment assay in a PathHunter U2OS cell line coexpressing μ and δ receptors (U2OS-OPRM1D1) (DiscoverX, Fremont, CA) (Zhao *et al.*, 2008; Bassoni *et al.*, 2012). The screen was executed in PAM mode by measuring activity in the presence of an EC₁₀ concentration of both endomorphin 1 (a μ -receptor-selective agonist) and leu-enkephalin which in this assay and cell line was a relatively selective agonist for the δ receptor (Burford *et al.*, 2014). Typically, when using HTS approaches to identify PAMs, an EC_{20–40} concentration of orthosteric agonist is used (Burford *et al.*, 2011). However, in this HTS the sum of the two EC₁₀ concentrations of agonists offered a compromise between the detection of both μ and δ receptor PAMs and the ability to maintain the overall signal window so that lower efficacy partial agonists could also be detected. Follow-up *in vitro* testing to determine structural features necessary for PAM activity was performed utilizing CHO-PathHunter cell lines (CHO-OPRD1 and CHO-OPRM1) obtained from

DiscoverX. Concentration-response curves (CRCs) for HTS hits were determined both in agonist mode (in the absence of orthosteric agonist) to determine agonist activity of the test compounds, and in PAM mode (in the presence of an EC₂₀ concentration of orthosteric agonist) to determine allosteric modulator activity using the β -arrestin recruitment assays. Compound **7** (Table B.1) was identified as a δ PAM, producing a robust potentiation of the response to an EC₂₀ concentration of leu-enkephalin.

As shown in Scheme 1, we synthesized a series of close analogs of **7** to optimize δ PAM potency and selectivity. None of the compounds exhibited significant agonist activity in a β -arrestin recruitment assay, but all of the compounds produced measurable PAM activity at the δ receptor. **1** with an unsubstituted benzyl ring acted as a δ PAM with an EC₅₀ value of 0.2 μ M and showed 30-fold selectivity in the β -arrestin recruitment assay compared with PAM activity at the



Scheme 1

μ receptor. Introduction of a methyl group in various positions around the phenyl ring (**2–4**) suggested that ortho substitution increased δ receptor PAM activity by an order of magnitude, with minimal effect on μ receptor PAM activity, while meta and para substitution did not significantly affect δ or μ receptor PAM activity. The corresponding ortho-F analog **5** was not significantly more active than **1**, suggesting that the increased δ receptor activity with the *o*-methyl was due to a steric rather than an electronic effect. Similarly, the meta- and para-F analogs **6** and **7** or the ortho-Cl analog **8** did not afford an increase in δ receptor activity. Introduction of a second Cl group in the meta position (**9**) provided a modest improvement in δ receptor activity while maintaining selectivity. A more pronounced effect was observed with the ortho-Br analog **10** which produced equipotent PAM activity to **2** at the δ receptor but no

observable PAM activity at the μ receptor, suggesting that 9 - (4-((2-bromobenzyl)oxy)phenyl)-3,3,6,6-tetramethyl-3,4,5,6,7,9-hexahydro-1*H*-xanthene-1,8(2*H*)-dione (**10**, BMS-986188) is the most δ receptor-selective analog we have identified to date. The effect of ortho substitution on δ receptor PAM potency and selectivity appears to be restricted to small substituents. As shown with analogs **11–15**, larger ortho substituents did not improve δ PAM activity and had no effect on selectivity. Similarly, more drastic changes to the chemotype, such as increasing the chain length between the ether oxygen and the phenyl ring, or replacement of the benzyl ether with a phenyl amide, yielded a significant loss in δ receptor PAM activity (data not shown). The most potent δ PAM identified was **2**, which in the presence of an EC₂₀ of leu-enkephalin produced a β -arrestin response with an average EC₅₀ of 33 nM in CHO-OPRD1 cells (Table B.1). Representative agonist and PAM mode CRCs for **2** at the μ and δ receptor are shown in Figure B.1. In this example, **2** produced little or no activity in agonist mode, but in PAM mode (in the presence of an EC₂₀ of leu-enkephalin (in CHO-OPRD1 cells) or endomorphin 1 (in CHO-OPRM1 cells)) produced a response with an EC₅₀ of 48 nM in CHO-OPRD1 cells and 2 μ M in CHO-OPRM1 cells.

Binding Characterization of 2

2 (at concentrations up to 30 μ M) does not inhibit binding of the orthosteric antagonist ³H-diprenorphine (DPN) to CHO-hDOPr cell membranes, suggesting that **2** is acting at an allosteric site to produce agonist and PAM activity (Figure B.2A). However, in competition binding experiments 10 μ M **2** increased the affinity of the orthosteric agonists, leu-enkephalin (Fig B.2B), SNC80 (Fig B.2C), and TAN67 (Fig B.2D) to displace ³H-DPN. This suggests that **2** is an affinity modulator (the α component of the cooperativity factor) in the system tested (Table B.2). The affinity shift with the partial agonist TAN67 is less than that seen with the full agonists leu-enkephalin and SNC80 (Table B.2).

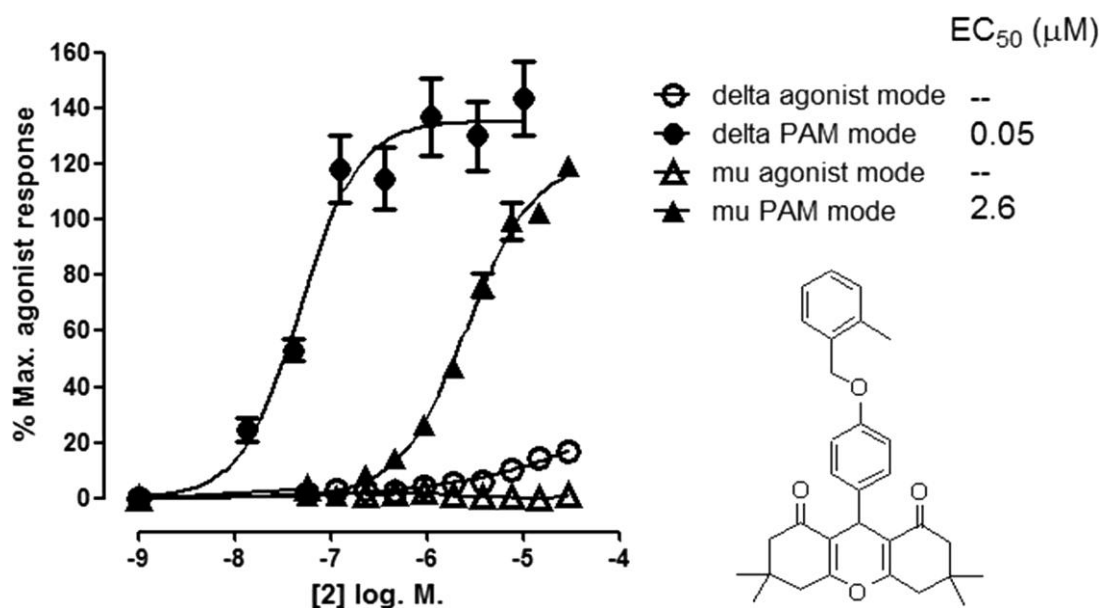


Figure B.1: β -Arrestin recruitment response to **2** in agonist mode (in the absence of orthosteric agonist) and in PAM mode (in the presence of an EC₂₀ of orthosteric agonist) in PathHunter cells expressing δ receptors (CHO-OPRD1) and μ receptors (CHO-OPRM1). For CHO-OPRD1 cells the orthosteric agonist was leu-enkephalin, and for CHO-OPRM1 cells the orthosteric agonist was endomorphin 1. In PAM mode, the EC₂₀ response of orthosteric agonist was normalized to 0%. 100% represents the response to a maximally effective concentration of orthosteric agonist. Data are presented as the mean \pm SEM, $n = 4$.

Table B.1: Structure–Activity Relationship of the δ -PAM Chemotype in PathHunter CHO-OPRD1 and CHO-OPRM1 Cells in a β -Arrestin Recruitment Assay

Compound	R ₁	R ₂	R ₃	Delta EC ₅₀ (μ M) (%Ymax)	Mu EC ₅₀ (μ M) (%Ymax)	Selectivity Mu / Delta
1	H	H	H	0.2 (126)	6 (130)	30
2 (BMS-986187)	CH ₃	H	H	0.03 (124)	3 (121)	100
3	H	CH ₃	H	0.2 (136)	3 (120)	15
4	H	H	CH ₃	0.3 (92)	4 (65)	13
5	F	H	H	0.1 (120)	5 (107)	50
6	H	F	H	1 (136)	7 (182)	7
7	H	H	F	0.1 (95)	2 (72)	20
8	Cl	H	H	0.3 (68)	>10 (>100)	>33
9	Cl	Cl	H	0.1 (116)	>10 (>87)	>100
10 (BMS-986188)	Br	H	H	0.05 (58)	>10 (>20)	>200
11	OCHF ₂	H	H	0.2 (109)	3 (80)	15
12	OCF ₃	H	H	0.3 (114)	2 (111)	7
13	SO ₂ CH ₃	H	H	0.9 (102)	5 (42)	6
14	CH ₂ OH	H	H	1 (92)	10 (112)	10
15	CF ₃	H	H	>10 (>40)	>10 (>20)	

No activity was observed in agonist mode (in the absence of orthosteric agonist (data not shown)). In PAM mode (in the presence of an EC₂₀ of leu-enkephalin for OPRD1 cells or an EC₂₀ of endomorphin I for OPRM1 cells), robust responses were observed. The mean EC₅₀ values, Y_{max} values, and potency ratio of δ receptor activity/ μ receptor activity in PAM mode are reported in the table ($n = 3$).

Functional Characterization of 2

The PAM activity of **2** was further characterized in four different functional assays. In the CHO-OPRD1 PathHunter cells, **2** effects on leu-enkephalin potency and efficacy were studied in both β -arrestin recruitment assays and inhibition of forskolin-stimulated cAMP accumulation assays. Unlike the U2OS cell lines used in the HTS, where forskolin was relatively ineffective at stimulating adenylyl cyclase activity, the recombinant CHO PathHunter cell lines allowed us to investigate both β -arrestin recruitment and inhibition of forskolin-stimulated cAMP accumulation in the same cell line. In the β -arrestin recruitment assay, **2** alone (up to 10 μ M) produced only marginal agonist activity (\sim 10% of a maximal response to leu-enkephalin) but produced a robust 18-fold increase in the potency of leu-enkephalin (Fig B.3A). A small increase in the maximal response to leu-enkephalin with **2**, relative to leu-enkephalin alone, was also observed. This suggests that **2** is a PAM with little or no intrinsic efficacy in this system. In contrast, in the inhibition of forskolin-stimulated cAMP assay, **2** alone produced robust activity resulting in full inhibition of cAMP accumulation at concentrations above 3 μ M (Fig B.3B). At lower concentrations, **2** increased the potency of leu-enkephalin. At a 370 nM concentration of **2** (the highest concentration at which a potency for leu-enkephalin could be determined) the potency of leu-enkephalin was increased by 56-fold. Similar findings were observed using the small molecule orthosteric agonist SNC80 in these two assays (Table B.3).

Similar to the findings in the cAMP functional assay, **2** was also shown to be a PAM in [³⁵S]GTP γ S binding (Fig B.4A) and in ERK1/2 phosphorylation (Fig B.4B) in CHO-hDOPr cells, showing agonist activity at higher concentrations and increases in the potency of

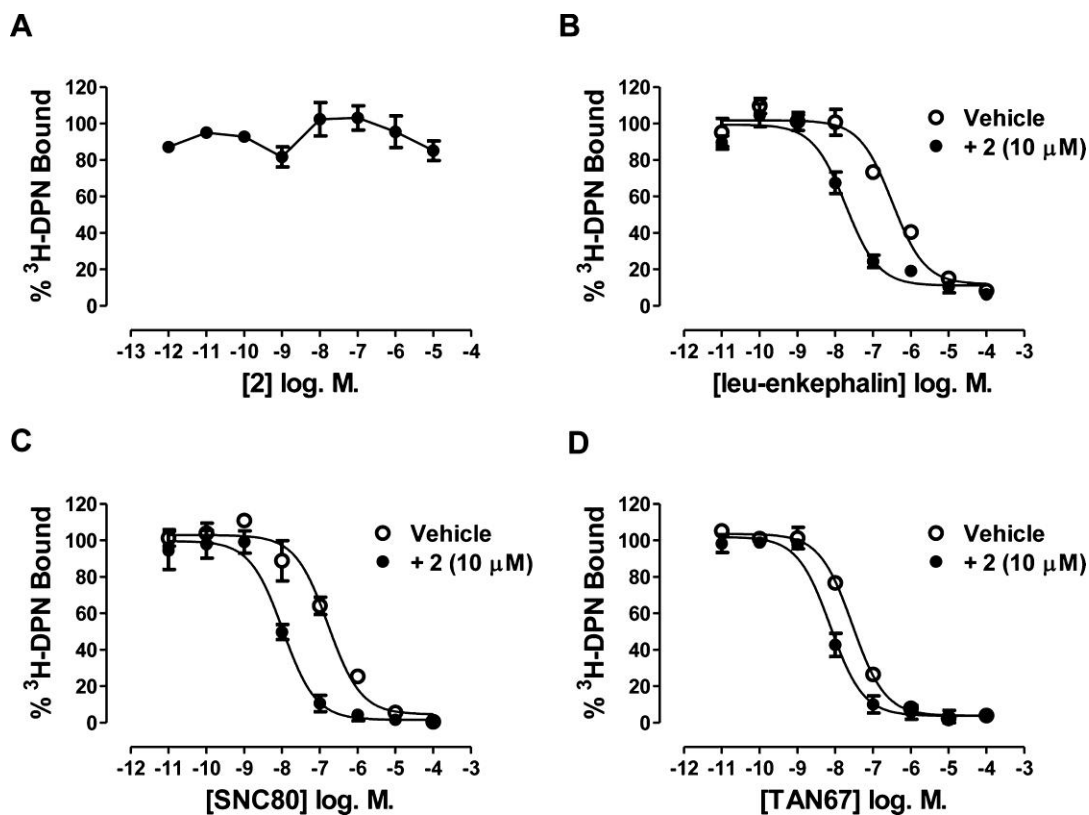


Figure B.2: Effect of 2 on 3H-diprenorphine (DPN) binding (A) and the effect of 10 μM 2 on leu-enkephalin (B), SNC80 (C), and TAN67 (D) competition binding curves in CHO-hDOPr membranes. *K_i* values are shown in Table 2. Data are presented as the mean ± SEM of three experiments.

Table B.2: Effect of 2 (10 μ M) on Orthosteric Agonist Competition Binding K_i Values in CHO-hDOPr Cell Membranes

Ligand	With Vehicle: K_i (nM) (95% C.I.) (nM)	With 2 (10 μ M): K_i (nM) (95% C.I.) (nM)	Affinity ratio Vehicle K_i / 2 K_i
Leu-Enkephalin	221 (119 to 324)	7 (3-12)	32
SNC80	71 (20 to 122)	5 (3-7)	14
TAN67	10 (7 to 14)	3 (0.2-5.8)	3

2 had no effect on $^3\text{H-DPN}$ binding (see Figure B.2) but increased the affinity of orthosteric agonist competition binding curves. Data are presented as the mean \pm SEM of three experiments.

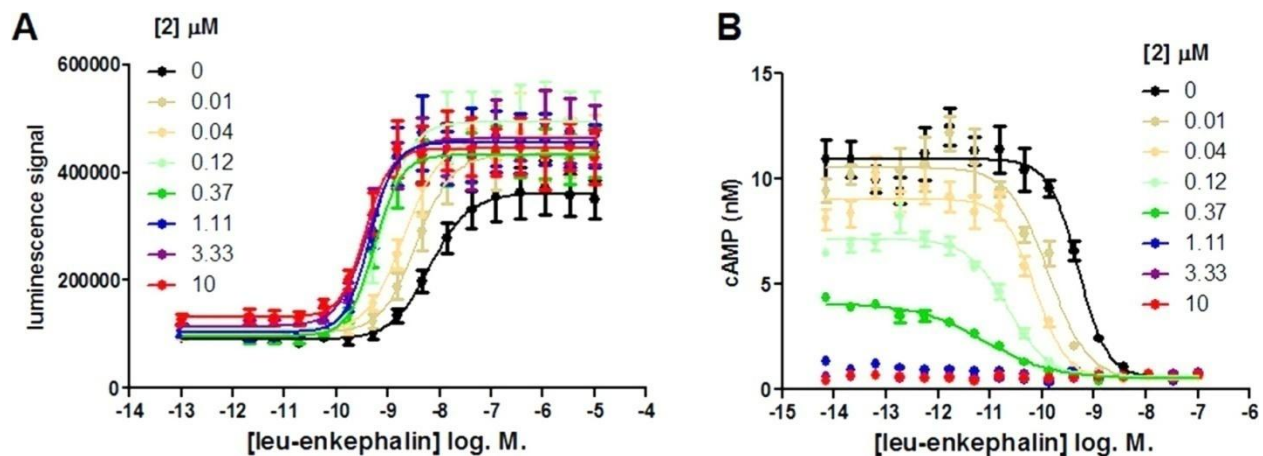


Figure B.3: Effect of increasing concentrations of 2 on leu-enkephalin concentration–response curves in β -arrestin recruitment (A) and in inhibition of forskolin-stimulated cAMP accumulation (B) in CHO-OPRD1 cells. Data are presented as the mean \pm SEM of four experiments. Data were fitted to the operational model of allosterism (see Table C.3).

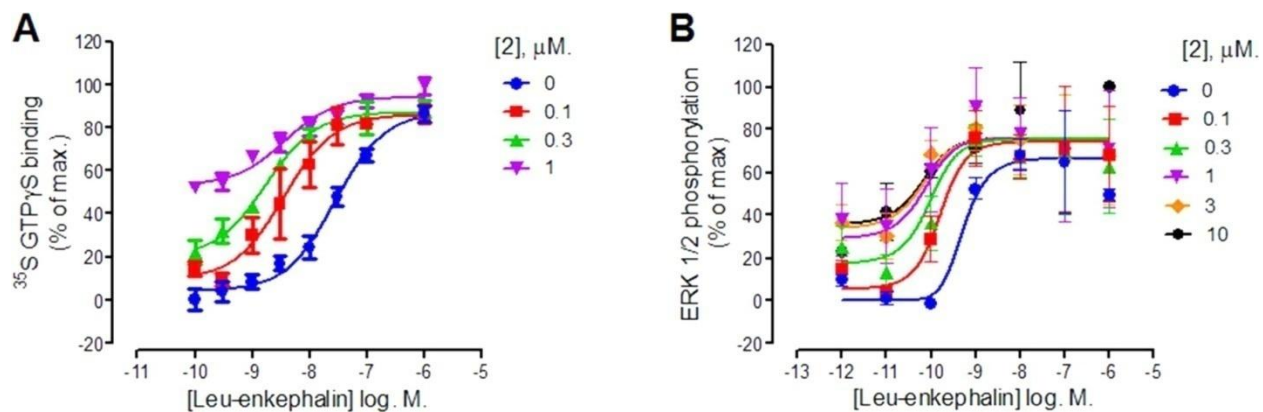


Figure B.4: Effect of increasing concentrations of 2 on leu-enkephalin concentration–response curves in [35S]GTP γ S binding in CHO-hDOPr membranes (A) and in pERK in CHO-hDOPr cells (B). In the [35S]GTP γ S binding assay, 0% and 100% represent the basal response and the maximal response produced, respectively. In the pERK assay, 0% represents basal activity in serum-free media and 100% represents the pERK response in the presence of 10% serum. Data are presented as the mean \pm SEM, $n = 3–7$. Data were fitted to the operational model of allosterism (see Table C.3).

Table B.3: Allosteric Parameters for 2 at the δ Receptor

	Leu-Enkephalin				SNC80				TAN-67	
	β -arr	GTP γ S	cAMP	pERK	β -arr	GTP γ S	cAMP	pERK	GTP γ S	pERK
Log $\cdot \tau_A$	0.28 \pm 0.04	0.94 \pm 0.06	2.8 \pm 0.03	0.25 \pm 0.16	0.66 \pm 0.08	0.56 \pm 0.10	0.86 \pm 0.03	1.06 \pm 0.15	0.67 \pm 0.09	0.22 \pm 0.07
Log $\cdot \tau_B$	-0.73 \pm 0.15	0.36 \pm 0.17	1.45 \pm 0.27	-0.16 \pm 0.15	-1.06 \pm 0.11	0.29 \pm 0.20	1.01 \pm 0.02	-0.04 \pm 0.15	0.45 \pm 0.07	0.11 \pm 0.08
pK _A	= 7.90 **	= 6.6 **	= 6.7 *	= 9.13 **	6.38 \pm 0.11	= 7.7 *	= 7.7 *	= 7.7 *	= 7.6 **	= 8.4 **
pK _B	7.06 \pm 0.11	5.85 \pm 0.23	5.45 \pm 0.02	6.13 \pm 0.30	6.45 \pm 0.05	6.23 \pm 0.32	5.52 \pm 0.02	5.66 \pm 0.30	=6.0 ***	5.80 \pm 0.32
Log ($\alpha\beta$)	1.18 \pm 0.07 (15)	1.67 \pm 0.21 (47)	2.80 \pm 0.08 (631)	0.99 \pm 0.28 (10)	1.33 \pm 0.05 (21)	1.00 \pm 0.30 (10)	2.11 \pm 0.07 (129)	0.89 \pm 0.29 (8)	1.11 \pm 0.19 (13)	1.41 \pm 0.29 (26)

Values for affinity, efficacy, and allosteric cooperativity for orthosteric ligands and **2** are derived from the operational model of allosterism. Three different orthosteric agonists were used (leu-enkephalin, SNC80, and TAN67), across up to four functional assays (β -arrestin recruitment, [³⁵S]GTP γ S binding, cAMP inhibition, and pERK). In the model τ_A and τ_B represent the efficacy of the orthosteric agonist and allosteric modulator, respectively; pK_A and pK_B represent the binding affinity of the orthosteric agonist and the allosteric modulator, respectively, to the free receptor; and $\alpha\beta$ represents the composite allosteric cooperativity factor. Data are presented as the mean \pm SEM of three to seven experiments.

*pK_A is fixed to its equilibrium binding affinity, as ligand is a full agonist in all end points tested.

**pK_A of leu-enkephalin and TAN67 in end points where they are partial agonists was obtained from fitting their concentration response curves to the operational model of agonism to obtain a functional affinity in each end point tested.

***the pK_B for TAN67 in [³⁵S]GTP γ S binding had to be fixed to the average of the pK_B obtained from Leu-enk and SNC80 as neither allosteric agonism or potentiation reached a limit.

orthosteric agonist at lower concentrations. No agonist activity to **2** was observed in the parental CHO cells (lacking the δ receptor) in ERK1/2 phosphorylation or in parental CHO cells in inhibition of cAMP accumulation assays (data not shown). **2** increased the potency of leu-enkephalin by 16-fold in the [³⁵S]GTP γ S binding assay in CHO-hDOPr membranes and by 8-fold in the ERK1/2 phosphorylation assay in CHO-hDOPr cells. Similar experiments were performed replacing leu-enkephalin with the orthosteric agonists SNC80 and the partial agonist TAN67. By use of an operational model of allosterism (Leach *et al.*, 2007) (see Methods and Materials), composite cooperativity ($\alpha\beta$) values and pK_B values (denoting the equilibrium dissociation binding constant for **2** at the δ receptor in the absence of orthosteric agonist, i.e., at the free receptor) were determined for **2** across these different assays and with different orthosteric agonists (Table B.3).

The mean \pm SEM pK_B across all the assays for **2** was 6.02 ± 0.16 ($\sim 1 \mu\text{M}$). One would expect that the pK_B values should be the same across all the cell lines, functional assays, and orthosteric agonists used, since the pK_B represents the binding affinity of **2** to the free receptor. Two way ANOVA with multiple comparison test of the pK_B values in Table B.3 showed no significant difference between the different orthosteric agonist ligands used in the same functional assay. For SNC80 and TAN67 there were also no significant differences in pK_B values across the different functional pathways tested. However, for leu-enkephalin there were significant differences in the pK_B values between β -arrestin recruitment and [³⁵S]GTP γ S binding ($p < 0.01$) and between β -arrestin recruitment and cAMP inhibition ($p < 0.001$).

Discussion

By use of a β -arrestin recruitment assay, the SAR of a δ PAM chemotype identified from HTS was explored, resulting in identification of compounds (**1–15**) with little or no agonist activity but which produced PAM activity at the δ and μ receptor. To compare the allosteric activity of the compounds, we used increasing concentrations with a single (EC_{20}) concentration of orthosteric agonist and analyzed the EC_{50} and Y_{max} values of the functional curves produced. Although the compounds exhibited a range of Y_{max} values in PAM mode (Table B.1) which can correlate with the allosteric cooperativity, the large proportion of the analogs tested exhibited efficacy close to or above 100% limiting the usefulness of the Y_{max} parameter for selecting

compounds for further study. Instead, potency of the PAM response was used and selectivity was determined using potency ratios between the PAM responses at the δ receptor compared to the μ receptor. While this procedure is useful for selecting δ receptor selective PAM candidates to pursue, one must bear in mind that different orthosteric agonist ligands were used in the PAM mode assays: leu-enkephalin for the δ receptor, and endomorphin I for the μ receptor. Since we currently know little about the possible probe dependence of these PAM compounds at the δ and μ receptor, we cannot necessarily assume that the reported selectivity will be the same with different orthosteric probe ligands.

The selected data set used for multivariate statistical analysis do not allow for thorough cross-validation of the presented linear models, but our results suggest initial physicochemical properties that can be used as searching criteria for additional compounds with potential PAM activity at δ and μ opioid receptors. **2** was selected for further characterization, since it had the highest PAM mode potency at the δ receptor and showed 100-fold selectivity compared to the μ receptor.

The multivariate statistical analysis initially suggested that the compounds may not be readily soluble in aqueous buffer at concentrations in the micromolar range. Also, nephelometry data (not shown) suggest that **2** and **10** show particulate matter in phosphate buffered saline solution at concentrations above 1 μ M. When nephelometry was repeated using the specific buffer used for the β -arrestin recruitment assays (HBSS + 25 mM HEPES and 10% FBS) in Table C.1, **2** and **10** produced particulate matter above 3 μ M. While the majority of responses to **2** in cells expressing the δ receptor were maximal at 1 μ M (and therefore, within the solubility window predicted for **2**), the μ receptor responses (e.g., see Figure B.1) also showed sigmoidal responses (i.e., the responses were not biphasic) up to 30 μ M **2**, suggesting that solubility was not an issue in these assays in the specific buffers used. However, compound solubility should be an important consideration in further studies and optimization of this chemical series.

From competition binding studies, **2** did not affect $^3\text{H-DPN}$ binding to the δ receptor but increased the affinity of orthosteric agonists, suggesting that **2** does not bind to the orthosteric site of the δ receptor but can increase the affinity of orthosteric agonists binding to the receptor (α cooperativity). The precise mechanism for this cooperativity remains unknown. However, in this context it is tempting to make comparisons to recently discovered PAMs of the μ opioid receptor (Burford *et al.*, 2013). The μ receptor PAM 2-(3-bromo-4-methoxyphenyl)-3-((4-

chlorophenyl)sulfonyl)thiazolidine (**16**, BMS-986122) has been found to differentially increase the affinity of various orthosteric agonists, and the magnitude of the affinity increase (α value) produced by **16** correlates with the intrinsic activity of the orthosteric ligand used (Chapter 3; Livingston and Traynor, 2014). The mechanism by which **16** induces this affinity modulation is suggested to be via reducing the affinity of Na^+ for its binding site on the μ receptor. The precise binding site for **16** on the μ receptor has not been clearly established, and it is unknown whether the δ receptor PAMs described here bind to an analogous binding site on the δ receptor or act via a similar mechanism. However, several analogs of **16** were found to exhibit weak activity at δ receptors, and most of the δ receptor PAMs described here also exhibit some degree of activity at μ receptors. Therefore, it is possible that these δ receptor PAMs may be binding to a site on the δ receptor that is analogous to the **16** binding site on the μ receptor and may work through a similar mechanism. The reduced affinity shift observed with **2** for the partial agonist TAN67 compared with the agonists with higher intrinsic activity, leu-enkephalin and SNC80 (Fig B.2, Table B.2), is consistent with this hypothesis. It will be interesting to determine whether these δ PAMs reduce the affinity of Na^+ for its binding site on the δ receptor. Sodium ions are known to stabilize a lower affinity state of the δ receptor, and the molecular basis for allosteric Na^+ control of opioid receptor signaling has been elucidated recently (Fenalti *et al.*, 2014; Shang *et al.*, 2014).

While TAN67 was a partial agonist in the CHO-hDOPr cell line for [^{35}S]GTP γ S binding giving 84% of maximal SNC80 response, it had even less intrinsic activity in a C6-DOPr cell line at 41% of maximal SNC80 response (data not shown). In the presence of **2** (300 nM), the maximal stimulation by TAN67 was increased to 67% of maximal SNC80 response. This suggests that **2** has some allosteric efficacy cooperativity (β), as well as the affinity cooperativity (α) observed above.

In all of the functional assays, **2** acted as a PAM, increasing the potency of the response to orthosteric agonists. No activity was observed in functional assays when **2** was added alone in CHO-parental cells (lacking the recombinant δ opioid receptor) in either the ERK activation assay or cAMP assay (data not shown). However, in cells expressing the δ receptor, **2** (when added alone) produced significant activity in cAMP inhibition, [^{35}S]GTP γ S binding, and ERK activation assays, suggesting that this activity is due to intrinsic efficacy of **2** at the τ receptor. Thus, **2** is a PAM-agonist in these systems. In cells expressing the δ receptor, **2** showed little to

no agonist activity in the β -arrestin recruitment assay, which measures an event proximal to receptor activation with limited signal amplification. The difference in observed agonist activity for **2** between the β -arrestin recruitment assay and the cAMP assay (Fig B.3) is likely reflective of a higher level of signal amplification and thus a higher receptor reserve in the cAMP assay compared to the β -arrestin recruitment assay in the same cell line (Ehlert, 2005; Kenakin *et al.*, 2012). Phosphorylation of the receptor by G protein-coupled receptor kinases (GRKs) is thought to be a prerequisite for β -arrestin recruitment (Pierce and Lefkowitz, 2001). It would be interesting to see how **2** impacts δ receptor phosphorylation by GRKs and consequently desensitization and internalization of the receptor.

Calculation of pK_B values for **2** across the various functional assays with leu-enkephalin, SNC80, and TAN67, using the allosteric operational model, showed some variability. These differences in pK_B values may result from the allosteric effect not reaching a plateau or ceiling. This could reflect that the allosteric effect was submaximal at concentrations below those at which full agonism was observed with **2** or that the highest concentrations of **2** used did not cause the allosteric EC_{50} shift to reach its ceiling. This can make accurate assessment of the allosteric parameters more difficult to estimate in the model. Other variables, including the use of different cell lines or use of a tagged receptor (in the case of the PathHunter CHO-OPRD1 cell line), may also contribute to the variability of values obtained in the model.

The fact that we observed PAM effects with **2** at concentrations lower than those which produced agonist effects is entirely consistent with the allosteric ternary complex model because the former effects (PAM effects) are observed in the presence of orthosteric agonist, and hence the affinity of the modulator for the receptor is higher, whereas the latter effects (agonist effects) reflect the actions of the modulator at the free receptor and thus require higher concentrations to achieve the same level of fractional occupancy. Therefore, a PAM with a large cooperativity factor ($\alpha\beta$) can exhibit functional activity that is far more potent than its K_B value. This has potential implications for PAM drug discovery programs, suggesting that it is important to track functional PAM activity rather than K_B values when designing assays to support SAR. Additionally, this suggests that assays assessing target engagement may dramatically underestimate the relevant receptor occupancy of a PAM, since the affinity of the PAM (and therefore its fractional receptor occupancy) will be much higher at sites where orthosteric agonist is present. While such sites may represent only a small fraction of the receptor population *in*

in vivo, they nonetheless represent the relevant receptor population, since positive allosteric modulation can only occur when and where orthosteric agonist is bound.

Despite the complexities discussed above, all available data suggest that **2** is a δ PAM or a δ PAM-agonist. In future studies, it will be important to confirm the activity of **2** and its analogs in cells or tissues natively expressing δ receptors. Further, it will be of significant interest to determine whether compounds such as **2** also exhibit direct agonist activity in native systems expressing endogenous levels of δ receptors. PAMs devoid of intrinsic agonist activity could theoretically have therapeutic advantages over PAM-agonists, particularly in the maintenance of the temporal and spatial fidelity of endogenous receptor activation *in vivo*, as they would effectively be silent when bound to the receptor until orthosteric (endogenous) agonist is presented to the receptor. A key issue will be the determination of these effects *in vivo*. We intend to evaluate the *in vivo* activity of **2** and its analogs in models of acute and chronic pain (Vanderah, 2010), migraine (Pradhan *et al.*, 2014), depression (Jutkiewicz, 2006) and convulsive activity (Broom *et al.*, 2002) which is a known liability of δ opioid receptor agonists that has limited the pursuit of δ receptor agonists as potential therapeutics.

In summary, we have identified and characterized δ receptor-selective PAMs including our lead compound **2**. Further studies are planned to assess probe dependence and signaling bias for these PAMs using a variety of orthosteric opioid receptor ligands and functional assays. Additional research is also ongoing to determine if this new class of compounds could represent a viable approach to develop new medicines for chronic pain, depression, and other therapeutic indications.

Methods

Chemistry

Analogues were purchased from external vendors (**1**, **3–5**, **7**) or synthesized according to Scheme 1 (**2**, **6**, **8–15**). All purchased and newly synthesized analogues provided analytical data consistent with their assigned structures and were >95% pure based on LCMS.

Synthesis of Intermediate A (Scheme 1)

To a solution of 4-hydroxybenzaldehyde (1.5 g, 12.28 mmol) in 2-propanol (35 mL) were added 5,5-dimethylcyclohexane-1,3-dione (3.44 g, 24.57 mmol) and H₂SO₄ (98%, 0.098 mL, 1.842

mmol). The reaction mixture was refluxed for 1.5 h in an oil bath and then cooled to room temperature, forming a white precipitate. After filtration, 3 g of 9-(4-hydroxyphenyl)-3,3,6,6-tetramethyl-3,4,5,6,7,9-hexahydro-1*H*-xanthene-1,8(2*H*)-dione was obtained in 65% yield (98% purity by LCMS analysis). ¹H NMR (400 MHz, CD₃Cl) δ 7.09 (d, *J* = 8.6 Hz, 2H), 6.56 (d, *J* = 8.6 Hz, 2H), 4.67 (s, 1H), 2.46 (s, 4H), 2.23 (s, 2H), 2.21 (s, 2H), 1.10 (s, 6H), 1.00 (s, 6H); ESI-MS *m/z* = 367.08 [M + H]⁺.

Synthesis of Analogs 1-15

General Procedure

To a solution of 9-(4-hydroxyphenyl)-3,3,6,6-tetramethyl-3,4,5,6,7,9-hexahydro-1*H*-xanthene-1,8(2*H*)-dione (100 μ mol, 36.6 mg) in DMF (1.2 mL) were added ArCH₂Br (200 μ mol) and Cs₂CO₃ (65.2 mg, 200 μ mol). The reaction mixture was stirred at room temperature overnight. Then 10 μ L of the reaction solution was taken, dissolved in MeOH (0.2 mL), and analyzed by LCMS. The LCMS showed that the reaction was complete and the desired product as a major peak was found. The product was purified via preparative LC/MS with the following conditions. Column: XBridge C18, 19 mm \times 200 mm, 5- μ m particles. Mobile phase A: 5:95 acetonitrile/water with 10 mM ammonium acetate. Mobile phase B: 95:5 acetonitrile/water with 10 mM ammonium acetate. Gradient: 70–100% B over 15 min, then a 5 min hold at 100% B. Flow: 20 mL/min. Fractions containing the desired product were combined and dried via centrifugal evaporation.

Two analytical LC/MS injections were used to determine the final purity. Injection 1 conditions were the following. Column: Waters BEH C18, 2.0 mm \times 50 mm, 1.7 μ m particles. Mobile phase A: 5:95 acetonitrile/water with 10 mM ammonium acetate. Mobile phase B: 95:5 acetonitrile/water with 10 mM ammonium acetate. Temperature: 50 °C. Gradient: 0% B, 0–100% B over 3 min, then a 0.5 min hold at 100% B. Flow: 1 mL/min. Detection: UV at 220 nm. Injection 2 conditions were the following. Column: Waters BEH C18, 2.0 mm \times 50 mm, 1.7 μ m particles. Mobile phase A: 5:95 methanol/water with 10 mM ammonium acetate. Mobile phase B: 95:5 methanol/water with 10 mM ammonium acetate. Temperature: 50 °C. Gradient: 0% B, 0–100% B over 3 min, then a 0.5 min hold at 100% B. Flow: 0.5 mL/min. Detection: UV at 220 nm.

Proton NMR was acquired in deuterated CDCl₃ or DMSO.

3,3,6,6-Tetramethyl-9-(4-((2-methylbenzyl)oxy)phenyl)-3,4,5,6,7,9-hexahydro-1H-xanthene-1,8(2H)-dione (2, BMS-986187)

¹H NMR (400 MHz, chloroform-d) δ 7.51–7.35 (m, 2H), 7.26–7.18 (m, 4H), 6.89 (dd, J = 14.2, 8.6 Hz, 2H), 5.05 (s, 2H), 4.72 (s, 1H), 2.49 (d, J = 5.9 Hz, 4H), 2.38 (d, J = 7.8 Hz, 4H), 2.27–2.21 (m, 3H), 1.16–1.10 (m, 6H), 1.07–1.00 (m, 6H). HRMS: calcd C₃₁H₃₅O₄, 471.2530; found, 471.2538

9-(4-((2-Bromobenzyl)oxy)phenyl)-3,3,6,6-tetramethyl-3,4,5,6,7,9-hexahydro-1H-xanthene-1,8(2H)-dione (10, BMS-986188)

The yield of the product was 20.6 mg, and its estimated purity by LCMS analysis was 100%. ¹H NMR (500 MHz, DMSO-d₆) δ 7.67 (d, J = 7.7 Hz, 1H), 7.56 (d, J = 7.3 Hz, 1H), 7.42 (t, J = 7.5 Hz, 1H), 7.31 (t, J = 7.3 Hz, 1H), 7.10 (d, J = 8.1 Hz, 2H), 6.88 (d, J = 8.4 Hz, 2H), 5.04 (s, 2H), 4.48 (s, 1H), 2.54 (d, J = 11.4 Hz, 4H), 2.26 (d, J = 16.1 Hz, 2H), 2.09 (d, J = 16.1 Hz, 2H), 1.04 (s, 6H), 0.91 (s, 6H). HRMS: calcd C₃₀H₃₂O₄Br, 535.1478; found, 535.1478.

Cell Lines

Chinese hamster ovary (CHO) PathHunter cells expressing enzyme acceptor (EA) tagged β -arrestin **2** and either ProLink (PK) tagged δ receptor (CHO-OPRD1) or PK-tagged μ receptor (CHO-OPRM1) were from DiscoverX (Fremont, CA). PathHunter is a trademark of DiscoverX. Cells were grown in F-12 media (Invitrogen 11765), containing Hyclone FBS 10%, Hygromycin 300 μ g/mL (Invitrogen 10687), G418 800 μ g/mL (Invitrogen 10131) and maintained at 37 °C in a humidified incubator containing 5% CO₂. These cells were used for β -arrestin recruitment assays and inhibition of forskolin-stimulated cAMP accumulation assays described below.

FlpIn CHO cells (Invitrogen, Carlsbad, CA, USA) were grown in Dulbecco's modified Eagle medium (DMEM) supplemented with 10% fetal bovine serum and maintained at 37 °C in a humidified incubator containing 5% CO₂. FlpIn CHO cells were transfected with the pOG44 vector encoding Flp recombinase and the pDEST vector encoding the human δ receptor (hDOPr) at a ratio of 9:1 using polyethylenimine as transfection reagent. At 24 h after transfection the cells (CHO-hDOPr) were subcultured and the medium was supplemented with 700 μ g/mL

HygroGold as selection agent. Cells were grown and maintained in DMEM containing 20 mM HEPES, 5% fetal bovine serum, and 200 $\mu\text{g}/\text{mL}$ Hygromycin-B. Cells were maintained at 37 °C in a humidified incubator containing 5% CO_2 . These cells were used for ERK phosphorylation assays, and membranes derived from these cells were used for [^{35}S]GTP γ S binding and ^3H DPN binding studies as described below.

Materials

PathHunter detection reagents were from DiscoverRx (Fremont, CA). Cell culture media and supplements were from Life Technologies (Carlsbad, CA). Lance-Ultra cAMP detection reagents, Surefire ERK assay reagents, [^3H]diprenorphine (DPN), and [^{35}S]GTP γ S (guanosine-5'-*O*-(3-thio)triphosphate) were from PerkinElmer Life Sciences (Cambridge, MA). Endomorphin I and TAN67 were obtained from Tocris. All other chemicals, unless otherwise specified, were purchased from Sigma (St. Louis, MO).

PathHunter β -Arrestin Assay

Confluent flasks of CHO-OPRM1 and CHO-OPRD1 cells were harvested with TrypLE Express and resuspended in F-12 media supplemented with 10% FBS and 25 mM HEPES, at a density of 6.67×10 cells/mL and plated (3 μL /well) into white solid TC-treated 1536-well plates (Corning, NY). Plates were incubated overnight at 37 °C in a 5% CO_2 humidified incubator. The next day, compounds (40 nL of 100 \times final concentration in 100% DMSO) were added to cell plates by acoustic dispense using an Echo-550 (Labcyte, Sunnyvale, CA) from Echo-qualified 1536-well source plates (Labcyte). Next, 1 μL of assay buffer (agonist mode), or assay buffer containing a low concentration ($\sim 4 \times \text{EC}_{20}$) of orthosteric agonist (PAM mode), was added to assay plates. The orthosteric agonists used are described in the Results and Discussion. Plates were covered with a lid and incubated at room temperature for 90 min. Incubations were terminated by the addition of 2 μL of PathHunter Reagent (DiscoverRx). One hour later luminescence was detected using a Viewlux imaging plate reader (PerkinElmer).

Inhibition of Forskolin-Stimulated cAMP Accumulation Assays

CHO-OPRD1 cells were grown to confluence (as described above). Cells were harvested and resuspended at 1×10 cells/mL in assay buffer (HBSS + 25 mM HEPES, +0.05% BSA).

Compounds (30 nL of $100 \times$ final concentration in 100% DMSO) were added to 1536-well white solid NT plates by acoustic dispense using an Echo-550 (Labcyte, CA) followed by a 1 μ L addition of cells (2000 cells/well) to all wells. Next, 1 μ L of either assay buffer (for agonist mode) or assay buffer containing a $3 \times EC_{20}$ concentration of orthosteric agonist (PAM mode) was added. Finally, 1 μ L of $3 \times$ forskolin (2 μ M final) was added. Plates were lidded and incubated for 45 min at rt. Incubations were terminated by the addition of Lance-Ultra cAMP detection reagent (PerkinElmer) (1.5 μ L of Eu-cryptate-labeled cAMP tracer in lysis buffer, followed by 1.5 μ L of U-light conjugated anti-cAMP antibody in lysis buffer). After a 1 h incubation at room temperature, time-resolved fluorescence (TRF) was detected on a Viewlux or Envision plate reader (PerkinElmer) with excitation at 337 nm and emission reads at 615 and 665 nm. The ratiometric data (665 nm read/615 nm read) $\times 10\,000$ were then converted to cAMP (nM) based on a standard curve for cAMP (replacing the cell addition step) run at the same time and under identical conditions to the assay.

Characterization of δ -opioid receptor-selective PAMs in the CHO-OPRD1 cAMP assay, using curve-shift assays, were performed as described above using orthosteric agonists described in the Results and Discussion.

Membrane Preparation

Confluent cells were rinsed with phosphate buffered saline and then detached using harvesting buffer (0.68 mM EDTA, 0.15 M NaCl, 20 mM HEPES, pH 7.4). Cells were pelleted by centrifugation at 300g for 3 min, followed by resuspension in cold 50 mM Tris-HCl buffer, pH 7.4. Pellet was rehomogenized using a Tissue Tearor and then centrifuged at 20 000g for 20 min at 4 °C. The supernatant was discarded, and the process was repeated for an additional rehomogenization and centrifugation. The supernatant was discarded, and the final pellet was resuspended in 50 mM Tris-HCl and flash-frozen in aliquots using liquid nitrogen. Aliquots were kept at -80 °C until assays. Protein concentration was determined using BCA protein assay with bovine serum albumin as the standard.

Radioligand Binding Assay

Cell membranes (as prepared above, 10 μ g/well) were incubated in the following mixture for 90 min at 25 °C: assay buffer (50 mM Tris-HCl, pH 7.4, 100 mM NaCl, 1 mM EDTA, 5 mM

MgCl₂, 10 μM GTPγS), various concentrations of orthosteric and allosteric ligand, and 0.35-0.45 nM [³H]DPN. Nonspecific binding was determined in the presence of 10 μM naloxone. Reactions were terminated by rapid filtration through glass microfiber GF/C filters (Whatman) using a Brandell harvester and washed three times using cold 50 mM Tris-HCl buffer. Filters were dried in a 50 °C oven, and radioactivity was measured by liquid scintillation counting with EcoLume liquid scintillation cocktail (MP Biomedicals) in a Wallac 1450 MicroBeta counter (PerkinElmer).

[³⁵S]GTPγS Assay

CHO-hDOPr cell membranes (as prepared above, 10 μg/well) were incubated for 1 h at 30 °C in buffer comprising 50 mM Tris-HCl (pH 7.4), 1 mM EDTA, 5 mM MgCl₂, 100 mM NaCl, 0.1 nM [³⁵S]GTPγS, and 30 μM GDP (guanosine 5-diphosphate) in a final volume of 200 μL. Orthosteric and allosteric ligands were also included, with SNC80 used as the maximal standard and assay buffer used to assess basal [³⁵S]GTPγS binding. The reaction was terminated by filtration through glass microfiber GF/C filters (Whatman) using a Brandell harvester. The filters were rinsed, dried, and radioactivity was counted by liquid scintillation counting using EcoLume liquid scintillation cocktail (MP Biomedicals) in a Wallac 1450 MicroBeta counter (PerkinElmer).

ERK1/2 Phosphorylation Assay

hDOPr FlpIn CHO cells (CHO-hDOPr) were seeded into 96-well plates at a density of 50 000 cells/well. After 5–7 h, cells were washed with phosphate buffered saline (PBS) and incubated overnight in serum-free DMEM. Initially, time-course experiments were conducted at least twice for each ligand to determine the time required to maximally promote ERK1/2 phosphorylation via the δ-receptor. Concentration–response experiments were performed for the orthosteric ligands in the absence or presence of increasing concentrations of the allosteric modulator at 37 °C. Stimulation of the cells was terminated by removal of the media and the addition of 100 μL of SureFire lysis buffer (PerkinElmer) to each well. The plate was shaken for 5 min at room temperature before transferring 5 μL of the lysates to a white 384-well Proxiplate (PerkinElmer). Then 8 μL of a 240:1440:7:7 mixture of Surefire activation buffer/Surefire reaction buffer/Alphascreen acceptor beads/Alphascreen donor beads was added to the samples and

incubated in the dark at 37 °C for 1.5 h. Plates were read using a Fusion plate reader (PerkinElmer).

Data Analysis

For all experiments data were analyzed and EC₅₀ or K_i values determined using nonlinear regression analysis to fit a logistic equation using GraphPad Prism, version 6 (GraphPad, San Diego, CA). pK_B and αβ values were determined using the “operational model of allosterism” (Leach *et al.*, 2007) (see eq 1), using Graphpad Prism, version 6.

$$E = \frac{E_m(\tau_A[A](K_B + \alpha\beta[B]) + \tau_B[B]K_A)n}{([A]K_B + K_A K_B + K_A[B] + \alpha[A][B])n + (\tau_A[A](K_B + \alpha\beta[B]) + \tau_B[B]K_A)n}$$

Within this model, E is the pharmacological effect, K_A and K_B denote the equilibrium binding constants for the orthosteric ligand A and the allosteric ligand B at the receptor. The binding cooperativity factor α represents the effect of the allosteric ligand on orthosteric agonist binding affinity and vice versa. An activation cooperativity factor β denotes the effect the allosteric ligand has on orthosteric agonist efficacy. Agonism constants τ_A and τ_B represent the intrinsic activity of the orthosteric agonist and any intrinsic activity of the allosteric ligand, respectively, which is dependent on the cell context and receptor expression level of the cell system and intrinsic efficacy of the ligands used. The remaining parameters E_m and n denote the maximal response of the system and the slope, respectively.

APPENDIX C

Ligand-Based Discovery of a New Scaffold for Allosteric Modulation of the μ -Opioid Receptor⁴

Summary

With the hope of discovering effective analgesics with fewer side effects, attention has recently shifted to allosteric modulators of the opioid receptors. In the past two years, the first chemotypes of positive or silent allosteric modulators (PAMs or SAMs, respectively) of μ - and δ -opioid receptor types have been reported in the literature. During a structure-guided lead optimization campaign with μ -PAMs BMS-986121 and BMS-986122 as starting compounds, we discovered a new chemotype that was confirmed to display μ -PAM or μ -SAM activity depending on the specific substitutions as assessed by endomorphin-1-stimulated β -arrestin2 recruitment assays in Chinese Hamster Ovary (CHO)- μ PathHunter cells. The most active μ -PAM of this series was analyzed further in competition binding and G-protein activation assays to understand its effects on ligand binding and to investigate the nature of its probe dependence.

Introduction

A prominent member of the G-protein-coupled receptor (GPCR) superfamily, the μ -opioid receptor is the main pharmacological target for both acute and chronic pain, as well as a target for the treatment of alcohol abuse, drug abuse, and addiction disorders (Spetea *et al.*, 2013; Pasternak, 2014). Although μ -opioid medications such as morphine and its derivatives remain the “gold-standard” for pain management, clinicians are rightly conservative in the administration of these drugs, owing to their dangerous adverse effects (e.g., respiratory

⁴ This research was originally published in the Journal of Chemical Information and Modeling. Bisignano P, Burford NT, Shang Y, Marlow B, Livingston KE, Fenton AM, Rockwell K, Budenholzer L, Traynor JR, Gerritz SW, Alt A, Filizola M. “Ligand-Based Discovery of a Novel Scaffold for Allosteric Modulation of the mu Opioid Receptor.” *J. Chem. Inform. and Modeling*. 2015 Sep 28;55(9):1836-43

© 2015 American Chemical Society.

depression, nausea, tolerance, dependence, and constipation), as well as social and legal issues. As a result, the development of new opioid analgesics that are free from side effects represents a critically important research objective for 21st century medicine.

Recent high-resolution structural information on the μ -opioid receptor (Manglik *et al.*, 2012), as well as novel paradigms of biased agonism (or functional selectivity) and allosterism at this receptor (N Burford *et al.*, 2015; Thompson *et al.*, 2015), may offer unprecedented opportunities for the discovery of opioid therapeutics with reduced adverse effects. Allosteric ligands are defined as binding to regions that are distinct from the site where the endogenous ligand binds (defined as the orthosteric binding site). Depending on whether they enhance or reduce the affinity and/or efficacy of the orthosteric ligand, they can be classified as positive allosteric modulators (PAMs) or negative allosteric modulators (NAMs), respectively. In principle, these ligands have several theoretical advantages over traditional orthosteric agonists and antagonists. First, because allosteric regions of GPCRs tend to be less evolutionarily conserved than orthosteric binding sites, allosteric ligands can attain improved receptor type selectivity, which can limit the occurrence of off-target effects (although this does not eliminate the possibility of on-target effects). In the case of opioid receptors, development of selective opioid drugs has not been a major impediment, and most of the untoward side effects of opioid agonists are target-mediated; therefore, this specific advantage of allosteric modulators may have limited applicability to opioid receptors. Another important advantage of allosteric modulators is that their effect is limited by their cooperativity, and therefore allosteric ligands may hold great potential as safer drugs with fewer on-target overdosing risks. This feature may be more important in the case of μ -opioid receptors, where safety risks associated with drug overdose are a very significant problem. Finally, another major theoretical advantage of PAMs compared to orthosteric agonists is that PAMs are likely to maintain the temporal and spatial fidelity of signaling *in vivo* as they only act in the presence of the endogenous ligand. Therefore, PAMs might be expected to produce significantly less desensitization and tolerance than direct-acting agonists, which continuously activate the receptor until the drug is cleared. Because tolerance and dependence produced by direct opioid agonists remain major issues limiting their therapeutic utility, this feature of PAMs may have great importance in the case of μ -opioid receptors specifically. Similarly, opioid PAMs may be able to avoid some of the on-target side effects produced by opioid agonists by virtue of acting only in tissues where native opioid signaling is

occurring. For a more thorough review on the potential advantages of opioid PAMs, see Burford et al (N Burford *et al.*, 2015). It is important to note that at present these potential advantages of opioid PAMs remain purely theoretical, as *in vivo* effects of opioid PAMs have not yet been reported.

Although several GPCR allosteric modulators have shown preclinical promise in neurodegenerative, psychiatric, or neurobehavioral diseases (Nickols *et al.*, 2014), the development and validation of drug-like allosteric modulators of the opioid receptors lags behind. The first opioid allosteric modulators were identified for the μ -opioid receptor from a recent high throughput screening campaign using a β -arrestin2 recruitment assay (Burford *et al.*, 2013). Specifically, this screen identified two PAMs and two silent allosteric modulators (SAMs) of the μ -opioid receptor. While the μ -SAMs exhibited neutral cooperativity with orthosteric ligands in spite of their competitive binding at the allosteric site, the two μ -PAMs BMS-986121 and BMS-986122 potentiated the effects of endomorphin-1, DAMGO ([d-Ala², N-MePhe⁴, Gly-ol]-enkephalin), and morphine in β -arrestin2 recruitment, G-protein activation, and adenylyl cyclase (AC) inhibition. Although a few PAMs of the δ -opioid receptor have also been recently identified (NT Burford *et al.*, 2014; Burford *et al.*, 2015; Appendix B), additional pharmacological tools are needed to investigate further the effect of allosterism on μ -opioid receptor signaling, and to test whether μ -opioid receptor PAMs will in fact provide the potential therapeutic advantages described above.

Here, we report the discovery of a new chemotype that, depending on the specific substitutions, exhibits μ -PAM or μ -SAM activity as assessed by endomorphin-1-stimulated β -arrestin2 recruitment assays in Chinese Hamster Ovary (CHO)- μ PathHunter cells. Further radioligand binding and G-protein activation assays were performed on the most active μ -PAM of this series (MS1) to understand both its effects on ligand binding and the nature of its probe dependence.

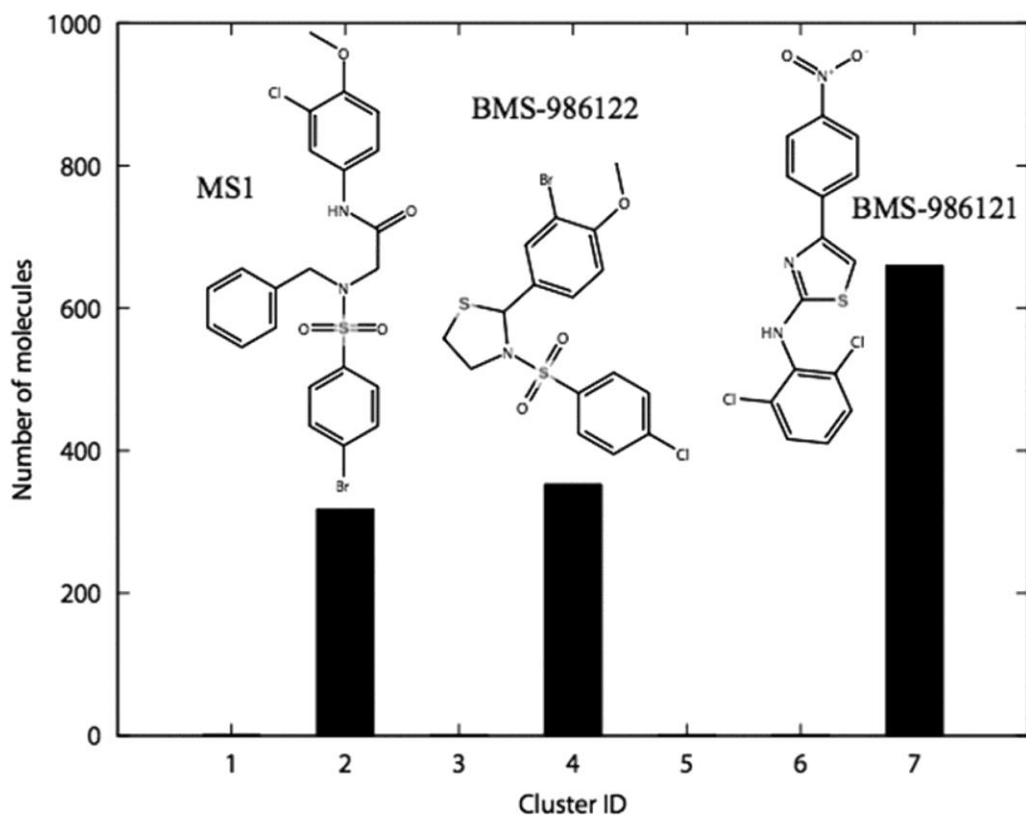


Figure C.1: Clustering results of the 1336 analogs of BMS-986121 and BMS-986122 extracted from eMolecules. The three most populated clusters 2, 4, and 7 included analogs of MS1, BMS-986122, and BMS-986121, respectively.

Results

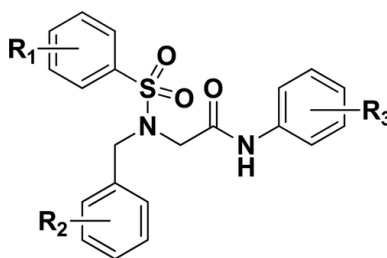
Discovery and Structure–Activity Relationship of a New μ -PAM/SAM Chemotype

In the hunt for more active allosteric modulators of the μ -opioid receptor, we searched the eMolecules database for analogs of the recently identified μ -PAMs BMS-986121 and BMS-986122 (Burford *et al.*, 2013), including significantly different chemical scaffolds. Clustering of the resulting 1336 molecules led to their grouping into 7 clusters (Fig C.1). While cluster 1 contained 2 elements and clusters 3, 5, and 6 contained 1 element only, clusters 2, 4, and 7 were highly populated (see Fig C.1). Specifically, clusters 4 and 7 contained 353 and 660 close analogs of BMS-986122 and BMS-986121, respectively, whereas the 318 molecules of cluster 2 corresponded to a significantly different chemotype (e.g., compare MS1 to BMS-986122 and BMS-986121 in Fig C.1). Additional analogs of this new chemotype were retrieved through a chemical similarity search to MS1 in both the eMolecules and ZINC databases (see Methods for details).

Twenty-eight of these compounds were purchased for experimental testing, and the results of a primary screen based on a PathHunter β -arrestin recruitment assay are shown in Table C.1. While none of these compounds displayed agonist activity alone, all of them but two (i.e, MS27 and MS28) displayed PAM or SAM activity in the presence of low concentration of endomorphin-1, a μ -opioid receptor agonist. No NAM activity (inhibition of an EC_{50} concentration of endomorphin-1) was detected (data not shown). As shown in Table C.1, most PAMs had low potencies in the single and low double digit μ M range with efficacy (Y_{max}) values below 40% compared to endomorphin-1 maximal stimulation. The exceptions were MS1, MS2, and MS3, which displayed a Y_{max} value larger than 44% in PAM mode with EC_{50} values in the single digit μ M range. The Y_{max} activity gives an indication of the degree of cooperativity exhibited by these compounds suggesting that MS1, MS2, and MS3 have greater cooperativity compared to the other MS compounds tested. The remaining 12 compounds are either SAMs or weak PAMs judging from their reduced PAM activity. As expected, SAMs behave as competitive antagonists at the allosteric site, having little to no allosteric efficacy themselves but inhibiting the binding of a higher efficacy PAM to the allosteric binding site.

For the most efficacious MS1–MS3 compounds, we assessed the K_B and α values of cooperativity by performing full concentration–response curves of the orthosteric ligand endomorphin-1 in the presence of increasing concentrations of the allosteric compounds in the β -

Table C.1: Structure Activity Relationship of a New μ -PAM/SAM Chemotype in a PathHunter β -Arrestin Recruitment Assay



<u>sample ID</u>	<u>R1</u>	<u>R2</u>	<u>R3</u>	<u>EC50, μM^a</u>	<u>PAM mode Y_{max} %</u>	<u>activity</u>
MS1	4-Br	H	3-Cl,4-MeO	6.5	85.1	PAM
MS2	4-Br	H	4-PhO	6.2	109.2	PAM
MS3	4-Cl	3-Me	3-Cl,4-MeO	5.7	44.6	PAM
MS4	4-Br	H	3-Cl	3.9	32.4	PAM
MS5	3-Me,4-MeO	H	3-Cl,4-MeO	4.7	21	PAM
MS6	4-Me	H	3-Cl,4-MeO	5.3	21.8	PAM
MS7	4-Br	H	4-MeO	5.4	22.1	PAM
MS8	4-Cl	H	4-EtO	6.4	31.8	PAM
MS9	4-F	H	3-Cl,4-MeO	7	24	PAM
MS10	4-Cl	H	4-MeO	8.9	26.4	PAM
MS11	4-OMe	H	3-Br	14.5	33	PAM
MS12	4-Me	4-Me	3-Cl,4-MeO	21.9	10.3	PAM
MS13	H	H	3-Br	> 30	20	PAM
MS14	H	H	3-Cl,4-MeO	76.1	28.4	PAM
MS15	H	2,4-di-Cl	3-Cl,4-MeO	6 ^a	NA ^b	SAM
MS16	4-Cl	H	3-MeO	6.5 ^a	NA ^b	SAM
MS17	H	4-F	3-Cl,4-MeO	6.9 ^a	NA ^b	SAM
MS18	4-Me	H	4-MeO	14.4 ^a	NA ^b	SAM
MS19	H	4-Me	3-Cl	16.2 ^a	NA ^b	SAM
MS20	H	4-Cl	4-MeO	16.6 ^a	NA ^b	SAM
MS21	H	4-Cl	3-Me	21.2 ^a	NA ^b	SAM
MS22	H	4-Br	4-MeO	22.7 ^a	NA ^b	SAM
MS23	4-Cl	H	3-Cl,6-MeO	23.5 ^a	NA ^b	SAM
MS24	H	4-Cl	3-Cl,4-MeO	24.2 ^a	NA ^b	SAM
MS25	H	4-Cl	2-MeO,5-Me	27.7 ^a	NA ^b	SAM
MS26	4-Cl	H	2-MeO,5-Me	>30 ^a	NA ^b	SAM
MS27	H	4-Me	3-Cl,4-MeO		NA ^b	inactive
MS28	4-MeO	H	2-CF3		NA ^b	inactive

^aSAM compounds were detected by incubating a serial dilution of the compound with cells in the presence of an EC₂₀ of endomorphin-1 plus an EC₈₀ of BMS-986121 PAM. Under these conditions, the SAM compound acts as an antagonist of PAM binding, reducing PAM activity. Control PAMs: BMS-986121 (EC₅₀ 2.2 μ M, Y_{max} 86%) and BMS-986122 (EC₅₀ 16.2 μ M, Y_{max} 108%).

^bNA = not active in PAM mode.

arrestin recruitment assay (see Fig C.2). The results confirm the ability of these molecules to act as PAMs with K_B and α cooperativity values slightly weaker, but comparable, to those observed for the previously reported BMS-986121 (Burford *et al.*, 2013).

The allosteric compound with the highest α value of cooperativity, MS1, was analyzed further in competition binding and G-protein activation assays to understand its effects on ligand binding and to investigate the nature of its probe dependence. Saturation binding using the neutral antagonist ^3H -diprenorphine (^3H -DPN) was performed in cell membranes prepared from C6 glioma cells stably expressing rat μ -opioid receptor (Fig C.3). The K_d of ^3H -DPN was unchanged in the presence of 10 μM MS1 (K_d with veh = 0.25 ± 0.10 nM; K_d with MS1 = 0.35 ± 0.15 nM, data not shown). In contrast, MS1 was able to enhance the affinity of the agonist l-methadone to bind μ -opioid receptor (Fig C.3A). The K_i of l-methadone in the absence or presence of 10 μM MS1 was enhanced by 7-fold (K_i in the presence of vehicle = 1177 ± 329 nM, K_i in the presence of MS1 = 161 ± 38 nM; $p = 0.04$). Notably, MS1 exhibited strong probe dependence in that it failed to alter the affinity of the agonists DAMGO, endomorphin-1, and morphine to bind μ -opioid receptor (Fig C.3B–D).

In addition to binding, the ability of MS1 to alter the activity of μ -opioid receptor agonists was investigated using $\text{GTP}\gamma^{35}\text{S}$ binding in C6- μ cell membranes. Although MS1 (up to 30 μM) failed to have any activity alone (data not shown), the presence of 10 μM MS1 enhanced the potency of l-methadone to activate G-protein by over 4-fold (Fig C.4A) but had no effect on the degree of maximal stimulation. Again, MS1 showed strong probe dependence and failed to alter the potency or maximal stimulation of DAMGO and endomorphin-1 to activate G-protein (Fig C.4B,C, respectively). However, MS1 did enhance the maximal activation by morphine to that of a full agonist while having no effect of morphine's potency (Fig C.4D). The lack of effect of MS1 on endomorphin-1 stimulation of $\text{GTP}\gamma^{35}\text{S}$ binding was unexpected in view of the enhancement of endomorphin-1 recruitment of β -arrestin, but is in line with reports that the endomorphins are arrestin-biased agonists (McPherson *et al.*, 2010; Rivero *et al.*, 2012).

Molecular Descriptors of μ -PAMs/SAM and Their Statistical Analysis

We calculated fifty-two physicochemical properties for each of the 14 μ -PAMs and 12 μ -SAMs reported in Table C.1. The numerical values of those descriptors that displayed nonzero variance across these twenty-six ligands are reported in Table S3 (see online). Considering

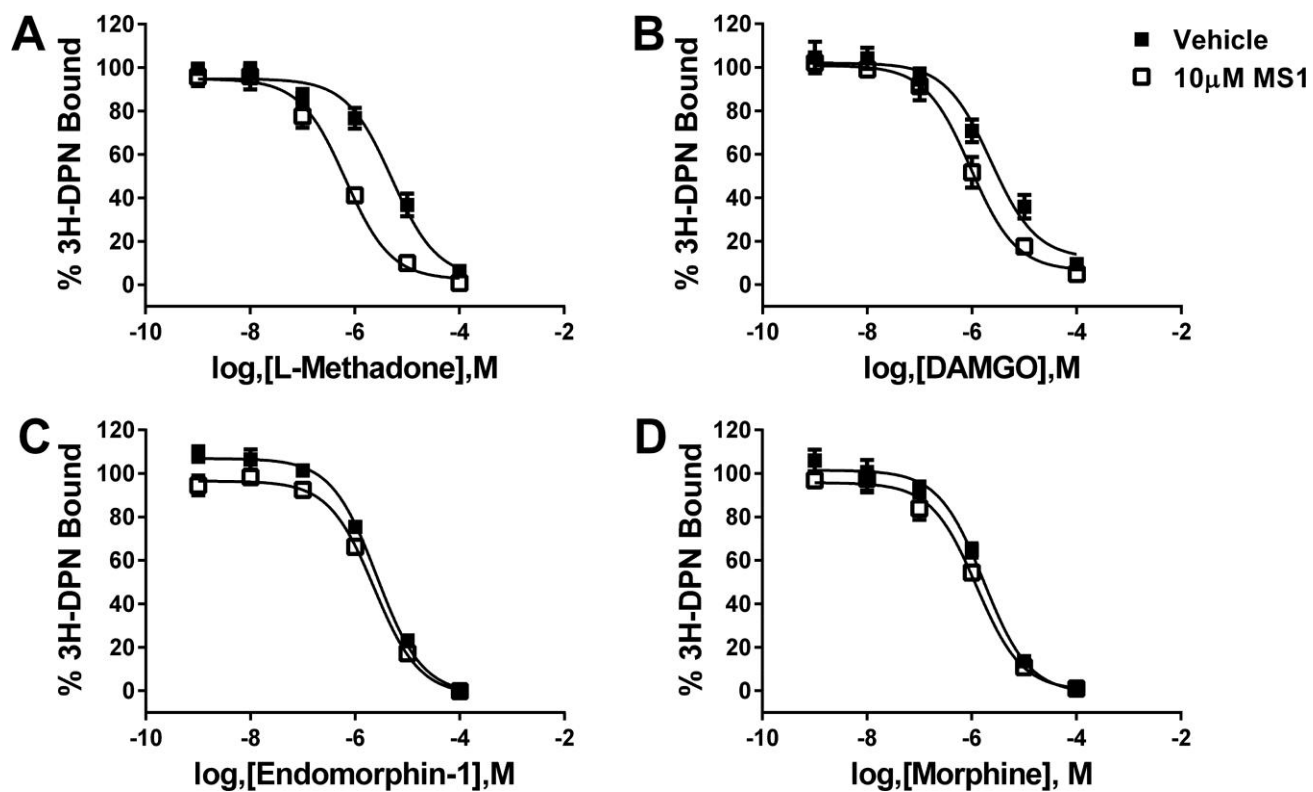


Figure C.3: Effects of MS1 on the binding of various orthosteric μ -opioid receptor agonists. Displacement of ^3H -DPN by l-methadone (A), DAMGO (B), endomorphin-1 (C), and morphine (D) was measured in the presence of vehicle (■) or 10 μM MS1 (□) using C6- μ cell membranes.

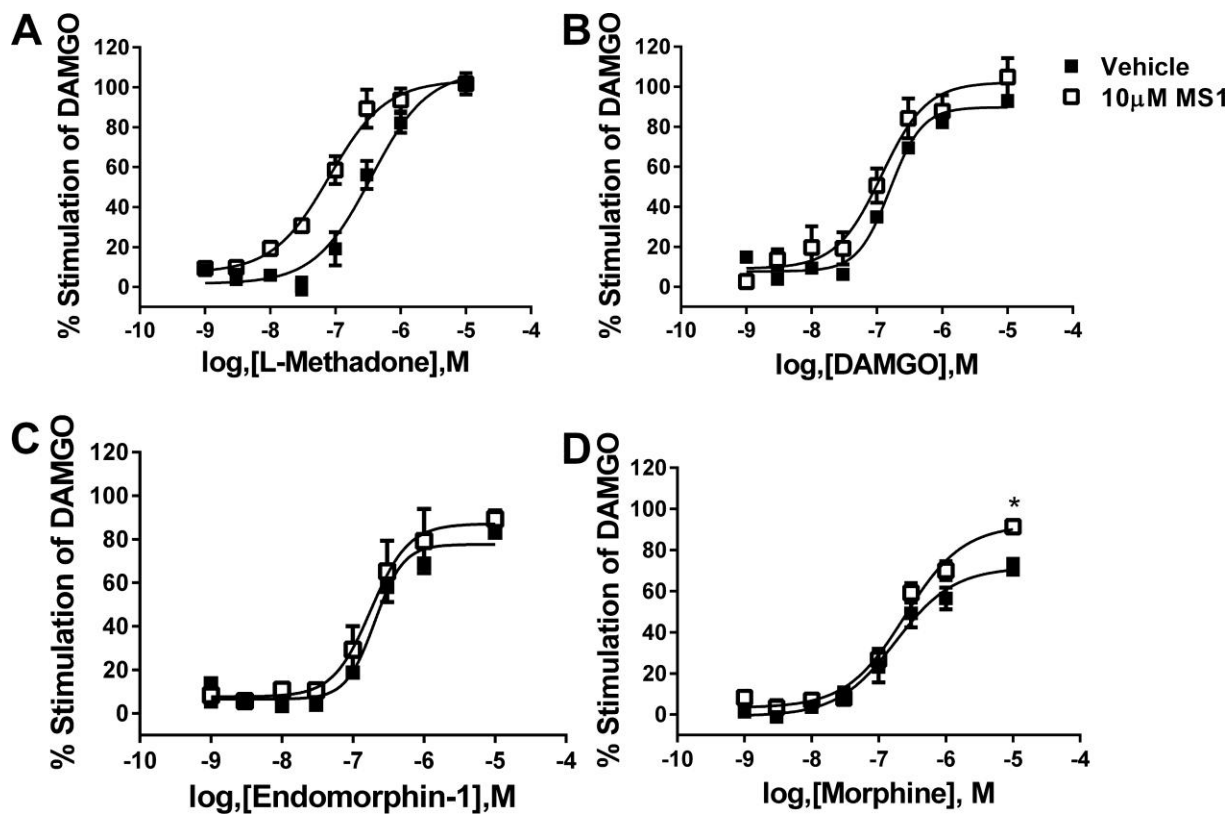


Figure C.4: Effects of MS1 on the potency of various orthosteric μ -opioid receptor agonists to activate G-protein. Agonist-stimulated $GTP\gamma^{35}S$ binding was measured for l-methadone (A), DAMGO (B), endomorphin-1 (C), and morphine (D) in the presence of vehicle (■) or 10 μ M MS1 (□) using C6- μ cell membranes.

combinations of up to 5 descriptors, Bayesian logistical regression analysis identified four descriptors that could best separate between μ -PAMs and μ -SAMs as assessed experimentally. Specifically, the best linear model according to AIC resulted from using the following four properties: the predicted central nervous system activity (CNS), the conformation-independent predicted aqueous solubility (CIQPlogS), the Parameterized Model Number 3 (PM3)-calculated electron affinity (EA.eV.), and the van der Waals surface area of polar nitrogen and oxygen atoms and carbonyl carbon atoms (PSA). Using this model, only four (MS12, MS13, MS14, and MS23) out of twenty-six compounds could not be confidently assigned the same μ -PAM or μ -SAM activity inferred from experiments owing to their predicted effect value below or above an arbitrary 0.5 cutoff, respectively. The remaining 11 PAMs exhibited calculated average values of -0.82 ± 0.40 , -7.12 ± 0.75 , $+1.07 \pm 0.14$, and $+76.51 \pm 3.62$ for CNS, CIQPlogS, PM3, and EA.eV., respectively, whereas the remaining 11 SAMs had corresponding values of -0.91 ± 0.54 , -6.54 ± 0.51 , $+0.94 \pm 0.08$, and $+74.04 \pm 2.78$.

Common 3D-Pharmacophore of μ -PAMs

We built a ligand-based 3D pharmacophore model to elaborate further on the molecular and structural determinants that differentiate μ -PAMs from μ -SAMs. The best 3D pharmacophore model of this kind (Fig C.5) includes: (i) two H-bond acceptors (i.e., the two oxygen atoms of the sulfur dioxide group) labeled A1 and A2 in the figure, (ii) one halogen substituent or hydrophobic group (i.e., R1 = Br, Cl, Me; see Table C.1) labeled Halo/Hyd in the figure, and (iii) the three aromatic rings R1–R3 related by the distances and angles reported in Tables S6 and S7 (see online), respectively. Using this model, all μ -PAMs (but MS13) could be separated from all μ -SAMs (but MS16 and MS23) according to an arbitrary cutoff of 1.7 for the pharmacophore alignment fitness scores. In the case of MS13, an optimal alignment of this compound to the best pharmacophore model could not be found because of competition in the alignment between the hydrophobic substituent on ring 3 (R3) and that of ring 1 (R1). Although MS16 and MS23 could indeed be successfully aligned to the pharmacophore model, the R3 methoxy substitution at the ortho- position might interfere with the position of the ligand amide atoms although it is also possible that the R3 methoxy substitution at ortho- or meta- positions clashes with the receptor environment. More sophisticated strategies than simple docking are

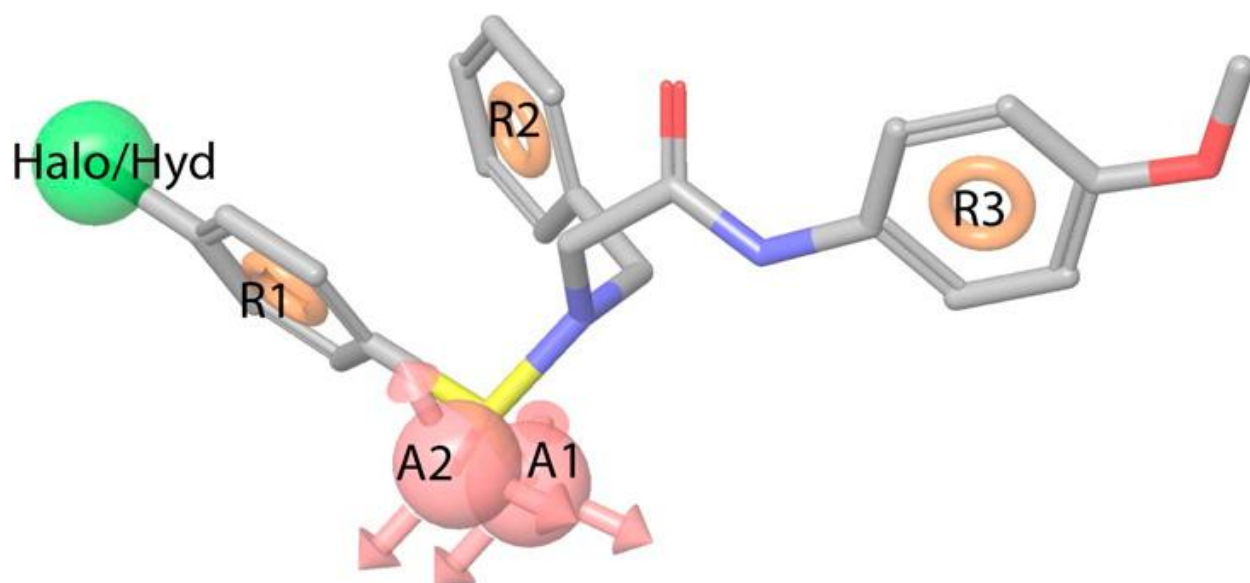


Figure C.5: Ligand-based 3D pharmacophore model built from μ -PAMs shown in Table C.1. The best 3D pharmacophore model that separates μ -PAMs and μ -SAMs includes two H-bond acceptors (i.e., the two oxygen atoms of the sulfur dioxide group), one halogen substituent or hydrophobic group (i.e., R1 = Br, Cl, Me; see Table 1), and three aromatic rings related by specific distances and angles listed in Tables S6 and S7 (see online).

currently being tested in our lab to be eventually be able to support or dispute unambiguously this possibility.

Discussion

Recently, attention has shifted to allosteric rather than orthosteric opioid ligands as a means of potentially providing effective pain relief that is free from debilitating adverse effects (Thompson *et al.*, 2015). These allosteric modulators are expected to be receptor type selective, and to act by enhancing the antinociceptive activity of endogenous opioid ligands. Therefore, μ -opioid receptor PAMs may have fewer on-target side effects and overdosing risks, and may produce less tolerance and dependence than currently used opioid agonists. It has been suggested that opioid ligands that bias receptor signaling toward the G-protein mediated pathway instead of β -arrestin2 may be therapeutically beneficial (Raehal *et al.*, 2011). Whether caused by the receptor conformational plasticity, allosterism, or dimerization/oligomerization, this G-protein-biased agonism has been suggested to remove the on-target side effects such as drug tolerance associated with the μ -opioid receptor internalization (e.g., see (Thompson *et al.*, 2015)). The current findings with endomorphin-1 suggest that the μ -opioid receptor PAM MS1 may promote signaling bias in the opposite direction (favoring β -arrestin versus G-protein activation), at least with this peptide. Further studies are needed in order to understand more fully both the signaling bias and probe-dependence of this PAM, and to determine whether these properties can be altered through modifications to the chemical structure.

The only two known μ -PAMs at the time of this work, i.e., BMS-986121 and BMS-986122, are limited in their ease of synthesis. Not only is the new allosteric modulator chemotype we identified easier to derivatize by synthetic chemistry, and offering an additional point of diversity for structure–activity relationship studies compared to previously published compounds, but the new scaffold increases the chemical diversity of known ligands for the allosteric site of the μ -opioid receptor. However, undesirable “off-target” effects may still be present for this scaffold, and must be evaluated before further development.

In competition binding and G-protein activation assays, MS1 displayed marked probe dependence. Indeed, the largest effects of MS1 were seen with l-methadone. The prototype μ -PAM BMS-986122 also showed the highest levels of cooperativity with methadone and its isomers (Chapter 3; Livingston and Traynor, 2014). Because MS1 is a new scaffold, this similar

probe dependence may be reflective of a similar mechanism of action and/or mode of binding. In addition, MS1 enhanced the maximal activation of the partial agonist morphine to activate G-protein. This again fits with the probe dependence of BMS-986122 in which the efficacy of partial agonists was increased. The mechanism of BMS-986122 action was found to be through allosteric disruption of sodium ion binding (Chapter 3; Livingston and Traynor, 2014) and it would be interesting to determine if this new chemotype also functions in a similar manner.

Cheminformatics analysis of the set of newly identified μ -PAMs and μ -SAMs suggested that physicochemical properties such as the predicted CNS, the CIQPlogS, the EA.eV., and the PSA may be used as searching criteria to identify additional compounds with potential PAM activity at μ -opioid receptors. Specifically, our best statistical model shows that μ -PAMs have higher predicted values of central nervous system activity, PM3-calculated electron affinity, and van der Waals surface area of polar nitrogen and oxygen atoms and carbonyl carbon atoms, but lower calculated values of conformation-independent predicted aqueous solubility, compared to μ -SAMs. However, it must be kept in mind that the dataset we used is limited in number and no thorough cross-validation of the presented statistical models could be performed. Although the same limitation exists for the predicted common 3D pharmacophore model of μ -PAMs vs μ -SAMs, the suggested model can be used as an initial criterion to either design more highly potent derivatives of the newly identified μ -PAM or to search for completely different chemotypes that retain the same pharmacophore features. These inferences can and will eventually be combined with structural studies using the crystal structure of the active μ -opioid receptor that has appeared in the literature during review of this paper (Huang *et al.*, 2015). In the meantime, additional ligand-based studies are ongoing in our laboratories to optimize the newly identified chemotype and to explore the potential of this scaffold for the development of new therapeutics.

Bibliography

- Ahn KH, Mahmoud MM, and Kendall D (2012) Allosteric modulator ORG27569 induces CB1 cannabinoid receptor high affinity agonist binding state, receptor internalization, and Gi protein-independent ERK1/2 kinase activation. *J Biol Chem* **287**:12070–12082.
- Allouche S, Noble F, and Marie N (2014) Opioid receptor desensitization: mechanisms and its link to tolerance. *Front Pharmacol* **5**:1–20.
- Alt A, McFadyen IJ, Fan CD, Woods JH, and Traynor JR (2001) Stimulation of guanosine-5'-o-(3-[35S]thio)triphosphate binding in digitonin-permeabilized C6 rat glioma cells: evidence for an organized association of mu-opioid receptors and G protein. *J Pharmacol Exp Ther* **298**:116–121.
- Appelmans N, Carroll JA, Rance MJ, Simon E, and Traynor JR (1986) Sodium ions increase the binding of the antagonist peptide ICI 174864 to the delta-opiate receptor. *Neuropeptides* **7**:139–143.
- Ariens E, and De Groot W (1954) Affinity and intrinsic-activity in the theory of competitive inhibition. III. Homologous decamethonium-derivatives and succinyl-choline-esters. *Arch Int Pharmacodyn Ther* **99**:193–205.
- Arunlakshana O, and Schild H (1959) Some quantitative uses of drug antagonists. *Br J Pharmacol* **14**:47–58.
- Baillie GL, Horswill JG, Anavi-Goffer S, Reggio PH, Bolognini D, Abood ME, McAllister S, Strange PG, Stephens GJ, Pertwee RG, and Ross R a (2013) CB(1) receptor allosteric modulators display both agonist and signaling pathway specificity. *Mol Pharmacol* **83**:322–338.
- Ballesteros JA, and Weinstein H (1995) Integrated methods for the construction of three-dimensional models and computational probing of structure-function relations in G protein-coupled receptors. *Methods Neurosci* **25**:366–428.
- Bartuzi D, Kaczor AA, and Matosiuk D (2016) Interplay between Two Allosteric Sites and Their Influence on Agonist Binding in Human μ Opioid Receptor. *J Chem Inf Model* [acs.jcim.5b00705](https://doi.org/10.1021/acs.jcim.5b00705).
- Bassoni D, Raab W, Achacoso P, Loh CY, and Wehrman TS (2012) Measurements of beta-arrestin recruitment to activated seven transmembrane receptors using enzyme complementation. *Recept Bind Tech* **897**:181–203.

- Bisignano P, Burford NT, Shang Y, Marlow B, Livingston KE, Fenton AM, Rockwell K, Budenholzer L, Traynor JR, Gerritz SW, Alt A, and Filizola M (2015) Ligand-Based Discovery of a New Scaffold for Allosteric Modulation of the μ -Opioid Receptor. *J Chem Inf Model* **55**:1836–1843.
- Black J, and Leff P (1983) Operational models of pharmacological agonism. *Proc R Soc London* **220**:141–162.
- Blane GF, Boura a L, Fitzgerald a E, and Lister RE (1967) Actions of etorphine hydrochloride, (M99): a potent morphine-like agent. *Br J Pharmacol Chemother* **30**:11–22.
- Bohn LM, Gainetdinov RR, Lin FT, Lefkowitz RJ, and Caron MG (2000) Mu-opioid receptor desensitization by beta-arrestin-2 determines morphine tolerance but not dependence. *Nature* **408**:720–3.
- Bohn LM, Lefkowitz RJ, and Caron MG (2002) Differential mechanisms of morphine antinociceptive tolerance revealed in (beta)arrestin-2 knock-out mice. *J Neurosci* **22**:10494–500.
- Bohn LM, Lefkowitz RJ, Gainetdinov RR, Peppel K, Caron MG, and Lin FT (1999) Enhanced morphine analgesia in mice lacking beta-arrestin 2. *Science* **286**:2495–8.
- Broadhead GK, Mun HC, Avlani VA, Jourdon O, Church WB, Christopoulos A, Delbridge L, and Conigrave AD (2011) Allosteric modulation of the calcium-sensing receptor by gamma-glutamyl peptides: Inhibition of pth secretion, suppression of intracellular cAMP levels, and a common mechanism of action with L-amino acids. *J Biol Chem* **286**:8786–8797.
- Broom DC, Nitsche JF, Pintar JE, Rice KC, Woods JH, and Traynor JR (2002) Comparison of receptor mechanisms and efficacy requirements for delta-agonist-induced convulsive activity and antinociception in mice. *J Pharmacol Exp Ther* **303**:723–9.
- Brownstein MJ (1993) A brief history of opiates, opioid peptides, and opioid receptors. *Proc Natl Acad Sci U S A* **90**:5391–5393.
- Buntin-Mushock C, Phillip L, Moriyama K, and Palmer PP (2005) Age-dependent opioid escalation in chronic pain patients. *Anesth Analg* **100**:1740–5.
- Burford N, Clark M, Wehrman T, Gerritz S, Banks M, O’Connell J, Traynor J, and Alt A (2013) Discovery of positive allosteric modulators and silent allosteric modulators of the μ -opioid receptor. *Proc Natl Acad Sci U S A* **110**:10830–10835.
- Burford N, Traynor J, and Alt A (2015) Positive allosteric modulators of the μ -opioid receptor: a novel approach for future pain medications. *Br J Pharmacol* **172**:277–286.
- Burford NT, Livingston KE, Canals M, Ryan MR, Budenholzer LML, Han Y, Shang Y, Herbst JJ, O’Connell J, Banks M, Zhang L, Filizola M, Bassoni DL, Wehrman TS, Christopoulos A, Traynor JR, Gerritz SW, and Alt A (2015) Discovery, Synthesis, and Molecular Pharmacology of Selective Positive Allosteric Modulators of the δ -Opioid Receptor. *J Med Chem* **58**:4220–4229.

- Burford NT, Watson J, Bertekap R, and Alt A (2011) Strategies for the identification of allosteric modulators of G-protein-coupled receptors. *Biochem Pharmacol* **81**:691–702.
- Burford NT, Wehrman T, Bassoni D, O’Connell J, Banks M, Zhang L, and Alt A (2014) Identification of Selective Agonists and Positive Allosteric Modulators for μ - and δ -Opioid Receptors from a Single High-Throughput Screen. *J Biomol Screen* **19**:1255–1265.
- Byun NE, Grannan M, Bubser M, Barry RL, Thompson A, Rosanelli J, Gowrishankar R, Kelm ND, Damon S, Bridges TM, Melancon BJ, Tarr JC, Brogan JT, Avison MJ, Deutch AY, Wess J, Wood MR, Lindsley CW, Gore JC, Conn PJ, and Jones CK (2014) Antipsychotic Drug-Like Effects of the Selective M4 Muscarinic Acetylcholine Receptor Positive Allosteric Modulator VU0152100. *Neuropsychopharmacology* 1–16.
- Campos AC, Ferreira FR, and Guimarães FS (2012) Cannabidiol blocks long-lasting behavioral consequences of predator threat stress: Possible involvement of 5HT1A receptors. *J Psychiatr Res* **46**:1501–1510.
- Canals M, Lane JR, Wen A, Scammells PJ, Sexton PM, and Christopoulos A (2012) A Monod-Wyman-Changeux mechanism can explain G protein-coupled receptor (GPCR) allosteric modulation. *J Biol Chem* **287**:650–659.
- Carroll J, Shaw J, and Wickenden A (1988) The physiological relevance of low agonist affinity binding at opioid mu-receptors. *Br J Pharmacol* **94**:625–631.
- Center for Substance Abuse Treatment (2004) Clinical Guidelines for the Use of Buprenorphine in the Treatment of Opioid Addiction. *Treat Improv Protoc Ser 40 DHHS Publ No 04-3939* 1–172.
- Chakrabarti S, Yang W, Law PY, and Loh HH (1997) The mu-opioid receptor down-regulates differently from the delta-opioid receptor: requirement of a high affinity receptor/G protein complex formation. *Mol Pharmacol* **52**:105–13.
- Charpentier N, Prezeau L, Carrette J, Bertorelli R, Le Cam G, Manzoni O, Bockaert J, and Homburger V (1993) Transfected Go1 alpha inhibits the calcium dependence of beta-adrenergic stimulated cAMP accumulation in C6 glioma cells. *J Biol Chem* **268**:8980–8989.
- Chavkin C, and Goldstein A (1981) Specific receptor for the opioid peptide dynorphin: structure-activity relationships. *Proc Natl Acad Sci U S A* **78**:6543–6547.
- Chen Y, Mestek A, Liu J, Hurley JA, and Yu L (1993) Molecular cloning and functional expression of a μ -opioid receptor from rat brain. *Mol Pharmacol* **44**:8–12.
- Cherezov V, Rosenbaum DM, Hanson MA, Rasmussen SGF, Thian FS, Kobilka TS, Choi H-J, Kuhn P, Weis WI, Kobilka BK, and Stevens RC (2007) High-resolution crystal structure of an engineered human beta2-adrenergic G protein-coupled receptor. *Science* **318**:1258–65.
- Christopoulos A (2014) Advances in G Protein-Coupled Receptor Allosterism: From Function to Structure. *Mol Pharmacol* **86**:463–478.

- Christopoulos A, and Kenakin T (2002) G Protein-Coupled Receptor Allostereism and Complexing. *Pharmacol Rev* **54**:323–374.
- Christopoulos A, Sorman JL, Mitchelson F, and El-Fakahany EE (1999) Characterization of the subtype selectivity of the allosteric modulator heptane-1,7-bis-(dimethyl-3'-phthalimidopropyl) ammonium bromide (c7/3-phth) at cloned muscarinic acetylcholine receptors. *Biochem Pharmacol* **57**:171–179.
- Chu Sin Chung P, Boehrer A, Stephan A, Matifas A, Scherrer G, Darcq E, Befort K, and Kieffer BL (2015) Delta opioid receptors expressed in forebrain GABAergic neurons are responsible for SNC80-induced seizures. *Behav Brain Res* **278**:429–434.
- Chu Sin Chung P, and Kieffer BL (2013) Delta opioid receptors in brain function and diseases. *Pharmacol Ther* **140**:112–120.
- Chung KY, Rasmussen SGF, Liu T, Li S, DeVree BT, Chae PS, Calinski D, Kobilka BK, Woods VL, and Sunahara RK (2011) Conformational changes in the G protein Gs induced by the β_2 adrenergic receptor. *Nature* **477**:611–615.
- Cichewicz DL (2004) Synergistic interactions between cannabinoid and opioid analgesics. *Life Sci* **74**:1317–1324.
- Clark MJ, Harrison C, Zhong H, Neubig RR, and Traynor JR (2003) Endogenous RGS Protein Action Modulates mu-Opioid Signaling through Galpha o. Effects on adenylyl cyclase, extracellular-regulated kinases, and intracellular calcium pathways. *J Biol Chem* **278**:9418–9425.
- Clark MJ, Linderman JJ, and Traynor JR (2008) Endogenous regulators of G protein signaling differentially modulate full and partial mu-opioid agonists at adenylyl cyclase as predicted by a collision coupling model. *Mol Pharmacol* **73**:1538–48.
- Conn P, Christopoulos A, and Lindsley CW (2009) Allosteric modulators of GPCRs: a novel approach for the treatment of CNS disorders. *Nat Rev Drug Discov* **8**:41–54.
- Connor M, and Traynor J (2010) Constitutively Active μ -Opioid Receptors, in *Methods in Enzymology* pp 445–469, Elsevier Inc.
- Cunningham CL, Gremel CM, and Groblewski PA (2006) Drug-induced conditioned place preference and aversion in mice. *Nat Protoc* **1**:1662–1670.
- Cussac D, Raully-Lestienne I, Heusler P, Finana F, Cathala C, Bernois S, and De Vries L (2012) μ -opioid and 5-HT1A receptors heterodimerize and show signalling crosstalk via G protein and MAP-kinase pathways. *Cell Signal* **24**:1648–1657.
- de Leon-Casasola OA, Myers DP, Donaparthi S, Bacon DR, Peppriell J, Rempel J, and Lema MJ (1993) A comparison of postoperative epidural analgesia between patients with chronic cancer taking high doses of oral opioids versus opioid-naive patients. *Anesth Analg* **76**:302–7.

- Debono DJ, Hoeksema LJ, and Hobbs RD (2013) Caring for patients with chronic pain: pearls and pitfalls. *J Am Osteopath Assoc* **113**:620–7.
- Del Castillo J, and Katz B (1957) Interaction at end-plate receptors between different choline derivatives. *Proc R Soc London Ser B, Contain Pap Bioloical Character* **146**:369–381.
- Dewire SM, Yamashita DS, Rominger DH, Liu G, Cowan CL, Graczyk TM, Chen X, Pitis PM, Gotchev D, Yuan C, Koblisch M, Lark MW, and Violin JD (2013) A G protein-biased ligand at the μ -opioid receptor is potently analgesic with reduced gastrointestinal and respiratory dysfunction compared with morphine. *J Pharmacol Exp Ther* **344**:708–17.
- Dhawan BN, Cesselin F, Raghubir R, Reisine T, Bradley PB, Portoghese PS, and Hamon M (1996) International Union of Pharmacology. XII. Classification of opioid receptors. *Pharmacol Rev* **48**:567–592.
- Divin MF, Bradbury FA, Carroll FI, and Traynor JR (2009) Neutral antagonist activity of naltrexone and δ -naltrexol in naive and opioid-dependent C6 cells expressing a μ -opioid receptor. *Br J Pharmacol* **156**:1044–1053.
- Divin MF, Holden Ko MC, and Traynor JR (2008) Comparison of the opioid receptor antagonist properties of naltrexone and δ -naltrexol in morphine-naive and morphine-dependent mice. *Eur J Pharmacol* **583**:48–55.
- Doll C, Konietzko J, Pöll F, Koch T, Höllt V, and Schulz S (2011) Agonist-selective patterns of μ -opioid receptor phosphorylation revealed by phosphosite-specific antibodies. *Br J Pharmacol* **164**:298–307.
- Dores RM, Lecaude S, Bauer D, and Danielson PB (2002) Analyzing the evolution of the opioid/orphanin gene family. *Mass Spectrom Rev* **21**:220–243.
- Dreborg S, Sundström G, Larsson T a, and Larhammar D (2008) Evolution of vertebrate opioid receptors. *Proc Natl Acad Sci U S A* **105**:15487–15492.
- Ehlert FJ (2005) Analysis of allosterism in functional assays. *J Pharmacol Exp Ther* **315**:740–754.
- Ehlert FJ (1985) The relationship between muscarinic receptor occupancy and adenylate cyclase inhibition in the rabbit myocardium. *Mol Pharmacol* **28**:410–421.
- El Kouhen R, Burd a L, Erickson-Herbrandson LJ, Chang CY, Law PY, and Loh HH (2001) Phosphorylation of Ser363, Thr370, and Ser375 residues within the carboxyl tail differentially regulates μ -opioid receptor internalization. *J Biol Chem* **276**:12774–80.
- Elliott J, Guo L, and Traynor JR (1997) Tolerance to μ -opioid agonists in human neuroblastoma SH-SY5Y cells as determined by changes in guanosine-5'-O-(3-[35S]-thio)triphosphate binding. *Br J Pharmacol* **121**:1422–8.
- Emmerson P, Clark M, Mansour A, Akil H, Woods J, and Medzihradsky F (1996) Characterization of opioid agonist efficacy in a C6 glioma cell line expressing the μ -opioid receptor. *J Pharmacol Exp Ther* **278**:1121–1127.

- Emmerson PJ, McKinzie JH, Surface PL, Suter TM, Mitch CH, and Statnick M a (2004) Na⁺ modulation, inverse agonism, and anorectic potency of 4-phenylpiperidine opioid antagonists. *Eur J Pharmacol* **494**:121–130.
- Farrell M, and Roth BL (2010) Allosteric Antipsychotics: M4 Muscarinic Potentiators as Novel Treatments for Schizophrenia. *Neuropsychopharmacology* **35**:851–852.
- Fawzi a B, Macdonald D, Benbow LL, Smith-Torhan A, Zhang H, Weig BC, Ho G, Tulshian D, Linder ME, and Graziano MP (2001) SCH-202676: An allosteric modulator of both agonist and antagonist binding to G protein-coupled receptors. *Mol Pharmacol* **59**:30–7.
- Felder CC, Bymaster FP, Ward J, and Delapp N (2000) Therapeutic Opportunities for Muscarinic Receptors in the Central Nervous System. *J Med Chem* **43**:4333–4353.
- Fenalti G, Giguere PM, Katritch V, Huang X-P, Thompson A a, Cherezov V, Roth BL, and Stevens RC (2014) Molecular control of δ -opioid receptor signalling. *Nature* **506**:191–196.
- Finn AK, and Whistler JL (2001) Endocytosis of the mu opioid receptor reduces tolerance and a cellular hallmark of opiate withdrawal. *Neuron* **32**:829–839.
- Frick S, Kramell R, Schmidt J, Fist AJ, and Kutchan TM (2005) Comparative qualitative and quantitative determination of alkaloids in narcotic and condiment *Papaver somniferum* cultivars. *J Nat Prod* **68**:666–73.
- Furchgott RF (1967) The pharmacological differentiation of adrenergic receptors. *Ann N Y Acad Sci* **139**:553–570.
- Gao Z, and Ijzerman A (2000) Allosteric modulation of A(2A) adenosine receptors by amiloride analogues and sodium ions. *Biochem Pharmacol* **60**:669–676.
- Gao ZG, Gross AS, and Jacobson KA (2004) Effects of the allosteric modulator SCH-202676 on adenosine and P2Y receptors. *Life Sci* **74**:3173–3180.
- Garbison KE, Heinz B a, Lajiness ME, and Weidner JR (2015) Phospho-ERK Assays Assay Guidance Manual. **1**:1–8.
- Gavériaux-Ruff C, and Kieffer BL (2011) Delta opioid receptor analgesia: recent contributions from pharmacology and molecular approaches. *Behav Pharmacol* **222**:405–414.
- Gesty-Palmer D, Chen M, Reiter E, Ahn S, Nelson CD, Wang S, Eckhardt AE, Cowan CL, Spurney RF, Luttrell LM, and Lefkowitz RJ (2006) Distinct beta-Arrestin- and G Protein-dependent Pathways for Parathyroid Hormone Receptor-stimulated ERK1/2 Activation. *J Biol Chem* **281**:10856–10864.
- Gesty-Palmer D, Flannery P, Yuan L, Corsino L, Spurney R, Lefkowitz RJ, and Luttrell LM (2009) A beta-arrestin-biased agonist of the parathyroid hormone receptor (PTH1R) promotes bone formation independent of G protein activation. *Sci Transl Med* **1**:1ra1.
- Ghosh E, Kumari P, Jaiman D, and Shukla AK (2015) Methodological advances: the unsung heroes of the GPCR structural revolution. *Nat Rev Mol Cell Biol* **16**:69–81.

- Goldstein A, Tachibana S, Lowney LI, Hunkapiller M, and Hood L (1979) Dynorphin-(1-13), an extraordinarily potent opioid peptide. *Proc Natl Acad Sci* **76**:6666–6670.
- Goupil E, Tassy D, Bourguet C, Quiniou C, Wisheart V, Pétrin D, Le Gouill C, Devost D, Zingg HH, Bouvier M, Uri Saragovi H, Chemtob S, Lubell WD, Claing A, Hébert TE, and Laporte SA (2010) A novel biased allosteric compound inhibitor of parturition selectively impedes the prostaglandin F₂ α -mediated Rho/ROCK Signaling Pathway. *J Biol Chem* **285**:25624–25636.
- Groer C, Tidgewell K, and Moyer R (2007) An Opioid Agonist that Does Not Induce μ -Opioid Receptor — Arrestin Interactions or Receptor Internalization. *Mol Pharmacol* **71**:549–557.
- Gutiérrez-de-Terán H, Massink A, Rodríguez D, Liu W, Han GW, Joseph JS, Katritch I, Heitman LH, Xia L, Ijzerman AP, Cherezov V, Katritch V, and Stevens RC (2013) The role of a sodium ion binding site in the allosteric modulation of the A(2A) adenosine G protein-coupled receptor. *Structure* **21**:2175–2185.
- Haga K, Kruse AC, Asada H, Yurugi-Kobayashi T, Shiroishi M, Zhang C, Weis WI, Okada T, Kobilka BK, Haga T, and Kobayashi T (2012) Structure of the human M2 muscarinic acetylcholine receptor bound to an antagonist. *Nature* **482**:547–551.
- Hassell AM, An G, Bledsoe RK, Bynum JM, Carter HL, Deng SJJ, Gampe RT, Grisard TE, Madauss KP, Nolte RT, Rocque WJ, Wang L, Weaver KL, Williams SP, Wisely GB, Xu R, and Shewchuk LM (2006) Crystallization of protein-ligand complexes. *Acta Crystallogr Sect D Biol Crystallogr* **63**:72–79.
- Hegde VL, Singh UP, Nagarkatti PS, and Nagarkatti M (2015) Critical Role of Mast Cells and Peroxisome Proliferator-Activated Receptor γ in the Induction of Myeloid-Derived Suppressor Cells by Marijuana Cannabidiol In Vivo. *J Immunol* **194**:5211–22.
- Herenbrink CK, Sykes DA, Donthamsetti P, Canals M, Coudrat T, Shonberg J, Scammells PJ, Capuano B, Sexton PM, Charlton SJ, Javitch JA, Christopoulos A, and Lane JR (2016) The role of kinetic context in apparent biased agonism at GPCRs. *Nat Commun* **7**:1–14, Nature Publishing Group.
- Heusler P, Tardif S, and Cussac D (2016) Agonist stimulation at human μ opioid receptors in a [(35)S]GTP γ S incorporation assay: observation of “bell-shaped” concentration-response relationships under conditions of strong receptor G protein coupling. *J Recept Signal Transduct Res* **36**:158–66.
- Hoyo M, Sudo Y, Ando Y, Minami K, Takada M, Matsubara T, Kanaide M, Taniyama K, Sumikawa K, and Uezono Y (2008) μ -Opioid Receptor Forms a Functional Heterodimer With Cannabinoid CB1 Receptor: Electrophysiological and FRET Assay Analysis. *J Pharmacol Sci* **108**:308–319.
- Hollinger S, and Hepler JR (2002) Cellular regulation of RGS proteins: modulators and integrators of G protein signaling. *Pharmacol Rev* **54**:527–59.

- Hu J, and El-Fakahany E (1993) Allosteric Interaction of Dynorphin and Myelin Basic Protein with Muscarinic Receptors. *Pharmacology* **47**:351–359.
- Huang W, Manglik A, Venkatakrisnan AJ, Laeremans T, Feinberg EN, Sanborn AL, Gmeiner P, Kato HE, Livingston KE, Thorsen TS, Kling RC, Husbands SM, Traynor JR, Weis WI, Steyaert J, Dror RO, and Kobilka BK (2015) Structural insights into mu-opioid receptor activation. *Nature* **524**:315–323.
- Hughes J, Smith TW, Kosterlitz HW, Fothergill L, Morgan B, and Morris HR (1975) Identification of two related pentapeptides from the brain with potent opiate agonist activity. *Nature* **258**:577–579.
- Huidobro F, Huidobro-Toro J, and Leong Way E (1976) Studies Single on Tolerance Doses of Development Morphine in Mice. *J Pharmacol Exp Ther* **198**:318–329.
- Irannejad R, Tomshine JC, Tomshine JR, Chevalier M, Mahoney JP, Steyaert J, Rasmussen SGF, Sunahara RK, El-Samad H, Huang B, and von Zastrow M (2013) Conformational biosensors reveal GPCR signalling from endosomes. *Nature* **495**:534–538.
- Jaffe JH (1985) Impact of scheduling on the practice of medicine and biomedical research. *Drug Alcohol Depend* **14**:403–418.
- Just S, Illing S, Trester-Zedlitz M, Lau EK, Kotowski SJ, Miess E, Mann A, Doll C, Trinidad JC, Burlingame AL, von Zastrow M, and Schulz S (2013) Differentiation of opioid drug effects by hierarchical multi-site phosphorylation. *Mol Pharmacol* **83**:633–9.
- Jutkiewicz EM (2006) The antidepressant-like effects of delta-opioid receptor agonists. *Mol Interv* **6**:162–169.
- Jutkiewicz EM, Baladi MG, Folk JE, Rice KC, and Woods JH (2006) The convulsive and electroencephalographic changes produced by nonpeptidic delta-opioid agonists in rats: comparison with pentylenetetrazol. *J Pharmacol Exp Ther* **317**:1337–48.
- Jutkiewicz EM, Rice KC, Traynor JR, and Woods JH (2005) Separation of the convulsions and antidepressant-like effects produced by the delta-opioid agonist SNC80 in rats. *Psychopharmacology (Berl)* **182**:588–596.
- Kalant H (1997) Opium revisited: A brief review of its nature, composition, non-medical use and relative risks. *Addiction* **92**:267–277.
- Kathmann M, Flau K, Redmer A, Tränkle C, and Schlicker E (2006) Cannabidiol is an allosteric modulator at mu- and delta-opioid receptors. *Naunyn Schmiedebergs Arch Pharmacol* **372**:354–61.
- Katritch V, Fenalti G, Abola EE, Roth BL, Cherezov V, and Stevens RC (2014) Allosteric sodium in class A GPCR signaling. *Trends Biochem Sci* **39**:233–244.
- Kenakin T (2002) Efficacy at G-protein-coupled receptors. *Nat Rev Drug Discov* **1**:103–110.

- Kenakin T (2013) New concepts in pharmacological efficacy at 7TM receptors: IUPHAR review 2. *Br J Pharmacol* **168**:554–575.
- Kenakin T, and Christopoulos A (2011) Analytical pharmacology: the impact of numbers on pharmacology. *Trends Pharmacol Sci* **32**:189–196.
- Kenakin T, and Christopoulos A (2012) Signalling bias in new drug discovery: detection, quantification and therapeutic impact. *Nat Rev Drug Discov* **12**:205–216.
- Kenakin T, Watson C, Muniz-Medina V, Christopoulos A, and Novick S (2012) A simple method for quantifying functional selectivity and agonist bias. *ACS Chem Neurosci* **3**:193–203.
- Keov P, Sexton PM, and Christopoulos A (2011) Allosteric modulation of G protein-coupled receptors: A pharmacological perspective. *Neuropharmacology* **60**:24–35.
- Kofuku Y, Ueda T, Okude J, Shiraishi Y, Kondo K, Maeda M, Tsujishita H, and Shimada I (2012) Efficacy of the β 2-adrenergic receptor is determined by conformational equilibrium in the transmembrane region. *Nat Commun* **3**:1045.
- Kosten TR, and George TP (2002) The neurobiology of opioid dependence: implications for treatment. *Sci Pract Perspect* **1**:13–20.
- Kosterlitz HW, Leslie FM, and Waterfield AA (1975) Rates of onset and offset of action of narcotic analgesics in isolated preparations. *Eur J Pharmacol* **32**:10–16.
- Kristensen K, Christensen C, and Christrup L (1995) The mu 1, mu 2, delta, kappa opioid receptor binding profiles of methadone stereoisomers and morphine. *Life Sci* **56**:PL45–50.
- Kromer W (1988) Endogenous and exogenous opioids in the control of gastrointestinal motility and secretion. *Pharmacol Rev* **40**:121–162.
- Kruse AC, Ring AM, Manglik A, Hu J, Hu K, Eitel K, Hübner H, Pardon E, Valant C, Sexton PM, Christopoulos A, Felder CC, Gmeiner P, Steyaert J, Weis WI, Garcia KC, Wess J, and Kobilka BK (2013) Activation and allosteric modulation of a muscarinic acetylcholine receptor. *Nature* **504**:101–106.
- Lamberts JT, Jutkiewicz EM, Mortensen RM, and Traynor JR (2011) Mu-Opioid Receptor Coupling to G α (o) Plays an Important Role in Opioid Antinociception. *Neuropsychopharmacology* **36**:2041–2053.
- Lane JR, Donthamsetti P, Shonberg J, Draper-Joyce CJ, Dentry S, Michino M, Shi L, López L, Scammells PJ, Capuano B, Sexton PM, Javitch J a, and Christopoulos A (2014) A new mechanism of allostery in a G protein-coupled receptor dimer. *Nat Chem Biol* **10**.
- Lane JR, Sexton PM, and Christopoulos A (2013) Bridging the gap: bitopic ligands of G-protein-coupled receptors. *Trends Pharmacol Sci* **34**:59–66.

- Lau EK, Trester-Zedlitz M, Trinidad JC, Kotowski SJ, Krutchinsky AN, Burlingame AL, and von Zastrow M (2011) Quantitative Encoding of the Effect of a Partial Agonist on Individual Opioid Receptors by Multisite Phosphorylation and Threshold Detection. *Sci Signal* **4**:ra52–ra52.
- Le Bourdonnec B, Windh RT, Ajello CW, Leister LK, Gu M, Chu G, Tuthill P a, Barker WM, Koblisch M, Wiant DD, Graczyk TM, Belanger S, Cassel J a, Feschenko MS, Brogdon BL, Smith S a, Christ DD, Derelanko MJ, Kutz S, Little PJ, DeHaven RN, DeHaven-Hudkins DL, and Dolle RE (2008) Potent, orally bioavailable delta opioid receptor agonists for the treatment of pain: discovery of N,N-diethyl-4-(5-hydroxyspiro[chromene-2,4'-piperidine]-4-yl)benzamide (ADL5859). *J Med Chem* **51**:5893–5896.
- Leach K, Loiacono RE, Felder CC, McKinzie DL, Mogg A, Shaw DB, Sexton PM, and Christopoulos A (2010) Molecular mechanisms of action and in vivo validation of an M4 muscarinic acetylcholine receptor allosteric modulator with potential antipsychotic properties. *Neuropsychopharmacology* **35**:855–869.
- Leach K, Sexton PM, and Christopoulos A (2007) Allosteric GPCR modulators: taking advantage of permissive receptor pharmacology. *Trends Pharmacol Sci* **28**:382–389.
- Lee KO, Akil H, Woods JH, and Traynor JR (1999) Differential binding properties of oripavines at cloned mu- and delta-opioid receptors. *Eur J Pharmacol* **378**:323–330.
- Lewandowicz AM, Vepsäläinen J, and Laitinen JT (2006) The “allosteric modulator” SCH-202676 disrupts G protein-coupled receptor function *via* sulphydryl-sensitive mechanisms. *Br J Pharmacol* **147**:422–429.
- Lipkowski A, Tam S, and Portoghese P (1986) Peptides as receptor selectivity modulators of opiate pharmacophores. *J Med Chem* **29**:1222–1225.
- Liu W, Chun E, Thompson AA, Chubukov P, Xu F, Katritch V, Han GW, Roth CB, Heitman LH, IJzerman AP, Cherezov V, and Stevens RC (2012) Structural Basis for Allosteric Regulation of GPCRs by Sodium Ions. *Science (80-)* **337**:232–236.
- Livingston KE, and Traynor JR (2014) Disruption of the Na⁺ ion binding site as a mechanism for positive allosteric modulation of the mu-opioid receptor. *Proc Natl Acad Sci U S A* **111**:1–6.
- Luttrell LM, and Kenakin TP (2011) *Signal Transduction Protocols* (Luttrell LM, and Ferguson SSG eds), Humana Press, Totowa, NJ.
- Lutz PE, and Kieffer BL (2013) Opioid receptors: Distinct roles in mood disorders. *Trends Neurosci* **36**:195–206.
- Mains RE, Eipper B a, and Ling N (1977) Common precursor to corticotropins and endorphins. *Proc Natl Acad Sci U S A* **74**:3014–8.
- Manglik A, Kruse AC, Kobilka TS, Thian FS, Mathiesen JM, Sunahara RK, Pardo L, Weis WI, Kobilka BK, and Granier S (2012) Crystal structure of the μ-opioid receptor bound to a morphinan antagonist. *Nature* **485**:321–326.

- Martini L, and Whistler JL (2007) The role of mu opioid receptor desensitization and endocytosis in morphine tolerance and dependence. *Curr Opin Neurobiol* **17**:556–64.
- Matthes HWD, Maldonado R, Simonin F, Valverde O, Slowe S, Kitchen I, Befort K, Dierich A, Le Meur M, Dollé P, Tzavara E, Hanoune J, Roques BP, and Kieffer BL (1996) Loss of morphine-induced analgesia, reward effect and withdrawal symptoms in mice lacking the μ -opioid-receptor gene. *Nature* **383**:819–823.
- May L, Avlani VA, Langmead CJ, Herdon HJ, Wood MD, Sexton PM, and Christopoulos A (2007) Structure-Function Studies of Allosteric Agonism at M₂ Muscarinic Acetylcholine Receptors. *Mol Libr* **72**:463–476.
- May L, Leach K, Sexton PM, and Christopoulos A (2007) Allosteric Modulation of G Protein–Coupled Receptors. *Annu Rev Pharmacol Toxicol* **47**:1–51.
- McPherson J, Rivero G, Baptist M, Llorente J, Al-Sabah S, Krasel C, Dewey WL, Bailey CP, Rosethorne EM, Charlton SJ, Henderson G, and Kelly E (2010) μ -Opioid Receptors: Correlation of Agonist Efficacy for Signalling with Ability to Activate Internalization. *Mol Pharmacol* **78**:756–766.
- Miller-Gallacher JL, Nehmé R, Warne T, Edwards PC, Schertler GFX, Leslie AGW, and Tate CG (2014) The 2.1 Å resolution structure of cyanopindolol-bound β 1-adrenoceptor identifies an intramembrane Na⁺ ion that stabilises the ligand-free receptor. *PLoS One* **9**:e92727.
- Monod J, Wyman J, and Changeux JP (1965) On the Nature of Allosteric Transitions: a Plausible Model. *J Mol Biol* **12**:88–118.
- Motulsky HJ, and Insel PA (1983) Influence of sodium on the alpha₂-adrenergic receptor system of human platelets Role for intraplatelet sodium in receptor binding. *J Biol Chem* **258**:3913–3919.
- Motulsky HJ, and Mahan LC (1984) The kinetics of competitive radioligand binding predicted by the law of mass action. *Mol Pharmacol* **25**:1–9.
- Neilan CL, Akil H, Woods JH, and Traynor JR (1999) Constitutive activity of the delta-opioid receptor expressed in C6 glioma cells: identification of non-peptide delta-inverse agonists. *Br J Pharmacol* **128**:556–62.
- Neilan CL, Husbands SM, Breeden S, Ko MC, Aceto MD, Lewis JW, Woods JH, and Traynor JR (2004) Characterization of the complex morphinan derivative BU72 as a high efficacy, long-lasting mu-opioid receptor agonist. *Eur J Pharmacol* **499**:107–116.
- Nickols HH, Conn PJ, and Conn JP (2014) Development of allosteric modulators of GPCRs for treatment of CNS disorders. *Neurobiol Dis* **61**:55–71.
- Nobles KN, Xiao K, Ahn S, Shukla AK, Lam CM, Rajagopal S, Strachan RT, Huang T, Bressler EA, Hara MR, Shenoy SK, Gygi SP, and Lefkowitz RJ (2011) Distinct phosphorylation sites on the β (2)-adrenergic receptor establish a barcode that encodes differential functions of β -arrestin. *Sci Signal* **4**:ra51.

- Nygaard R, Zou Y, Dror RO, Mildorf TJ, Arlow DH, Manglik A, Pan AC, Liu CW, Fung JJ, Bokoch MP, Thian FS, Kobilka TS, Shaw DE, Mueller L, Prosser RS, and Kobilka BK (2013) The dynamic process of $\beta(2)$ -adrenergic receptor activation. *Cell* **152**:532–542.
- O'Brien J, Lemaire W, Wittman M, Jacobson M, Ha S, Wisnoski D, Lindsley C, Shaffhauser H, Rowe B, Sur C, Duggan M, Pettibone D, Conn P, and Williams D (2004) A novel selective allosteric modulator potentiates the activity of native metabotropic glutamate receptor subtype 5 in rat forebrain. *J Pharmacol Exp Ther* **309**:568–577.
- O'Callaghan JP, and Holtzman SG (1975) Quantification of the analgesic activity of narcotic antagonists by a modified hot-plate procedure. *J Pharmacol Exp Ther* **192**:497–505.
- O'Connor EC, Chapman K, Butler P, and Mead AN (2011) The predictive validity of the rat self-administration model for abuse liability. *Neurosci Biobehav Rev* **35**:912–938, Elsevier Ltd.
- Palczewski K, Kumasaka T, Hori T, Behnke C a, Motoshima H, Fox B a, Le Trong I, Teller DC, Okada T, Stenkamp RE, Yamamoto M, and Miyano M (2000) Crystal structure of rhodopsin: A G protein-coupled receptor. *Science* **289**:739–45.
- Pasternak GW (2014) Opiate pharmacology and relief of pain. *J Clin Oncol* **32**:1655–1661.
- Patel MB, Patel CN, Rajashekara V, and Yoburn BC (2002) Opioid agonists differentially regulate mu-opioid receptors and trafficking proteins in vivo. *Mol Pharmacol* **62**:1464–70.
- Paulozzi L, Mack K, Hockenberry J, and Division of Unintentional Injury Prevention, National Center for Injury Prevention and Control C (2014) Vital signs: variation among States in prescribing of opioid pain relievers and benzodiazepines - United States, 2012. *Centers Dis Control Prev Morb Mortal Wkly Rep* **63**:563–568.
- Pert C, and Snyder S (1974) Opiate receptor binding of agonists and antagonists affected differentially by sodium. *Mol Pharmacol* **1**:868–879.
- Pert CB, Pasternak G, and Snyder SH (1973) Opiate agonists and antagonists discriminated by receptor binding in brain. *Science* **182**:1359–61.
- Pert CB, and Snyder SH (1976) Correlation of opiate receptor affinity with analgetic effects of meperidine homologues. *J Med Chem* **19**:1248–50.
- Pierce KL, and Lefkowitz RJ (2001) Classical and new roles of beta-arrestins in the regulation of G-protein-coupled receptors. *Nat Rev Neurosci* **2**:727–733.
- Polastron J, Jauzac P, and Meunier JC (1992) The delta-opioid receptor in neuroblastoma x glioma NG 108-15 hybrid cells is strongly precoupled to a G-protein. *Eur J Pharmacol* **226**:133–9.
- Pradhan A a, Befort K, Nozaki C, Gavériaux-Ruff C, and Kieffer BL (2011) The delta opioid receptor: an evolving target for the treatment of brain disorders. *Trends Pharmacol Sci* **32**:581–90.

- Pradhan AA, Smith ML, Kieffer BL, and Evans CJ (2012) Ligand-directed signalling within the opioid receptor family. *Br J Pharmacol* **167**:960–969.
- Pradhan AA, Smith ML, Zyuzin J, and Charles A (2014) δ -Opioid receptor agonists inhibit migraine-related hyperalgesia, aversive state and cortical spreading depression in mice. *Br J Pharmacol* **171**:2375–2384.
- Price M, Baillie G, Thomas A, Stevenson L, Easson M, Goodwin R, McLean A, McIntosh L, Goodwin G, Walker G, Westwood P, Marrs J, Thomson F, Cowley P, Christopoulos A, Pertwee R, and Ross R (2005) Allosteric modulation of the cannabinoid CB1 receptor. *Mol Pharmacol* **68**:1484–1495.
- Raehal KM, and Bohn LM (2011) The role of beta-arrestin2 in the severity of antinociceptive tolerance and physical dependence induced by different opioid pain therapeutics. *Neuropharmacology* **60**:58–65.
- Raehal KM, Schmid CL, Groer CE, and Bohn LM (2011) Functional selectivity at the μ -opioid receptor: implications for understanding opioid analgesia and tolerance. *Pharmacol Rev* **63**:1001–19.
- Raehal KM, Walker JKL, and Bohn LM (2005) Morphine side effects in beta-arrestin-2 knockout mice. *J Pharmacol Exp Ther* **314**:1195–1201.
- Rasmussen SGF, Choi H-J, Fung JJ, Pardon E, Casarosa P, Chae PS, Devree BT, Rosenbaum DM, Thian FS, Kobilka TS, Schnapp A, Konetzki I, Sunahara RK, Gellman SH, Pautsch A, Steyaert J, Weis WI, and Kobilka BK (2011) Structure of a nanobody-stabilized active state of the $\beta(2)$ adrenoceptor. *Nature* **469**:175–80, Nature Publishing Group.
- Rasmussen SGF, DeVree BT, Zou Y, Kruse AC, Chung KY, Kobilka TS, Thian FS, Chae PS, Pardon E, Calinski D, Mathiesen JM, Shah ST, Lyons J, Caffrey M, Gellman SH, Steyaert J, Skiniotis G, Weis WI, Sunahara RK, and Kobilka BK (2011) Crystal structure of the β_2 adrenergic receptor-Gs protein complex. *Nature* **477**:549–55.
- Remmers A, Clark M, Alt A, Medzihradsky F, Woods JH, and Traynor JR (2000) Activation of G protein by opioid receptors: role of receptor number and G-protein concentration. *Eur J Pharmacol* **396**:67–75.
- Rivero G, Llorente J, McPherson J, Cooke A, Mundell SJ, McArdle C a, Rosethorne EM, Charlton SJ, Krasel C, Bailey CP, Henderson G, and Kelly E (2012) Endomorphin-2: a biased agonist at the μ -opioid receptor. *Mol Pharmacol* **82**:178–88.
- Rodríguez-Muñoz M, de la Torre-Madrid E, Sánchez-Blázquez P, and Garzón J (2007) Morphine induces endocytosis of neuronal μ -opioid receptors through the sustained transfer of Galpha subunits to RGSZ2 proteins. *Mol Pain* **3**:19.
- Roerig SC, Fujimoto JM, and Lange DG (1987) Development of tolerance to respiratory depression in morphine- and etorphine-pellet-implanted mice. *Brain Res* **400**:278–84.
- Russo EB, Burnett A, Hall B, and Parker KK (2005) Agonistic properties of cannabidiol at 5-HT1a receptors. *Neurochem Res* **30**:1037–1043.

- Sánchez-Blázquez P, Gómez-Serranillos P, and Garzón J (2001) Agonists determine the pattern of G-protein activation in μ -opioid receptor-mediated supraspinal analgesia. *Brain Res Bull* **54**:229–235.
- Schutz J, Spetea M, Hoch M, Aceto MD, Harris LS, Coop A, and Schmidhammer H (2003) Synthesis and biological evaluation of 14-alkoxymorphinans. 20.1 14-Phenylpropoxymetopon: An extremely powerful analgesic. *J Med Chem* **46**:4182–4187.
- Schwartz TW, and Holst B (2007) Allosteric enhancers, allosteric agonists and ago-allosteric modulators: where do they bind and how do they act? *Trends Pharmacol Sci* **28**:366–373.
- Schwyzler R, Kriwaczek V, and Wunderlin R (1981) A method for mapping peptide receptors. *Naturwissenschaften* 4–5.
- Scott C, Robbins E, and Chen K (1948) Pharmacological comparison of the optical isomers of methadone. *J Pharmacol Exp Ther* **93**:282–286.
- Seager M, Wittmann M, Jacobson M, Bickel D, Burno M, Jones K, Kuzmick V, Xu G, Pearson M, Mc- A, Gaspar R, Shughrue P, Danziger A, Regan C, Flick R, Pascarella D, Gar- S, Doran S, Kreatsoulas C, Veng L, Lindsley W, Shipe W, Kuduk S, Sur C, Seabrook GR, Ray WJ, Ma L, Seager MA, Graufelds VK, Mccampbell A, Garson S, Lindsley CW, Kinney G, Seabrook R, Naylor RL, Hardy RW, Bureau P, Chiu A, Elliott M, Farrell AP, Forster I, Gatlin DM, Goldberg RJ, Dominique P, Anthony P, and Rebecca J (2009) Selective activation of the M1 muscarinic acetylcholine receptor achieved by allosteric potentiation. *Proc Natl Acad Sci* **106**:15950–15955.
- Seki T, Minami M, Nakagawa T, Ienaga Y, Morisada A, and Satoh M (1998) DAMGO recognizes four residues in the third extracellular loop to discriminate between μ - and κ -opioid receptors. *Eur J Pharmacol* **350**:301–310.
- Selent J, Sanz F, Pastor M, and De Fabritiis G (2010) Induced Effects of Sodium Ions on Dopaminergic G-Protein Coupled Receptors. *PLoS Comput Biol* **6**:e1000884.
- Selley D, Cao C, Liu Q, and Childers S (2000) Effects of sodium on agonist efficacy for G-protein activation in μ -opioid receptor-transfected CHO cells and rat thalamus. *Br J Pharmacol* **130**:987–996.
- Semple G, Skinner PJ, Gharbaoui T, Shin Y-J, Jung J-K, Cherrier MC, Webb PJ, Tamura SY, Boatman PD, Sage CR, Schrader TO, Chen R, Colletti SL, Tata JR, Waters MG, Cheng K, Taggart AK, Cai T-Q, Carballo-Jane E, Behan DP, Connolly DT, and Richman JG (2008) 3-(1H-tetrazol-5-yl)-1,4,5,6-tetrahydro-cyclopentapyrazole (MK-0354): a partial agonist of the nicotinic acid receptor, G-protein coupled receptor 109a, with antilipolytic but no vasodilatory activity in mice. *J Med Chem* **51**:5101–8.
- Shang Y, LeRouzic V, Schneider S, Bisignano P, Pasternak GW, and Filizola M (2014) Mechanistic insights into the allosteric modulation of opioid receptors by sodium ions. *Biochemistry* **53**:5140–9.

- Shang Y, Yeatman HR, Provasi D, Alt A, Christopoulos A, Canals M, and Filizola M (2016) Proposed Mode of Binding and Action of Positive Allosteric Modulators at Opioid Receptors. *ACS Chem Biol*, doi: 10.1021/acscchembio.5b00712.
- Shenoy SK, and Lefkowitz RJ (2011) B-Arrestin-Mediated Receptor Trafficking and Signal Transduction. *Trends Pharmacol Sci* **32**:521–533, Elsevier Ltd.
- Simon EJ, and Groth J (1975) Kinetics of opiate receptor inactivation by sulfhydryl reagents: evidence for conformational change in presence of sodium ions. *Proc Natl Acad Sci U S A* **72**:2404–2407.
- Sounier R, Mas C, Steyaert J, Laeremans T, Manglik A, Huang W, Kobilka BK, Déméné H, and Granier S (2015) Propagation of conformational changes during μ -opioid receptor activation. *Nature* **524**:375–378.
- Spetea M, Asim MF, Wolber G, and Schmidhammer H (2013) The μ opioid receptor and ligands acting at the μ opioid receptor, as therapeutics and potential therapeutics. *Curr Pharm Des* **19**:7415–34.
- Srivastava A, Yano J, Hirozane Y, Kefala G, Gruswitz F, Snell G, Lane W, Ivetac A, Aertgeerts K, Nguyen J, Jennings A, and Okada K (2014) High-resolution structure of the human GPR40 receptor bound to allosteric agonist TAK-875. *Nature* **513**:124–7.
- Stafford K, Gomes AB, Shen J, and Yoburn BC (2001) μ -Opioid receptor downregulation contributes to opioid tolerance in vivo. *Pharmacol Biochem Behav* **69**:233–237.
- Stephenson RP (1956) A modification of receptor theory. *Br J Pharmacol* **11**:379–393.
- Steyaert J, and Kobilka BK (2011) Nanobody stabilization of G protein-coupled receptor conformational states. *Curr Opin Struct Biol* **21**:567–572.
- Strange PG (2008) Agonist binding, agonist affinity and agonist efficacy at G protein-coupled receptors. *Br J Pharmacol* **153**:1353–63.
- Szekeres PG, and Traynor JR (1997) Delta opioid modulation of the binding of guanosine-5'-O-(3-[35S]thio)triphosphate to NG108-15 cell membranes: characterization of agonist and inverse agonist effects. *J Pharmacol Exp Ther* **283**:1276–1284.
- Tan Q, Zhu Y, Li J, Chen Z, Han GW, Kufareva I, Li T, Ma L, Fenalti G, Li J, Zhang W, Xie X, Yang H, Jiang H, Cherezov V, Liu H, Stevens RC, Zhao Q, and Wu B (2013) Structure of the CCR5 Chemokine Receptor-HIV Entry Inhibitor Maraviroc Complex. *Science* **341**:1387–1390.
- Thompson GL, Kelly E, Christopoulos A, and Canals M (2015) Novel GPCR paradigms at the μ -opioid receptor. *Br J Pharmacol* **172**:287–96.
- Traynor JR, and Nahorski SR (1995) Modulation by mu-opioid agonists of guanosine-5'-O-(3-[35S]thio)triphosphate binding to membranes from human neuroblastoma SH-SY5Y cells. *Mol Pharmacol* **47**:848–854.

- Tso PH, and Wong YH (2000) G(z) can mediate the acute actions of mu- and kappa-opioids but is not involved in opioid-induced adenylyl cyclase supersensitization. *J Pharmacol Exp Ther* **295**:168–176.
- Valant C, Felder CC, Sexton PM, and Christopoulos A (2012) Probe dependence in the allosteric modulation of a G protein-coupled receptor: implications for detection and validation of allosteric ligand effects. *Mol Pharmacol* **81**:41–52.
- van der Westhuizen ET, Valant C, Sexton PM, and Christopoulos A (2015) Endogenous Allosteric Modulators of G Protein-Coupled Receptors. *J Pharmacol Exp Ther* **353**:246–260.
- Vanderah TW (2010) Delta and kappa opioid receptors as suitable drug targets for pain. *Clin J Pain* **26 Suppl 1**:S10–5.
- Virk MS, Arttamangkul S, Birdsong WT, and Williams JT (2009) Buprenorphine Is a Weak Partial Agonist That Inhibits Opioid Receptor Desensitization. *J Neurosci* **29**:7341–7348.
- Waldhoer M, Bartlett SE, and Whistler JL (2004) Opioid Receptors. *Annu Rev Biochem* **73**:953–990.
- Walker E, Picker M, Granger A, and Dykstra L (2004) Effects of opioids in morphine-treated pigeons trained to discriminate among morphine, the low-efficacy agonist nalbuphine, and saline. *J Pharmacol Exp Ther* **310**:150–158.
- Walsh SK, Hepburn CY, Keown O, Åstrand A, Lindblom A, Ryberg E, Hjorth S, Leslie SJ, Greasley PJ, and Wainwright CL (2015) Pharmacological profiling of the hemodynamic effects of cannabinoid ligands: a combined in vitro and in vivo approach. *Pharmacol Res Perspect* **3**:e00143.
- Walters RW, Shukla AK, Kovacs JJ, Violin JD, DeWire SM, Lam CM, Chen JR, Muehlbauer MJ, Whalen EJ, and Lefkowitz RJ (2009) beta-Arrestin1 mediates nicotinic acid-induced flushing, but not its antilipolytic effect, in mice. *J Clin Invest* **119**:1312–21.
- Wang M, Yao Y, Kuang D, and Hampson DR (2006) Activation of Family C G-protein-coupled Receptors by the Tripeptide Glutathione. *J Biol Chem* **281**:8864–8870.
- Whistler JL, Chuang HH, Chu P, Jan LY, and von Zastrow M (1999) Functional dissociation of mu opioid receptor signaling and endocytosis: implications for the biology of opiate tolerance and addiction. *Neuron* **23**:737–46.
- Whistler JL, and von Zastrow M (1998) Morphine-activated opioid receptors elude desensitization by beta-arrestin. *Proc Natl Acad Sci U S A* **95**:9914–9.
- Whorton MR, Bokoch MP, Rasmussen SGF, Huang B, Zare RN, Kobilka B, and Sunahara RK (2007) A monomeric G protein-coupled receptor isolated in a high-density lipoprotein particle efficiently activates its G protein. *Proc Natl Acad Sci U S A* **104**:7682–7.
- Williams JT, Christie MJ, and Manzoni O (2001) Cellular and synaptic adaptations mediating opioid dependence. *Physiol Rev* **81**:299–343.

- Williams JT, Ingram SL, Henderson G, Chavkin C, von Zastrow M, Schulz S, Koch T, Evans CJ, and Christie MJ (2013) Regulation of μ -opioid receptors: desensitization, phosphorylation, internalization, and tolerance. *Pharmacol Rev* **65**:223–54.
- Woolfe G, and MacDonald A (1944) The Evaluation of the Analgesic Action of Pethidine Hydrochloride (Demerol). *J Pharmacol Exp Ther* **80**:300–307.
- Wootten D, Christopoulos A, and Sexton PM (2013) Emerging paradigms in GPCR allostery: implications for drug discovery. *Nat Rev Drug Discov* **12**:630–44.
- Yoburn BC, Gomes B a, Rajashekara V, Patel C, and Patel M (2003) Role of G(i)alpha2-protein in opioid tolerance and mu-opioid receptor downregulation in vivo. *Synapse* **47**:109–16.
- Yoburn BC, Purohit V, Patel K, and Zhang Q (2004) Opioid agonist and antagonist treatment differentially regulates immunoreactive mu-opioid receptors and dynamin-2 in vivo. *Eur J Pharmacol* **498**:87–96.
- Zadina J, Hackler L, Ge L, and Kastin A (1997) A potent and selective endogenous agonist for the μ -opiate receptor. *Nature* **386**:499–502.
- Zhang C, Srinivasan Y, Arlow DH, Fung JJ, Palmer D, Zheng Y, Green HF, Pandey A, Dror RO, Shaw DE, Weis WI, Coughlin SR, and Kobilka BK (2012) High-resolution crystal structure of human protease-activated receptor 1. *Nature* **492**:387–92.
- Zhang J, Ferguson SS, Barak LS, Bodduluri SR, Laporte S a, Law PY, and Caron MG (1998) Role for G protein-coupled receptor kinase in agonist-specific regulation of mu-opioid receptor responsiveness. *Proc Natl Acad Sci U S A* **95**:7157–62.
- Zhao X, Jones A, Olson KR, Peng K, Wehrman T, Park A, Mallari R, Nebalasca D, Young SW, and Xiao S-H (2008) A Homogeneous Enzyme Fragment Complementation-Based - Arrestin Translocation Assay for High-Throughput Screening of G-Protein-Coupled Receptors. *J Biomol Screen* **13**:737–747.
- Zheng H, Loh HH, and Law P (2008) Extracellular Signal-Regulated Kinases (ERKs) Translocate to Nucleus in Contrast to G Protein-Dependent ERK Activation. *Mol Pharmacol* **73**:178–190.